VOLUME 37 FEBRUARY 1959 NUMBER 2

Canadian Journal of Chemistry

Editor: LÉO MARION

Associate Editors:

HERBERT C. BROWN, *Purdue University*
A. R. GORDON, *University of Toronto*
C. B. PURVES, *McGill University*
SIR ERIC RIDEAL, *Imperial College, University of London*
J. W. T. SPINKS, *University of Saskatchewan*
E. W. R. STEACIE, *National Research Council of Canada*
H. G. THODE, *McMaster University*
A. E. VAN ARKEL, *University of Leiden*

Published by THE NATIONAL RESEARCH COUNCIL

OTTAWA CANADA

Canadian Journal of Chemistry

Under the authority of the Chairman of the Committee of the Privy Council on Scientific and Industrial Research, the National Research Council issues THE CANADIAN JOURNAL OF CHEMISTRY and five other journals devoted to the publication, in English or French, of the results of original scientific research. Matters of general policy concerning these journals are the responsibility of a joint Editorial Board consisting of: members representing the National Research Council of Canada; the Editors of the Journals; and members representing the Royal Society of Canada and four other scientific societies.

The Chemical Institute of Canada has chosen the Canadian Journal of Chemistry as its medium of publication for scientific papers.

EDITORIAL BOARD

Representatives of the National Research Council

A. Gauthier, *University of Montreal*
R. B. Miller, *University of Alberta*
H. G. Thode, *McMaster University*
D. L. Thomson, *McGill University*

Editors of the Journals

D. L. Bailey, *University of Toronto*
T. W. M. Cameron, *Macdonald College*
H. E. Duckworth, *McMaster University*
K. A. C. Elliott, *Montreal Neurological Institute*
Léo Marion, *National Research Council*
R. G. E. Murray, *University of Western Ontario*

Representatives of Societies

D. L. Bailey, *University of Toronto*
Royal Society of Canada
T. W. M. Cameron, *Macdonald College*
Royal Society of Canada
H. E. Duckworth, *McMaster University*
Royal Society of Canada
Canadian Association of Physicists
K. A. C. Elliott, *Montreal Neurological Institute*
Canadian Physiological Society
P. R. Gendron, *University of Ottawa*
Chemical Institute of Canada
R. G. E. Murray, *University of Western Ontario*
Canadian Society of Microbiologists
T. Thorvaldson, *University of Saskatchewan*, Royal Society of Canada

Ex officio

Léo Marion (Editor-in-Chief), *National Research Council*
J. B. Marshall (Administration and Awards), *National Research Council*

Manuscripts for publication should be submitted to Dr. Léo Marion, Editor-in-Chief, Canadian Journal of Chemistry, National Research Council, Ottawa 2, Canada.
(For instructions on preparation of copy, see **Notes to Contributors** (inside back cover).)

Proof, correspondence concerning proof, and orders for reprints should be sent to the Manager, Editorial Office (Research Journals), Division of Administration and Awards, National Research Council, Ottawa 2, Canada.

Subscriptions, renewals, requests for single or back numbers, and all remittances should be sent to Division of Administration and Awards, National Research Council, Ottawa 2, Canada. Remittances should be made payable to the Receiver General of Canada, credit National Research Council.

The journals published, frequency of publication, and prices are:

Canadian Journal of Biochemistry and Physiology	Monthly	$9.00 a year
Canadian Journal of Botany	Bimonthly	$6.00 a year
Canadian Journal of Chemistry	Monthly	$12.00 a year
Canadian Journal of Microbiology	Bimonthly	$6.00 a year
Canadian Journal of Physics	Monthly	$9.00 a year
Canadian Journal of Zoology	Bimonthly	$5.00 a year

The price of regular single numbers of all journals is $2.00.

Canadian Journal of Chemistry

Issued by THE NATIONAL RESEARCH COUNCIL OF CANADA

VOLUME 37 FEBRUARY 1959 NUMBER 2

ω-HALOALKYL AND ω-AMINOALKYL SULPHIDES

CLEAVAGE OF THE ALKYL–SULPHUR BOND[1]

MARSHALL KULKA

ABSTRACT

In the homologous series of *p*-chlorophenyl ω-chloroalkyl sulphides (I), the first and second members reacted abnormally with amines to yield 1,ω-bis(*p*-chlorophenylmercapto)alkanes (II). The fourth member of the series reacted normally to produce 4-aminobutyl *p*-chlorophenyl sulphide (III). The formation of II is explained on the basis of an alkyl–sulphur bond cleavage. The members of the *p*-chlorobenzyl series (VI) in general reacted with amines to form the expected aminoalkyl sulphides (VII). However, the *p*-chlorobenzyl chloroalkyl sulphides (VI) were thermally labile and decomposed to *p*-chlorobenzyl chloride and a sulphur component. A cyclic sulphur component originated from VI whose chloroalkyl carbon chain was 4, 5, or 6. The thermal degradation of VI is explained through a sulphonium salt cleavage.

INTRODUCTION

It has been recently shown that *p*-chlorophenyl chloromethyl sulphide (I, $n = 1$) can undergo an unusual bimolecular reaction to form 2,8-dichloro-6H,12H-dibenzo(*b*,*f*)-1,5-dithiocin (1). Now another anomalous reaction of I has been discovered and is the subject

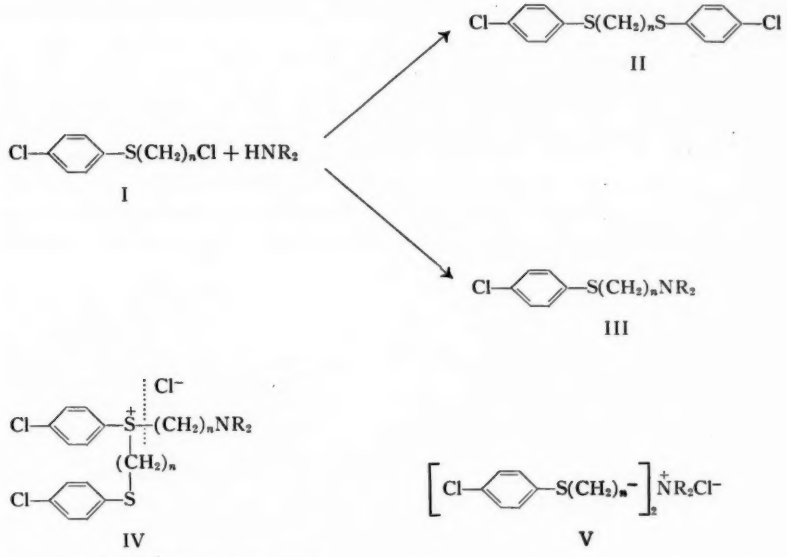

[1]*Manuscript received September 18, 1958.*
Contribution from the Dominion Rubber Company Limited Research Laboratories, Guelph, Ontario.

of this paper. When I ($n = 1$) was heated with ammonia, di-*n*-butylamine, or *t*-butylamine, the expected aminomethyl, *p*-chlorophenyl sulphide (III, $n = 1$), was not obtained. Instead, bis(*p*-chlorophenylmercapto)methane (II, $n = 1$) was the product.

On treatment of higher members of the homologous series of I with amines, it was found the 2-chloroethyl *p*-chlorophenyl sulphide (I, $n = 2$) also reacted abnormally in boiling di-*n*-butylamine to form 1,2-bis(*p*-chlorophenylmercapto)ethane (II, $n = 2$). However, when the temperature of the reaction was lowered to about 120° the only product was N,N-di-*n*-butylaminoethyl *p*-chlorophenyl sulphide (III, $n = 2$). Normal reaction only was indicated with higher members of the homologous series, since *p*-chlorophenyl 4-chlorobutyl sulphide (I, $n = 4$) with boiling di-*n*-butylamine gave *p*-chlorophenyl 4-di-*n*-butylaminobutyl sulphide (III, $n = 4$) in high yield. In this connection it was interesting to note that III ($n = 2$ and 4) forms a hydrochloride which is soluble in benzene and which distills readily without decomposition.

Any mechanism which attempts to explain the formation of II from I must take into account the observation that neither I nor III thermally decomposed to II, but that an equimolecular mixture of I and III on heating at 180° yielded II. This observation suggests two possible intermediates in the mechanism of the reaction, the sulphonium salt IV and the quaternary ammonium salt V, each of which could arise by the reaction of I with III. The dissociation of the sulphonium salt IV (indicated by the dotted line) would lead to II and chloroalkylamine. However, evidence is against this sulphonium salt mechanism since phenyl sulphides in general resist sulphonium chloride formation.

The formation of II ($n = 1$ and 2) from I might be attributed to a side reaction of I with *p*-chlorothiophenol in the presence of the amine. *p*-Chlorothiophenol could arise through an alkyl–sulphur bond cleavage of the quaternary ammonium salt V of I and III. A similar alkyl–sulphur bond cleavage has been experienced previously in the hydrazinolysis of β-*p*-chlorophenylmercapto-ethyl N,N-dimethyldithiocarbamate to *p*-chlorothiophenol (2).

The alkyl–sulphur bond in compounds of the benzyl series VI, unlike that of the phenyl series I, appeared to resist amine cleavage. Thus in the reaction of *p*-chlorobenzyl ω-chloroalkyl sulphides (VI) with amines only the normal products, VII, were formed and little if any of the neutral sulphides VIII could be detected.

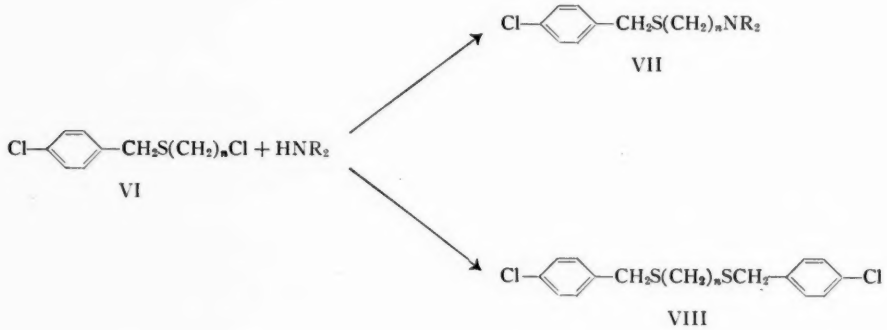

However, an alkyl–sulphur bond cleavage of a different nature was encountered in this series. It was found that the *p*-chlorobenzyl ω-haloalkyl sulphides (VI) were thermally

labile (unlike the members of the phenyl series I) and cleaved to *p*-chlorobenzyl chloride and a sulphur component. ω-Bromoalkyl *p*-chlorobenzyl sulphides were even more sensitive to heat and yielded *p*-chlorobenzyl bromide.

The lower members of the series VI could be distilled *in vacuo* with little if any decomposition but the higher members (n = 4 and 5) were too labile. Thus vacuum distillation of IX (Y = 0), IX (Y = CH_2), IX (Y = S), and IX (Y = 0) yielded *p*-chlorobenzyl chloride (XI) in each case together with tetrahydrothiophene (XII, Y = 0) (not isolated),

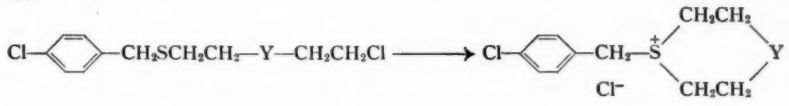

IX X

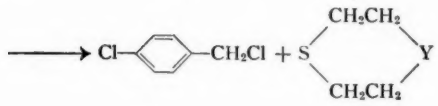

XI XII

pentamethylene sulphide (XII, Y = CH_2), 1,4-dithiane (XII, Y = S), and 1,4-oxathiane (XII, Y = 0) respectively. An attempt to prepare 4-bromo-2-butenyl *p*-chlorobenzyl sulphide from *p*-chlorobenzyl mercaptan and 1,4-dibromo-2-butene resulted in a mixture of *p*-chlorobenzyl bromide and a malodorous liquid which was probably dihydrothiophene.

The explanation for these reactions must involve sulphonium salt formation. Thus intramolecular sulphonium salt cyclization of IX could occur to form the ring X, which by dissociation would yield *p*-chlorobenzyl chloride (XI) and the cyclic sulphur compound (XII). Similar alkyl–sulphur bond cleavages with and without cyclizations have been reported by other workers (3, 4, 5). Bell, Bennett, and Hock (3) showed that mustard gas when heated at 180° yielded *p*-dithiane and ethylene dichloride. They proposed a mechanism for this reaction which consisted of both intermolecular and intramolecular sulphonium salt formation followed by dissociation.

An interesting example is provided of an alkyl–sulphur bond cleavage which must involve a seven-membered sulphonium salt ring (XIV). Thus when 2-β-chloroethoxy-5-methylbenzyl *p*-chlorobenzyl sulphide (XIII) was slowly distilled at 11 mm pressure, a

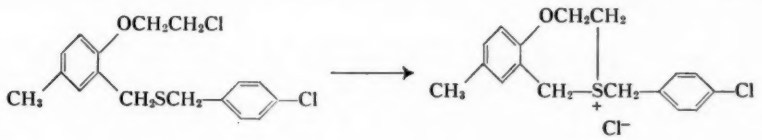

XIII XIV

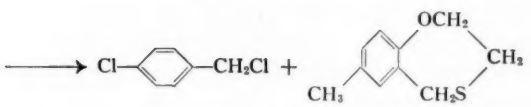

XI XV

mixture of low-boiling compounds was obtained. These compounds proved to be *p*-chlorobenzyl chloride (XI) and 2,3-dihydro-7-methylbenzo(*f*)-1,4-oxathiepin (XV) (6).

EXPERIMENTAL

Bis(p-chlorophenylmercapto)methane (II, $n = 1$) *from p-Chlorophenyl Chloromethyl Sulphide* (I, $n = 1$)

To *p*-chlorophenyl chloromethyl sulphide (7) (20 g) was added *t*-butylamine (40 ml) and the solution was heated under reflux for 4 hours. The precipitated *t*-butylamine hydrochloride was filtered off from the cooled reaction mixture and the filtrate freed of excess *t*-butylamine by distillation. The residue was dissolved in benzene, the solution washed with water, and the solvent removed. The residue distilled at 160–162° (0.5 mm) and the distillate (12 g or 77%) when crystallized from methanol melted at 42–43° alone or in admixture with bis(*p*-chlorophenylmercapto)methane (8).

In another experiment *p*-chlorophenyl chloromethyl sulphide was heated in a sealed bomb with excess liquid ammonia at 50–55° for 15 hours. This yielded only bis(*p*-chlorophenylmercapto)methane.

1,2-Bis(p-chlorophenylmercapto)ethane (II, $n = 2$) *from p-Chlorophenyl 2-Chloroethyl Sulphide* (I, $n = 2$)

A solution of *p*-chlorophenyl 2-chloroethyl sulphide (20 g) and di-*n*-butylamine (40 ml) was heated under reflux for 5 hours. The excess di-*n*-butylamine was removed *in vacuo* and the residue was crystallized from methanol. The white prisms (9 g) melted at 92–93° and did not depress the melting point of 1,2-bis(*p*-chlorophenylmercapto)ethane (9).

In another experiment *p*-chlorophenyl 2-chloroethyl sulphide was heated in a sealed bomb with methylamine at 140° for 6 hours. The product was 1,2-bis(*p*-chlorophenylmercapto)ethane.

2-(Di-n-butylamino)ethyl p-Chlorophenyl Sulphide (III, $n = 2$, R = C_4H_9)

A solution of *p*-chlorophenyl 2-chloroethyl sulphide (50 g) and di-*n*-butylamine (100 ml) was heated at 115–125° for 18 hours. The excess di-*n*-butylamine was removed *in vacuo*, the residue dissolved in benzene, and the solution washed with dilute hydrochloric acid. The benzene was removed and the residue distilled yielding a very viscous distillate (52 g) boiling at 160° (0.5 mm). When it was rubbed and warmed, it solidified and the white solid melted at 86–88°. This proved to be the hydrochloride of 2-(di-*n*-butylamino)-ethyl *p*-chlorophenyl sulphide (it is rather unusual that an amine salt should distill and be soluble in benzene). Anal. Calc. for $C_{16}H_{27}NCl_2S$: C, 57.14; H, 8.03. Found: C, 56.68; H, 7.79.

The free base was liberated from the hydrochloride by dissolving the latter in benzene and shaking with aqueous sodium hydroxide. 2-(Di-*n*-butylamino)ethyl *p*-chlorophenyl sulphide boiled at 137–140° (0.5 mm), $n_D^{20} = 1.5350$ and remained a colorless mobile liquid. Anal. Calc. for $C_{16}H_{26}NClS$: C, 64.11; H, 8.68. Found: C, 63.58, 63.27; H, 8.34, 8.52.

In another experiment when *p*-chlorophenyl 2-chloroethyl sulphide was heated with di-*n*-butylamine at 130–150° for 5 hours, a mixture of 2-(di-*n*-butylamino)ethyl *p*-chlorophenyl sulphide and 1,2-bis(*p*-chlorophenylmercapto)ethane was obtained.

4-(Di-n-butylamino)butyl p-Chlorophenyl Sulphide (III, $n = 4$, R = C_4H_9)

A solution of *p*-chlorophenyl 4-chlorobutyl sulphide (1) (17 g) and di-*n*-butylamine

(50 ml) was heated under reflux for 5 hours. The excess amine was removed *in vacuo*, the residue was dissolved in benzene, and the solution washed with aqueous sodium hydroxide and with water. Removal of the solvent and distillation of the residue yielded a colorless liquid (18 g), b.p. = 155° (0.5 mm); $n_D^{22} = 1.5288$. Anal. Calc. for $C_{18}H_{30}NClS$: C, 65.95; H, 9.16. Found: C, 65.43; H, 8.98.

2-(Diethylamino)ethyl p-Chlorophenyl Sulphide (III, $n = 2$, R = C_2H_5)

A solution of *p*-chlorophenyl 2-chloroethyl sulphide (20 g) and 98% diethylamine (35 ml) was heated at 120–130° in a sealed bomb for 6 hours. The product which was worked up as above boiled at 163–165° (11 mm); $n_D^{22} = 1.5535$. The yield was 12 g. Anal. Calc. for $C_{12}H_{18}NClS$: C, 59.14; H, 7.39. Found: C, 58.81, 59.25; H, 7.53, 7.50.

2-Aminoethyl p-Chlorophenyl Sulphide (III, $n = 2$, R = H)

To a solution of sodium hydroxide (10 g) in water (100 ml) was added *p*-chlorothiophenol (16 g) and 2-bromoethylamine hydrobromide (20 g) in water (30 ml). The resulting solution was heated on the steam bath for ½ hour and the precipitated oil was extracted with benzene. The benzene solution was washed with water, the solvent removed, and the residue distilled, b.p. = 152° (11 mm); $n_D^{25} = 1.6025$. The yield was 15 g. Anal. Calc. for $C_8H_{10}NClS$: C, 51.20; H, 5.33. Found: C, 50.27, 50.87; H, 5.25, 5.31.

2-Aminoethyl Pentachlorophenyl Sulphide

This was prepared in 60% yield from pentachlorobenzenethiol and 2-bromoethylamine hydrobromide as above. The white prisms crystallized from benzene – petroleum ether and melted at 89–90°. Anal. Calc. for $C_8H_6NCl_5S$: C, 29.46; H, 1.81. Found: C, 30.17, 29.81; H, 2.23, 2.12.

p-Chlorobenzyl 2-(Di-n-butylamino)ethyl Sulphide (VII, $n = 2$, R = C_4H_9)

A solution of *p*-chlorobenzyl 2-chloroethyl sulphide (9) (20 g) and di-*n*-butylamine (40 ml) was heated under reflux for 3 hours. The excess amine was removed *in vacuo*, the residue dissolved in benzene and washed with water. The solvent was removed and the residue fractionally distilled. The first fraction consisted of low-boiling material. The second fraction (7 g), which boiled at 137–140° (0.5 mm); $n_D^{27} = 1.5320$, was the required *p*-chlorobenzyl 2-(di-*n*-butylamino)ethyl sulphide. Anal. Calc. for $C_{17}H_{28}NClS$: C, 65.07; H, 8.93. Found: C, 65.26; H, 8.75.

The third fraction (3 g) boiled at 180–210° (0.5 mm) and the distillate on crystallization from methanol yielded white prisms (1.2 g) which melted at 74–76° alone or in admixture with 1,2-bis(*p*-chlorobenzylmercapto)ethane (9).

Pyrolysis of p-Chlorobenzyl 5-Chloropentyl Sulphide (VI, $n = 5$)

The crude *p*-chlorobenzyl 5-chloropentyl sulphide (40 g) (see below) was distilled at 12 mm first, and the distillate was then fractionated.

Fraction 1 consisted of 9 g of colorless malodorous liquid boiling at 140°; $n_D^{20} = 1.5060$. These properties agree with those of pentamethylene sulphide (10, 11). When a portion of fraction 1 was dissolved in acetic acid and treated with 30% hydrogen peroxide, pentamethylene sulphone (12), m.p. 96–97°, was formed.

Fraction 2 consisted of 19 g of colorless lachrymatory liquid; $n_D^{20} = 1.5560$ boiling at 87–89° (11 mm). It solidified on cooling and melted at 29°. Recrystallization from petroleum ether yielded long white needles melting at 29–30° alone or in admixture with *p*-chlorobenzyl chloride.

Pyrolysis of p-Chlorobenzyl 4-Chlorobutyl Sulphide (VI, $n = 4$)

Crude *p*-chlorobenzyl 4-chlorobutyl sulphide was prepared and pyrolyzed as above. *p*-Chlorobenzyl chloride was obtained in 74% yield but no tetrahydrothiophene could be isolated.

Pyrolysis of p-Chlorobenzyl 4-Bromo-2-butenyl Sulphide

To a stirred solution of potassium hydroxide (11 g) in methanol (200 ml) and *p*-chlorobenzyl mercaptan (30 g), cooled to 0°, was added a chilled solution of 1,4-dibromo-2-butene (100 g) in benzene (100 ml). The reaction mixture was stirred with cooling at 5–10° for 1 hour. The precipitated potassium bromide was filtered off and the solvents were removed from the filtrate. The residue was dissolved in benzene, the solution washed with water, and the solvent removed. The residue was distilled at 11 mm and the distillate then fractionated. Fraction 1 was a colorless malodorous liquid boiling at 40–60° (11 mm) and was probably dihydrothiophene. Fraction 2, boiling at 60–95° (11 mm), consisted mainly of 1,4-dibromo-2-butene. Fraction 3 (14 g) boiled at 95–102° (11 mm) and on crystallization from methanol yielded white needles melting at 49–50° alone or in admixture with *p*-chlorobenzyl bromide (13).

β-p-Chlorobenzylmercaptoethyl 2-Hydroxyethyl Sulphide

To a solution of potassium hydroxide (6 g) in methanol (100 ml) was added 2-mercaptoethanol (9 ml) and *p*-chlorobenzyl 2-chloroethyl sulphide (9) (20 g). The resulting solution was heated under reflux for 2 hours and then the methanol distilled off. The residual oil was extracted with benzene, the solution washed with water, and the solvent removed. The residue distilled at 175–178 (0.5 mm) yielding 19 g of a colorless liquid, $n_D^{26} = 1.5992$. Anal. Calc. for $C_{11}H_{15}OClS_2$: C, 50.28; H, 5.71. Found: C, 50.59; H, 5.82.

β-o-Chlorobenzylmercaptoethyl 2-Hydroxyethyl Sulphide

This was prepared in 87% yield from *o*-chlorobenzyl 2-chloroethyl sulphide as above, b.p. = 170–175° (0.5 mm); $n_D^{22} = 1.6020$. Anal. Calc. for $C_{11}H_{15}OClS_2$: C, 50.28; H, 5.71. Found: C, 50.55; H, 5.76.

Pyrolysis of β-p-(IX, Y = S) *and β-o-Chlorobenzylmercaptoethyl 2-Chloroethyl Sulphide*

A solution of *β-o*-chlorobenzylmercaptoethyl 2-hydroxyethyl sulphide (30 g), benzene (100 ml), and thionyl chloride (12 ml) was heated under reflux for 2 hours. The benzene and excess thionyl chloride were removed *in vacuo* and the residue was slowly distilled at 11 mm. The distillate was cooled and the white malodorous precipitate (6 g) filtered, washed with cold methanol, and dried. It sublimed readily and melted at 111–112°. This was *p*-dithiane (14).

The filtrate on distillation yielded *o*-chlorobenzyl chloride.

When *β-p*-chlorobenzylmercaptoethyl 2-hydroxyethyl sulphide was converted to the 2-chloroethyl derivative IX, (Y = S) with thionyl chloride and treated as above, a separable mixture of *p*-dithiane and *p*-chlorobenzyl chloride was obtained.

Pyrolysis of β-p-Chlorobenzylmercaptoethyl 2-Chloroethyl Ether (IX, Y = 0)

β-p-Chlorobenzylmercaptoethyl 2-chloroethyl ether (10 g) (see below) was heated at 160–170° for 7 hours. A malodorous liquid (3 g) distilled into the receiver which on redistillation boiled at 147–150°; $n_D^{22} = 1.5070$. The properties of this compound are in agreement with those given for 1,4-oxathiane (15, 16).

The residue on distillation yielded 5 g of *p*-chlorobenzyl chloride.

Pyrolysis of 2-β-Chloroethoxy-5-methylbenzyl p-Chlorobenzyl Sulphide (XIII)

To a solution of potassium hydroxide (5 g) in methanol (100 ml) was added *p*-chlorobenzyl mercaptan (11 g) and 2-β-chloroethoxy-5-methylbenzyl chloride (6) (15 g) in that order. The resulting reaction mixture was heated under reflux for 15 minutes. The methanol was removed, the residue dissolved in benzene, the solution washed with water, and the solvent removed. The residue was distilled slowly at 11 mm pressure up to 200° and the distillate was fractionated. Fraction 1 (5 g) which boiled at 80–135° (11 mm) was treated with thiourea in ethanol. The resulting isothiuronium salt melted at 205–207° and did not depress the melting point of the isothiuronium salt of *p*-chlorobenzyl chloride. Fraction 2 (9 g) boiled at 135–150° (11 mm) and when crystallized from methanol yielded white prisms melting at 45–46° alone or in admixture with 2,3-dihydro-7-methylbenzo(*f*)-1,4-oxathiepin (XV) (6).

Preparation of ω-Chloroalkyl Sulphides

These were prepared by the method used for 2-chloroethyl aryl and aralkyl sulphides previously described (9).

(*a*) *p-Chlorobenzyl 3-chloropropyl sulphide* (VI, $n = 3$) was obtained in 87% yield from 1,3-dichloropropane and *p*-chlorobenzyl mercaptan, b.p. = 115–118 (0.5 mm); $n_D^{22} = 1.5720$. Anal. Calc. for $C_{10}H_{12}Cl_2S$: C, 51.06; H, 5.10. Found: C, 50.63, 50.91; H, 4.89, 4.64.

(*b*) *p-Chlorobenzyl 3-bromopropyl sulphide* was prepared in 60% yield from 1,3-dibromopropane and *p*-chlorobenzyl mercaptan, b.p. = 120–125° (0.5 mm); $n_D^{22} = 1.5884$. Anal. Calc. for $C_{10}H_{12}ClBrS$: C, 42.93; H, 4.29. Found: C, 42.21, 42.27; H, 3.39, 3.50.

(*c*) *p-Chlorobenzyl 2-bromoethyl sulphide* could not be prepared in pure form because pyrolysis occurred during distillation to form *p*-chlorobenzyl bromide.

(*d*) *n-Amyl 4-chlorobutyl sulphide* was prepared in 20% yield from *n*-amyl mercaptan and 1,4-dichlorobutane, b.p. = 120–130° (11 mm); $n_D^{23} = 1.4775$. Anal. Calc. for $C_9H_{19}ClS$: C, 55.53; H, 9.76. Found: C, 56.33, 56.74; H, 9.75, 9.84.

(*e*) *β-p-Chlorobenzylmercaptoethyl 2-chloroethyl ether* (IX, Y = 0) was prepared in 75% yield from *p*-chlorobenzyl mercaptan and excess β,β′-dichloroethyl ether, b.p. = 137–140° (0.5 mm); $n_D^{22} = 1.5618$. Anal. Calc. for $C_{11}H_{14}OCl_2S$: C, 49.81; H, 5.28. Found: C, 49.94, 49.82; H, 5.08, 5.12.

(*f*) *p-Chlorobenzyl 5-chloropentyl sulphide* (VI, $n = 5$) was prepared from *p*-chlorobenzyl mercaptan and 1,5-dichloropentane (17). No attempt was made to distill the crude product because it pyrolyzed very readily.

(*g*) *Crude p-chlorobenzyl 4-chlorobutyl sulphide* (VI, $n = 4$) was prepared similarly.

o-Chlorobenzyl 2-Hydroxyethyl Sulphide

To a stirred mixture of sodium hydroxide (70 g) in 2-mercaptoethanol (200 ml) and benzene (200 ml) was added, over ½ hour, a solution of *o*-chlorobenzyl chloride (250 g) in benzene (150 ml). The reaction mixture boiled vigorously. It was heated under reflux for 2 hours, washed with water, the solvent removed, and the residue distilled, b.p. = 175–178° (11 mm); $n_D^{20} = 1.5832$. The yield was 293 g. Anal. Calc. for $C_9H_{11}OClS$: C, 53.33; H, 5.43. Found: C, 53.73; H, 5.58.

o-Chlorobenzyl 2-Chloroethyl Sulphide

To a stirred solution of *o*-chlorobenzyl 2-hydroxyethyl sulphide (200 g) in benzene (250 ml) was added, over ½ hour, thionyl chloride (125 g) with cooling. The reaction

mixture was heated under reflux for 1 hour, the solvent removed, and the residual oil distilled, b.p. = 155–158° (11 mm); n_D^{23} = 1.5827. The yield was 190 g. Anal. Calc. for $C_9H_{10}Cl_2S$: C, 48.87; H, 4.52. Found: C, 48.76; H, 4.05.

β-p-t-Butylphenoxyethyl 2-Hydroxyethyl Sulphide

This was prepared in 90% yield from *p-t*-butylphenyl 2-chloroethyl ether and 2-mercaptoethanol in the same way as was *o*-chlorobenzyl 2-hydroxyethyl sulphide above. The colorless liquid boiled at 205–210° (11 mm); n_D^{23} = 1.5410. Anal. Calc. for $C_{14}H_{22}O_2S$: C, 66.14; H, 8.66. Found: C, 65.49; H, 8.86.

β-p-t-Butylphenoxyethyl 2-Chloroethyl Sulphide

This was prepared in 94% yield by treatment of *β-p-t*-butylphenoxyethyl 2-hydroxyethyl sulphide with thionyl chloride. It distilled at 145–148° (0.5 mm) as a colorless liquid, n_D^{22} = 1.5400. Anal. Calc. for $C_{14}H_{21}OClS$: C, 61.65; H, 7.70. Found: C, 61.83; H, 7.79.

Preparation of the Aminoalkyl Sulphides

These were prepared by the same method as was (*a*).

(*a*) *p-Chlorobenzyl 2-aminoethyl sulphide* (VII, $n = 2$, R = H) was prepared by the addition of liquid ammonia (about 100 ml) to 30 g *p*-chlorobenzyl 2-chloroethyl sulphide cooled by dry ice, and the reaction mixture was sealed in a hydrogenation bomb and heated at 135–140° for 6 hours. The excess ammonia was allowed to evaporate, the residue treated with aqueous sodium hydroxide and extracted with benzene. The benzene solution was washed with water, the solvent removed, and the residue distilled. Most of it (20 g) distilled at 103–105° (0.2 mm) as a colorless liquid; n_D^{25} = 1.5850. Anal. Calc. for $C_9H_{12}NClS$: C, 53.59; H, 5.95. Found: C, 52.83, 53.01; H, 5.83, 6.02. The residue from the distillation on treatment with hydrochloric acid and crystallization from methanol yielded 3 g of bis(*β-p*-chlorobenzylmercaptoethyl)amine hydrochloride melting at 140–141°. Anal. Calc. for $C_{18}H_{21}NCl_2S_2$: C, 51.07; H, 5.20. Found: C, 51.22, 51.32; H, 5.26, 5.36.

(*b*) *o-Chlorobenzyl 2-aminoethyl sulphide* was prepared from *o*-chlorobenzyl 2-chloroethyl sulphide in 76% yield. The almost colorless liquid boiled at 160–165° (13 mm); n_D^{24} = 1.5862. Anal. Calc. for $C_9H_{12}NClS$: C, 53.59; H, 5.95. Found: C, 53.86, 53.38; H, 5.56, 5.93.

(*c*) *β-p-Chlorobenzylmercaptoethyl 2-aminoethyl ether* was prepared from *β-p*-chlorobenzylmercaptoethyl 2-chloroethyl ether in 45% yield. It distilled as a colorless liquid boiling at 135–137° (0.5 mm); n_D^{22} = 1.5640. Anal. Calc. for $C_{11}H_{16}NOClS$: C, 53.77; H, 6.42. Found: C, 53.68, 52.97; H, 6.25, 6.21.

(*d*) *p-Chlorobenzyl 5-aminopentyl sulphide* (VII, $n = 5$, R = H) was prepared in 25% yield from crude *p*-chlorobenzyl 5-chloropentyl sulphide. It distilled at 145–150° (0.5 mm); n_D^{25} = 1.5580. Anal. Calc. for $C_{12}H_{18}NClS$: C, 59.14; H, 7.39. Found: C, 58.94, 59.41; H, 7.10, 7.14.

(*e*) *p-Chlorobenzyl 3-amino-2-hydroxypropyl sulphide* was prepared from *p*-chlorobenzyl 3-chloro-2-hydroxypropyl sulphide (9) in 68% yield. It distilled at 170–175° (0.5 mm) and crystallized from ether containing a little methanol as white prisms which melted at 85–86°. Anal. Calc. for $C_{10}H_{14}NOClS$: C, 51.84; H, 6.04. Found: C, 51.96; H, 5.80. The residue from the distillation crystallized from methanol to yield bis(1-*p*-chlorobenzylmercapto-2-hydroxypropyl)amine melting at 97–100°. Anal. Calc. for $C_{20}H_{25}NO_2Cl_2S_2$: C, 53.81; H, 5.60. Found: C, 54.25, 53.85; H, 5.47, 5.31.

(*f*) *p-Chlorobenzyl 3-aminopropyl sulphide* (VII, $n = 3$, R = H) was prepared from *p*-chlorobenzyl 3-chloropropyl sulphide in 67% yield. It distilled as a colorless liquid with b.p. = 112–115° (0.5 mm); $n_D^{22} = 1.5754$. Anal. Calc. for $C_{10}H_{14}NClS$: C, 55.68; H, 6.49. Found: C, 54.91, 55.13; H, 6.47, 5.99.

(*g*) *n-Amyl 4-aminobutyl sulphide* was prepared from *n*-amyl 4-chlorobutyl sulphide in 42% yield. It distilled as a colorless liquid with b.p. = 112° (11 mm); $n_D^{23} = 1.4790$. Anal. Calc. for $C_9H_{21}NS$: C, 61.71; H, 12.00. Found: C, 60.99, 61.17; H, 11.91, 12.17.

(*h*) *n-Dodecyl 2-aminoethyl sulphide* was prepared from *n*-dodecyl 2-chloroethyl sulphide (18) in 50% yield. It distilled as a yellow liquid with b.p. = 120–123° (0.5 mm); $n_D^{23} = 1.4755$. Anal. Calc. for $C_{14}H_{31}NS$: C, 68.57; H, 12.65. Found: C, 68.56, 68.76; H, 12.21, 12.62.

(*i*) *β-p-t-Butylphenoxyethyl 2-aminoethyl sulphide* was prepared from *β-p-t*-butylphenoxyethyl 2-chloroethyl sulphide in 73% yield. It distilled as an almost colorless liquid with b.p. = 138–140° (0.5 mm); $n_D^{24} = 1.5400$. Anal. Calc. for $C_{14}H_{23}NOS$: C, 66.40; H, 9.09. Found: C, 66.44; H, 9.16.

REFERENCES

1. KULKA, M. Can. J. Chem. **36**, 750 (1958).
2. KULKA, M. Can. J. Chem. **34**, 1093 (1956).
3. BELL, E. V., BENNETT, G. M., and HOCK, A. L. J. Chem. Soc. 1803 (1927).
4. FUSON, R. C. and ZIEGLER, J. B. J. Org. Chem. **11**, 510 (1946).
5. MEADOW, J. R. and REID, E. E. J. Am. Chem. Soc. **56**, 2177 (1934).
6. KULKA, M. Can. J. Chem. **33**, 1442 (1955).
7. SCHERER, O. and FINK, K. German Pat. No. 845,511 (1952); Chem. Abstr. **47**, 5442 (1953).
8. FAITH, H. E. J. Am. Chem. Soc. **72**, 837 (1950).
9. KULKA, M. and VAN STRYK, F. Can. J. Chem. **35**, 519 (1957).
10. NAYLOR, R. F. J. Chem. Soc. 1106 (1947).
11. YUREV, Yu. K., PERVOVA, E. YA., and SAZONOVA, V. A. J. Gen. Chem. (U.S.S.R.) **9**, 590 (1939); Chem. Abstr. **33**, 7779 (1939).
12. BIRCH, S. F. and FIDLER, F. A. Brit. Pat. No. 654,464 (1951); Chem. Abstr. **46**, 3573 (1952).
13. BAKER, J. W. J. Chem. Soc. 1448 (1936).
14. FUSON, R. C., LIPSCOMB, R. D., MCKUSICK, B. C., and REED, L. J. J. Org. Chem. **11**, 513 (1946).
15. CLARKE, H. T. J. Chem. Soc. **101**, 1806 (1912).
16. JOHNSON, D. A. J. Chem. Soc. 1530 (1933).
17. PUMMERER, R. and SCHÖNAMSGRUBER, M. Ber. B, **72**, 1834 (1939).
18. FINKE, J. K. U.S. Pat. No. 2,598,640 (1952); Chem. Abstr. **47**, 2199 (1953).

THE STUDY OF HYDROGEN BONDING AND RELATED PHENOMENA BY ULTRAVIOLET LIGHT ABSORPTION

PART II. THE EFFECT OF SOLVENT–SOLUTE INTERACTIONS ON THE INTERMOLECULAR HYDROGEN BOND IN BENZOIC ACIDS[1]

W. F. Forbes and A. R. Knight

ABSTRACT

The concentration dependence of some electronic absorption bands, which has previously been ascribed to intermolecular hydrogen bonding, is reinvestigated. The concentration dependences are compared for a number of substituted benzoic acids in inert solvents, and in solvent mixtures containing various amounts of ether. The results are discussed in terms of current theories of hydrogen bonding.

INTRODUCTION

In Part I (1) of this series it was found convenient to classify environmental influences affecting ultraviolet absorption spectra as follows: (i) intermolecular hydrogen bonding acting between solute molecules only; (ii) intermolecular hydrogen bonding acting between solute and solvent molecules; and (iii) solvent–solute interactions which do not involve hydrogen bonding.

The first of these effects was shown in Part I to be qualitatively susceptible to spectral analysis, and the concentration dependence of the electronic spectra of benzoic acids in cyclohexane media was ascribed to intermolecular hydrogen bonding. The next aim was to obtain quantitative relations between absorption spectra and solution concentrations for these and other substituted benzoic acids. It was then found that a number of substituted benzoic acids were not sufficiently soluble in cyclohexane to permit the determination of the concentration dependence of their spectra, and ether had to be added in order to obtain solution. The characteristic concentration dependence was still obtained under these conditions, but the question arose whether addition of ether affects the dimeric hydrogen bond, or whether addition of small amounts of ether does not unduly disturb the spectral effect associated with the formation of the dimeric hydrogen bond. In order to decide, the spectra of a number of cyclohexane-soluble benzoic acids were determined in cyclohexane and in solvent mixtures containing various proportions of cyclohexane and ether.

EXPERIMENTAL

The ultraviolet absorption spectra were determined as previously described in this series (1). For each compound the concentration dependence was determined at least in duplicate. A considerable extension of the concentration range was achieved by using progressively more concentrated solutions in the solvent cell instead of pure solvents. By using solutions of biphenyl in cyclohexane, which do not show any appreciable concentration dependence, it was shown that this modification does not introduce any additional errors.* By extremely careful manipulation, ϵ_{max} values could be measured with a precision estimated to be $\pm 2\%$ or better, and the day-to-day reproducibility was also well within this margin. Results are listed in Figs. 2, 3, 4, and 5 where the vertical brackets indicate the $\pm 2\%$ reproducibility.

[1]*Manuscript received September 15, 1958.*
Contribution from the Memorial University of Newfoundland, St. John's, Newfoundland.
**We are indebted to Dr. O. H. Wheeler for suggesting this modification to us.*

Solvent mixtures were prepared by mixing together the corresponding volume percentages. The cyclohexane used was Fisher Certified Reagent, spectroanalyzed, and the ethyl ether used was Eastman white label, spectrograde. No evidence was found to indicate the presence of traces of acids or base in the solvents. The benzoic acids were purified by standard methods and carefully dried. Elemental analyses showed the absence of any appreciable amounts of water of crystallization in the benzoic acids. For example, *p*-toluic acid analyzed for C, 70.7% (calc. C, 70.6%), whereas $C_8H_8O_2.H_2O$ requires C, 62.3%.

THE EFFECT OF ADDITION OF ETHER ON THE O–H---O BOND IN BENZOIC ACID DIMERS

The absorption spectrum of benzoic acid in cyclohexane solution at different concentrations is shown in Fig. 1.

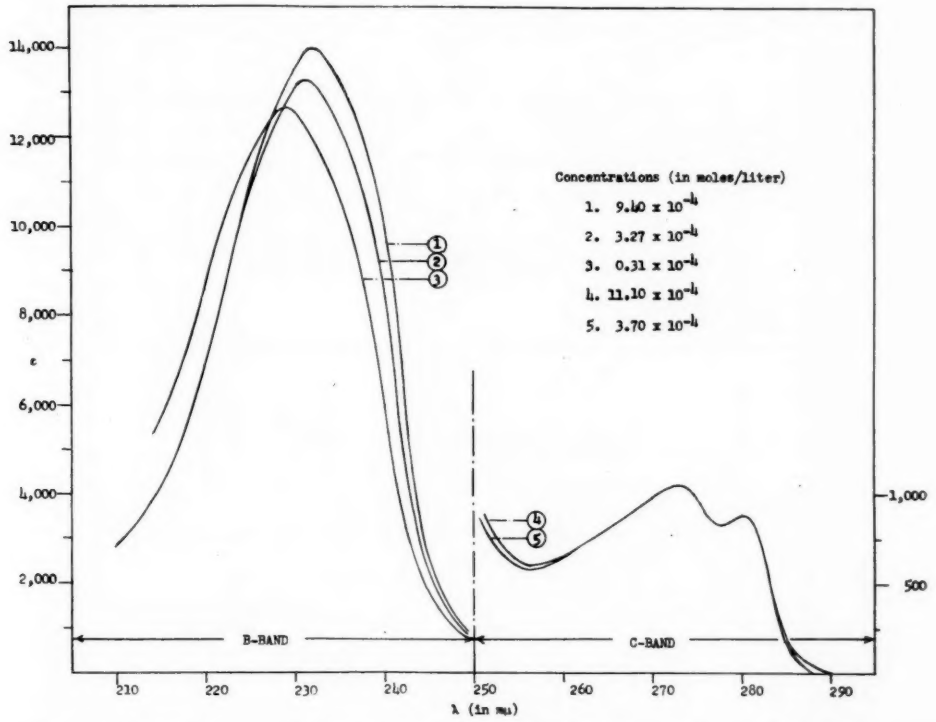

FIG. 1. The effect of concentration on the ultraviolet absorption spectrum of benzoic acid in cyclohexane solution. The description of the absorption bands as *B*- and *C*-bands follows the nomenclature adopted in Part I (1, cf. also ref. 2).

The following observations lead us to ascribe this concentration dependence to intermolecular hydrogen bonding between solute molecules, that is, to dimerization as shown in I:

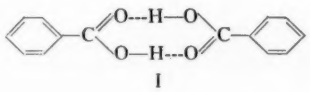

I

(i) A similar concentration dependence is not observed for a number of other molecules within the investigated concentration range (1).

(ii) The concentration dependence practically disappears for methyl benzoate (1, 3). Hence, the hydroxyl group is necessary.

(iii) The concentration dependence for benzoic acid relates with the supposed dimerization of benzoic acids at concentrations similar to those of the present investigation (cf. refs. 4, 5).

(iv) Addition of ether decreases the concentration dependence (see Figs. 2, 3, 4, and 5).

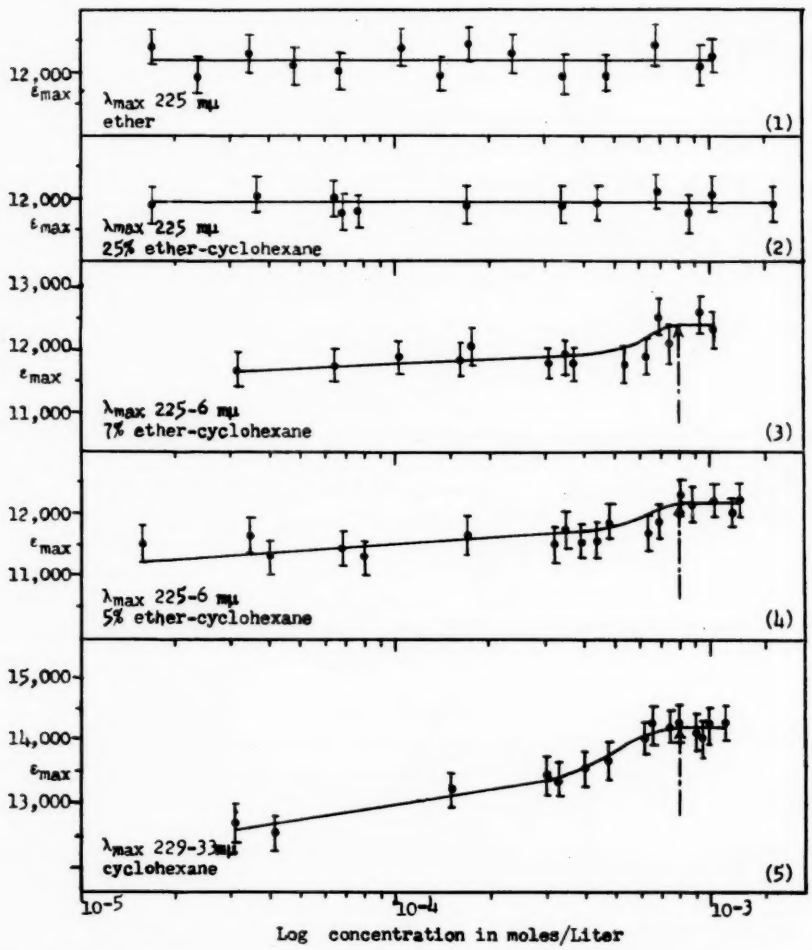

FIG. 2. The variation of ϵ_{max} on changing the concentration of acid for benzoic acid in (1) ether solution, (2) cyclohexane solution containing 25% ether, (3) cyclohexane solution containing 7% ether, (4) cyclohexane solution containing 5% ether, and (5) cyclohexane solution. In this and subsequent figures the lower λ_{max} value shown indicates the maximal wavelength at the smallest concentration, and the higher λ_{max} value indicates the maximal wavelength at the largest concentration. In this way, for example in Fig. 2 for benzoic acid in cyclohexane solution, λ_{max} 229 mμ represents the maximal wavelength for the most dilute solution.

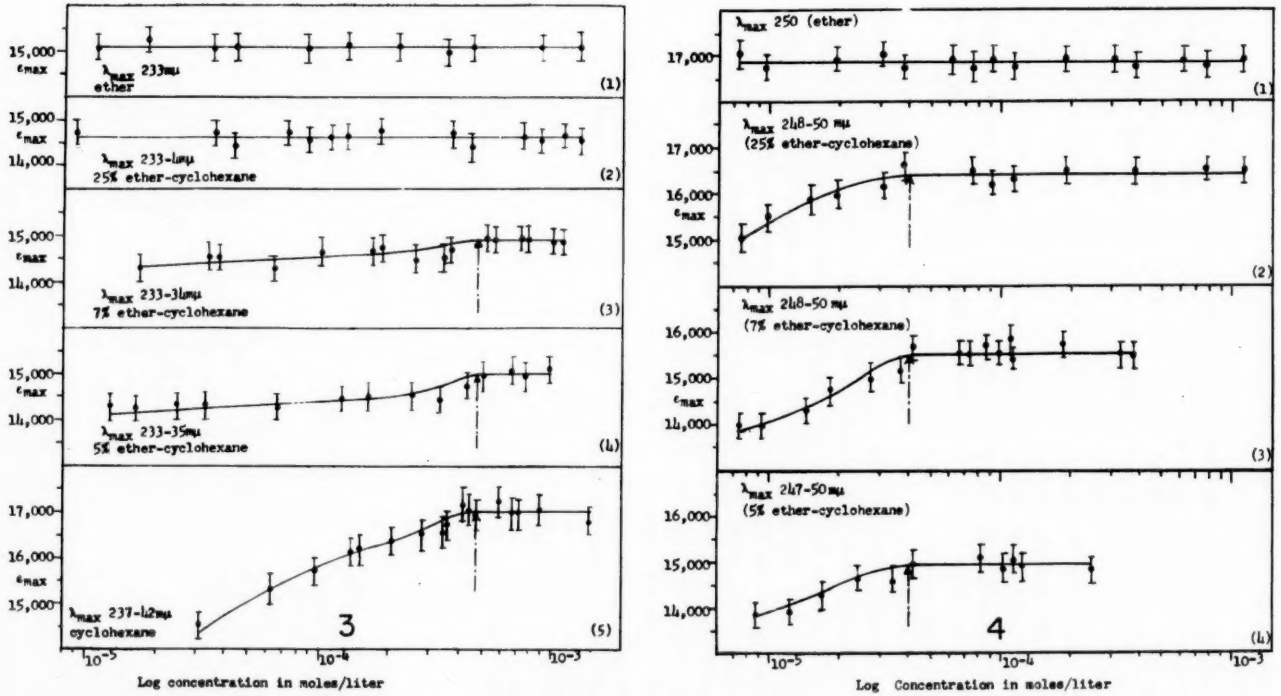

FIG. 3. The variation of ϵ_{max} on changing the concentration of acid for *p*-toluic acid in (1) ether solution, (2) cyclohexane solution containing 25% ether, (3) cyclohexane solution containing 7% ether, (4) cyclohexane solution containing 5% ether, and (5) cyclohexane solution.

FIG. 4. The variation of ϵ_{max} on changing the concentration of acid for *p*-hydroxybenzoic acid in (1) ether solution, (2) cyclohexane solution containing 25% ether, (3) cyclohexane solution containing 7% ether, and (4) cyclohexane solution containing 5% ether.

This indicates a competitive intermolecular hydrogen bonding, and hence indirectly suggests solute–solute hydrogen bonding as an explanation of the observed concentration dependence.

(v) Intramolecular hydrogen bonding in salicylic acid apparently reduces the strength of the dimeric hydrogen bond (cf. Figs. 2 and 5, and subsequent discussion). Since various forms of hydrogen bonding would be expected to compete with each other, this again indicates that association is responsible for the observed concentration dependence (cf. ref. 6).

Figure 1 also shows that the shape of both *B*- and *C*-bands remains approximately similar on changing the solute concentration; similar curves are also obtained for the substituted benzoic acids on changing the concentration. Consequently, maximal molecular extinction coefficients (ϵ_{max}) are used as a first approximation to measure the actual absorption intensities. Figure 2 shows the observed changes in ϵ_{max} with solute concentration for benzoic acid in cyclohexane solution and in various cyclohexane–ether solvent mixtures.

Figure 2 shows that it is possible to determine the concentration above which the values of ϵ_{max} become approximately independent of concentration changes. These values, as shown in Figs. 2, 3, 4, and 5 by vertical arrows, are assumed to represent the concentrations below which the particular benzoic acids exist appreciably in the monomeric form. Figure 2 also shows that in ether solution no concentration dependence is observed. On the other hand, in cyclohexane solution containing 5% of ether, a concentration dependence is observed, and generally, in solutions containing intermediate percentages of ether, intermediate concentration dependences are observed.

It also follows from the argument set out in the previous paragraph, that the *lower* the concentration at which a particular benzoic acid begins to exist appreciably in the monomeric form, the *stronger* will be the dimeric hydrogen bond. Figures 3 and 4 show

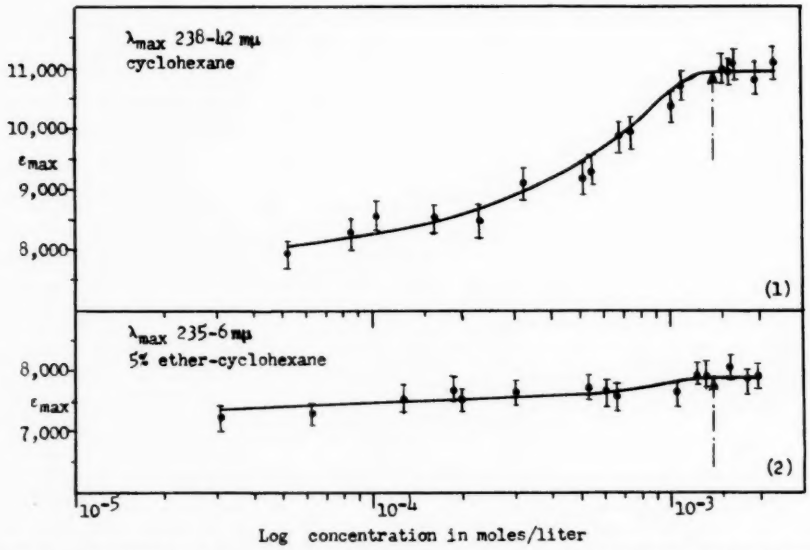

FIG. 5. The variation of ϵ_{max} on changing the concentration of acid for salicyclic acid in (1) cyclohexane, (2) cyclohexane solution containing 5% ether.

that a *p*-methyl- or a *p*-hydroxyl-group in benzoic acid apparently has this effect of strengthening the dimeric hydrogen bond, and the *p*-hydroxyl group appears to be more effective than the *p*-methyl group. Further, for *p*-hydroxybenzoic acid the concentration dependence, ascribed to intermolecular hydrogen bonding, is readily discernible in 25% ether (see Fig. 4), whereas for benzoic and *p*-toluic acid no concentration dependence could be observed under those conditions (see Figs. 2 and 3).

The effect of solute concentration on the maximal extinction coefficient of salicylic acid is shown in Fig. 5. Figure 5 indicates that the intramolecular hydrogen bond in salicylic acid decreases the strength of the dimeric hydrogen bond in this acid, compared with benzoic acid or *p*-hydroxybenzoic acid. On addition of 5% of ether to the solution of salicylic acid in cyclohexane the concentration dependence is only recognized with difficulty, whereas under similar conditions the concentration dependence in benzoic acid may readily be discerned (see Figs. 2 and 5).

DISCUSSION

Three conclusions may be reached from the data. First, the vertical arrows in Figs. 2, 3, 4, and 5, indicating the appearance of monomeric forms, occur at approximately the same concentration, irrespective of whether a small amount of ether has been added to the solvent or not. Hence in comparing the relative strengths of the dimeric hydrogen bond for substituted benzoic acids by this method, *the concentration dependence may be determined either in cyclohexane or in cyclohexane containing small amounts of ether.* This allows the extension of the comparison to benzoic acids which are only slightly soluble in cyclohexane; applications of this extension will be reported in Part III of this series.

Secondly, as expected (cf. ref. 4), for the four benzoic acids studied, *the dimeric hydrogen bond is stronger than any competing intermolecular hydrogen bonding occurring between benzoic acid and ether molecules.* This follows because if hydrogen-bonded forms of type II were to compete with dimeric forms of type I and if in addition the intermolecular

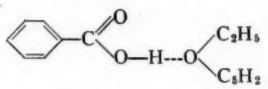

II

hydrogen bond in II were stronger than the bond in I, structures of type II would be formed preferentially. It would then be inconceivable that the very small amounts of benzoic acid present in cyclohexane solution, containing relatively large amounts of ether, would have the opportunity to dimerize to any appreciable extent. However, dimerization occurs, and hence the initial conclusion follows.

Notwithstanding the conclusion deduced in the previous paragraph, the spectra of the three benzoic acids in 100% ether are believed to correspond to the spectra of monomeric forms. We arrive at this conclusion thus: the absence of concentration dependence in 100% ether suggests that there is present predominantly only one molecular species of acid. At the same time, there is no evidence that, for example, in benzoic acid dimerization predominates below an acid concentration of *ca.* 8×10^{-4} moles/l. (see Fig. 2). Hence the absorption in the concentration region below 8×10^{-4} moles/l. can hardly correspond to dimer absorption, and consequently, since only one acid species is believed to be present, this is assumed to be a monomeric species. A satisfactory way to account for these two, apparently contradictory, observations—that is, that the dimeric hydrogen

bond is stronger than the ether – benzoic acid linkage while at the same time the observed spectra are frequently ascribed to ether – benzoic acid hydrogen-bonded complexes—is to postulate that *neither the dimeric hydrogen bond between benzoic acid molecules nor the intermolecular hydrogen bond between acid and ether molecules represents a stable hydrogen-bonded complex under the conditions of the experiment.* That is, it is assumed that both intermolecular bonds are continuously formed, broken, and re-formed; and the characteristic spectral effect, ascribed to intermolecular hydrogen bonding, will only be observed if bond formation occurs sufficiently often or if the bond formed is sufficiently strong. According to this view benzoic acid molecules, in solution containing large amounts of ether, are sufficiently surrounded by ether molecules so that the spectral effect, ascribed to dimerization, is no longer observed. According to this view also, a stronger dimeric hydrogen bond, as has been postulated in *p*-hydroxybenzoic acid compared with benzoic acid, would be anticipated to require a greater ether concentration to obscure the concentration dependence ascribed to dimerization; whereas a weaker dimeric hydrogen bond, as has been postulated in salicylic acid, would be anticipated to require a smaller ether concentration to achieve the same effect. That these predictions are borne out is indicated from Figs. 2, 4, and 5. Finally, the hypothesis receives indirect support from the work of Coggeshall and Lang (7), who showed the absence of spectral changes for solutions of phenol or aniline at different temperatures, although the temperature change was quite adequate to destroy any hydrogen-bonded complexes. They conclude that for these compounds spectral differences between solutions in polar and non-polar solvents do not depend on stable hydrogen-bonded complexes.

ACKNOWLEDGMENTS

The authors are pleased to acknowledge the assistance of Miss V. M. Walsh and Mr. J. F. Templeton in some of the preliminary work, and they are indebted to Mr. J. C. Dearden for a number of valuable discussions.

The major part of this work was carried out under a contract between the Fisheries Research Board of Canada and the Memorial University of Newfoundland. Preliminary studies were supported from grants of the National Research Council of Canada and the Research Corporation of New York.

REFERENCES

1. Forbes, W. F. and Templeton, J. F. Can. J. Chem. **36**, 180 (1958).
2. Forbes, W. F., Mueller, W. A., Ralph, A. S., and Templeton, J. F. Can. J. Chem. **35**, 1049 (1957).
3. Ungnade, H. E. and Lamb, R. W. J. Am. Chem. Soc. **74**, 3789 (1952).
4. Jones, R. N. and Sandorfy, C. *In* Chemical applications of spectroscopy. *Edited by* W. West. Interscience Publishers, Inc., New York. 1956. p. 426.
5. Banewicz, J. J., Reed, C. W., and Levitch, M. E. J. Am. Chem. Soc. **79**, 2693 (1957).
6. Simova, P. D. and Skorchev, B. Izvest. Bulgar. Akad. Nauk., Otdel. Fiz.-Mat. i Tekh. Nauki Ser. Fiz. **4**, 47 (1954); Chem. Abstr. **50**, 6923 (1956).
7. Coggeshall, N. D. and Lang, E. M. J. Am. Chem. Soc. **70**, 3283 (1948).

THE QUENCHING OF POTASSIUM RESONANCE RADIATION BY HYDROCARBONS[1]

E. A. CHERNIAK[2] AND W. M. SMITH

ABSTRACT

The quenching of the resonance radiation of potassium by some unsaturated and saturated hydrocarbons has been examined at 67° C. The behavior was found to be almost identical with that previously observed with sodium, the saturated hydrocarbons quenching to a negligible extent, the unsaturated hydrocarbons exhibiting cross sections with potassium not significantly different from those exhibited towards sodium.

INTRODUCTION

An examination of the quenching of excited potassium ($4^2P \rightarrow 4^2S$) by hydrogen and deuterium was described in an earlier publication (1). We report here on an extension of the measurements to quenching by some saturated and unsaturated hydrocarbons, work undertaken with a view to obtaining information about the comparative behavior of the various excited alkali metals.

METHOD

The method used to measure the cross sections for the quenching process was the same as that described before (1) except that pyrex resonance vessels were used during all measurements. The features of the method are as follows. Potassium atoms in the 4^2P state are produced at constant rate by irradiation of potassium vapor in a resonance vessel by a filtered beam from a G.E. K-1 lamp. The intensity of the "resonance radiation" (due to return of the excited atoms to the 4^2S state) is estimated in the presence and in the absence of quenching gas. The ratio of these intensities is known as the quenching ratio Q and its values for various pressures of quenching gas are the primary data from which a cross section σ^2 may be estimated (1). Also required is the mean life of a 4^2P potassium atom, and we have taken Stephenson's value 2.71×10^{-8} seconds (2). All measurements were made at $66.7 \pm 0.4°$ C.

MATERIALS

Potassium was purified and introduced into the quenching vessels in the manner described previously (1).

Methane was prepared by the reduction of ethanolic methyl iodide by a zinc–copper couple (3). The gas was passed through fuming sulphuric acid, and potassium hydroxide solution, and was collected for intermediate storage over water in an aspirator bottle. This gas was then passed through a dry-ice trap, fractionally distilled with the aid of liquid air, and dried over potassium before final storage.

Propane was Phillips Research Grade hydrocarbon.

Ethene was from two sources. One sample was Matheson C.P. grade. The other was made by dehydrating ethanol with freshly prepared pyrophosphoric acid (4). The impure ethene was then dried and fractionally distilled as was the methane.

The butenes were Phillips Research Grade hydrocarbons.

[1]*Manuscript received September 26, 1958.*
Contribution from the Department of Chemistry, Queen's University, Kingston, Ontario.
[2]*Holder of a National Research Council Bursary, 1955–56. Present address: Department of Chemistry, University of Leeds, England.*

RESULTS

It was found that the unsaturated hydrocarbons quench strongly, and that the saturated hydrocarbons quench to an almost negligible extent. Data for the unsaturated hydrocarbons are summarized in Figs. 1 and 2 as plots of $1/Q$ against pressure. These data are in reasonable accord with the Stern-Volmer relation (a linear relation between $1/Q$ and pressure). On the other hand, the saturated hydrocarbons methane and propane led to a significant increase rather than a decrease in the intensity of the resonance radiation. At a pressure of 5 mm of mercury the quenching ratios were 1.03 and 1.10 respectively. Apparently these gases were leading to an increase in the rate of production

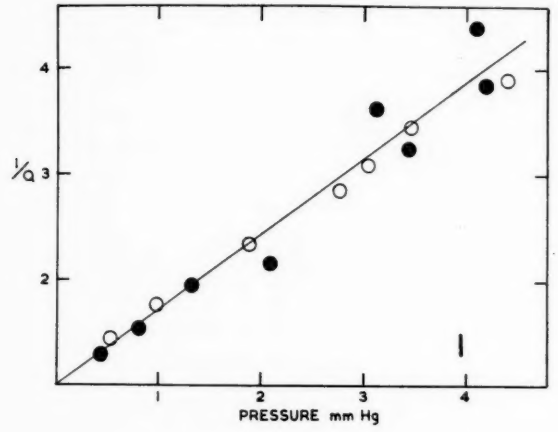

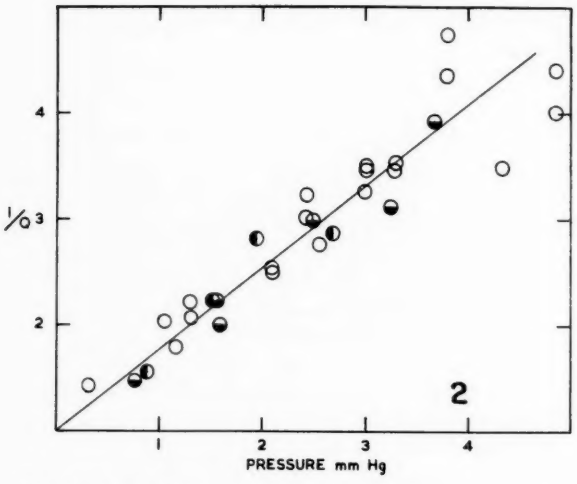

FIG. 1. Plot of $1/Q$ against pressure of ethene.
● Ethene from ethanol. ○ Ethene (Matheson C.P.).
FIG. 2. Plot of $1/Q$ against pressure for the butenes.
○ Butene-1. ◒ *trans*-Butene-2. ◐ *cis*-Butene-2.

of excited potassium atoms, probably through broadening of the absorption line of the potassium vapor. It is not possible to estimate quenching cross sections for methane and propane from these data, but they must be very small.

Cross sections (σ^2) for quenching by the unsaturated hydrocarbons estimated from the data summarized in Figs. 1 and 2 are given in Table I, along with previously reported values for the quenching of excited potassium by hydrogen (1), and the quenching of excited sodium (5) by all those substances whose behavior with potassium are recorded.

TABLE I

Quenching cross sections ($cm^2 \times 10^{16}$)

Gas	With potassium	With sodium
Ethene	44	44[a]
Butene-1	57	58[a]
cis-Butene-2	57	58[a]
trans-Butene-2	57	
Hydrogen	1.56[b]	7.4[a]

[a]From ref. 5.
[b]From ref. 1.

The cross sections were estimated from values of the slopes of the plots of $1/Q$ against pressure, the effects of added gas on the rate of production of excited atoms being ignored. We do not have data which would enable corrections to be made for this effect, but the fact that methane and propane do apparently increase the absorption suggests that the true values of $1/Q$ and σ^2 for the unsaturated hydrocarbons may be a little greater than recorded in the table. The data for the different butenes have been grouped together in determining a single slope and a single cross section.

DISCUSSION

The hydrocarbons which were investigated exhibit quenching characteristics towards excited potassium (4^2P) which are almost identical with those exhibited by the same gases towards sodium (3^2P) in spite of the difference in the excitation energies of the two metals. On the other hand hydrogen was previously found to exhibit significantly different behavior with the two metals (1).

The data for the saturated and unsaturated hydrocarbons indicate that it is the unsaturated center which is decisive in controlling quenching efficiency. As has been pointed out by Laidler (6) there is no excited singlet level in the alkenes low enough to be excited by either alkali atoms in the ^2P state. It follows that the electronic state of the hydrocarbons does not change in a quenching encounter, and that the electronic excitation energy of potassium is transferred directly into vibrational and rotational.

Theories developed by Laidler (7) and Magee and Ri (8) for processes involving degradation of electronic excitation energy of the excited alkali metals to vibrational and translational suggest that quenching occurs with high cross section only when the excited atom, and quenching molecule, are held in association for periods much in excess of the time of a normal collision, the magnitude of the quenching cross section depending on the probability of change of electronic state during the lifetime of the complex as well as on the cross section for complex formation. No attempt was made to estimate the probability of change of electronic state, and it was assumed that it approached unity unless the rotational energy was unduly high. Magee and Ri's treatment of quenching

of the excited alkali metals by hydrogen led to such a picture, and also to the prediction that potassium would be quenched by hydrogen less effectively than sodium, essentially because the smaller stability of the complex involving potassium implied a smaller cross section for the association reaction yielding the complex.

The large values of the quenching cross sections for processes involving the alkenes suggest that the probability of change in electronic state approaches unity, and along with the nearly identical values exhibited by a given alkene with both alkali metals, could be taken to imply that the interactions leading to complex formation are very similar. However, cross sections for complex formation considerably in excess of the values implied by atomic radii appear possible, particularly where there are strong ionic contributions to the interaction and it may be that the cross sections for complex formation are somewhat greater than the admittedly large values noted for quenching and that the probabilities of electronic transition are appreciably less than unity. If this were so, the increase in quenching cross sections with increasing molecular weight of the alkene might be due in part to an associated increase in the probability of electronic transition during the lifetime of the complex. It would be enlightening in this connection to have independent means, experimental or theoretical, for estimating the cross sections for complex formation between the alkenes and excited alkali metals in the gas phase.

ACKNOWLEDGMENT

This work was supported by a grant from the Committee on Scientific Research of Queen's University.

REFERENCES

1. SMITH, W. M., STEWART, J. A., and TAYLOR, G. W. Can. J. Chem. **32**, 961 (1954).
2. STEPHENSON, G. Nature, **167**, 112 (1951).
3. GLADSTONE, J. H. and TRIBE, A. J. Chem. Soc. **45**, 154 (1884).
4. MICHELS, A., DE GRUYTER, J., and NIELSON, F. Physica, **III**, 346 (1936).
5. NORRISH, R. G. W. and SMITH, W. M. Proc. Roy. Soc. (London), A, **176**, 295 (1940).
6. LAIDLER, K. J. The chemical kinetics of excited states. Oxford University Press. 1955. p. 104.
7. LAIDLER, K. J. J. Chem. Phys. **10**, 34 (1942).
8. MAGEE, J. L. and RI, T. J. Chem. Phys. **9**, 638 (1941).

BROMINATION OF STEROID 20-KETALS[1]

ARTHUR A. AMOS AND P. ZIEGLER

ABSTRACT

Bromination of 3α,12α-diacetoxypregnan-20-one ethylene ketal provided in good yield the corresponding 21-monobromo compound. This product, on acid hydrolysis and subsequent acetolysis, gave the known 3α,12α,21-triacetoxypregnan-20-one. Acid hydrolysis of the bromoketal, followed by Faworsky rearrangement, led to 3α,12α-diacetoxy-17α-methyletiocholanic acid methyl ester.

In order to prepare 11-keto steroids from the readily available 3α,12α-diacetoxypregnan-20-one (I*b*), it had been planned to apply the elegant Glaxo procedure (1, 2) to 3α-acetoxy-12,20-diketopregnane 20-ethylene ketal (VIII*b*), obtained from I. However, when VIII*b* was treated with varying amounts of bromine in methylene chloride at low temperature and in the presence of calcium oxide, the reaction products consisted of mixtures of brominated 20-keto steroids. At no time could VIII*b* be brominated exclusively at C-11; it was apparent that, during the reactions, the ketal group was removed and that bromine also had been substituted at C-17 and/or C-21. It had been observed before (3) that 3β-acetoxy-12,20-diketoallopregnane 12-ethylene ketal could be brominated at C-17, but only with simultaneous hydrolysis of the 12-ketal group. As will be seen later on, 3α,12α-diacetoxypregnan-20-one ethylene ketal (II*b*) could be brominated, under the same conditions as described above, to the corresponding 21-bromoketal (III); this reaction had no effect on the ketal group which remained intact. It is therefore assumed that α-monobromination of the ketal II*b* proceeded by a free radical mechanism during which the substitution of bromine at C-21 and the formation of hydrogen bromide took place without preliminary or concurrent formation of hydrogen ions. The hydrogen bromide did not dissociate rapidly in methylene chloride and the protons that did form were immediately taken up by the calcium oxide. On the other hand, α-brominations of ketones proceed via the enol form of the ketone by an ionic mechanism, during which protons as such are believed to be transferred. In the bromination of VIII*b*, enolization of the 12-keto group and subsequent bromination at C-11 probably produced hydrogen ions in proximity of the 20-ketal group, which then rapidly decomposed. The liberated 20-keto steroid then reacted with more bromine at C-17 and C-21.

Very little information is available on the bromination of ketals. Sapogenins react with bromine in the spiroketal side chain at C-23 giving compounds in which the bromine atom is in the α-position to the potential carbonyl group (4). Similarly, aliphatic acetals react with bromine (5, 6, 7) or N-bromosuccinimide (8) to yield the corresponding α-bromoacetals. An indication that steroidal 3-ketals react with bromine at C-4 has been reported (9). When 3α,12α-diacetoxypregnan-20-one ethylene ketal (II*b*) was brominated, only 1 mole of bromine was taken up, and there was obtained 70–80% of a crystalline monobromo derivative. This compound did not exhibit a ketone band in the ultraviolet region, and it was therefore assumed that the 20-ketal structure had remained unchanged during bromination; elemental analyses indicated structure III or the corresponding 17-bromo isomer. The latter formulation was at first preferred mainly because the reaction of 3α,12α-diacetoxypregnan-20-one (I*b*) with 1 mole of bromine has been reported (10) to provide predominantly the 17-bromo derivative of I*b*. This is in agreement with other

[1]*Manuscript received September 8, 1958.*
Contribution from the Research and Development Laboratories of Canada Packers Ltd., Toronto, Ontario.

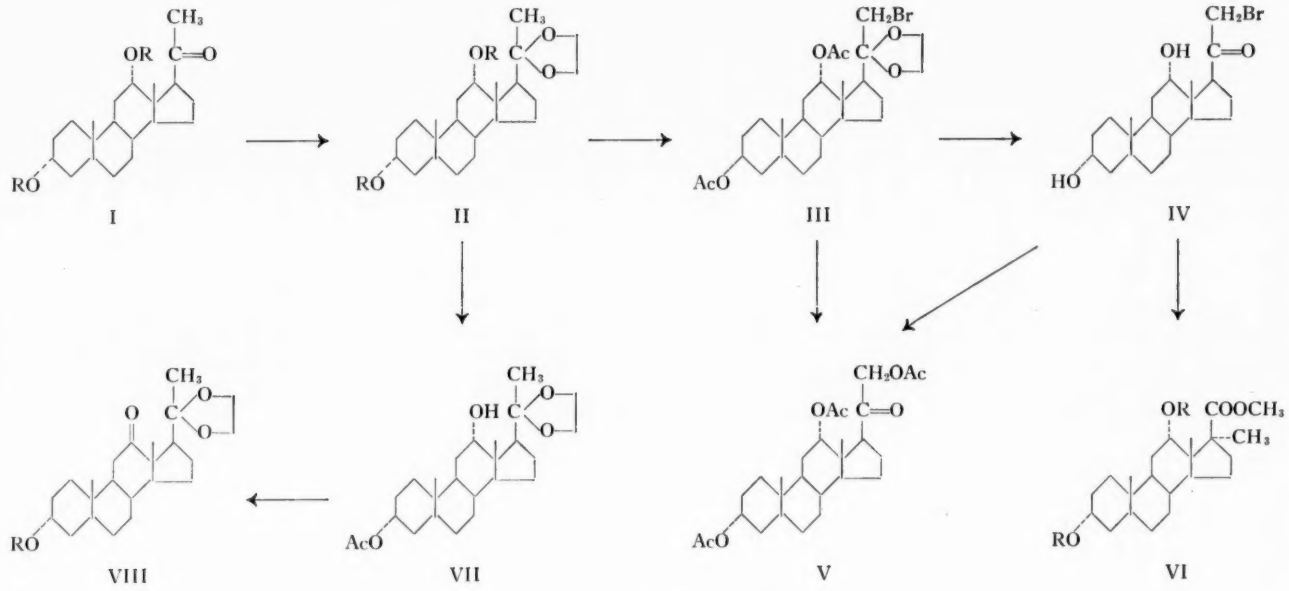
CH3
OR
C=O
RO
I
CH3
OR
O
O
RO
II
CH2Br
OAc
AcO
III
CH2Br
OH
C=O
HO
IV
CH2OAc
OAc
C=O
AcO
V
OR
COOCH3
CH3
RO
VI
CH3
O
O
O
RO
VIII
CH3
OH
O
O
AcO
VII

a, R = H
b, R = Ac

data (11, 12) which indicate that 20-keto steroids with equimolar amounts of bromine provide the related 17-bromo compounds. The bromoketal III was then found to yield, after treatment with 80% acetic acid and subsequent acetolysis, the known (13) 3α,12α,21-triacetoxypregnan-20-one (V); this clearly proved that the bromine atom in III was attached to C-21, and that compounds I*b* and II*b* react in a different manner towards bromine.

The bromoketal III was then converted quantitatively, by vigorous acid hydrolysis, to the bromoketone IV; carbon and hydrogen analyses for this compound did not correspond to the assigned empirical formula, a finding which had been made previously (13) when IV was obtained by an entirely different route. This discrepancy was ascribed to partial decompositon during recrystallization. The identity of IV was verified by its conversion to V by acetolysis and acetylation. As expected, the bromoketone IV underwent a Faworsky rearrangement upon mild alkaline treatment to afford, after acetylation, the known (10, 14) methyl 3α,12α-diacetoxy-17α-methyletiocholanate (VI*b*). This type of rearrangement has been described both in the case of 17- and 21-halogenated 20-keto steroids (15).

Preliminary results show that ketals, closely related to II*b* but which lack the 12α-acetoxy group, cannot be monobrominated at C-21 in good yield. Thus 3α-acetoxypregnan-20-one ethylene ketal with equimolar amounts of bromine yields a dibromoketal of as yet unknown constitution.

EXPERIMENTAL*

3α,12α-Diacetoxypregnan-20-one Ethylene Ketal (II*b*)

Compound I*b* (10 g) and *p*-toluenesulphonic acid (0.25 g), dissolved in a mixture of dry benzene (150 ml) and ethylene glycol (20 ml), were stirred and refluxed for 16 hours. During this time 1.05 ml of water was collected in a Dean-Stark trap. The reaction mixture was then neutralized by addition of sodium bicarbonate (2.2 g), the solvents were evaporated *in vacuo*, and the residue was taken up in water and ether. The ether extract, after being washed with water, dried over sodium sulphate, and evaporated, provided the crude products (10.8 g) which crystallized readily from methanol to yield 8.75 g (80%) of crystals, m.p. 141–142°. One crystallization from ether–hexane and three from methanol gave pure II*b*, m.p. 145–146° and $[\alpha]_D^{25}$ +124.2° (*c*, 0.512, ethanol). Anal. Calc. for $C_{27}H_{42}O_6$: C, 70.09; H, 9.15; O, 20.77. Found: C, 69.79; H, 9.21; O, 21.00.

3α,12α-Dihydroxypregnan-20-one Ethylene Ketal (II*a*)

The diacetoxyketal II*b* (10 g) was saponified by refluxing for 17 hours with potassium hydroxide (10 g), water (5 ml), and ethanol (95 ml). The solution was cooled to 20°, poured into water (600 ml), and the gummy mixture was stirred for ½ hour. The solid was then filtered off, washed with water, and dried to yield 8.05 g (98.5%) of product, m.p. 157–158°. After three recrystallizations from ether, this material had m.p. 157–159° but did not give satisfactory elemental analyses. It was dissolved in benzene, the solvent was distilled off, and the residue was crystallized twice from ether–iso-octane to give m.p. 146.5–148° and $[\alpha]_D^{25}$ +82.8° (*c*, 0.528, ethanol). Anal. Calc. for $C_{23}H_{38}O_4$: C, 72.97; H, 10.12. Found: C, 73.19, 73.10; H, 10.36, 10.28.

3α-Acetoxy-12α-hydroxypregnan-20-one Ethylene Ketal (VII)

Compound II*a* (2 g) was acetylated at 25° with pyridine (1.35 ml) and acetic anhydride (0.81 ml). After 20 hours the solution was diluted with water and ether, the solvent

**Microanalyses were kindly performed by Mr. E. Thommen, Basel, Switzerland.*

extract was washed several times with water, dried, and evaporated. The residue (2.4 g) crystallized from ether–hexane to provide 1.55 g (70%) of product, m.p. 154–156°. Three recrystallizations from methanol gave pure VII, m.p. 163–164° and $[\alpha]_D^{25}$ +72° (*c*, 0.541, ethanol). Anal. Calc. for $C_{25}H_{40}O_5$: C, 71.39; H, 9.59; O, 19.02. Found: C, 71.46; H, 9.74; O, 19.22.

3α-Acetoxy-12,20-diketopregnane 20-Ethylene Ketal (VIII*b*)

Compound VII (3 g) in *t*-butanol (45 ml) and pyridine (1.35 ml) was oxidized with N-bromosuccinimide (2.47 g) at 20° under constant stirring. After 6 hours the orange-red solution was poured into water (200 ml), the mixture was stirred briefly, then refrigerated overnight. The solid was filtered off, washed with dilute sodium sulphite solution and then with water. The dry material (3 g), m.p. 195–200°, was crystallized first from ethyl acetate, then from ether to afford VIII*b*, m.p. 226–228° and $[\alpha]_D^{25}$ +111.8° (*c*, 0.214, ethanol). Anal. Calc. for $C_{25}H_{38}O_5$: C, 71.73; H, 9.15; O, 19.11. Found: C, 71.85, 71.92; H, 9.35, 9.27; O, 19.02.

3α-Hydroxy-12,20-diketopregnane 20-Ethylene Ketal (VIII*a*)

Saponification of VIII*b* by refluxing with methanolic potassium hydroxide and subsequent isolation by precipitation with water, afforded quantitatively crude VIII*a*, m.p. 166–168°. Several recrystallizations from ethyl acetate gave the analytical specimen, m.p. 171–172° and $[\alpha]_D^{25}$ +105.5° (*c*, 0.679, ethanol). Anal. Calc. for $C_{23}H_{36}O_4$: C, 73.36; H, 9.64. Found: C, 73.30, 73.40; H, 9.81, 9.78.

Bromination of 3α-Acetoxy-12,20-diketopregnane 20-Ethylene Ketal (VIII*b*)

The reactions were carried out in methylene chloride at 0° to −10° in the presence of calcium oxide. With stirring, 1–4 molar equivalents of bromine was added within 10–20 minutes, whereupon the mixtures were poured into dilute sodium bicarbonate solution. The organic solvent extracts were then washed with water, dried, and evaporated to a residue.

Using 1, 2.4, 3, or 4 molar equivalents of bromine and resorting to fractional crystallization of the crude reaction products, two compounds could be isolated. The first of these had m.p. 210–213° (decomp.), $[\alpha]_D^{25}$ −19.1° (*c*, 0.404, chloroform), and contained 42.64% C, 4.31% H, and 42.6% Br. On refluxing with 80% acetic acid, the material remained unchanged which indicated that the ketal group was hydrolyzed during bromination. The same product, having m.p. 212–215° (decomp.) and $[\alpha]_D^{25}$ −19.2° (*c*, 0.414, chloroform), was also obtained when 3α-acetoxypregnan-12,20-dione was brominated under similar conditions. The second compound, isolated in only small amounts, had m.p. 200–202° (decomp.) and $[\alpha]_D^{25}$ −31.8° (*c*, 0.432, chloroform). Since monobromination of VIII*b* at C-11 could not be effected, these experiments were discontinued.

3α,12α-Diacetoxy-21-bromopregnan-20-one Ethylene Ketal (III)

To a solution of II*b* (10 g) in methylene chloride (170 ml) there was added calcium oxide (4.35 g), and the mixture was cooled to −10°. With constant stirring, a solution of bromine (4.66 g; 1.34 molar equivalents) in methylene chloride (30 ml) was added dropwise and, after ½ hour, the red mixture was poured into water (150 ml) containing sodium bicarbonate (8 g). The organic solvent extract was washed with sodium thiosulphate solution, then with water, dried over sodium sulphate, and evaporated. Crystallization of the residue (12.6 g) from aqueous methanol provided 8.2 g (74%) of product, m.p. 138–140°. Repeated recrystallization from methanol gave pure III, m.p. 145–147° and $[\alpha]_D^{25}$ +100.7° (*c*, 0.35, ethanol). Anal. Calc. for $C_{27}H_{41}O_6Br$: C, 59.88; H, 7.63; Br, 14.76. Found: C, 59.91, 59.78; H, 7.60, 7.71; Br, 14.80.

3α,12α-Dihydroxy-21-bromopregnan-20-one (IV)

Compound III (6 g) was refluxed for 1¼ hours with methanol (60 ml) and concentrated hydrochloric acid (3 ml). Dilution with water (100 ml) produced a precipitate which was filtered off, washed with water, and dried; the solid (4 g; 94%), m.p. 147–150°, was crystallized once from aqueous methanol and twice from ether to afford a sample for analysis, m.p. 147–150°, $[\alpha]_D^{25}$ +151° (*c*, 0.284, chloroform). Anal. Calc. for $C_{21}H_{33}O_3Br$: C, 61.01; H, 8.05. Found: C, 64.74, 64.43; H, 8.56, 8.88. This compound has been reported (13) to have m.p. 148–150°, $[\alpha]_D^{25}$ +148.5° (*c*, 0.793, chloroform), and giving the following analyses: C, 64.57; H, 8.85; Br, 17.54.

3α,12α,21-Triacetoxypregnan-20-one (V)

(*a*) *From* III.—The bromoketal III (2.5 g) was heated on the steam bath for 2¼ hours with 80% acetic acid (65 ml) in order to hydrolyze the ketal grouping. After addition of water, the products were extracted with ether, the ether extract was washed with dilute sodium bicarbonate and then with water. The residue (2.3 g) from evaporation of solvent was refluxed for 16 hours with potassium acetate (9.2 g), potassium iodide (35 mg), acetic acid (1.4 ml), and acetone (138 ml). After the mixture had been cooled the salts were filtered off, the filtrate was evaporated to a small volume, and the residue was taken up in ether and water. From the ether extract a gum (2.3 g) was obtained, which crystallized from ether–hexane to yield 0.89 g of material, m.p. 143–148°. Four recrystallizations gave pure V, m.p. 151–152° and $[\alpha]_D^{25}$ +151.7° (*c*, 0.23, acetone). Anal. Calc. for $C_{27}H_{40}O_7$: C, 68.04; H, 8.46. Found: C, 68.16, 68.24; H, 8.33, 8.37. This compound was reported (13) to have m.p. 153–153.5° and $[\alpha]_D^{25}$ +159.5° (*c*, 1.03, acetone).

(*b*) *From* IV.—Compound IV (100 mg) was refluxed for 17 hours with freshly fused potassium acetate (200 mg), potassium iodide (5 mg), acetic acid (0.25 ml), and acetone (10 ml). The cooled solution was diluted with water, extracted with ether, and the solvent extract was washed and dried. Acetylation of the residue (90 mg) with pyridine (2.5 ml) and acetic anhydride (5 ml) at 25° for 18 hours, followed by solvent extraction of the products and working up in the usual manner, yielded a gum which crystallized from ether–hexane. There was obtained 81 mg (71.5%) of V, m.p. 148–152°, giving no depression in melting point on admixture with a sample of V obtained in the previous experiment.

3α,12α-Diacetoxy-17α-methyletiocholanic Acid Methyl Ester (VI*b*)

Compound IV (1 g) was dissolved in methanol (75 ml), a solution of sodium hydroxide (0.8 g) in water (25 ml) was added, and the resulting solution was kept at 25° for 20 hours. After neutralization of the alkali with acetic acid (1.2 ml), most of the methanol was evaporated, and the products were taken up in ether and water. The solvent extract, after having been washed with water, dried, and evaporated, provided a residue (0.95 g); this was acetylated at 20° with pyridine (2.5 ml) and acetic anhydride (5 ml) to afford, subsequent to the usual work-up, 1.08 g of material which failed to crystallize. Chromatography on alumina finally yielded 0.15 g of crystals, m.p. 160–162°, eluted from the column with benzene–hexane (2:3 and 3:2). One recrystallization from hexane gave pure VI*b*, m.p. 163–164° and $[\alpha]_D^{25}$ +121.9° (*c*, 0.305, chloroform). This compound has been reported (10, 14) to have m.p. 161–161.5°, 163–165°, and $[\alpha]_D^{25}$ +117.4° (*c*, 0.78, chloroform).

3α,12α-Dihydroxy-17α-methyletiocholanic Acid Methyl Ester (VI*a*)

Saponification of VI*b* (100 mg) with 5% methanolic potassium hydroxide (10 ml) for 4 hours at reflux temperature and precipitation of the product by addition of water

(40 ml) gave crude VI*a* (80 mg), having double m.p. 95–100° and 155–156°. This was crystallized from ether–hexane to yield the pure compound, m.p. 155–157° and $[\alpha]_D^{25}$ +51.1° (*c*, 0.351, chloroform). The literature (10) reports m.p. 152–152.5° and $[\alpha]_D^{22}$ +42.3° (*c*, 0.79, chloroform).

REFERENCES

1. CHAPMAN, J. H., ELKS, J., and WYMAN, L. J. Chem. & Ind. 603 (1955).
2. ROTHMAN, E. S. and WALL, M. E. J. Am. Chem. Soc. **79**, 3228 (1957).
3. CALLOW, R. K. and JAMES, V. H. T. J. Chem. Soc. 4744 (1956).
4. WALL, M. E. and JONES, H. W. J. Am. Chem. Soc. **79**, 3222 (1957).
5. HARTUNG, W. H. and ADKINS, H. J. Am. Chem. Soc. **49**, 2517 (1927).
6. MCELVAIN, S. M. and WALTERS, P. M. J. Am. Chem. Soc. **64**, 1963 (1942).
7. ALEXANDER, E. R. J. Am. Chem. Soc. **70**, 2592 (1948).
8. MARVELL, E. N. and JONCICH, M. J. J. Am. Chem. Soc. **73**, 973 (1951).
9. OLIVETO, E. P., SMITH, H. Q., GEROLD, C., WEBER, L., RAUSSER, R., and HERSHBERG, E. B. J. Am. Chem. Soc. **77**, 2224 (1955).
10. ENGEL, CH. R., JENNINGS, K. F., and JUST, G. J. Am. Chem. Soc. **78**, 6153 (1956).
11. ENGEL, CH. R. J. Am. Chem. Soc. **78**, 4727 (1956).
12. WENDLER, N. L., GRABER, R. P., and HAZEN, G. G. Tetrahedron, **3**, 144 (1958).
13. MEYSTRE, CH. and WETTSTEIN, A. Helv. Chim. Acta, **30**, 1037 (1947).
14. KOECHLIN, B. and REICHSTEIN, T. Helv. Chim. Acta, **27**, 549 (1944).
15. HEUSSER, H., BERIGER, E., and ENGEL, CH. R. Helv. Chim. Acta, **37**, 2166 (1954).

STERIC INHIBITION OF RESONANCE

I. 9-NITROANTHRACENE AND 9,10-DINITROANTHRACENE[1]

JAMES TROTTER[2]

ABSTRACT

Detailed X-ray analyses of the crystal structures of 9-nitroanthracene and 9,10-dinitroanthracene have shown that the nitro groups are tilted out of the planes of the aromatic rings by 84.7° in the nitro derivative and 63.7° in the dinitro. The decreases in resonance interaction resulting from these deviations from coplanarity have been correlated with the characteristic vibration frequencies of the nitro groups.

INTRODUCTION

Examination of some of the physical properties of the nitro and acetyl derivatives of durene and mesitylene suggests that the steric effect of the methyl groups prevents the attainment of a completely coplanar configuration, and reduces the resonance interaction between the aromatic π-electrons and the substituent nitro and acetyl groups. Consideration of Raman and infrared frequencies, dipole moments, ultraviolet spectra, acid-base strengths, and rates of reaction indicates a great amount of inhibition of resonance in this type of molecule (1). Few direct measurements of the deviations from coplanarity have been made however.

Huse and Powell (2) have investigated the crystal structure of picryl iodide (I) by X-ray diffraction methods; their results indicate that the para-nitro group is coplanar with the benzene nucleus and, owing to resonance with ionic structures (II), the para C–N bond length (1.35 Å) is much shorter than the normal single bond distance, but the planes of the ortho-nitro groups are approximately at right angles to the benzene ring, there is no resonance with the aromatic π-electrons, and the ortho C–N bond length (1.45 Å) corresponds closely to the single bond distance. The molecular geometry and dimensions have not been determined very accurately, however, owing to the presence of the heavy iodine atom.

Francel (3) has investigated the infrared spectra of five ortho-substituted nitrobenzenes in the solid state using polarized radiation. The polarization of the absorption band arising from the asymmetric NO_2 stretching vibration in *o*-nitrobromobenzene indicates that the nitro group is rotated well out of the plane of the benzene ring owing to the steric effect of the bromine atom, and is probably almost perpendicular to the ring. The polarization of the bands in the corresponding chloro derivative is assumed to indicate a smaller angle between the benzene ring and the nitro group, which would be expected because of the difference in the van der Waals radii of chlorine and bromine. Again, however, no accurate measure of the deviation from coplanarity has been possible.

The present investigations, which are confined chiefly to nitro derivatives, were undertaken to obtain accurate measurements of the tilts of the planes of the substituent groups out of the aromatic planes, using X-ray diffraction methods, and to correlate these values with the reduction in resonance interaction, the bond lengths in the molecules, the infrared frequencies, dipole moments, and other physical data.

[1]*Manuscript received October 8, 1958.*
Contribution from the Division of Pure Physics, National Research Council, Ottawa, Canada.
Issued as N.R.C. 5002.
[2]*National Research Council Postdoctorate Fellow.*

Such steric effects and resonance inhibition should be observable also in 9- and 9,10-substituted anthracenes, where the environments of the substituent groups are very similar to those in durene and mesitylene derivatives. Contributions to the ground state of the 9-nitroanthracene molecule from structures such as III and IV would be greatest when the nitro group is coplanar with the anthracene nucleus, but this involves distances which are much less than the usual van der Waals separations, between the oxygen atoms and the hydrogen atoms bonded to carbons 1 and 8. It would be expected that the strain due to this 'overcrowding' would be relieved by rotation of the nitro group about the C–N bond. Jones (4, 5) has examined the ultraviolet spectra of certain 9,10-diarylanthracenes, and observes that the introduction of phenyl groups, for example, at positions 9 and 10 causes very little change in the anthracene spectrum, and indeed methyl groups actually produce a greater displacement towards longer wavelengths. He concludes that the phenyl groups are hindered to such an extent that they probably lie more or less perpendicular to the main plane of the anthracene nucleus.

The infrared spectra of 9-nitroanthracene and 9,10-dinitroanthracene have now been measured, and the characteristic nitro group vibration frequencies have been correlated with the angles between the planes of the nitro groups and the anthracene nuclei. These angles have been determined by accurate X-ray analyses of the crystalline materials. Extension of these investigations to durene and mesitylene derivatives will be described in subsequent communications.

EXPERIMENTAL

Preparation and Purification of Materials

Commercial 9-nitroanthracene was purified by chromatography on alumina and crystallization from petroleum ether, giving yellow crystals melting at 146°. From this material 9,10-dinitroanthracene was prepared by nitration with nitric acid in acetic anhydride, and then purified by chromatography and crystallization, giving yellow crystals, melting point 310°. Crystals of each substance grown by slow crystallization from petroleum ether were suitable for the X-ray examinations.

Infrared Spectra

The spectra measured (Fig. 1) were those of 1 mg of the pure solids dispersed in potassium bromide disks of thickness 1 mm and weighing 400 mg as observed with a Perkin–Elmer model 21 infrared spectrophotometer with a rock salt prism. The peak positions of the NO_2 symmetrical stretching frequencies in the region of 1370 cm^{-1} were more accurately determined using a Perkin–Elmer spectrometer model 12C, but these more accurate values agreed closely with the previously measured frequencies.

X-Ray Analyses

Crystals of 9-nitroanthracene are monoclinic with four molecules in a unit cell of dimensions $a = 7.49$, $b = 13.77$, $c = 11.44$ Å, $\beta = 115°11'$, space group $P2_1/a$. The structure was determined from projections along the three principal crystallographic axes. The nitro group is very markedly tilted out of the plane of the anthracene nucleus about the C–N bond, the angle between the planes of the aromatic ring and of the nitro group being 84.7°. Figure 2 shows a projection of the structure along the *c*-axis; the individual atoms are not separately resolved in this projection, but the large deviation from coplanarity is well illustrated.

9,10-Dinitroanthracene is triclinic with one molecule in a unit cell of dimensions $a = 3.95$, $b = 8.68$, $c = 8.76$ Å, $\alpha = 106°46'$, $\beta = 98°59'$, $\gamma = 98°01'$, space group

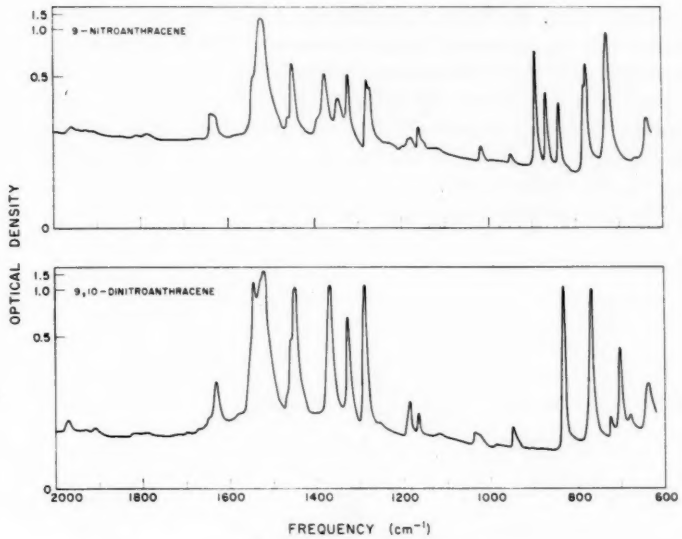

FIG. 1. Infrared spectra.

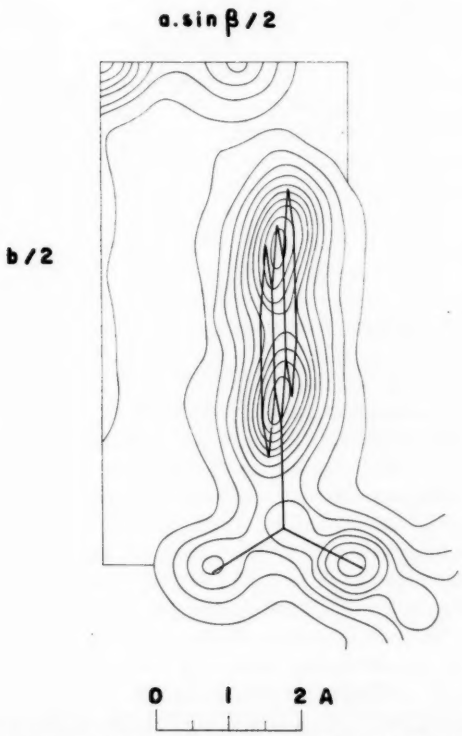

FIG. 2. Projection of the structure of 9-nitroanthracene along the *c*-axis, showing the tilt of the nitro group.

$P\bar{1}$. In the projection along the short *a*-axis all the atoms are very well resolved. Figure 3 shows a projection of the structure along the *b*-axis, in which the resolution of the individual atoms is not so good, but which shows very clearly the tilt of the nitro groups. The molecule is centrosymmetrical and the angle between the planes of a nitro group and the aromatic nucleus is in this case 63.7°. This deviation from planarity is just sufficient to increase the separations between the oxygen atoms and neighboring carbon and hydrogen atoms to the normal van der Waals distances. Full details of the crystal structure analyses are published elsewhere (6, 7).

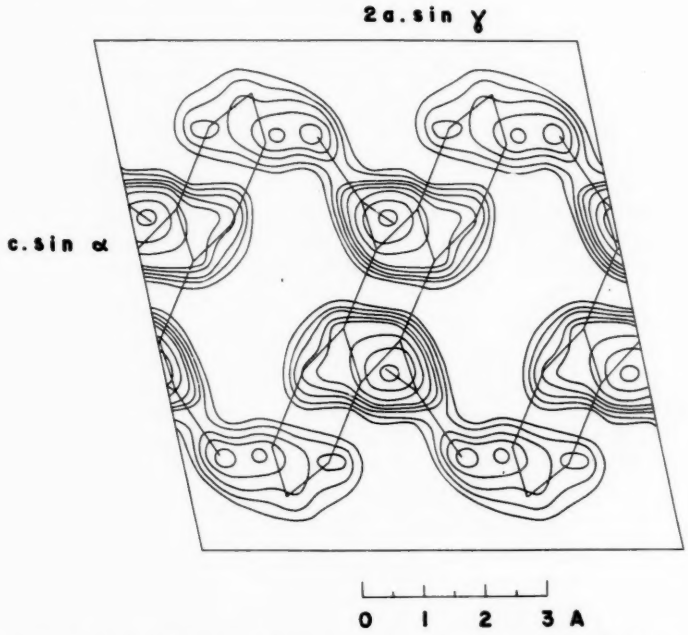

FIG. 3. Projection of the 9,10-dinitroanthracene structure along the *b*-axis, showing the nitro-group tilts.

DISCUSSION

The spectra of 9-nitroanthracene and 9,10-dinitroanthracene in the range 2000 cm^{-1} to 600 cm^{-1} are shown in Fig. 1, and the peak positions and intensities of the absorption bands are listed in Table I. The maxima at 1374 cm^{-1} in 9-nitroanthracene and at 1367 cm^{-1} in 9,10-dinitroanthracene can be assigned to the NO_2 symmetrical stretching vibrations, the intensity of the absorption in the dinitro compound being about double that in the mononitro derivative. The NO_2 asymmetrical stretching vibrations cannot be assigned quite so unambiguously. In 9,10-dinitroanthracene there are bands of about equal intensity at 1519 cm^{-1} and 1542 cm^{-1}, while in the 9-nitro there is a band at 1519 cm^{-1} corresponding in intensity to that of the dinitro derivative and a shoulder at 1540 cm^{-1} of about half this intensity, and on this basis the bands around 1540 cm^{-1} have been assigned to the NO_2 asymmetrical stretching vibrations.

The C–N stretching frequency in nitromethane (8) is at 918 cm^{-1}, although it is at rather lower frequencies in the higher nitroparaffins (at 804 cm^{-1} in 1-nitropropane for

TABLE I

Frequencies and intensities of absorption bands

9-Nitroanthracene		9,10-Dinitroanthracene		
Frequency (cm^{-1})	Intensity	Frequency (cm^{-1})	Intensity	Vibration
1623–1639	w	1631	w	C=C (conjugated) stretching
1540	m (sh)	1542	s	NO_2 asymmetrical stretching
1519	s	1519	s	C=C (conjugated) stretching
1458	w	1458	m (sh)	
1449	m	1447	s	
1374	m	1367	s	NO_2 symmetrical stretching
1344	w→m			
1322	m	1327	m	
1279	m	1288	s	
1271	m			
1186	w (sh)	1190	w (sh)	
1179	w	1186	w	
1159	w	1166	w	Characteristic anthracene bands
1017	w	1023–1037	w	
949	w	949	w	
890	s			C_{10}—H out-of-plane vibration
866	m			
836	m	831	s	C—N stretching
778	m (sh)			
773	s	768	s	
724	s	724	w	Characteristic anthracene band
		702	m	
		678	w	
637	m	639	m	NO_2 symmetrical bending

example), while in aromatic nitro compounds (9) it is at 849 cm^{-1}. The absorption maxima at 836 cm^{-1} and 831 cm^{-1} in the meso-nitroanthracenes can be assigned to the C–N stretching vibrations. The strong absorption at 890 cm^{-1} in the mononitro derivative, which is not observed in the dinitro, corresponds to the C_{10}–H out-of-plane vibration.

In Table II the characteristic nitro group frequencies in 9-nitroanthracene and 9,10-dinitroanthracene are compared with those in nitromethane and those in typical aromatic nitro compounds (9). In aromatic nitro compounds contributions from ionic structures of type V lead to a decrease in the force constant of the N–O bonds and a consequent decrease in the NO_2 symmetrical and asymmetrical stretching frequencies (1349 cm^{-1} and 1518 cm^{-1}) compared with non-conjugated nitro compounds (1377 cm^{-1} and 1586 cm^{-1} in nitromethane). The frequency of the NO_2 symmetrical stretching vibration in 9-nitroanthracene is much higher than in nitrobenzene, and nearly equal to the frequency in nitromethane, corresponding to a negligible amount of resonance interaction between the nitro group and the anthracene nucleus. In 9,10-dinitroanthracene the band is at 1367 cm^{-1}, indicating a very marked reduction in resonance interaction compared with nitrobenzene, but also suggesting that the resonance is not inhibited to such an extent as in the 9-nitro derivative.

These frequencies are in accord with the tilts of the nitro groups out of the aromatic planes, which are given in the final column of Table II. The tilt has been assumed to be zero in nitrobenzene, although this is not quite certain; X-ray crystal analyses of *p*-dinitrobenzene for example have shown that the nitro group is tilted 9°25′ out of the plane of the benzene ring in this molecule (10). Resonance interaction is at a maximum in nitrobenzene (corresponding to $\theta = 0°$) and zero in nitromethane (corresponding effectively to $\theta = 90°$). The frequencies of the NO_2 symmetrical stretching vibrations indicate that resonance between aromatic rings and nitro groups is almost completely inhibited

TABLE II

Characteristic nitro-group frequencies (cm^{-1}) and deviations from coplanarity

Molecule	NO_2 stretching		C–N stretching	NO_2 tilt (θ in degrees)
	Symmetrical	Asymmetrical		
Nitromethane	1377	1586	918	90
9-Nitroanthracene	1374	1540	836	84.7
9,10-Dinitroanthracene	1367	1542	831	63.7
Aroamtic nitro compounds	1349	1518	849	0

in 9-nitroanthracene ($\theta = 85°$) and inhibited to a large extent in 9,10-dinitroanthracene ($\theta = 64°$). The NO_2 asymmetrical stretching vibrations in 9-nitro and 9,10-dinitroanthracene are also in accord with resonance inhibition, although quantitatively the agreement is not so good.

Resonance inhibition decreases the weight of ionic structures such as III and IV, and the resulting decrease in the force constant of the C–N bond should lead to lower frequencies for the C–N stretching vibration in 9-nitroanthracene and 9,10-dinitro-

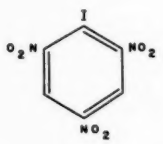

I

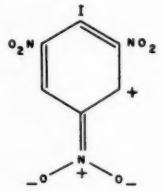

II

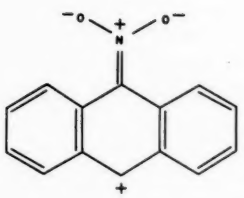

III

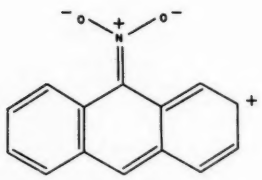

IV

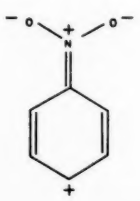

V

anthracene than in nitrobenzene, in agreement with the observed frequencies. The C–N stretching frequency in nitromethane would then appear to be anomalous, but the higher frequency in this case is not unexpected as the carbon atom can vibrate more freely than those in the more rigid aromatic molecules.

The characteristic NO_2 vibration frequencies in meso-nitroanthracenes then indicate a marked inhibition of the resonance interaction between the nitro groups and the aromatic π-electrons, in complete agreement with the effect which would be predicted from a measure of the tilts of the nitro groups out of the aromatic planes. For the NO_2 symmetrical stretching frequencies the results would appear to be semiquantitative, but this is probably fortuitous, since only qualitative agreement is obtained with the other characteristic vibrations. Only qualitative agreement is to be expected of course, since the nitro-group frequencies are not entirely independent of the remainder of the molecule, and small frequency variations are observed among quite similar aromatic molecules where no steric effects are involved. Quantitative information concerning the resonance interaction may be obtained from an examination of the bond lengths in these molecules, since structures of types III and IV would impart a considerable amount of double bond character to the C–N bond, reduce the double bond character of the N–O bonds, and also influence the bond lengths in the aromatic rings. Discussion of these quantitative relations obtainable from a study of the bond length variations will be given in later communications.

ACKNOWLEDGMENTS

The author wishes to thank Dr. W. G. Schneider for samples of 9-nitroanthracene and 9,10-dinitroanthracene, and Mr. R. Lauzon for recording the infrared spectra.

REFERENCES

1. WHELAND, G. W. Resonance in organic chemistry. John Wiley & Sons, Inc., New York. 1955.
2. HUSE, G. and POWELL, H. M. J. Chem. Soc. 1398 (1940).
3. FRANCEL, R. J. J. Am. Chem. Soc. **74**, 1265 (1952).
4. JONES, R. N. J. Am. Chem. Soc. **67**, 2127 (1945).
5. JONES, R. N. Chem. Revs. **41**, 353 (1947).
6. TROTTER, J. Acta Cryst. **11**, 564 (1958).
7. TROTTER, J. Acta Cryst. (In press).
8. SMITH, D. C., PAN, C., and NIELSEN, J. R. J. Chem. Phys. **18**, 706 (1950).
9. RANDLE, R. R. and WHIFFEN, D. H. J. Chem. Soc. 4153 (1952).
10. ABRAHAMS, S. C. Acta Cryst. **3**, 194 (1950).

THE SYNTHESIS OF 4-*O*-β-D-GALACTOSYL-D-GLUCOSE (LACTOSE)[1]

E. J. C. CURTIS AND J. K. N. JONES

ABSTRACT

4-*O*-β-D-Galactosyl-D-glucose (lactose) has been synthesized using a modification of the Koenigs–Knorr reaction.

INTRODUCTION

4-*O*-β-D-Galactosyl-D-glucose (lactose) occurs in all mammalian milk to the extent of about 5%. It has also been reported in the long-styled pollen of forsythia flowers. It was prepared in 1942 by Haskins, Hann, and Hudson (1) from epilactose (4-*O*-β-D-galactosyl-D-mannose), but has not previously been synthesized directly.

One of the most useful methods of disaccharide synthesis is that due to Koenigs and Knorr (2). They prepared tetra-*O*-acetyl-α-D-glucopyranosyl-bromide and found that this, in the presence of silver carbonate or dry pyridine, reacted with methanol to form methyl-β-D-glucopyranoside. The reaction—essentially the elimination of hydrogen halide between a glycosyl halide and a hydroxyl group—was adapted for disaccharide synthesis by Helferich (3) and by Hudson (4). They allowed the acetobrom sugar to react with a suitably substituted sugar derivative in a dry inert medium in the presence of silver carbonate or silver oxide. With modern refinements—use of "Drierite" as drying agent and small amounts of iodine as catalyst—good yields can be obtained in the case of $1 \rightarrow 6$ linked hexose disaccharides, where a primary hydroxyl group is involved. However, up to the present only small yields have been obtained in the case of disaccharides where a secondary hydroxyl group is involved. This is due to the lesser reactivity of the secondary hydroxyl group and to steric hindrance by the alcohol component due to the presence of the hemiacetal ring and the substituent groups. It was thought that this second factor might be lessened—and thus greater yields obtained—by the use of an open-chain sugar derivative as the alcohol reactant. Here the accessibility of the hydroxyl group is much greater than in the corresponding ring compound.

In the present work 2,3-5,6-di-*O*-isopropylidene-D-glucose diethyl acetal was condensed with acetobrom-D-galactose under standard Koenigs–Knorr conditions (5). The reaction mixture was boiled with sodium hydroxide solution to remove acetyl groups from the product and to destroy excess acetobrom-galactose, cooled, and deionized. Hydrolysis of isopropylidene and acetal groups was carried out with hot dilute acetic acid. The resulting mixture of mono- and di-saccharides was separated by charcoal- and paper-chromatography. Lactose was obtained crystalline in 35% yield, which is well in excess of the yields usually obtained from Koenigs–Knorr syntheses where a secondary hydroxyl group is involved. Two other disaccharide fractions were obtained in small yield. These have not been completely identified but presumably result from isomers of 2,3-5,6-di-*O*-isopropylidene-D-glucose diethyl acetal. These are inevitably present in small amount as a result of the method of preparation of this compound (via a mercaptal mixture (8) consisting mainly of the 2,3-5,6-di-*O*-isopropylidene derivative).

EXPERIMENTAL

Optical rotations were measured in water at 21°±2° C. The following solvent systems (v/v) were used to separate sugars on paper chromatograms: (A) ethyl acetate: acetic acid: formic acid: water, 18:3:1:4; (B) *n*-butanol:ethanol: water, 3:1:1. Sugars were

[1]*Manuscript received August 11, 1958.*
Contribution from the Department of Chemistry, Queen's University, Kingston, Ontario.

detected with the *p*-anisidine hydrochloride spray (6). Solutions were concentrated under reduced pressure at 40° C.

D-Glucose Diethyl Thioacetal (Ref. 7)

D-Glucose (60 g), ice-cold ethanethiol (60 ml), and ice-cold concentrated hydrochloric acid (60 ml) were shaken together in a stoppered flask, and left at room temperature. After 3 hours the material had formed a crystalline mass. Methanol (*ca.* 300 ml) was added and sufficient lead carbonate to neutralize the solution, which was then filtered and the precipitate washed with boiling methanol. The crude product crystallized from the filtrate on cooling and was recrystallized from methanol. Yield: 62 g (65%), m.p. 119–120° C.

Di-O-isopropylidene-D-glucose Diethyl Thioacetal (Ref. 8)

Glucose diethyl thioacetal (36 g) was added to a mixture of dry acetone (350 ml) and concentrated sulphuric acid (8.5 g) and the resulting solution was left at room temperature for 72 hours. The solution was neutralized with a solution of barium hydroxide in methanol, and filtered. The filtrate was evaporated to a pale yellow mobile syrup. Yield: 35 g.

Di-O-isopropylidene-D-glucose Diethyl Acetal

The method used was similar to that employed by Wolfrom *et al.* (9) in the preparation of D-galactose diethyl acetal pentaacetate. Di-*O*-isopropylidene-D-glucose diethyl thioacetal (40 g), mercuric oxide (80 g), and lead carbonate (20 g) were added to dry ethanol (400 ml) and the solution heated to 70–80° C while it was being stirred. A solution of mercuric chloride (176 g) in dry ethanol (300 ml) was then added and the solution stirred for 5 hours at 70–80° C with occasional addition of mercuric oxide. The solution was filtered hot and the precipitate washed with hot ethanol. The filtrate was evaporated to a small volume and then diluted with chloroform (400 ml). This chloroform solution was extracted with water until chloride-free and dried over Drierite. Filtration and subsequent evaporation yielded a syrup (30 g), which was purified by distillation, a fraction (22 g) being collected with b.p. 130–140° C at 0.05 mm.

Condensation of Di-O-isopropylidene-D-glucose Diethyl Acetal with Acetobromo-D-galactose

Di-*O*-isopropylidene-D-glucose diethyl acetal (15 g, 0.0449 mole) was dissolved in dry, alcohol-free chloroform (200 ml) and to the solution were added Drierite (20 g), silver oxide (20 g), and glass beads (35 g). The solution was shaken in the dark. After 4 hours acetobrom-D-galactose (46 g, 0.112 mole) in dry, alcohol-free chloroform (150 ml) and iodine (1 g) were added and the shaking continued. After 42 hours a test for ionizable bromine was negative. The solution was filtered, evaporated to a syrup, and dissolved in a solution of sodium hydroxide (20 g) in methanol (400 ml). This was heated under reflux for 3.5 hours, cooled, and de-cationized on Amberlite IR-120 resin in the cold. The acidic eluate was heated at 65° C for 1 hour in order to hydrolyze isopropylidene and acetal groups, and then de-ionized by passage through a column of Duolite A-4 resin. Concentration of the eluate yielded a syrup (20 g) which was shown by paper chromatography to consist, in addition to glucose and galactose, of a main fraction with R_{gal} 0.45 (solvent A) and 0.28 (solvent B) and two much smaller spots running slightly in front of, and behind, this spot.

A portion of the syrup (8.1 g) was fractionated on a column of Darco charcoal (4×5 cm) (10). Elution with water removed all the monosaccharide and in the final stages a faint trace of the slower-moving components: subsequent elution with ethanol/water (5:95) removed the bulk of the slower-moving components (2.9 g). This latter syrup

was dissolved in a little moist methanol, nucleated with authentic lactose, and the solvent allowed to evaporate at room temperature. Part of the material crystallized, 1.8 g being obtained. It was recrystallized from moist methanol and was found chromatographically to be a single substance indistinguishable from lactose. Hydrolysis yielded galactose and glucose in equal amounts. It had m.p. 201–202° C undepressed by admixture with an authentic specimen of lactose monohydrate, and $[\alpha]_D$ +86.3 (5 min) → +58.1° (16 hr). The infrared spectra of the material and of authentic lactose monohydrate were identical. Calculated for $C_{12}H_{22}O_{11}.H_2O$: C, 40.00%; H, 6.67%. Found: C, 40.19%; H, 6.82%.

Part of the syrup which failed to crystallize (0.6 g) was separated on filter paper (Whatman No. 3 MM). A further quantity of lactose (0.20 g) was obtained in addition to two other fractions: I (51.2 mg) and II (49.9 mg). Fraction I had R_{gal} 0.33 (solvent A) and 0.15 (solvent B) while II had R_{gal} 0.47 (solvent A) and 0.32 (solvent B). Both fractions yielded galactose and glucose in equal amounts on hydrolysis.

Periodate Oxidation of Fractions I and II

Portions of fractions I and II were oxidized with aqueous sodium metaperiodate solution using standard procedures. The periodate uptake was estimated by the method of Neumüller and Vasseur (11) and the formic acid liberation by that of Andrews *et al.* (12).

The molar periodate consumptions per mole of disaccharide were as follows: fraction I, 3.90 (after 25 min), 4.44 (1 hr), 4.75 (3.5 hr), and 4.83 (22 hr); fraction II, 2.35 (0.5 hr), 2.84 (1 hr), 3.08 (4 hr), and 3.56 (22 hr). The molar productions of formic acid were: fraction I, 3.77 (after 40 min), 4.29 (1.5 hr), 4.92 (4 hr), and 5.34 (22.5 hr); fraction II, 1.01 (40 min), 1.25 (1.5 hr), 1.41 (4 hr), and 2.12 (22.5 hr). Extrapolation of the flat part of the curve to zero time gave values of: fraction I, periodate uptake = 4.78 moles per mole of sugar, formic acid production = 4.41 moles per mole; fraction II, periodate uptake = 2.95 moles per mole sugar, formic acid production = 1.17 moles per mole.

The figures for fraction I are difficult to interpret. The large amount of formic acid could not have come from any normal type of sugar and it may be that this fraction is a mixture of disaccharide and some other material. The figures for fraction II—where the slope of the flat part of the periodate and formic acid curves indicates that over-oxidation was taking place—are those to be expected of a 1 → 3 linked hexopyranose disaccharide. Crystalline derivatives of fractions I and II have not yet been obtained.

ACKNOWLEDGMENTS

The authors are indebted to the National Research Council for a grant. One of them (E.J.C.C.) thanks Queen's University for the award of a fellowship.

REFERENCES

1. Haskins, W. T., Hann, R. M., and Hudson, C. S. J. Am. Chem. Soc. **64**, 1852 (1942).
2. Koenigs, W. and Knorr, E. Ber. **34**, 957 (1901).
3. Helferich, B. Advances in carbohydrate chemistry. Vol. 3. Academic Press, Inc., New York. 1948. p. 79.
4. Knauf, A. E., Hann, R. M., and Hudson, C. S. J. Am. Chem. Soc. **63**, 1447 (1941).
5. Evans, W. L., Reynolds, D. D., and Talley, E. A. Advances in carbohydrate chemistry. Vol. 6. Academic Press, Inc., New York. 1951. p. 27.
6. Hough, L., Jones, J. K. N., and Wadman, W. H. J. Chem. Soc. 1702 (1950).
7. Hough, L. and Taylor, T. J. J. Chem. Soc. 1212 (1955).
8. Munro, J. and Percival, E. G. V. J. Chem. Soc. 873 (1935).
9. Wolfrom, M. L., Tanghe, L. T., George, R. W., and Waisbrot, S. W. J. Am. Chem. Soc. **60**, 132 (1938).
10. Andrews, P., Hough, L., and Powell, D. B. Chem. & Ind. 658 (1956).
11. Neumüller, G. and Vasseur, E. Arkiv Kemi, **2**, 235 (1953).
12. Andrews, P., Hough, L., and Jones, J. K. N. J. Chem. Soc. 806 (1954).

THE INFRARED SPECTRA OF SOME CYCLIC MALONATES[1]

R. A. ABRAMOVITCH

ABSTRACT

The infrared spectra of isopropylidene malonate and some of its derivatives have been examined and compared with those of open-chain malonate esters and of 5,5-dimethylcyclohexane-1,3-dione. Two bands in the carbonyl stretching region are attributed to vibrational coupling of the carbonyl groups in the cyclic esters. There is no evidence that isopropylidene malonate exists in the enolic form either in the solid state or in chloroform solution. This cyclic ester structure for "Meldrum's acid" is thus confirmed.

In an investigation of the infrared spectra of a number of malonate esters it was shown (1) that most of them exhibited two ester carbonyl stretching bands, and that these were not due to enolization and conjugate chelation, or to association. It was not possible, at that stage, to decide whether these double carbonyl bands were due to vibrational coupling or to rotational isomerism, or yet perhaps to another still unknown cause.

It was of interest to determine whether, in the absence of the possibility of rotational isomerism, two ester carbonyl groups beta- to each other could undergo vibrational coupling. For this purpose the spectra of isopropylidene malonate and some of its derivatives have been examined, since apart from ethylene glycolyl malonate (2) (which is not unambiguously characterized), no other simple cyclic esters of malonic acid seem to be known. Vibrational coupling does not appear to have been observed in cyclic 6-membered β-diketones: here, enolization with intermolecular chelation has been reported (3). The carbonyl groupings, which are beta- to each other, in cyclic anhydrides are known to undergo coupling (4), and it has recently been suggested that this type of interaction also occurs in substituted isatoic anhydrides (5) though in this case the carbonyl groups are different in nature and one would have expected each to exhibit its own stretching frequency.

Isopropylidene malonate (I) poses an interesting structural problem which was largely clarified by the work of Davidson and Bernhard (6). The cyclic ester, also known as "Meldrum's acid", is prepared by the action of acetone on malonic acid in a cold acetic anhydride – sulphuric acid medium, and was originally attributed the structure of β,β-dimethyl-β-propiolactone-α-carboxylic acid (II). On the basis of chemical evidence Davidson and Bernhard were able to suggest structure (I) for the product and structure (III) for the dimethylated derivative.

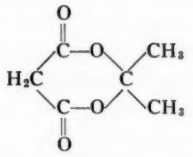

(I)

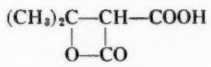

(II)

They compared the reactions of the cyclic ester with those of 5,5-dimethylcyclohexane-1,3-dione (IV) and attributed the acidity of the ester (pK_a 5.1) to enolization ((I $\rightleftarrows$ V) in the same way as the acidity of 5,5-dimethylcyclohexane-1,3-dione (pK_a 5.2) is

[1]*Manuscript received September 22, 1958.*
Contribution from the Chemistry Department, University of Saskatchewan, Saskatoon, Saskatchewan.

Can. J. Chem. Vol. 37 (1959)

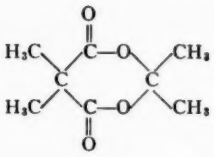

(III)

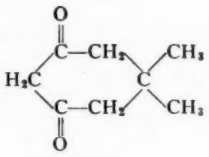

(IV)

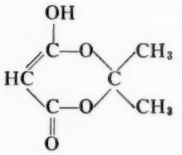

(V)

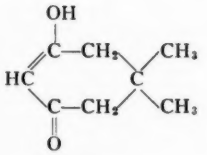

(VI)

attributed to a similar enolization (IV ⇄ VI). In fact, the dione (IV) is 95% in the enolic form in water solution (7). On the other hand, isopropylidene dimethylmalonate, which cannot exist in an enolic form, exhibits no acidic properties (6). It should be pointed out, however, that diethyl malonate itself is not enolized to any appreciable extent ((1), and references cited therein).

EXPERIMENTAL

Isopropylidene malonate and isopropylidene dimethylmalonate were prepared by the method of Davidson and Bernhard (6). Isopropylidene malonate could be recrystallized either from acetone–water, or more conveniently from water or anhydrous carbon tetrachloride giving needles, m.p. 96°. 5,5-Dimethylcyclohexane-1,3-dione had m.p. 147–148.5°.

Isopropylidene ethylmalonate.—To a suspension of ethylmalonic acid (6.6 g) in acetic anhydride (6 ml) was added concentrated sulphuric acid (0.2 ml) with stirring. Most of the solid dissolved. Acetone (4 ml) was added dropwise to the suspension kept at 20–25° and the resulting solution was kept in the refrigerator overnight. The solid which separated was filtered and washed repeatedly with ice water, and the filtrate and washings combined to give a further amount of isopropylidene ethylmalonate. The product (6.09 g), m.p. 108–109° (depressed to 86–88° on admixture with ethylmalonic acid, m.p. 111°), was recrystallized from distilled water giving long, colorless needles, m.p. 108–109°. Found: C, 55.5; H, 7.1. Calc. for $C_8H_{12}O_4$: C, 55.8; H, 7.0.

Isopropylidene deuteromalonate.—An attempt to replace the reactive hydrogen atoms by sodium (with sodium ethoxide) followed by evaporation to dryness and treatment with D_2O, as in the case of diethyl ethylmalonate (1), only led to hydrolysis of the cyclic ester. Exchange of the active hydrogens of isopropylidene malonate took place readily when the compound was recrystallized from 99.9% deuterium oxide; seven such recrystallizations gave the deuterated ester as flat needles, m.p. 93–94°.

Infrared spectra.—A Perkin–Elmer model 21 double beam spectrophotometer with sodium chloride optics was used. The chloroform used for the solution spectra was AnalaR grade, dried and redistilled before use. The solution cell thickness was 0.028 mm and the concentrations were in the range of 20–22 mg/ml. Carbon tetrachloride was also of AnalaR grade and was dried before use.

Compound	Nujol mull			Chloroform solution		
	$\nu_{C=O}$ cm^{-1}	Mean value	$\Delta\nu_{C=O}$ cm^{-1}	$\nu_{C=O}$ cm^{-1}	Mean value	$\Delta\nu_{C=O}$ cm^{-1}
Isopropylidene malonate	1785, 1753	1769	32	1778, 1749	1763	29
Isopropylidene deutero-malonate	1778 (br), 1740 (br)	1759	38	1782, 1745	1763	37
Isopropylidene ethylmalonate	1777, 1737	1757	40	1783, 1747	1765	36
Isopropylidene dimethyl-malonate	1780 (br), 1745 (br)	1758	35	1770, 1735 1787, 1749*	1753 1768	35 38
5,5-Dimethylcyclohexane-1,3-dione	1612 (br)	—	—	1733, 1710, 1612 (br)	—	—
Diethyl malonate (1)	1760, 1742†	1751	22	1761, 1742	1752	19

br = Broad band.
*Carbon tetrachloride solution.
†Liquid film.

RESULTS

The 3–5 μ region.—5,5-Dimethylcyclohexane-1,3-dione is the only compound which shows OH stretching absorption in that region: in the solid state a very broad band is observed at 2505 cm^{-1} with a shoulder at 2380 cm^{-1}. These bands are attributed to the enolic OH group, which is strongly intermolecularly bonded. The intensities of these bands are decreased considerably in dilute chloroform solution and vanish altogether at high dilution. Isopropylidene deuteromalonate exhibits a band at 2155 cm^{-1} (Nujol mull) attributed to the CD_2 vibration, indicating that at least a large proportion of the active hydrogen atoms have been exchanged for deuterium; if only one of the two hydrogen atoms had been replaced no appreciable band corresponding to the tertiary C—D stretching mode would have been observed (1). None of the other compounds examined showed any O—H stretching bands either in the solid state or in chloroform solution.

The 5–6 μ region.—The cyclic malonates exhibited two bands in this region above 1730 cm^{-1} whether in the solid state or in solution. In the solid state 5,5-dimethylcyclohexane-1,3-dione exhibited only a single broad band at 1612 cm^{-1}, whereas in dilute chloroform solution three bands were observed at 1733 (m), 1710 (s), and 1612 cm^{-1} (s) (broad). Bellamy and Beecher (8) reported bands at 1733, 1706, and 1603 cm^{-1} which they attributed to the keto, free enol, and intermolecularly chelated forms respectively. Though the positions of the double maxima of the cyclic malonates are altered on going from the solid state to the solutions, or, in the case of isopropylidene dimethylmalonate on changing from a chloroform solution to a carbon tetrachloride solution, $\Delta\nu_{C=O}$ for each individual compound remains approximately the same. The effect of deuteration does not change the mean of the positions of the two bands of isopropylidene malonate in chloroform solution though the positions of the bands themselves are altered, as is also $\Delta\nu_{C=O}$ (which becomes closer to that of isopropylidene dimethylmalonate).

DISCUSSION

Structure (II) for "Meldrum's acid" is eliminated owing to absence of the broad peaks characteristic of the carboxyl group in the 3–4 μ region, as well as of a band at around 1700 cm^{-1}. It is clear, however, that neither in the solid state nor in chloroform solution is isopropylidene malonate (I) enolized to any appreciable extent. This is shown by the absence of any O—H stretching bands, whether bonded or unbonded, by the absence of a definite band corresponding to an α,β-unsaturated ester carbonyl group as would be present in the free enol, as well as by the non-appearance of a band corre-

sponding to a chelated ester carbonyl group. Also, since isopropylidene dimethylmalonate shows two bands above 1730 cm^{-1} these cannot be due to an equilibrium between keto and enol forms. The possibility that the two bands are due to different conformations of the 6-membered ring is rendered very unlikely by the fact that in isopropylidene dimethylmalonate there would be large 1,4-interactions in the boat form (VII).

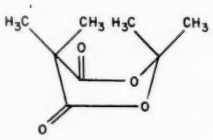

(VII)

Vibrational coupling is, therefore, the most logical answer. The fact that vibrational coupling can occur in cyclic malonates where rotational isomerism is not possible does not, however, mean that this is necessarily the explanation for the appearance of two ester carbonyl bands in open-chain malonates; all it does show is that coupling can occur between suitably situated ester carbonyl groups beta- to each other. The acidity of isopropylidene malonate must be due to the ease with which it undergoes enolization *in the presence of base.*

The difference in behavior between malonates and β-diketones is interesting. The greater degree of enolization of β-diketones has been attributed to the larger —M effect of the acyl group over that of the ester group (9) as well as in the added stabilization due to internal hydrogen bonding of the enol form (10). The cyclic β-diketone 5,5-dimethylcyclohexane-1,3-dione is enolized to an even larger extent than acetylacetone and this may be due to greater steric ease of intermolecular hydrogen bonding between two molecules of the enol existing in semichair conformations. It is tempting, therefore, to suggest that, since cyclic malonates are not enolized to any appreciable extent in the solid state or in solution whereas 5,5-dimethylcyclohexane-1,3-dione is almost completely enolized and intermolecularly chelated in the solid state, ketonic carbonyl groups have a greater tendency to undergo hydrogen bonding than similarly situated ester carbonyl groups. This could be rationalized if it were assumed that ease of hydrogen bonding in such cases depended among other things on the availability of electrons at the oxygen atom, since in ketones the alkyl group has a +I effect whereas in ester groups the alkoxyl group has a −I effect.

Some comments may also be made about the two bands at 1733 and 1710 cm^{-1} in the spectrum of 5,5-dimethylcyclohexane-1,3-dione in chloroform solution, which were previously observed by Bellamy and Beecher (8) at 1733 and 1706 cm^{-1}, and which they attributed to the unenolized keto form and to the free enol respectively. These authors observed that the band at 1603 cm^{-1}, due to the intermolecularly chelated form, vanished on great dilution owing to the breaking of the intermolecular hydrogen bonds, as expected. They found, however, that the 1710 cm^{-1} band also vanished at very high dilutions; they suggested that this band was due to the free enol form and that at these high dilutions in non-polar solvents the compound existed only in the keto form. If, after breaking the intermolecular hydrogen bonds by solution in chloroform, the free enol form were stable in that solvent it is difficult to see why further dilution with the same solvent should have rendered this form less stable. On the other hand, it is not stated whether after dilution a proportionally greater cell thickness was used in the

measurements. It may be possible that the two bands at 1733 and 1710 cm^{-1} are again due to vibrational coupling of the two unenolized carbonyl groups. A 6-membered ring ketone normally absorbs at *ca.* 1720–1710 cm^{-1} (though this might conceivably be raised to 1733 cm^{-1} if a strongly electron-attracting substituent is attached to the α-carbon atom as is the case here); an α,β-unsaturated 6-membered ring ketone, on the other hand, might be expected to absorb below 1700 cm^{-1} (11). The position of the two bands observed would fit in with the trend of one band being above, the other below, the common frequency in cases where vibrational coupling occurs (12).

ACKNOWLEDGMENTS

The author wishes to thank Dr. L. C. Leitch for a generous gift of deuterium oxide and the National Research Council for a grant-in-aid of this research. Useful discussions with Drs. J. M. Pepper and R. A. Heacock are gratefully acknowledged.

REFERENCES

1. ABRAMOVITCH, R. A. Can. J. Chem. **36**, 151 (1958).
2. TILICHEEV, M. D. J. Russ. Phys.-Chem. Soc. **58**, 447 (1927).
3. RASMUSSEN, R. S., TUNNICLIFF, D. D., and BRATTAIN, R. R. J. Am. Chem. Soc. **71**, 1068 (1949).
4. THOMPSON, H. W. J. Chem. Soc. 328 (1948).
5. O'SULLIVAN, D. G. and SADLER, P. W. J. Chem. Soc. 2916 (1957).
6. DAVIDSON, D. and BERNHARD, S. A. J. Am. Chem. Soc. **70**, 3426 (1948).
7. SCHWARZENBACH, G. and FELDER, E. Helv. Chim. Acta, **27**, 1044 (1944).
8. BELLAMY, L. J. and BEECHER, L. J. Chem. Soc. 4487 (1954).
9. INGOLD, C. K. Structure and mechanism in organic chemistry. Bell & Sons, Ltd., London. 1953. p. 555.
10. HINE, J. Physical organic chemistry. McGraw-Hill Book Co., Inc., New York. 1956. p. 233.
11. JONES, R. N., HUMPHRIES, P., and DOBRINER, K. J. Am. Chem. Soc. **72**, 956 (1950).
12. JONES, R. N. and SANDORFY, C. Techniques of organic chemistry. Vol. IX. Chemical applications of spectroscopy. Interscience Publishers, Inc., London. 1956. p. 495.

PERACETIC ACID OXIDATION OF HALOGENATED AZOBENZENES[1]

PAUL E. GAGNON AND BRIAN T. NEWBOLD[2]

ABSTRACT

A series of dihalogenated and five tetrachloroazobenzenes were oxidized to the corresponding azoxy compounds by means of 30% hydrogen peroxide in glacial acetic acid, the reaction being carried out at about 60–70° C, for 24 hours.

As expected, the yields, in general, obtained from azobenzenes containing substituents in the 2,2′-positions were lower than those from compounds having substituents in the 3,3′- and 4,4′-positions, which gave very good results.

INTRODUCTION

One of the most useful methods for the preparation of azoxybenzenes is the reduction of the appropriate nitrobenzene with a suitable reagent. However, azoxy compounds have also been obtained by oxidation of amines by means of peracids. For example, aniline when oxidized with an equimolar quantity of perbenzoic acid (1), or with peracetic acid (2), gave rise to azoxybenzene. D'Ans and Kneip (2) stated that primary amines can give rise to azo and azoxy compounds when treated with concentrated peracids under various conditions. Later, Greenspan (3) obtained a much better yield, 85%, of azoxybenzene from aniline by oxidation with 45% peracetic acid.

A third method of obtaining azoxybenzenes is the oxidation of the corresponding azobenzenes. For instance, azobenzene gave azoxybenzene when treated with an acetic acid solution of chromic acid in a sealed tube at 150–250° C (4) and 4,4′-dinitroazoxybenzene was obtained from the azo compound by the action of fuming nitric acid at room temperature (5).

The direct oxidation of azobenzenes to azoxybenzenes by means of organic peracids has been a subject of interest for many years. Angeli and others (6, 7, 8, 9) studied this reaction. For example, when azobenzene was treated for several days with peracetic acid, made by combining glacial acetic acid with 30% hydrogen peroxide, azoxybenzene was obtained (6). In a review (10), Swern states that this reaction proceeds readily under mild conditions and quantitative yields are frequently obtained, and he lists the azoxybenzenes prepared by this method up to 1949. In recent work, azobenzene was also oxidized by perbenzoic acid (11).

There are some examples of peracid oxidation of halogenated azobenzenes mentioned in the literature. For instance, 4-bromo-, 4,4′-dibromo-, and 2-bromo-4-nitro-azobenzene have been oxidized to the corresponding azoxy compounds by 30% hydrogen peroxide in glacial acetic acid (12, 13). Badger *et al.* (14) recently oxidized 3-bromo-, 4-bromo-, and 4-chloro-azobenzene with perbenzoic acid. However, only one dichloroazobenzene, namely, the 4,4′-derivative, has been oxidized to the azoxy compound by means of peracetic acid (15). Recently (16), 3,3′- and 4,4′-difluoroazoxybenzenes were prepared from the azo compounds by oxidation with peracetic acid using the method of Angeli.

The main object of the present work was to oxidize a series of dihalogenated and tetrachloroazobenzenes to the corresponding azoxy derivatives by means of 30% hydrogen peroxide in glacial acetic acid and to compare the yields obtained.

[1]*Manuscript received August 22, 1958.*
Contribution from the Department of Chemistry, Laval University, Quebec, Que., and St. Joseph's University, Moncton, New Brunswick.
[2]*Head of the Department of Chemistry, St. Joseph's University, Moncton, New Brunswick.*

THEORETICAL PART

In the present work, many oxidations of dihalogenated azobenzenes were carried out using 30% hydrogen peroxide in glacial acetic acid. The manner in which the hydrogen peroxide was added to the solution of the azo compound was found to be important. The best results were obtained when most of the hydrogen peroxide was added regularly in small portions during the first 2 hours. The solubility of the azobenzene in glacial acetic acid was of considerable importance. It was found that the azobenzenes which were very soluble were the most easily oxidized. The time of the reaction was also critical, for instance, when the period of heating at 60–70° C was only a few hours, the yields of the azoxy derivatives were low. Therefore, the period of heating for the oxidations described in this work was extended to 24 hours.

The experimental conditions for the best yields of the dihalogenated azoxybenzenes are given in Table I. It is seen that only a low yield, 28%, of 2,2′-dichloroazoxybenzene was obtained, and that almost half of the starting material was recovered. It is evident that 2,2′-dichloroazobenzene was quite stable to oxidation with peracetic acid. Bigelow *et al.* (17) found that 4-amino-azobenzene was very difficult to oxidize, there being incomplete oxidation even after 6 days of refluxing in 30% hydrogen peroxide. In the present work, however, very good yields of 3,3′- and 4,4′dichloroazoxybenzene were obtained.

TABLE I

Oxidation of halogenated azobenzenes

Azobenzenes	Amount, g	30% H_2O_2, ml	CH_3COOH, ml	Temp., °C	Azoxy compound Yield, %	M.p., °C	Lit. m.p., °C		Starting material rec., %
Dihalogenated azobenzenes									
2,2′-Dichloro-	2.000	41	150	60–70	28	56	56	(23)	47
3,3′-Dichloro-	2.000	41	200	62–75	93	98–99	97	(24)	Nil
4,4′-Dichloro-	0.512	31	200	60–82	89	154–155	155–156	(21)	"
2,2′-Dibromo-	0.232	10	50	63–66	13	112–113	114	(25)	"
3,3′-Dibromo-	0.300	10	50	64–65	Quant.	111–112	111.5	(26)	"
4,4′-Dibromo-	0.202	16	100	65–68	Quant.	171–171.5	172	(27)	"
3,3′-Diiodo-	0.200	10	100	62–67	96	116–117	117–118	(20)	"
Tetrachloroazobenzenes									
2,2′;3,3′-Tetrachloro-	0.042	20	150	66–70	71	136–138	—	*	Nil
2,2′;4,4′- "	0.098	30	100	65–67	26	128–129	130.5	(20)	72
2,2′;5,5′- "	0.088	35	100	65–68	25	145–146	147	(28)	75
3,3′;4,4′- "	0.160	22	150	62–68	98	137.5–138.5	137–138	(29)	Nil
3,3′;5,5′- "	0.095	20	150	61–70	71	172–173	171–172	(30)	"

*2,2′;3,3′-Tetrachloroazoxybenzene also prepared from 2,2-dichloronitrobenzene using dextrose in alkaline medium was pale yellow, m.p. 138–138.5° C. Yield, 2%. Anal. calc. for $C_{12}H_6N_2OCl_4$: Cl, 42.20%. Found: Cl, 41.22%.

By contrast, the yield of 2,2′-dibromoazoxybenzene was low, 13%, and there was apparently considerable complete oxidation, there being no recovery of unreacted starting material. Bigelow *et al.* (17) showed that both 4-nitro-4′-hydroxyazobenzene and 4-hydroxyazobenzene were completely oxidized to carbon dioxide and nitrogen by prolonged refluxing with 30% hydrogen peroxide. Quantitative yields of 3,3′- and 4,4′-dibromoazoxybenzene were obtained in the present study. As shown in Table I, the yield of 3,3′-diiodoazoxybenzene was very good, but here again, in some experiments, considerable decomposition occurred.

As far as we know, there are no instances of oxidation of tetrachloroazobenzenes with

peracetic acid that have been recorded in the literature. In the present work, five tetrachloroazoxybenzenes were prepared from the azo compounds by oxidation with 30% hydrogen peroxide in glacial acetic acid. The solubility of the tetrachloroazobenzene in glacial acetic acid, the manner in which the hydrogen peroxide was added, and the time of heating were of importance.

The experimental conditions and best results are given in Table I. It is seen that the yield of 2,2′;3,3′-tetrachloroazoxybenzene, which is described for the first time, was 71%, whereas the yields of 2,2′;4,4′- and 2,2′;5,5′-tetrachloroazoxybenzene were only 26 and 25% respectively. By comparison, both 3,3′;4,4′- and 3,3′;5,5′-tetrachloroazobenzene gave good yields of the azoxy derivatives.

In general, it may be said that oxidation of halogenated azobenzenes with peracetic acid is a good method for the preparation of azoxybenzene derivatives having no substituents in the 2,2′-positions.

EXPERIMENTAL PART*

Preparation of Halogenated Azobenzenes

The halogenated azobenzenes were prepared from the corresponding nitrobenzenes by standard methods given in the literature. For example, 4,4′-dichloroazobenzene was made by reducing 4-chloronitrobenzene with magnesium and absolute methanol (18). In the case of 3,3′;4,4′-tetrachloroazobenzene, the azoxy compound (19) was reduced with zinc dust and sodium hydroxide, followed by oxidation in air, as previously described (20).

Peracetic Acid Oxidation

The procedure followed was essentially the same in every case; therefore the preparation of only one compound needs to be described in detail.

4,4′-Dichloroazobenzene (0.512 g) was dissolved in glacial acetic acid (200 ml) at 80° C, and then 30% hydrogen peroxide (2 ml) was added. Further additions of 30% hydrogen peroxide (2 ml) were made every 15 minutes during the first 2 hours, when a further 5 ml was added. The heating was continued at about 65° C, then after 3 hours, 3 ml of 30% hydrogen peroxide was added. To complete the reaction, after 19 and 20 hours 2- and 5-ml portions of hydrogen peroxide, respectively, were added. Heating was continued until the 24-hour period was over, the solution being then allowed to cool to room temperature. The original orange color had changed to pale yellow. The solution was poured into an excess of water (300 ml) and a pale yellow product separated out. It was washed with water and dried. Crude yield, 89%. The 4,4′-dichloroazoxybenzene was recrystallized several times from ethanol as pale yellow needles, m.p. 154–155° C, alone or with an authentic sample (lit. m.p. 155–156° C (21)).

In some cases, the aqueous filtrate, obtained after precipitation with water and filtration, yielded a small amount of product after standing in a refrigerator. In some experiments, precipitation took place after several portions of hydrogen peroxide had been added and glacial acetic acid was used to restore the solution. In cases where there was incomplete oxidation, that is, where a mixture of azoxy compound and starting material was obtained, separation was achieved either by crystallization or chromatography. The latter method was used particularly for the separation of products obtained from the oxidation of the tetrachloroazobenzenes. The chromatography was carried out with columns containing a (4:1) mixture of salicylic acid – celite as absorbant. The celite was celite 535. The products were placed on the column in ligroin solution and

All melting points are uncorrected.

development was carried out with ligroin (b.p. 66–75° C). Elution was achieved with 95% ethanol. The azoxy compound was absorbed high on the column as a yellow band and the starting material (orange band) moved down to the bottom or was passed into the filtrate. The products separated by chromatography were further purified by recrystallizations from ethanol. In order to verify the oxidation method used in the present work, azobenzene was employed as a reference compound. Azobenzene (2 g), glacial acetic acid (50 ml), 30% hydrogen peroxide (18 ml) were heated at 65° C for 24 hours. The crude yield of azoxybenzene was 83%: m.p. 35–36° C, alone or with an authentic sample (lit. m.p. 35.5–36.5° C (22)).

The experimental details and results for all the halogenated azoxybenzenes prepared are given in Table I.

ACKNOWLEDGMENT

The authors wish to express their sincere thanks to Dr. Karl F. Keirstead, who gave them some halogenated azo- and azoxy-benzene samples.

REFERENCES

1. PRILESCHAJEW, N. Ber. **42**, 4811 (1909).
2. D'ANS, J. and KNEIP, A. Ber. **48**, 1136 (1915).
3. GREENSPAN, F. P. Ind. Eng. Chem. **39**, 847 (1947).
4. PETRIEW, H. Ber. **6**, 557 (1873).
5. WEINER, A. and STIASMY, E. Ber. 3263 (1899).
6. ANGELI, A. Atti accad. nazl. Lincei, **19** [I], 793 (1910).
7. ANGELI, A. and ALESSANDRI, L. Atti accad. nazl. Lincei, **20** [I], 896 (1911).
8. ANGELI, A. Gazz. chim. ital. **46** (2), 67 (1916).
9. BIGIAVI, D. and SABATELLI, V. Gazz. chim. ital. **57**, 559 (1927).
10. SWERN, D. Chem. Revs. **45**, 1 (1949).
11. BADGER, G. M., BUTTERY, R. C., and LEWIS, G. E. J. Chem. Soc. 2143 (1953).
12. ANGELI, A. and VALORI, B. Atti. accad. nazl. Lincei, **21** [I], 155 (1912).
13. BIGIAVI, D., ALBANESE, C., and POGGI, I. Gazz. chim. ital. **61**, 392 (1931).
14. BADGER, G. M., BUTTERY, R. C., and LEWIS, G. E. J. Chem. Soc. 2147 (1953).
15. BURNS, J., MCCOMBIE, H., and SCARBOROUGH, H. A. J. Chem. Soc. 2928 (1928).
16. GORE, P. H. and WHEELER, O. H. J. Am. Chem. Soc. **78**, 2160 (1956).
17. BIGELOW, H. E., HOLDER, C. H., and LINTON, E. P. Can. J. Research, B, **19**, 132 (1941).
18. KEIRSTEAD, K. F. Can. J. Chem. **31**, 1064 (1953).
19. GAUDRY, R. and KEIRSTEAD, K. F. Can. J. Research, B, **27**, 893 (1949).
20. GAUDRY, R. and KEIRSTEAD, K. F. Can. J. Research, B, **27**, 900 (1949).
21. HEUMANN, K. Ber. **5**, 911 (1872).
22. BIGELOW, H. E. and PALMER, A. Org. Syntheses, Collective Vol. **II**, 57 (1943).
23. BRAND, K. J. prakt. Chem. **67**, 145 (1903).
24. LAUBENHEIMER, A. Ber. **8**, 1623 (1875).
25. ZECHMEISTER, L. and ROM, P. Ann. **468**, 117 (1928).
26. GABRIEL, S. Ber. **9**, 1405 (1876).
27. FARROW, M. D. and INGOLD, C. K. J. Chem. Soc. 2543 (1924).
28. DE CRAUW, T. Rec. trav. chim. **50**, 782 (1931).
29. DAINS, F. B. and KENYON, W. O. J. Am. Chem. Soc. **52**, 2357 (1931).
30. BEILSTEIN, F. and KURBATOW, A. Ann. **197**, 84 (1879).

A NEW SPECTROPHOTOMETRIC PROCEDURE FOR PLATINUM WITH TIN (II) CHLORIDE[1]

S. S. Berman and E. C. Goodhue

ABSTRACT

A spectrophotometric procedure has been developed for microgram quantities of platinum utilizing an absorption peak at 310 mμ formed when platinum salts react with tin (II) chloride. The method offers a 5-fold increase in sensitivity over the conventional platinum – tin (II) chloride procedure. Several factors influencing the intensity and stability of the absorbing species, whose nature is unknown, are described. Palladium and rhodium produce gross interferences, but small quantities of iridium, iron, copper, and chromium can be tolerated. The procedure is applicable to fumed sulphuric acid solutions of platinum and to solutions of platinum in nitric acid. The recommended concentration range is 0.4 to 6 p.p.m. when measurements are made in 1.0-cm cells.

INTRODUCTION

Tin (II) chloride has long enjoyed wide use as a satisfactory colorimetric reagent for platinum. The earliest reported application was in 1921 by Davis (1). Several workers have since investigated this reagent (2, 3, 4, 5, 6, 7), the most extensive report being produced by Ayres and Meyer (4). In spite of its relatively low sensitivity tin (II) chloride has been preferred in many laboratories because it offered a wide freedom from interference and range of applicability. Two other reagents have also found a wide use. These are potassium iodide (3) and *p*-nitrosodimethylaniline (8). The potassium iodide procedure is less sensitive than that involving tin (II) chloride and suffers gross interferences. The *p*-nitrosodimethylaniline method is the most sensitive procedure for platinum published to date. It is fairly tolerant to the presence of some base metals but is not applicable to solutions of platinum in sulphuric acid and the conditions for the development of the colored species must be followed rather rigorously. (The diacetoimidoplatinum method of Barkovskiĭ and Kul'berg (9) has been reported in Chemical Abstracts (10) to be applicable to platinum concentrations "varying between 25 and 90 μg per liter". However, a study of the original paper has shown that this should have read "250 to 900 μg per ml".)

A comparison of the sensitivities of some of the usefully developed spectrophotometric procedures for platinum is given in Table I.

Ayres and Meyer (4) in their examination of the tin (II) chloride procedure (absorption maximum at 403 mμ) noted the existence of a second absorption peak at about 310 mμ

TABLE I

Sensitivity of spectrophotometric methods for platinum

Method	Molar absorptivity
Thiosemicarbazide (13)	2.46
Diacetoimidoplatinum (9)	2.4×10^2
Potassium iodide (3)	6.05×10^3
Tin (II) chloride (403 mμ) (4)	7.83×10^3
Hexachloroplatinate (14)	8.40×10^3
Phenylthiosemicarbazide (15)	1.35×10^4
Tin (II) chloride (310 mμ)	3.95×10^4
p-Nitrosodimethylaniline (8)	5.29×10^4

[1]*Manuscript received August 25, 1958.*
Contribution from the Division of Applied Chemistry, National Research Council, Ottawa, Canada. Issued as N.R.C. No. 5008.

but stated that the absorption of the reagent blank was so great below 325 mμ as to render this peak unsuitable for use. The authors have succeeded in establishing conditions whereby this absorption peak can be used as the basis for a precise and sensitive determination of platinum. This was done primarily by a gross reduction in the quantity of tin (II) chloride used to produce the absorbing species, and the addition of sulphuric and perchloric acids to stabilize the species and affect a hypsochromic shift in the absorption band due to the tin (II) chloride reagent. A spectral curve (A) of a solution containing 3.92 p.p.m. of platinum treated by the procedure described below is shown in Fig. 1. The absorbance at 310 mμ is five times that at 403 mμ, and the spectral curve (B) of the reagent blank against water shows that the absorbance of the blank is quite low at 310 mμ.

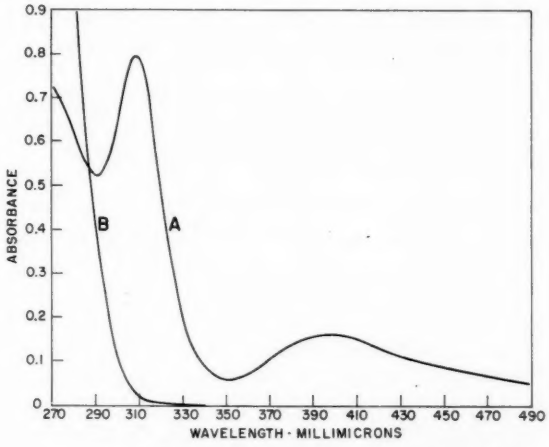

FIG. 1. A: Spectral curve of a solution containing 3.92 p.p.m. platinum against a reagent blank.
B: Spectral curve of the reagent blank against water.

EXPERIMENTAL

Apparatus and Solutions

Absorption measurements were made with a Beckman Model DU quartz spectrophotometer equipped with a hydrogen lamp source and matched 1.00-cm quartz cells. Spectral curves and some studies of the stability of the absorbing species under various conditions were made with a Beckman Model DK-1 recording spectrophotometer.

A standard platinum solution was prepared by dissolving pure platinum sponge in aqua regia, evaporating several times to dryness with hydrochloric acid, and then dissolving the residue and diluting with 0.1 *M* hydrochloric acid. The solution was standardized by precipitation with 4-phenylthiosemicarbazide (11). A 5-ml aliquot of this solution was diluted to 1000 ml with 0.1 *M* hydrochloric acid. The resulting solution contained 9.80 μg of platinum per milliliter of solution.

The reagent was a 2% w/v solution of tin (II) chloride dihydrate in 1.5 *M* hydrochloric acid. The reagent was prepared by dissolving the tin (II) chloride in concentrated hydrochloric acid and then diluting the solution with water.

All chemicals used were of analytical reagent grade.

DEVELOPMENT OF THE METHOD

Preliminary experiments using 5-ml aliquots of the dilute stock platinum solution, 5 ml of concentrated hydrochloric acid, and 2 ml of the reagent solution diluted to 25 ml with water, showed that a stable absorption peak was produced at 310 mμ. The absorbance of the reagent blank measured against water was 0.080. A slit width of about 0.3 mm was required when making measurements on the platinum solutions against a reagent blank.

However, very erratic results were obtained when the stock solution was treated in any way prior to the development of the color in an effort to simulate an actual sample in practice (e.g. boiling with hydrochloric acid, addition of sulphuric acid). Furthermore, it was found that in all these cases the absorption species was not stable, tending to fade rather rapidly, the rate of fading being proportional to the amount of light to which the sample was subjected. The addition of perchloric acid to the system prior to the addition of the reagent succeeded in stabilizing the color but did not increase the precision.

It was found that very precise results could be obtained, regardless of prior treatment of the platinum solution, if sulphuric acid was added and the solution heated to expel all volatile acids (care being taken not to fume the sample).

THE REAGENT

There was no difference in the absorbance produced when 1, 2, or 4 ml of reagent were used. However, 0.5 ml of reagent was insufficient to produce maximum absorbance. In order to keep the absorbance of the reagent blank at 310 mμ at a minimum, 2 ml was chosen as the optimum quantity.

Some experiments were carried out in which the hydrochloric acid concentration of the reagent was 3 *M* instead of 1.5 *M*. This difference in acid concentration had no apparent effect on the absorbance of the resulting solutions.

Low results were sometimes obtained when the color was developed with reagent solution that was one or two days old. It is therefore recommended that fresh reagent solution be prepared daily.

EFFECT OF PERCHLORIC ACID

The addition of concentrated perchloric acid (70–72%) had the effect of stabilizing the system. Solutions which contained no perchloric acid faded quickly, especially when exposed to light.

Some experiments were carried out in which the solutions were entirely shielded from light. The rate of fading was much less in these cases but still too fast to produce reliable results. The same phenomenon was noticed by one of the authors (S.S.B.) in the development of a similar spectrophotometric procedure for rhodium with tin (II) bromide (12). In this case perchloric acid also stabilized the system.

No differences in absorbance were apparent when quantities of concentrated perchloric acid ranging from 5 to 10 ml were used. Five milliliters was chosen as the optimum amount.

When 5 ml of concentrated perchloric acid was used the yellow color of the solution developed totally within a few minutes of the addition of the reagent. The absorbance was stable for at least 4 hours and decreased by only a few per cent in 18 hours.

Another effect of the addition of perchloric acid was to produce a hypsochromic shift in the absorption band due to the tin (II) chloride reagent. The absorbance of the reagent blank containing 5 ml of perchloric acid measured against water at 310 mμ

was 0.020. Slit widths of only about 0.13 mm were required when making absorbance measurements against reagent blanks.

EFFECT OF SULPHURIC ACID

After the preliminary experiments it was evident that all platinum solutions would have to be pretreated in some manner in order to convert the platinum to some species which would react favorably with the tin (II) chloride reagent.

Boiling with hydrochloric acid and with aqua regia were tried unsuccessfully.

It was found, however, that if sulphuric acid and hydrochloric acid were added to the platinum solution and the solution heated, but not fumed, until all the hydrochloric acid was evolved, quite reproducible results could be obtained regardless of the previous history of the sample.

Quantities of concentrated sulphuric acid ranging from 5 to 10 ml produced no differences in the absorbance of replicate samples. Six milliliters was chosen as the optimum value as less than 5 ml proved to be inadequate (low results being obtained) and there is always the danger of losing some acid by fuming.

Fumed samples generally gave low results unless the precaution was taken of adding several milliliters of concentrated hydrochloric acid again and boiling until the volatile acid had been expelled.

Several samples which were fumed quite strongly and then treated with hydrochloric acid as described above gave excellent results.

RECOMMENDED PROCEDURE

Transfer the solution containing the platinum to a small beaker. Add 6 ml of concentrated sulphuric acid and 5 ml of concentrated hydrochloric acid. Cover and boil the solution gently on a hot plate until all the hydrochloric acid is expelled taking care not to bring the solution to fumes of sulphuric acid. Cool and transfer the sulphuric acid solution to a 25-ml volumetric flask with a small quantity of water. Add 5 ml of concentrated perchloric acid followed by 2.0 ml of the reagent. Dilute to volume with water and mix thoroughly. Measure the absorbance at 310 mμ using a reagent blank for comparison.

PRECISION ATTAINABLE

The mean absorbance of 12 replicate samples each containing 49.0 μg of platinum in a final volume of 25 ml was 0.397. The mean deviation of these results was 0.002 or 0.5%.

ADHERENCE TO BEER'S LAW

The solutions adhered to Beer's law throughout the whole range of concentrations tested, which was from 0.4 to 6 p.p.m. This is demonstrated in Table II.

A solution containing 0.078 p.p.m. of platinum was prepared and the absorbance measured in 5-cm quartz cells. The absorbance was 0.080 giving an absorbance to

TABLE II

Adherence to Beer's law

P.P.M. Pt (C)	Absorbance (A)	Ratio A/C
0.392	0.081	0.206
1.18	0.240	0.202
1.96	0.397	0.201
3.92	0.796	0.202
5.88	1.190	0.201

concentration ratio (when corrected for the longer path length) of 0.204. This agreed very well with the ratios obtained for the more concentrated solutions and indicated that the procedure was quite applicable for these small quantities of platinum.

The recommended range for this procedure is 0.4 to 6 p.p.m. when measurements are made in 1-cm cells, and 0.08 to 1.2 p.p.m. when measurements are made in 5-cm cells.

INTERFERENCES

Gross quantities of nitric acid can be tolerated as this acid is expelled along with the hydrochloric acid in the pretreatment of the sample.

Several metals commonly associated with platinum were tested to ascertain their effect on the procedure. The results of these tests are shown in Table III. In each case the metal was added prior to the sulphuric acid – hydrochloric acid treatment of the sample.

TABLE III

Effect of diverse metals on 49.0 μg Pt

Metal added	Absorbance
—	0.397
47.8 μg Pd^{++}	0.741
45.4 μg Ir^{++++}	0.410
49.9 μg Rh^{+++}	0.890
1.0 mg Cu^{++}	0.410
1.0 mg Ni^{++}	0.355
1.0 mg Fe^{+++}	0.406
1.0 mg Cr^{+++}	0.399

It is apparent that small quantities (up to 1 mg) of chromium, iron, and copper and equivalent amounts of iridium produce a maximum error of 3% in the estimation of platinum.

EFFECT OF USING A TUNGSTEN LAMP AND COREX CELLS

All the work reported above was done using a hydrogen lamp source and quartz cells, since 310 mμ is beyond the recommended limit (320 mμ) for Corex-glass cells. Since many laboratories do not have an ultraviolet accessory it was decided to test the procedure using a tungsten lamp source and Corex-glass cells. It was found that measurements could be made quite conveniently, the only effect being the increase in slit width from 0.13 to 0.34 mm due to the loss of energy at this wavelength.

REFERENCES

1. Davis, C. W. U.S. Bur. Mines, Tech. papers, **270** (1921).
2. Wölbling, H. Ber. **67**, 773 (1934).
3. Sandell, E. B. Colorimetric determination of traces of metals. Interscience Publishers Inc., New York. 2nd ed. 1950.
4. Ayres, G. H. and Meyer, A. S. Anal. Chem. **23**, 299 (1951).
5. Ayres, G. H. Anal. Chem. **25**, 1622 (1953).
6. Meyer, A. S. and Ayres, G. H. J. Am. Chem. Soc. **77**, 2671 (1955).
7. Milner, O. I. and Shipman, G. F. Anal. Chem. **27**, 1476 (1955).
8. Kirkland, J. J. and Yoe, J. H. Anal. Chem. **26**, 1340 (1954).
9. Barkovskiĭ, V. F. and Kul'berg, L. M. Izvest. Sektora Platiny i Drug. Blagorod. Metal., Inst. Obschei i Neorg. Khim., Akad. Nauk S.S.S.R. **29**, 141 (1955).
10. Chemical Abstracts, **50**, 9932 (1956).
11. Fraser, J. G. M.A. Thesis, University of Toronto, Toronto, Ontario, Canada. 1951.
12. Berman, S. S. and Ironside, R. Can. J. Chem. **36**, 1151 (1958).
13. De Trecco, D. R. Rev. asoc. Bioquím. arg. **15**, 355 (1951).
14. Kirkland, J. J. and Yoe, J. H. Anal. Chim. Acta, **9**, 441 (1953).
15. Komatsu, S. and Oonishi, K. J. Chem. Soc. Japan, Pure Chem. Sect. **76**, 661 (1955).

MICROCALORIMETRY OF ADSORPTION OF WATER VAPOR ON LEAD DI-IODIDE[1]

HENRY M. PAPÉE[2]

ABSTRACT

Using a microcalorimeter of the Calvet type, measurements of the total heat of adsorption of water vapor on microcrystals of lead di-iodide have been made. By comparing the results obtained with those relating to the kinetic process of surface sintering by water vapor, heats for the process of sintering were calculated. The same sintering characteristics were found for preheated and unheated samples, but it was found that the heated product adsorbs more water than the original salt. Qualitative experiments on lead mono-iodide show a different pattern of heat evolution with time, and the over-all process requires more water to reach completion than in the case of di-iodide. The heats evolved are much greater, probably partly due to the reaction of water with the surface.

INTRODUCTION

The activity of lead iodide crystals towards ice nucleation and cloud precipitation (1, 2, 3, 4, 5) has recently resulted in studies with the object of gaining insight into the mechanism of the process. Much information was obtained by Birstein (6), who studied the process using conventional adsorption techniques and established that a considerable number of layers of water molecules can be formed on lead iodide particles. A study of the phenomenon by use of microcalorimetry was attempted in this laboratory under a U.S.A.F. contract, with the object of directly measuring the energies of the steps involved.

EXPERIMENTAL

Apparatus

A microcalorimeter of the Tian–Calvet type was used, and the general pattern of the experimentation followed closely that used recently in this laboratory for the study of the process of adsorption of water vapor on sodium chloride microcrystals (7).

Reagents

Pure lead di-iodide of large specific surface areas was prepared by a method previously described, and the specific areas of the product were changed, when required, by heating (8).

Procedure

Three series of experiments* were carried out as follows:

Series 1.—In this series of measurements, the microcalorimetry was carried out using different amounts of salt originating from a batch product of an initial surface area of 2.05 m^2/g. The original material was never heated above 25° C.

Series 2.—The work was done on samples of different specific surface areas. These were obtained by heating the original product under vacuum.

Series 3.—Two measurements were carried out on samples of lead mono-iodide. This product was obtained from the di-iodide by thermal decomposition at 240° C under dry nitrogen and at atmospheric pressure. The product obtained in this way had been outgassed by pumping it to a high vacuum for several days at 25° C.

[1]*Manuscript received August 28, 1958.*
Contribution of the Department of Chemistry, University of Ottawa, Canada.
[2]*Present address: Division of Applied Chemistry, National Research Council, Ottawa, Canada.*
**All calorimetry experiments were carried out at the pressure of water vapor at 25° C. Every experiment lasted 24 hours and was performed at 25.00° C.*

RESULTS

The admission of water vapor into the cell containing lead iodide leads to a pattern of heat evolution with time, such as the one shown in Fig. 1. The process is slow and takes several hours to finish. Since it is to be expected that an initial fast process of adsorption will be followed by a slow process of sintering of the surface, and since the kinetic aspect of this second phenomenon is known, heats corresponding to both processes can be estimated graphically from the experimental curves.

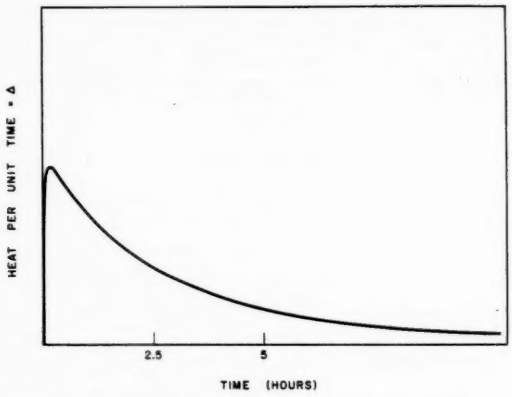

FIG. 1. Schematic plot of rate of heat evolution against time.

The decrease of lead iodide surface with time upon hydration has been shown previously (8) to follow a first-order pattern according to the equation

$$[1] \qquad \log(S-S_\infty) = -0.245t+A.$$

The symbols used in this paper are:

S: specific surface in meters^2 per gram, at time t,
t: time in hours,
S_0: initial specific surface of the product,
S_∞: specific surface of the product after long exposure to water vapor,
Q: heat of sintering,
A, a, b: constants,
w: weight of salt used in experiment,
Δ: deviation of galvanometer, approximately equal to (rate of heat evolution) $\times$ (proportionality constant).*

1st Series

The values of S_0 and S_∞ in this series were determined by B.E.T. nitrogen adsorption, and were $S_0 = 2.05$ and $S_\infty = 0.82$. Constant A of equation [1] is therefore $A = 0.090$ and

$$[2] \qquad S-S_\infty = \exp\{2.303(-0.245t+0.090)\}.$$

The process of heat evolution representative of the sintering of the crystalline surface under exposure to water vapor will follow the general equation

**Because of the slowness of the process this approximation is very good.*

$$[3] \qquad \frac{dQ}{dt} = a\left(w\frac{d(S-S_\infty)}{dt}\right) = b\Delta\,.$$

Substituting eq. [2] in [3] and taking logarithms

$$[4] \qquad \log \Delta = \log((-a/b)0.564)+\log w-0.245t+0.090$$

or

$$[4'] \qquad \log \Delta = \log w - 0.245t+K$$

in which the constant K contains all constants of eq. [4].

Figure 2 shows a series of calorimetric heat evolution curves in logarithmic form and represents examples of patterns obtained when working with different amounts of substance. The dotted line through the origin represents a line of gradient -0.245, which was obtained by measuring the kinetics of sintering by B.E.T. nitrogen estimation of surfaces at different times. Good agreement between the two methods can be seen.

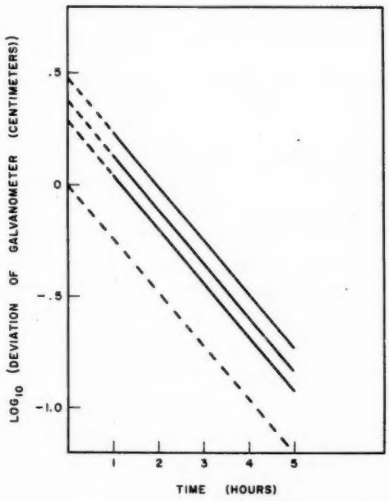

FIG. 2. Plot of decimal logarithm of rate of heat evolution against time, in microcalorimetry salt container. The lines represent experiments with different weights of the product. The dotted line gives the slope of the process as obtained by other means, and using B.E.T. surface measurements.

It was noticed that the curves become linear after about 30 minutes, initial irregularities being partly due to the heat of adsorption which superposes itself on the heat of sintering of the surface. Furthermore, for rapid initial heat evolution, the expression for Δ is no longer accurate enough (see also ref. 9). Because of this, the curves are shown after the first hour has elapsed, by which time they obey with good approximation the law of eq. [1].

Extrapolating the plots to zero time, the hypothetic value of the parameter Δ at the start of the process can be obtained. Under such conditions eq. [4'] becomes

$$[4''] \qquad [\log \Delta]_{t=0} = \log w+K.$$

Thus constant K can be obtained. Based on 9 experimental values it is found to be:

$$K = -0.08 \pm 0.02.$$

Substitution of the value for K in eq. [4'] gives, for unit weight of salt,

$$[4'''] \qquad \Delta = 10^{(-0.245t - 0.08)}.$$

Taking the calibration coefficients of the instrument into account, and integrating eq. [4'''] between zero and infinite time, the value of 0.084 ± 0.006 cal/g is obtained, and corresponds to the sintering of the surface of 1 g of lead di-iodide from 2.05 to 0.82 m^2/g.*

The over-all heat of the process is obtained by planimetric integration of the recorded curves. The results obtained are shown in Fig. 3. The heat evolved by 1 g of di-iodide when put in contact with water vapor is given by the slope of the line and is found to be 0.179 ± 0.007 cal.

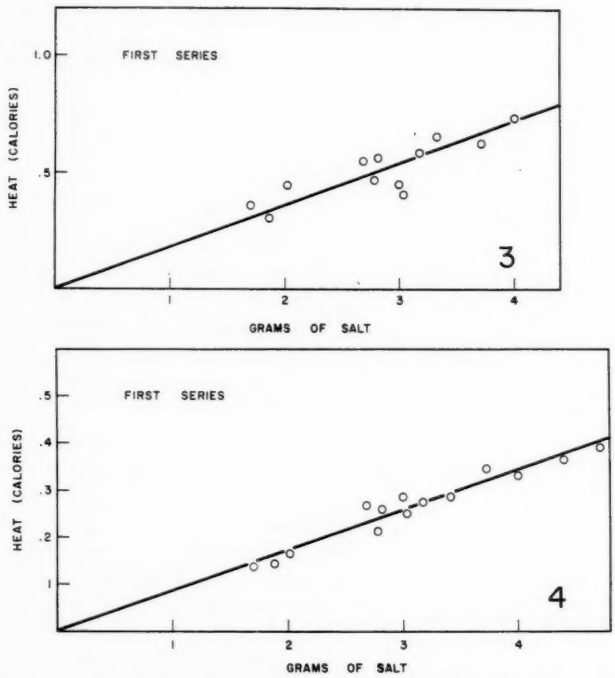

FIG. 3. Plot of over-all heat obtained by planimetric integration of areas under curves recorded, for cell in which salt was contained, against weight of salt.
FIG. 4. Plot of heat absorbed in cell from which water was evaporating, against weight of salt.

The evaporation of water necessary to induce the process described above was followed simultaneously, and the recorded curves showed rapid initial evaporation of water, but this was of short duration and only very small amounts of water evaporated per unit time after several hours. No relationship between kinetics of sintering and the amount of water used could be established. The heats of evaporation of water were therefore estimated by planimetric integration of the area obtained experimentally, and the

*The values quoted in the present paper are 'thermochemical' calories, equal to 4.1840 joules. The instrument was calibrated electrically.

results representing the over-all process are shown in Fig. 4. The slope of the line gives the heat of evaporation of water required for the process of adsorption on, and sintering of, the salt, and is 0.086 ± 0.002 cal/g.

Since the specific surface of the salt is equal to 0.82 m^2/g, at the end of the process, the amount of the water adsorbed by unit surface will be deduced from the heat absorbed and the latent heat of evaporation of water. The heat of evaporation of the amount of water used in the process just discussed is

$$(0.086 \pm 0.002)/0.82 = 0.105 \pm 0.0024 \text{ cal/m}^2$$

and assuming 10.6 $Å^2$ for the area occupied by a water molecule, the coverage is calculated to be 0.68 ± 0.02 layers.

*2nd Series**

Since samples of different initial surface areas were used in this case, eq. [1] will become

$$[5] \qquad (S - S_\infty) = (S_0 - S_\infty) \exp(-0.5642t),$$

which after substitution in eq. [3] becomes on taking logarithms

$$[6] \qquad \log \Delta = -0.245t + \log\{w(S_0 - S_\infty)\} + K$$

where K is constant.

Experiments were performed on 4 batches of salt, each of which was heated for 24 hours, to a different temperature. The specific areas of the products were determined by B.E.T. nitrogen adsorption both before exposure to water vapor and after long periods of exposure. Plots of ($\log \Delta$) against time were found to follow linear patterns of the type previously discussed and the gradients of the lines were the same as before. From these K is obtained following the method previously described. Seven separate runs give $K = -0.25 \pm 0.03$. This shows that sintering of lead di-iodide crystals that were moderately heated under vacuum by exposure to water vapor proceeds along a pattern similar to that of unheated salt. Substitution of the calculated value of K in eq. [6] leads after rearrangement and integration of Δ between zero and infinite time to a value of 0.056 ± 0.006 cal and represents the heat that is developed when 1 g of

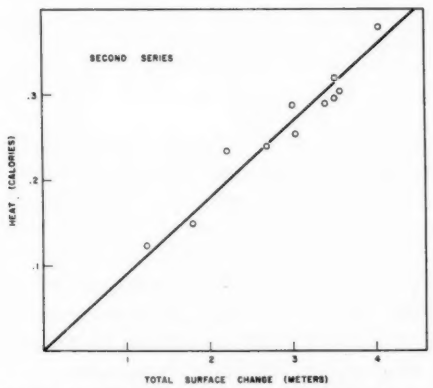

FIG. 5. Plot of over-all heat obtained by planimetric integration of areas under curves recorded for cell in which salt was contained, against $w(S_0 - S_\infty)$.

**Salt sintered by heat under vacuum in the range between 50 and 150° C.*

salt sinters by 1 m². Planimetric integration of the over-all phenomenon leads to results shown in Fig. 5, where the heat obtained is plotted against $w(S_0-S_\infty)$. The over-all heat that is evolved when the total surface changes by 1 meter is obtained from the slope of the line, and is 0.089 ± 0.002 cal.

As in the previous series, the heats of evaporation of water required to induce the phenomena described above were estimated by planimetric integration of the over-all areas under the curve. In contrast to Series 1, the phenomenon seemed to last longer, and the rate of heat evolution after 24 hours, although very small, could still be detected, and was fairly constant over the last 10 hours. However, no counterpart of this could be detected in the salt container. The heats are given in Fig. 6, which shows furthermore that the amount of water used in the process is a function not of the surface change but of the final surface S_∞.

The slope of the line gives the heat per unit surface, and is in this case 0.278 ± 0.004 cal/m² and the corresponding coverage is 1.79 ± 0.03 layers.

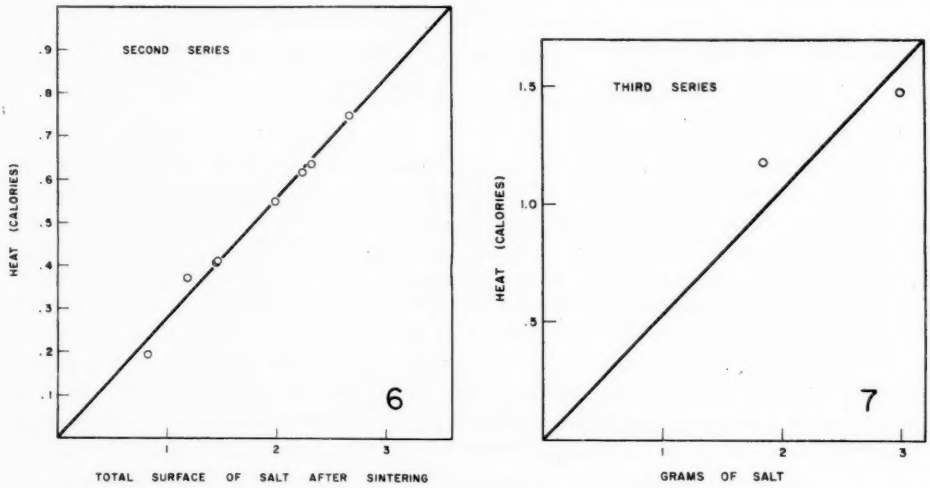

FIG. 6. Plot of heat absorbed in cell from which water was evaporating against product of weight of salt multiplied by its surface area after hydration.
FIG. 7. Plot of over-all heat evolved in salt container against weight of salt.

3rd Series

Although the conversion of the lead di-iodide by heating at 240° under dry nitrogen gave a mono-iodide 98.6% pure, it is not certain whether the subsequent outgassing in vacuum at 25° C liberated completely the surface of the product from elementary iodine which must have certainly been adsorbed there. The results reported in this series are therefore to be considered only as a by-product of the main experimentation, and are reported for the purpose of a tentative comparison with the previous data. Furthermore, the preparation of lead iodide for cloud-seeding experiments (cf. refs. 1, 2, 3, 4, 5) must invariably result in partial alteration of the salt (8). It is thought therefore that a brief discussion of the results obtained in this series is justified, since it might be helpful towards further studies of the subject.

Two runs were made on samples originating from the same batch. This consisted of salt of specific surface area of 0.84_8 m²/g. No determinations were made of the surface after hydration.

Plots of [log Δ] against time in both cases gave straight lines of gradients -0.12_2 hours^{-1}.

Heats evolved in the salt cell were estimated planimetrically and are plotted in Fig. 7 against the weight of salt. The line was fixed through the origin, and its gradient is 0.53 ± 0.06 cal/g.

Finally, the heat absorbed in the water container is given in Fig. 8 as a function of the amount of salt on which adsorption was carried out. The slope of the line is 0.31 ± 0.08 cal/g $= 0.4 \pm 0.1$ cal/m². This corresponds to the amount of water required to form 2.4 ± 0.61 layers.

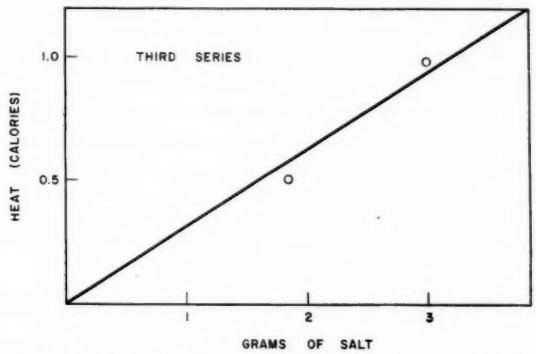

FIG. 8. Plot of heat absorbed in cell from which water was evaporating, against weight of salt.

DISCUSSION

The results obtained are summarized in the table.

Series	Nature of salt	Heat of sintering of surface under exposure to water vapor, cal/m²	Total heat measured, cal/m²	Heat of evaporation of water, cal/m² of sintered salt	Water coverage layers
1	PbI_2 salt handled only at temperatures below 25° C	0.068 ± 0.005	0.145 ± 0.006	0.105 ± 0.002	0.68 ± 0.02
2	PbI_2 salt heated between 50 and 150° C before adsorption measurements	0.056 ± 0.006	0.089 ± 0.002	0.278 ± 0.004	1.79 ± 0.03
3	PbI obtained from PbI_2 by thermal decomposition		0.53 ± 0.06	0.31 ± 0.08	2.4 ± 0.6

It can be seen that for PbI_2 no difference in the kinetic pattern of sintering of the surface by exposure to water vapor takes place, whether the surface was moderately heated or not, since the rate plots obey the same law. As expected, this is different in case of lead mono-iodide, although the general pattern probably remains of the first order with respect to surface.

In the case of preheated samples, the results are slightly lower than in the case of samples that were handled at room temperature. It is interesting to note, however, that the product which has been 'activated' by heat adsorbs a considerably larger amount of water than a non-activated salt. Since the heat evolved in the salt container in the first two series of experiments does not indicate condensation of water on the surface, or chemical reaction such as hydrolysis etc., this result can be tentatively interpreted in terms of 'electrostriction' of water molecules around charges appearing in the original area of imperfections induced by heat, after the surface is placed in contact with water vapor. Detailed analysis of the absorption of heat in the water container with time is indicative of a similar pattern. It can be seen that the rate drops almost to zero after a few hours, and then gradually slightly increases. A slow downward trend of the rate is observed again after about 20 hours, but a small process of heat absorption can be detected in most cases even after the period of 24 hours. If similar mechanism occurs in the case of silver iodide, which, like lead iodide is known to be an excellent ice-nucleating agent, the time lag (10) in formation of ice crystals after injection into supercooled water vapor might tentatively be explained along these lines.

The heat evolved in the salt container is much larger in the case of lead mono-iodide, than in the case of the previous series. Although the amount of water used in the process is also larger it does not explain the difference between the values obtained and those related to the process occurring on lead di-iodide. The result points therefore to

(i) a different heat of sintering of the surface of the product; and/or,
(ii) condensation of water on the surface; and/or,
(iii) hydrolysis of the salt.

The number of water layers on the surface is found to be very small in comparison with the measurements of Birstein (6) and the heats obtained, although of the same order of magnitude, are lower than his isosteric data. This might be due to one or both of the following factors:

(i) Small leaks in our calorimetry system, which would reduce the number of layers adsorbed.
(ii) Small temperature differences between the source of water vapor and the salt in Birstein's system. Calibration evidence points in our case to a thermal stability of the apparatus to within 10^{-5} degrees centigrade over long time periods.

Since all of our experiments were performed in the same system, and without disturbing the apparatus, it is thought that experimental abnormalities would show up in individual cases, and major leaks would be therefore easily detected. No sign of this was found during the experimentation. Furthermore, as implied previously, the process does not appear to be controlled by diffusion of H_2O. Because of this controversy, however, it appears that the relative behavior towards adsorption of water vapor of the three products under study is of more immediate significance than the direct data obtained.

ACKNOWLEDGMENTS

The author is indebted to Drs. G. C. Benson, J. A. Morrison, and A. R. Blake of the National Research Council for many helpful discussions, and to Professor K. J. Laidler of this Department for reading the manuscript and his interest in this project. The work was performed under a contract between the U.S. Air Force Cambridge Research Center, and the University of Ottawa.

REFERENCES

1. SCHAEFER, V. J. J. Meteorol. **11**, 417 (1954).
2. HASLER, C. L. and SPALDING, G. R. Artificial stimulation of rain (Symposium). Pergamon Press, New York. 1957. p. 369.
3. BIRSTEIN, S. J. and ANDERSON, C. E. J. Meteorol. **12**, 68 (1954).
4. PRUPPACHER, H. R. and SÄNGER, R. Z. angew. Math u. Phys. **VI**, 407 (1955).
5. FUKUTA, N. J. Meteorol. **15**, 17 (1958).
6. BIRSTEIN, S. J. Geophys. Research Paper No. 32 (1954).
7. PAPÉE, H. M. and LAIDLER, K. J. Can. J. Chem. **36**, 1338 (1958).
8. PAPÉE, H. M. Can. J. Chem. **36**, 1443 (1958).
9. CALVET, E. and PRAT, H. Microcalorimetric, applications physiques et biologiques. Masson et Cie, Paris. 1956. p. 66.
10. VONNEGUT, B. Chem. Revs. **44**, 277. (1949).

POTATO X VIRUS

PART III. LIGHT SCATTERING STUDIES[1]

M. E. REICHMANN

ABSTRACT

Light scattering studies were made on a non-aggregated potato X virus preparation. The data are consistent with a cylindrical model 5400 Å long having a molecular weight of 35×10^6. The weight average length of 4700 Å was determined from the high angle measurements. The low value of the weight average length, as compared with the length of the most frequent particle from electron microscopy, is interpreted in terms of a slight tendency to aggregate side-by-side. The insignificant extent of this aggregation is demonstrated by a direct evaluation of the weight average diameter. The value of 109 Å obtained is only 9% higher than the number average diameter reported in the literature.

INTRODUCTION

The spontaneous end-to-end aggregation of potato X virus in the process of purification has been the main obstacle in physicochemical studies of its properties in solution. The molecular weight of this virus has not been previously determined. The value of 37.5×10^6 used by Niu *et al.* (1) from data of Bode and Kohler (2) does not appear in the original paper, and was probably calculated from the electron microscope dimensions. These dimensions have now been corrected by Bode and Paul (3). Loring estimated the molecular weight to be 26×10^6 from sedimentation and viscosity measurements (4). Assuming a cylindrical shape, Loring also derived the dimensions of the virus particle as being 98 Å in diameter and 4330 Å in length.

From flow-birefringence studies on the virus in untreated tobacco sap and from a partially fractionated preparation, we reported a particle length of 5400–6200 Å (5).

The diameter of the dry virus particle has been determined from electron micrographs as 160 Å (6) and 100 Å (7). More recently, the length of the most probable particle has been given as 5000–5250 Å, and the diameter of 100 Å was confirmed (3).

In a previous publication, we reported a method for preparing purified, non-aggregated potato X virus from tobacco sap (8). The availability of this method facilitated further studies of the properties of the virus in solution, which are the subject of this paper.

MATERIAL AND METHODS

The method of virus preparation used in these studies has been described (8). Virus concentrations were determined by nitrogen analysis and checked by measurements of optical density at 260 mμ in 0.1 phosphate buffer pH 5.7 (8).

The angular distribution of the intensity of scattered light was measured in a Brice–Phoenix Universal Light Scattering Photometer manufactured by Phoenix Precision Instrument Co., Philadelphia, Penn. (9), using the cylindrical cell furnished with the instrument. The symmetry of the envelope of the cell was checked with a fluorescein solution and the cell was calibrated with a Ludox solution (10, 11). Reflectance corrections (12, 13) were made as described in other publications (10, 11). Dust-free solvents were obtained by filtration through a U.F. sintered-glass filter. Dust was removed from the virus solution by centrifuging the stock solutions in a Servall centrifuge at $15{,}000 \times g$ for 30 minutes. A small amount of virus was precipitated under these conditions. Light

[1]*Manuscript received September 22, 1958.*
Contribution No. 6, Chemistry Division, Science Service, Canada Department of Agriculture Research Laboratory, Vancouver, B.C.

scattering measurements were therefore also made on solutions that were centrifuged 20 and 60 minutes. Within the error of the experiment the same data were obtained, indicating that no fractionation of the virus material had taken place. Although the light scattering measurements were made at room temperature, the virus stock solution was kept in the cold. The manner in which dilutions were made has been described (14).

The specific refractive index increment, dn/dc, was determined with a Brice–Speiser differential refractometer (15). As mentioned previously (8), the non-aggregated virus was insoluble in water in the absence of electrolytes. Errors can be anticipated in refractive index increments determined in the presence of electrolytes as a result of differences in electrolyte concentrations between dialyzate and solvent due to the Donnan term. It was therefore preferable to measure the refractive index increment of an aggregated preparation obtained by 5 cycles of high and low speed centrifugation in distilled water. The dn/dc value found was 0.189 ± 0.004.

THEORETICAL CONSIDERATIONS

The relationship between the angular distribution of the intensity of scattered light and the molecular parameters in the case of rigid rods has been discussed (16). It has been shown that the weight average molecular weight and the z average length can be determined provided that the parameter $x^2 = (2L\pi/\lambda' \sin \theta/2)^2$ does not exceed 15 in the low angle range of measurements. Table I gives the values of x and x^2, for a monodisperse rod whose length L is 5000 Å, in the angular range $\theta = 30°$–$90°$ at a wave length $\lambda' = 3280$ Å ($= 4360$ Å$/1.33$). Between the angles 30° and 50°, x^2 is smaller than 15 and Kc/R_θ should be linear in $\sin^2 \theta/2$. In the case of a polydisperse system with a number average length of 5000 Å, the downward curvature will set in at lower angles, depending on the width of the distribution function (17). It should, however, be possible to determine the z average length and the weight average molecular weight of potato X virus, provided only that the polydispersity is not too great.

TABLE I

Theoretical values of the parameter x (see text) for angles at which light scattering measurements were made. Monodisperse rigid rods 5000 Å long. Wave length (4360/1.33) Å

θ	x	x^2
30°	2.50	6.25
35°	2.90	8.40
40°	3.30	10.90
45°	3.70	13.70
50°	4.10	16.80
60°	4.80	23.00
70°	5.50	30.25
80°	6.20	38.45
90°	6.80	46.25

From the asymptotic value of Kc/R_θ vs. $\sin \theta/2$, the number average length and molecular weight can be determined (18, 19, 20). In addition, if the weight average molecular weight is known, the weight average length can also be evaluated (16). The approximations made in the theoretical treatment require that $x > 2$. As can be seen from Table I this condition is fulfilled for a monodisperse particle 5000 Å long over the

entire range of angles tabulated. In the case of polydispersity the smaller particles may contribute significantly to the scattering and cause a deviation from linearity at low angles.

RESULTS AND DISCUSSION

Figures 1 and 2 represent typical Zimm plots of the angular distribution of the intensity of light scattered by four different virus concentrations in 0.1 *M* potassium chloride and 0.005 *M* sodium citrate, respectively. The plots are practically linear between 30° and 50°, and the weight average molecular weight and z average length were determined from the intercept and slope respectively. To check the reproducibility of the purification procedure three different virus preparations were investigated. The molecular weights were $34–36\times10^6$ and the length was 5300–5500 Å. Within the error of the experiment, the data in 0.005 *M* sodium citrate were the same as in 0.1 *M* potassium chloride. Therefore, no change in shape occurred, although the net charge on the virus particles increased as indicated by the increase of the second virial coefficient. The rigidity of the virus particle, as demonstrated previously by flow-birefringence measurements (5), was thus confirmed.

Figure 3 represents a plot of $(Kc/R_\theta)_{c=0}$ vs. sin $\theta/2$ corresponding to the data in Fig. 1. The linear relationship was followed. The slope of the regression line corresponds to

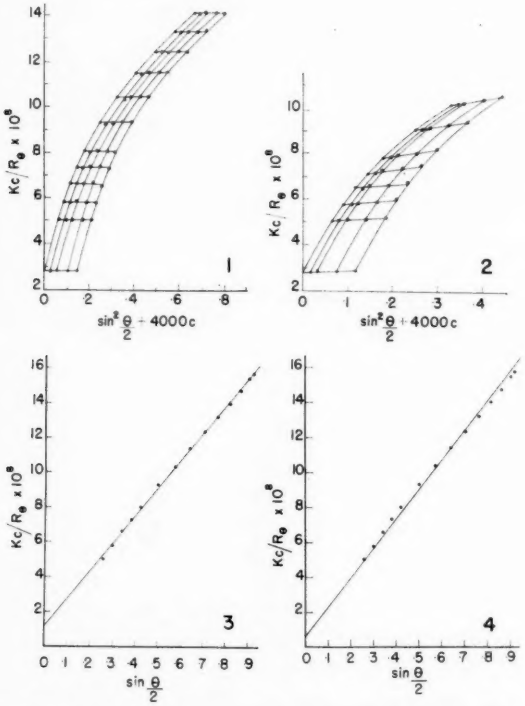

FIG. 1. Typical Zimm plot of light scattering data of potato X virus in 0.1 *M* potassium chloride.
FIG. 2. Typical Zimm plot of light scattering data of potato X virus in 0.005 *M* sodium citrate.
FIG. 3. The angular distribution of the intensity of scattered light from potato X virus solutions in 0.1 *M* potassium chloride as a function of sin $\theta/2$. Virus concentration was extrapolated to zero. Solid line is regression line: $(Kc/R_\theta)_{c=0} = (0.12+1.60 \sin \theta/2)\times10^{-7}$.
FIG. 4. Same data as in Fig. 3. Solid line is regression line with average slope 1.675×10^{-7} (see text).

1.60×10^{-7}. Taking the weight average molecular weight from Fig. 1 as 35.7×10^6 a weight average length of 4700 Å was calculated. From the best fit of the experimental values of $1/P$ vs. $\sin^2\theta/2$ with a theoretical curve at high angles, the value of 4800 Å was derived. As could be anticipated (16) this value is very close to the weight average length.

The uncertainty in the determination of number averages has been discussed (16). This can be illustrated with the data in Fig. 3. From the intercept and slope of the straight line in Fig. 3 the following number averages were derived: molecular weight 17×10^6, length 2200 Å. Obviously these data are unreasonably low. A more reasonable value can be obtained in the following manner. Taking the best straight lines through the points between 30° and 60° and between 90° and 135° separately, an average slope of 1.675×10^{-7} can be evaluated. Using this as the slope, the regression line through all the points will be given by $(Kc/R_\theta)_{c=0} = (0.063+1.675\sin\theta/2)\times10^{-7}$ (Fig. 4). The number average molecular weight and length from this line would be 32×10^6 and 4400 Å respectively. It should be noticed that while the slope has been changed by 5%, the molecular parameters increased by a factor of two. On the other hand the weight average length from Fig. 4 would be 4900 Å, not very different from the value derived from Fig. 3.

It was somewhat surprising that the weight average length was found to be lower than the most probable particle length as determined from electron microscopy. Inspection of light scattering data on tobacco mosaic virus will show that a similar discrepancy can also be found there (21, 22). We have pointed out that this can be anticipated in the case of polydispersity in thickness (16). The low value of the number average length could therefore be interpreted as indicating a tendency for side-to-side aggregation. The extent of this aggregation can be estimated by evaluating the radius of the cylinder, rather than the weight average length, from the slope in Fig. 3. The particle width determined from this slope should be independent of the distribution of length (19) and if the shape is known, can be determined unambiguously. Assuming a cylindrical shape the weight average radius is given by (16): $\sqrt{(r^2)_w} = \sqrt{4/\pi\rho N\lambda'\times(\text{slope})} = 54.5$ Å giving a diameter of 109 Å. This is only 9% higher than the number average value determined with the electron microscope.

The difference between the weight average and z average length, a measure of the total polydispersity, was relatively small (15%). We would therefore anticipate a sharp distribution function of lengths in our preparation.*

Assuming a cylinder 5100 Å long, 100 Å in diameter (3), with a partial specific volume of 0.73 ml/g (23), the predicted molecular weight is 33×10^6, in good agreement with the light scattering data. The value of 26×10^6 calculated by Loring (4) can be considered only as a rough estimate. The sedimentation constant and viscosity on which this estimate was based were determined at finite concentrations and the viscosity was measured at relatively high gradients (Ostwald Viscometer). From what is known about the dependence of the sedimentation constant on concentration and the viscosity on gradient in the case of large elongated particles, it is obvious that both values must have been too low. This is also apparent from the particle length derived from these data, which is 4330 Å.†

Finally, it should be mentioned that as in the case of tobacco mosaic virus (21), the

*A comparison with a uniform tobacco mosaic virus preparation can be made (21, 22). The difference in length determined from high values of $1/P$ and from the limiting slope of this function was 10%. In our potato X virus preparation the difference was 13% (4800 Å and 5460 Å).

†We have also determined the molecular weight from sedimentation–diffusion measurements. Because of the very slow rate of diffusion, the diffusion constant could not be determined accurately. We found, however, that at low virus concentrations the boundary remained Gaussian over a period of 8 days in the Spinco electrophoresis–diffusion apparatus. We obtained $D_{20} = 3.2\times10^{-8}$. The molecular weight obtained from this value and $S_{20} = 117.8\times10^{-13}$ (8) was 33×10^6.

light scattering particle length of potato X virus is significantly lower than the hydrodynamic length determined from flow birefringence (5). The inadequacy of the ellipsoid of revolution to represent a cylinder has been discussed in detail (21). Since the same considerations apply in the case of potato X virus, a similar discrepancy between the light scattering and flow-birefringence length can be anticipated.

REFERENCES

1. NIU, C. I., SHORE, V., and KNIGHT, C. A. Virology, **6**, 226 (1958).
2. BODE, O. and KOHLER, E. Naturforsch, **76**, 598 (1952).
3. BODE, O. and PAUL, H. L. Biochim. et Biophys. Acta, **16**, 343 (1955).
4. LORING, H. S. J. Biol. Chem. **126**, 455 (1938).
5. REICHMANN, M. E. Can. J. Chem. **36**, 1603 (1958).
6. TAKAHASHI, N. W. and RAWLINS, T. E. Am. J. Botany, **33**, 740 (1946).
7. KLECZKOWSKI, A. and NIXON, H. L. J. Gen. Microbiol. **4**, 220 (1950).
8. REICHMANN, M. E. Can. J. Chem. **37**, 4 (1959).
9. BRICE, B., HALVER, M., and SPEISER, R. J. Opt. Soc. Am. **40**, 768 (1950).
10. HOLTZER, A. M., BENOIT, H., and DOTY, P. J. Phys. Chem. **58**, 624 (1954).
11. BOEDTKER, H. and DOTY, P. J. Phys. Chem. **58**, 968 (1954).
12. SHEFFER, H. and HYDE, J. C. Can. J. Chem. **30**, 817 (1952).
13. OTH, A., OTH, J., and DESREUX, V. J. Polymer Sci. **10**, 551 (1953).
14. REICHMANN, M. E., BUNCE, B. H., and DOTY, P. J. Polymer Sci. **10**, 109 (1953).
15. BRICE, B. and HALVER, M. J. Opt. Soc. Am. **41**, 1033 (1951).
16. REICHMANN, M. E. Can. J. Chem. **37** (1959) (In press).
17. GOLDSTEIN, M. J. Chem. Phys. **21**, 1255 (1953).
18. HOLTZER, A. M. J. Polymer Sci. **17**, 432 (1955).
19. CASASSA, E. F. J. Chem. Phys. **23**, 596 (1955).
20. STACEY, K. A. Light scattering in physical chemistry. Butterworth Scientific Publications, London. 1956.
21. BOEDTKER, H. and SIMMONS, N. S. J. Am. Chem. Soc. **80**, 2550 (1958).
22. HALL, C. E. J. Am. Chem. Soc. **80**, 2556 (1958).
23. LAUFFER, M. A. and CARTWRIGHT, T. E. Arch. Biochem. Biophys. **38**, 371 (1952).

FREE RADICALS BY MASS SPECTROMETRY

XV. THE MERCURY-PHOTOSENSITIZED DECOMPOSITION OF FORMIC ACID, ACETIC ACID, AND METHYL FORMATE[1]

P. KEBARLE[2] AND F. P. LOSSING

ABSTRACT

The Hg($^3P_1$) photosensitized decomposition of formic acid proceeds by two intramolecular rearrangement reactions, leading respectively to H_2O and CO, and to H_2 and CO_2. No free radicals are produced. The decomposition reactions of methyl formate and of acetic acid proceed predominantly by the formation of free radicals, but intramolecular rearrangements also occur to a significant extent. For both these latter compounds the evidence suggests the occurrence of two modes of dissociation into free radicals:

$$RC(=O)—OR' + Hg^* \rightarrow RC(=O) + OR' + Hg$$

$$RC(=O)—OR' + Hg^* \rightarrow R + C(=O)—OR' + Hg.$$

No evidence for the alternative mode of dissociation

$$RC(=O)—OR' + Hg^* \rightarrow RC(=O)—O + R' + Hg$$

was found.

INTRODUCTION

In the photolytic decomposition of molecules of the type RCOOR′, several types of primary steps appear to occur. A bond rupture to give two free radicals may occur at one of several bonds, and an intramolecular shift of a hydrogen atom to give two molecular products appears to be also an important mode of decomposition.

The simplest molecule of the RCOOR′ type, formic acid, has been examined both by direct photolysis and by mercury photosensitization. Ramsperger and Porter (1) found that in the region 2260 Å – 2500 Å two molecular rearrangements occurred:

$$HCOOH + h\nu \rightarrow CO + H_2O \ (64\%), \qquad [1]$$

$$HCOOH + h\nu \rightarrow CO_2 + H_2 \ (36\%). \qquad [2]$$

Reaction [1] accounted for 64% of the molecules reacted, and reaction [2] accounted for the remainder.

Bates and Taylor (2) examined the mercury-photosensitized decomposition at 2537 Å and found a similar situation:

$$Hg^* + HCOOH \rightarrow Hg + CO + H_2O \ (76\%), \qquad [3]$$

$$Hg^* + HCOOH \rightarrow Hg + CO_2 + H_2 \ (24\%). \qquad [4]$$

The same products were found by Herr and Noyes (3). A more comprehensive examination of the direct photolysis over the region 1900–2540 Å was made by Gorin and Taylor (4). They found the ratio of reaction [1] to reaction [2] to vary with wavelength, shorter wavelengths and higher temperatures favoring reaction [2]. Molecules of the dimeric

[1]*Manuscript received September 16, 1958.*
Contribution from the Division of Pure Chemistry, National Research Council, Ottawa, Canada.
Issued as N.R.C. No. 5012.
[2]*National Research Council of Canada Postdoctorate Fellow 1956–58.*

form of formic acid $(HCOOH)_2$ decomposed solely into CO_2 and H_2 at all wavelengths used. From experiments with parahydrogen the authors concluded that a primary split

$$HCOOH + h\nu \rightarrow H + COOH \quad [5]$$

did not occur to any significant extent. A similar conclusion was reached by Burton (5), who found that antimony mirrors were not removed in the direct photolysis. The only evidence for a free radical mode of dissociation comes from the observations of Terenin (6) of the OH radical in emission during photolysis.

The next simplest molecules of the RCOOR′ type are methyl formate, $HCOOCH_3$, and acetic acid, CH_3COOH. Very little data is available on the photodecomposition of methyl formate. Ausloos (7) found the photolysis of liquid methyl formate to yield CH_4, CO_2, CO, and H_2 as products. No runs on gaseous methyl formate were reported.

The photolysis of CH_3COOH was examined by Burton (8), who, on the basis of mirror removal experiments, rejected the primary split

$$CH_3COOH + h\nu \rightarrow CH_3 + COOH \quad [6]$$

in favor of the process

$$CH_3COOH + h\nu \rightarrow CH_3COO + H. \quad [7]$$

No CH_3 radicals or radicals such as CH_3CO which would decompose to form CH_3 could be detected. A molecular process

$$CH_3COOH + h\nu \rightarrow CH_4 + CO_2 \quad [8]$$

was reported by Farkas and Wansbrough-Jones (9). A recent investigation of the photolysis by Ausloos and Steacie (10) using deuterium labelling provides good evidence that reaction [8] occurs to the extent of about 10%. Three other primary processes were possible, reactions [6], [7], and a split into acetyl and hydroxyl radicals:

$$CH_3COOH \rightarrow CH_3CO + OH. \quad [9]$$

From the behavior with temperature, it was evident that dimers $(CH_3COOH)_2$ played no part in the primary process.

EXPERIMENTAL

The reactor and mercury lamp have been described in previous publications (11, 12). A new ion source, similar in some respects to that used by Leger in a rapid-scan mass spectrometer (13), was constructed for this work and is shown in Fig. 1. It possessed a number of features designed to improve the sensitivity of detection for oxygenated radicals. The plates of the source were rectangular in shape, 2 in. long by $\frac{5}{8}$ in. wide. The side walls of the ionization chamber facing the orifice and the pumping lead consisted only of tungsten mesh screen of high transparency (> 90%). Owing to the open construction of the ionization chamber relatively little obstruction was placed in the flight path of a molecule from the orifice to the pumping lead, and the proportion of radicals ionized after colliding with surfaces should consequently be much less than in the design used previously. Although this feature is probably of little advantage for radicals which are not reactive toward metal surfaces, such as the alkyl radicals (14), it might be expected that oxygenated radicals are more sensitive to such collisions. A further advantage, that fewer molecules are able to enter the analyzer tube, permitted a higher differential pressure to be maintained between the ionization chamber and the analyzer tube. A rough estimate based on the ratio of the pressures in the pumping leads in the two designs indicated a four- or five-fold improvement in this ratio.

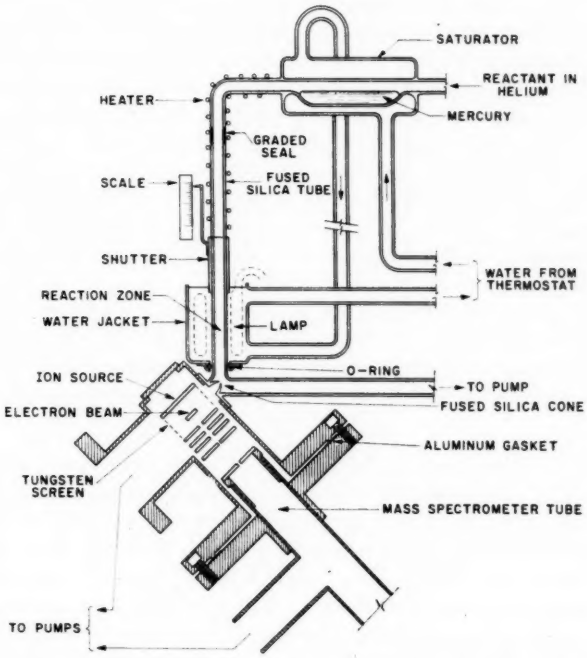

FIG. 1. Diagram of photochemical reactor and mass spectrometer ion source.

MATERIALS

The formic acid, methyl formate, and acetic acid were samples of commercial grades of high purity which were carefully degassed before using. The deuterated methyl formate and acetic acid were kindly supplied by Dr. L. C. Leitch.

RESULTS AND DISCUSSION

Before discussing the results in detail, it will not be amiss to point out some differences in reaction conditions between the reactor used in this work and those used in conventional photochemical experiments. In previous investigations using the same apparatus a number of compounds were found to decompose by a primary split into free radicals. In all these cases no evidence was found for the occurrence of reactions between free radicals and the parent compound. The reason for this is easily understood. Such abstraction reactions require an activation energy of 8–10 kcal/mole while radical combination and disproportionation reactions require considerably less, probably 0–1 kcal/mole. At 55° C the rate constant for abstraction reactions is consequently only 10^{-5} to 10^{-6} as large as for radical–radical reactions. In conventional photochemical systems this large factor is counterbalanced by the very small steady-state concentration of radicals relative to the parent compounds, and an abstraction reaction may consequently be of great importance. In the reactor used in this work the situation is quite different. For example, in the mercury-photosensitized decomposition of acetone (12) the concentration of methyl radicals was about $\frac{1}{10}$ of the concentration of acetone during most of the contact time. With such relatively high concentrations of radicals, radical–radical interactions will be

at least 10^4 times faster than reactions of radicals with the parent compound, and the formation of radicals or other products by such reactions can be neglected.

The situation is similar in many respects to that produced in the flash photolysis experiments of Khan, Norrish, and Porter (15) in which radical–radical reactions were considered to predominate. It is of interest to note that in the flash experiments the average decomposition was about 1% for a flash duration of about 10^{-4} second. No chains were found to participate and the entire decomposition resulted from the primary act. In the present system the extent of decomposition was 10–20% of the parent compound in a time of 10^{-3} second. The rates of radical production and consequently the ratio of concentrations of radicals and parent compound in the two reaction systems are, therefore, of about the same order.

A further consequence of the high concentration of radicals in the present experiments is the possibility of reaction of a radical with an excited mercury atom, leading to dissociation of the radical. Such reactions had to be postulated for allyl radicals (11) and for acetyl radicals (12) to explain the formation of certain products.

Formic Acid

In the mercury photosensitized decomposition of formic acid vapor, only four products were found: CO, H_2O, CO_2, and H_2. No free radicals could be detected. The amounts of products formed at two partial pressures of formic acid, and at various positions of the shutter (i.e. various exposure times) are given in Table I. Some difficulties were encountered in measuring the sensitivity coefficients for formic acid and for water, on account of the absorption effects of the glass surfaces in the sample line, and the mass balances of the products are therefore somewhat different from 100%. The analysis of formic acid and of the products at short exposure times were quite uncertain since only small changes in the composition were produced. The amounts of HCOOH decomposed and of products formed are shown in Figs. 2 and 3, as a function of the exposure time. It is evident that within the experimental error $\phi_{CO} = \phi_{H_2O}$ and $\phi_{CO_2} = \phi_{H_2}$. The equality of these pairs of products and the lack of variation with exposure time indicates that the only modes of decomposition are the two intramolecular rearrangement reactions found in earlier work, reactions [3] and [4]. From the present data the ratio of occurrence of these two reactions is about $\phi_3/\phi_4 \approx 70/30$. This ratio is slightly different from the

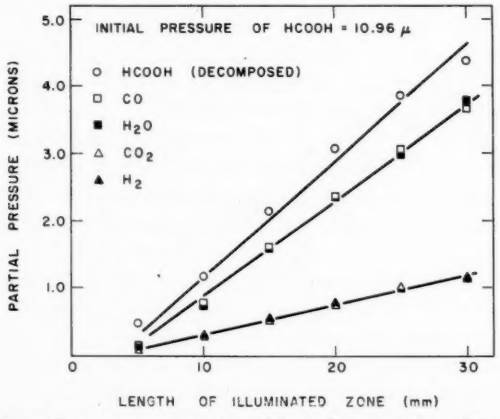

FIG. 2. Products from mercury-photosensitized decompositon of formic acid vapor.

ratio 76–24 found by Bates and Taylor, but in view of the uncertainty in the analysis of HCOOH and H_2O in the present work it is not entirely certain that the difference is significant. The present work does, however, confirm the view that a dissociation into free radicals or into an atom and a free radical occurs to a very small extent or not at all.

TABLE I

Decomposition of formic acid

Length of illuminated zone (mm)	Formic acid (μ) present		Formic acid decomposed		Products (μ)				Mass balance (%) for:			$CO_2 + H_2$
	Lamp off	Lamp on	μ	%	CO	H_2O	CO_2	H_2	C	O	H	$CO + H_2O$
5	10.96	10.48	0.48	4.38	0.14	0.13	0.10	0.06	(50)	(49)	(40)	(0.59)
10	10.96	9.79	1.17	10.7	0.77	0.71	0.25	0.27	87	85	84	0.35
15	10.96	8.83	2.13	19.4	1.58	1.56	0.50	0.51	98	97	97	0.32
20	10.96	7.90	3.06	27.9	2.37	2.36	0.73	0.79	102	101	103	0.32
25	10.96	7.12	3.84	35.0	3.09	2.96	1.00	0.99	107	105	103	0.33
30	10.96	6.59	4.37	39.9	3.65	3.78	1.14	1.19	110	100	114	0.31
5	25.84	25.47	0.37	1.43	0.23	0.22	0.08	0.04	(71)	(70)	(59)	(0.27)
10	25.84	24.54	1.30	5.03	1.05	1.03	0.34	0.30	107	106	102	0.31
15	25.84	23.23	2.61	10.1	2.09	2.16	0.60	0.62	103	104	107	0.29
20	25.84	21.76	4.08	15.8	3.11	3.25	0.92	0.94	98.8	100	103	0.29
25	25.84	20.32	5.52	21.4	4.26	4.48	1.16	1.31	98.2	100	105	0.28
30	25.84	19.27	6.57	25.4	5.16	5.55	1.38	1.58	99.5	103	109	0.28

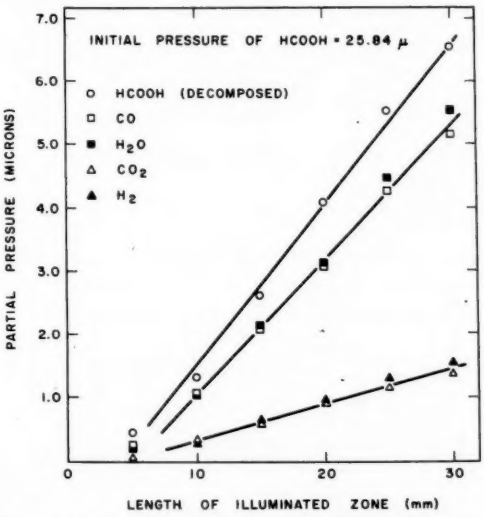

FIG. 3. Products from mercury-photosensitized decomposition of formic acid vapor.

Methyl Formate

The distribution of products formed by the mercury-photosensitized decomposition of methyl formate with different lengths of illuminated zone are given in Table II. In addition to these products very small amounts of methyl acetate and dimethyl ether were also produced. Two other minor products could be detected only by their parent peaks at mass 58 and mass 62. A search for free radicals was made using initial pressures

TABLE II

Decomposition of methyl formate

Length of illuminated zone (mm)	Methyl formate (μ) present		Methyl formate decomposed		Products (μ)							Mass balance (%) for:		
	Lamp off	Lamp on	μ	%	CO_2	CH_3OH	C_2H_6	CH_2O	CO	CH_4	H_2	O	C	H
5	19.87	19.21	.66	3.32	.070	$.04_1$	$.01_1$	$.06_9$	$.23_4$	$.01_5$	$.15_7$	36.7	34.2	28.1
10	19.87	18.43	1.44	7.25	$.14_1$	$.42_0$	$.02_9$	$.19_4$	$.65_4$	$.04_0$	$.46_2$	53.4	52.2	66.3
15	19.87	17.97	1.90	9.56	$.23_7$	$.94_1$	$.04_7$	$.39_9$	1.32	$.07_9$	$.68_7$	82.8	81.2	86.2
20	19.87	17.34	2.53	12.73	$.33_1$	1.18_7	$.07_8$	$.56_6$	1.86	$.11_7$	$.92_4$	84.5	83.4	85.6
25	19.87	16.54	3.33	16.76	$.44_1$	1.54_5	$.10_0$	$.69_4$	2.23	$.14_0$	1.22	80.3	78.9	83.9
30	19.87	16.00	3.87	19.48	$.49_0$	1.81_1	$.12_7$	$.83_3$	2.80	$.18_6$	1.41	83.1	82.5	85.6

of methyl formate two or three times higher than in the quantitative experiments. Using low electron energies, at which only parent ions should be formed, the peaks at mass 15, 29, 31, and 59 were found to increase when the lamp was on. These mass numbers correspond to the parent ions of CH_3, CHO, CH_3O, and $COOCH_3$ radicals. The presence of these radicals is also indicated by the formation of a number of products which evidently arise from the corresponding radical–radical interactions. Ethane undoubtedly was formed by the combination of two methyl radicals, the dimethyl ether from the combination of a methyl and a methoxy radical, and the methyl acetate from the combination of a methyl and a $COOCH_3$ radical. The unidentified peaks at mass 58 and mass 62 might be the parent peaks of glyoxal, the dimer of CHO radical, and dimethyl peroxide, the dimer of CH_3O, but a positive identification could not be made.

In order to obtain a further confirmation for some of these findings a separate experiment was carried out in which mercury dimethyl was added to the helium stream carrying the methyl formate. With the lamp on, a small additional increase in the peaks at mass 74 and mass 43 was observed. The increased portions of these peaks had a ratio mass 74/mass 43 = 0.15. The ratio of these peaks in the mass spectrum of methyl acetate measured in a separate experiment was 0.18. An increase was also observed for the mass 46 and 45 peaks, in the ratio mass 46/mass 45 = 0.34. The ratio for dimethyl ether measured separately was 0.40. Although the agreement is somewhat approximate, there can be little doubt that the corresponding increases in the peaks were caused by the formation of methyl acetate and dimethyl ether by reaction of $COOCH_3$ and OCH_3 radicals with the additional CH_3 radicals provided by the decomposition of mercury dimethyl.

The presence of the CH_3O and HCO radicals indicate that the following primary step must occur:

$$Hg^* + HCOOCH_3 \rightarrow Hg + HCO + OCH_3. \qquad [10]$$

The presence of the $COOCH_3$ radical suggests the occurrence of a second primary dissociation process:

$$Hg^* + HCOOCH_3 \rightarrow Hg + H + COOCH_3. \qquad [11]$$

The formation of the $COOCH_3$ radical by a primary step, and not by abstraction of a H atom from methyl formate by one of the radicals produced in reaction [10] depends on the validity of the discussion given above concerning the occurrence of radical–substrate reactions.

The presence of methyl radicals might result from a third primary mode of dissociation:

$$Hg^* + HCOOCH_3 \rightarrow Hg + HCOO + CH_3. \qquad [12]$$

It is not necessary, however, to postulate this reaction since the dissociation of the $COOCH_3$ radical by the reaction:

$$COOCH_3 \rightarrow CO_2 + CH_3 \qquad [13]$$

might be expected to be quite rapid at 55° C. Although the strength of the COO—CH_3 bond is unknown, it can be shown from thermochemical data that it cannot be very strong. From the relation

$$D(H—COOCH_3) + D(COO—CH_3) = \Delta H_f(H) + \Delta H_f(CH_3) + \Delta H_f(CO_2) - \Delta H_f(HCOOCH_3)$$

and standard thermochemical data, the sum of the two bonds is 73.6 kcal/mole. Since it might be expected that the C—H bond alone must be nearly this strong, D(COO—CH_3)

must be certainly not greater than 10–15 kcal/mole. It is rather surprising that the $COOCH_3$ radical could be detected at all in the present experiments.*

The quantitative data given in Table II were obtained from the mass spectra of the products in the reaction stream taken with 50-v electrons. After subtracting the contributions of the stable reaction products from the mass spectra, a small residual peak remained for mass 59, and somewhat larger ones for mass 31, 29, and 15. It is probable that these peaks were caused by the presence of the $COOCH_3$, CH_3O, CHO, and CH_3 free radicals. Since the mass spectrum of the CH_3O radical is not known, its contribution to the mass 15 peak could not be evaluated. Thus the concentration of the CH_3 radical, which is the only one whose sensitivity coefficient is known, could not be determined. The mass balances given in Table II therefore do not include free radical contributions. Contributions from the minor products methyl acetate, dimethyl ether, and the tentatively identified methyl peroxide and glyoxal are also not included.

Two approximate relations between the amounts of the various products given in Table II can be seen:

$$[CO] \approx [CH_3OH] + [CH_2O] \qquad \text{I}$$

$$[CO_2] \approx [CH_4] + [C_2H_6]. \qquad \text{II}$$

TABLE III

Product balances—methyl formate

Length of illuminated zone (mm)	Methyl formate		Products (μ)			
	Initial pressure (μ)	% Decomposed	[CO]	$[CH_3OH + CH_2O]$	$[CO_2]$	$[2C_2H_6 + CH_4]$*
20	19.87	12.73	1.86	1.75	.331	.273
25	19.87	16.76	2.23	2.24	.441	.340
30	19.87	19.48	2.80	2.64	.490	.440

*This sum should include $[CH_3]$, which could not be measured.

Numerical values for these product balances are given in Table III. Product balance I can be related to the primary reaction [10] if it is assumed that all of the HCO radicals produced by [10] are converted to CO by subsequent reactions, and that essentially all the CH_3O radicals disproportionate to CH_3OH and CH_2O. Similarly, product balance II will hold provided that essentially all the $COOCH_3$ radicals produced by reaction [11] are converted by subsequent reactions to CO_2, C_2H_6, and CH_4. A reaction mechanism fulfilling the requirements of product balances I and II is given below:

$$Hg^* + HCOOCH_3 \rightarrow Hg + HCO + OCH_3 \qquad [10]$$

$$Hg^* + HCOOCH_3 \rightarrow Hg + H + COOCH_3 \qquad [11]$$

$$COOCH_3 \rightarrow CO_2 + CH_3 \qquad [13]$$

$$Hg^* + OCH_3 \rightarrow Hg + H + CH_2O \qquad [14]$$

$$Hg^* + HCO \rightarrow Hg + H + CO \qquad [15]$$

$$2CH_3O \rightarrow CH_3OH + CH_2O \qquad [16]$$

$$2HCO \rightarrow H_2 + 2CO \qquad [17]$$

**Some further support for the instability of* $COOCH_3$ *is given by a comparison with the* CH_3CO *radical. From the relation:*

$$D(H—COCH_3) + D(CO—CH_3) = \Delta H_f(H) + \Delta H_f(CH_3) + \Delta H_f(CO) - \Delta H_f(CH_3CHO)$$

the sum of the two bonds is 97.5 kcal/mole. If, as might reasonably be expected, $D(H—COCH_3)$ *is not much less than* $D(H—COOCH_3)$ *it is evident that* $D(COO—CH_3)$ *is significantly weaker than* $D(CO—CH_3)$.

$$CH_3O + HCO \rightarrow CH_3OH + CO \quad [18]$$

$$CH_3O + HCO \rightarrow 2CH_2O \quad [19]$$

$$H + CH_3O \rightarrow CH_2O + H_2 \quad [20]$$

$$H + HCO \rightarrow CO + H_2 \quad [21]$$

$$CH_3 + CH_3O \rightarrow CH_4 + CH_2O \quad [22]$$

$$CH_3 + HCO \rightarrow CH_4 + CO \quad [23]$$

$$2CH_3 \rightarrow C_2H_6 \quad [24]$$

The evidence for reactions [10], [11], and [13] has been discussed. It is evident that with at least four free radicals, H atoms, and excited mercury atoms present as reactive species it is not possible to distinguish between alternative methods of producing many of the secondary products. The reactions listed above are all probable ones, but other modes of radical–radical interaction may, of course, occur. Reactions [14] and [15], for which there is no direct evidence, were included on the basis of previous work on the decomposition of acetone (12), using the same apparatus, in which the formation of ketene could only be explained by the reaction of acetyl radicals with excited mercury atoms. Reactions [16] to [23] are radical disproportionation steps, all of which may not be active in the mechanism. However, since products of radical combination, with the exception of ethane, were found only in minute amounts, it is to be expected that disproportionation reactions must account for the largest part of the products found.

In the preceding discussion the possibility of a dissociation involving an intramolecular rearrangement was not considered. It is clear that product balance I will still hold if part of the decomposition proceeds by the reaction

$$Hg^* + HCOOCH_3 \rightarrow Hg + CH_3OH + CO \quad [25]$$

since for every CO molecule one CH_3OH molecule is also produced. Similarly, product balance II will be obeyed if the intramolecular rearrangement

$$Hg^* + HCOOCH_3 \rightarrow Hg + CH_4 + CO_2 \quad [26]$$

is one of the primary reactions. These are analogous to reactions [3] and [4] respectively, as found to occur in the decomposition of formic acid. In order to establish whether methyl formate decomposes partly by reaction [25] some experiments were carried out using mixtures of $HCOOCH_3$ and $DCOOCD_3$. The total pressure of the two isomers in the helium stream was kept approximately equal to the pressure of methyl formate used in the previous experiments. In a series of runs, the mole fraction of deuterated methyl formate was varied from unity to almost zero. For each composition the amount of CD_3OD formed and the percentage of decomposition of $DCOOCD_3$ were measured. In these experiments the length of the illuminated zone was 30 mm. The results are summarized in Table IV. A plot of the ratio CD_3OD formed/$DCOOCD_3$ decomposed versus the mole fraction of $DCOOCD_3$ is shown in Fig. 4. If CD_3OD were formed entirely by the intramolecular rearrangement reaction [25], the ratio would not be affected by the addition of $HCOOCH_3$. Conversely, if CD_3OD were formed entirely by a free radical process, the ratio should approach zero as the mole fraction of $DCOOCD_3$ approaches zero. The observed dependence shows an intermediate behavior indicating the participation of both a molecular and a free radical process. The ratio obtained by extrapolation is approximately 0.12. Thus about 12% of the methyl formate decomposes by the rearrangement reaction [25]. In the experiments with $HCOOCH_3$ reported in Table II (for a 30-mm illuminated zone) the yield of CO was 72.4% of the methyl formate

decomposed. Since the yield of CO represents the fraction of methyl formate decomposing by reactions [10] and [25], it follows that the methyl formate decomposing by reaction [10] alone is approximately $72.4-12.0 = 60.4\%$.

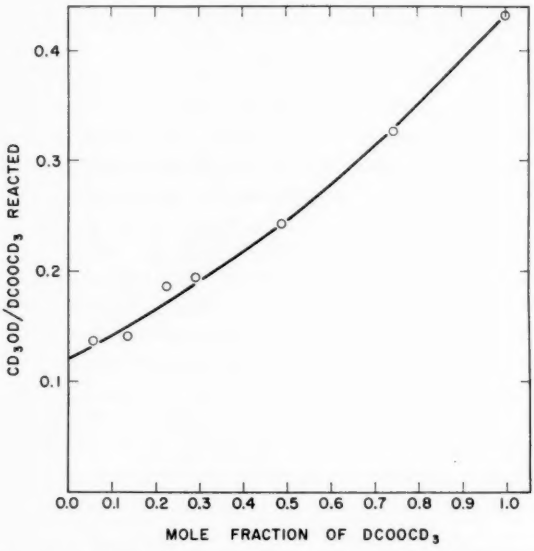

FIG. 4. Formation of CD_3OD in $DCOOCD_3$–$HCOOCH_3$ mixtures.

TABLE IV

CD_3OD Production in $DCOOCD_3$–$HCOOCH_3$ mixtures

$DCOOCD_3$ (μ), initial	$HCOOCH_3$ (μ), initial	Mole fraction $DCOOCD_3$	$DCOOCD_3$ decomposed		CD_3OD formed	CD_3OD formed
			μ	%	(μ)	$DCOOCD_3$ decomposed
1.21	19.6	.058	.226	18.7	.031	.137
2.64	16.7	.136	.516	19.5	.073	.141
4.89	16.7	.226	.909	18.6	.170	.187
6.94	16.7	.293	1.37	19.7	.266	.194
8.48	8.8	.490	1.81	21.3	.440	.243
14.97	5.1	.747	2.96	19.8	.968	.327
20.93	0.0	1.00	4.05	19.3	1.75	.432

Similarly, the methyl formate decomposing by reactions [11] and [26] should be equal to the yield of CO_2, that is 12.7% (Table II). Assuming that all the methane is formed by reaction [26] an upper limit for the participation of this reaction would be given by the methane yield, which is 4.8%. Since methane could also be formed by reactions [22] and [23], it is probable that the true extent for the occurrence of reaction [26] is much smaller than 4.8%, and possibly zero.

Acetic Acid

The yields of products obtained in the mercury-photosensitized decomposition of acetic acid are given in Table V. The full intensity of the lamp was used in this experiment by withdrawing the shutter completely out of the reaction zone. The principal

products were water, carbon dioxide, ketene, methane, ethane, methyl radicals, and acetone. The formation of a polymeric substance on the walls of the reactor, which was visible as a brown stain after several minutes' exposure, may account for the deficiency in the mass balances given in Table V. This deposit may result from the polymerization of the ketene formed in the reaction. In the mercury-photosensitized reaction of acetone (12) in which ketene was a product, a similar deposit was formed.

TABLE V

Decomposition of acetic acid

Acetic acid (μ) present		Acetic acid decomposed		Products (μ)								Mass balance (%) for:		
Lamp off	Lamp on	μ	%	CO_2	CO	C_2H_6	H_2O	CH_4	CH_3	Acetone	Ketene	O	C	H
7.35	6.12	1.23	16.7	0.461	0.260	0.224	0.654	0.231	0.073	0.015	0.292	87.7	87	91.6

Using electrons of low energy, the only radical which could be detected was methyl. However, the formation of acetone as a product can be explained only by the presence of acetyl radicals, which must have been present in concentrations too low to detect. Addition of mercury dimethyl to the reaction stream caused an increase in the amount of acetone formed, thus confirming the presence of CH_3CO radicals. The presence of CH_3CO radicals, together with the formation of substantial amounts of water, indicates that the following step must occur:

$$Hg^* + CH_3COOH \rightarrow Hg + CH_3CO + OH. \qquad [27]$$

Although the CH_3 radicals detected might arise by dissociation of CH_3CO, the presence of large amounts of CO_2 together with the fact that the yield of CO is not nearly twice the yield of ethane indicates that a second primary process, in which CH_3 radical and a radical ultimately forming CO_2 are produced, must occur: one possibility is that this reaction is the following:

$$Hg^* + CH_3COOH \rightarrow Hg + CH_2 + COOH. \qquad [28]$$

CO_2 would then be formed by the decomposition of the COOH radical as follows:

$$COOH \rightarrow CO_2 + H. \qquad [29]$$

Reaction [29] appears to be a much more probable mode of dissociation of COOH than the more frequently proposed dissociation into CO and OH, since $\Delta H_f(CO_2)+\Delta H_f(H)$ is some 25 kcal/mole less than $\Delta H_f(CO)+\Delta H_f(OH)$. A difference in dissociation energy of this magnitude between the O—O and O—H bonds in COOH should be sufficient to ensure that COOH dissociates mainly by reaction [29]. However, an alternative primary decomposition step

$$Hg^* + CH_3COOH \rightarrow Hg + CH_2COO + H \qquad [30]$$

would ultimately form CH_3 and CO_2 by dissociation. Reaction [30] was proposed by Burton (8) and by Ausloos and Steacie (10) as the primary dissociation step in the direct photolysis. A search for the $CH_3C\dot{O}O$ radical, using low electron energies, showed no indication of its presence. In experiments in which mercury dimethyl was added to the reaction stream, no sign of methyl acetate, the combination product of $CH_3C\dot{O}O$ and CH_3, could be found. It must be concluded that either the $CH_3C\dot{O}O$ radical was not formed in appreciable amounts, or alternatively that this radical has an extremely short lifetime at 55° C. (Care should be taken to distinguish between this radical, $CH_3C\dot{O}O$, and the isomeric radical $\dot{C}OOCH_3$ produced from methyl formate.) Since four

radical products can result from these primary steps, 10 radical recombination products are possible. Two of these lead to re-formation of acetic acid. A search was made for the parent peaks of the other eight, but aside from acetone and ethane no other recombination products could be detected. The observed products must then arise mainly by radical decomposition and disproportionation reactions. The following set of reactions appear probable:

$$COOH \rightarrow CO_2 + H \quad [29]$$

$$Hg^* + COOH \rightarrow Hg + CO_2 + H \quad [31]$$

$$CH_3CO \rightarrow CH_3 + CO \quad [32]$$

$$Hg^* + CH_3CO \rightarrow Hg + CH_2{=}CO + H \quad [33]$$

$$COOH + CH_3 \rightarrow CH_4 + CO_2 \quad [34]$$

$$COOH + OH \rightarrow H_2O + CO_2 \quad [35]$$

$$2CH_3 \rightarrow C_2H_6 \quad [24]$$

$$CH_3 + COCH_3 \rightarrow CH_3COCH_3. \quad [36]$$

Reactions [29] and [32] could be either thermal decompositions or decompositions of excited radicals produced in the primary splits. Reactions [31] and [33] have been assumed on the basis of previous experience with the apparatus as discussed above. Reactions [34] and [35] are plausible disproportionation reactions, and reactions [24] and [36] account for the formation of ethane and acetone.

These reactions lead to a number of relations between the yields of various products which can be compared with the analytical results. There are two modes of formation of methyl radicals, the primary reaction [28] and the decomposition reaction [32]. Since all the COOH produced by reaction [28] is evidently converted to CO_2 by subsequent reactions, the sum of the yields of CO and CO_2 should equal the total amount of methyl formed, that is:

$$[CO] + [CO_2] = [CH_3] + [CH_4] + 2[C_2H_6] + [CH_3COCH_3].$$

From Table V $[CO] + [CO_2] = 0.752\ \mu$, and the total methyl yield is $0.721\ \mu$, in reasonable agreement. The OH radicals produced by the primary step [27] are evidently all converted to H_2O. The quantity of H_2O should then be equal to the sum of the products derived from CH_3CO radicals, i.e.

$$[H_2O] = [CH_2{=}CO] + [CO] + [CH_3COCH_3].$$

From Table V, $[H_2O] = 0.65\ \mu$ and the sum of the acetyl products is 0.57. If allowance is made for the fact that some ketene may have polymerized, this agreement is reasonably close.

However, these two product balances would also apply if part of the primary decomposition occurred by one or both of the intramolecular rearrangement steps:

$$Hg^* + CH_3COOH \rightarrow Hg + CH_4 + CO_2, \quad [37]$$

$$Hg^* + CH_3COOH \rightarrow Hg + H_2O + CH_2{=}CO. \quad [38]$$

In order to determine the extent to which these reactions occur, an attempt was made to carry out experiments with CD_3COOD–CH_3COOH mixtures similar to those with deuterated methyl formate. It was found that the acidic hydrogen and deuterium atoms exchanged so rapidly in the reaction system that useful experiments with mixtures could not be carried out. It is possible, however, to set upper limits to the extent of

these reactions from an examination of the data in Table V. The proportion of acetic acid decomposing by reactions [28] and [37] should be given by the yield of CO_2, that is, 37.5%. On the assumption that all the methane was produced by reaction [37], the upper limit for the occurrence of this reaction is 18.8%, and a lower limit for sum of reactions [28] and [30] is 37.5%−18.8%, i.e. 18.7%. Since methane could also be produced by reaction [34] the actual extent was probably significantly less. The proportion of acetic acid decomposing by the primary reactions [27] and [38] should be given by the yield of H_2O, that is, 53%. On the assumption that all the ketene was formed by reaction [38], this reaction accounted for 23.7%, and a lower limit for reaction [27] would be 29.3%. The approximate extent of the various primary processes can be summarized as follows:

$$Hg^* + CH_3COOH \rightarrow Hg + CH_3CO + OH \quad \sim 29\% \quad [27]$$

$$\rightarrow \begin{Bmatrix} Hg + CH_3 + COOH \\ Hg + CH_3COO + H \end{Bmatrix} \sim 18\% \quad \begin{Bmatrix} [28] \\ [30] \end{Bmatrix}$$

$$\rightarrow Hg + CH_4 + CO_2 \quad \sim 19\% \quad [37]$$

$$\rightarrow Hg + H_2O + CH_2{=}CO \sim 24\%. \quad [38]$$

CONCLUSION

It is evident that the modes of mercury-photosensitized decomposition of compounds of the type $RC(=O)OR'$ do not by any means conform to a pattern. It is quite surprising that although HCOOH decomposes solely by molecular rearrangement reactions, methyl formate and acetic acid decompose predominantly by a split into free radicals. Two parallels in behavior can, however, be observed. In all three compounds the molecular rearrangement involving the transfer of a hydrogen atom to the oxygen atom of the hydroxy- or methoxy-group occurs with a greater probability than other molecular rearrangements. This reaction may be visualized as follows for the three compounds:

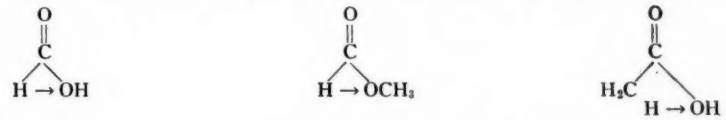

Secondly, in methyl formate and acetic acid the present experiments indicate that the predominating mode of dissociation into free radicals is the recation:

$$RC(=O)OR' \rightarrow RC(=O) + OR'. \quad [39]$$

Of secondary importance is the reaction:

$$RC(=O)OR' \rightarrow R + C(=O)OR'. \quad [40]$$

It may be noted further that when R is H, reaction [39] is much faster than [40], but when R′ is H the difference in rate is much smaller.

It is evident from the tables that the amount of formic acid decomposed is considerably greater than the amounts of methyl formate and acetic acid decomposed in an equal time under the same conditions. Provided that the quenching cross sections of the three compounds are not greatly different, it appears that the formic acid molecule

possesses a much greater facility for molecular rearrangements than do methyl formate or acetic acid. The lack of a free radical mode of decomposition for formic acid is therefore probably a consequence of the rapidity with which molecular rearrangements can occur. On the basis of structural considerations it is not clear why formic acid and methyl formate should differ so greatly in this respect.

REFERENCES

1. RAMSPERGER, H. C. and PORTER, C. W. J. Am. Chem. Soc. **48**, 1267 (1926).
2. BATES, J. R. and TAYLOR, H. S. J. Am. Chem. Soc. **49**, 2438 (1927).
3. HERR, D. S. and NOYES, W. A., JR. J. Am. Chem. Soc. **50**, 2345 (1928).
4. GORIN, E. and TAYLOR, H. S. J. Am. Chem. Soc. **56**, 2042 (1934).
5. BURTON, M. J. Am. Chem. Soc. **58**, 1155 (1936).
6. TERENIN, A. Acta Physicochim. U.R.S.S. **3**, 181 (1935).
7. AUSLOOS, P. Can. J. Chem. **36**, 383 (1958).
8. BURTON, M. J. Am. Chem. Soc. **58**, 1644 (1936).
9. FARKAS, L. and WANSBROUGH-JONES, O. H. Z. physik. Chem. B, **18**, 124 (1932).
10. AUSLOOS, P. and STEACIE, E. W. R. Can. J. Chem. **33**, 1530 (1955).
11. LOSSING, F. P., MARSDEN, D. G. H., and FARMER, J. B. Can. J. Chem. **34**, 701 (1956).
12. LOSSING, F. P. Can. J. Chem. **35**, 305 (1957).
13. LÉGER, E. G. Can. J. Phys. **33**, 74 (1955).
14. FABIAN, D. J. and ROBERTSON, A. J. B. Trans. Faraday Soc. **53**, 363 (1957).
15. KHAN, M. A., NORRISH, R. G. W., and PORTER, G. Proc. Roy. Soc. A, **219**, 312 (1953).

DÉRIVÉS DU TRIMÉTHYL-1,8,8 BICYCLO[3,2,1]OCTANE

III. SYNTHÈSE DES TRIMÉTHYL-1,8,8 BICYCLO[3,2,1]OCTANOLS-2α ET -2β ET DES TRIMÉTHYL-5,8,8 BICYCLO[3,2,1]OCTANOLS-2α ET -2β[1]

H. FAVRE, M. LEFEBVRE[2] ET (EN PARTIE) J-C. RICHER[3]

RÉSUMÉ

Le (+)-triméthyl-1,8,8 bicyclo[3,2,1]octanol-2α et le (+)-triméthyl-5,8,8 bicyclo[3,2,1]-octanol-2α ont été préparés en réduisant par le sodium et l'alcool le (−)-homocamphre et le (+)-homoépicamphre respectivement. L'hydrogénation catalytique de ces cétones par le platine dans l'acide acétique conduit au (−)-triméthyl-1,8,8 bicyclo[3,2,1]octanol-2β et au (+)-triméthyl-5,8,8 bicyclo[3,2,1]octanol-2β respectivement. Les rendements stériques de ces opérations sont supérieurs à 90%. Les configurations ont été attribuées à la suite de l'analyse des modes de formation, des pouvoirs rotatoires et des vitesses d'oxydation chromique des alcools.

Nous rapportons dans ce mémoire des travaux relatifs à la réduction du (−)-homocamphre (I) et du (+)-homoépicamphre (II)[4] et à la détermination de la configuration de chacun des 4 alcools[5] (III–VI) obtenus. L'obtention des alcools stériquement purs n'offre pas de grandes difficultés. Pour chaque cétone la réduction par le sodium et l'éthanol conduit en prépondérance à l'un des épimères (alcool au sodium), tandis que l'autre s'obtient facilement par l'hydrogénation catalytique sur platine dans l'acide acétique (alcool au platine). Après chaque réduction, l'alcool brut fut transformé en *p*-nitrobenzoate; ce dérivé fut cristallisé jusqu'à point de fusion et pouvoir rotatoire constants, puis saponifié. Les quatre alcools obtenus de cette manière (Tableau I) sont

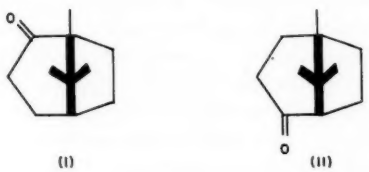

(I) (II)

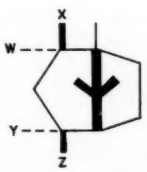

III.	W = OH; X,Y,Z = H	Triméthyl-1,8,8 bicyclo[3,2,1]octanol-2α
IV.	X = OH; W,Y,Z = H	Triméthyl-1,8,8 bicyclo[3,2,1]octanol-2β
V.	Y = OH; W,X,Z = H	Triméthyl-5,8,8 bicyclo[3,2,1]octanol-2α
VI.	Z = OH; W,X,Y = H	Triméthyl-5,8,8 bicyclo[3,2,1]octanol-2β

[1]*Manuscrit reçu le 27 août, 1958.*
Contribution du Département de Chimie de l'Université de Montréal, Montréal, P.Q.; elle est tirée du mémoire de maîtrise de M. Lefebvre et de la thèse de doctorat de J-C. Richer.

[2]*Boursier de l'Office de Recherches Scientifiques de la Province de Québec, 1955–1956. Adresse actuelle: Shawinigan Chemicals Ltd., Shawinigan, P.Q.*

[3]*Boursier du Conseil National de Recherches du Canada, 1954–1958. Adresse actuelle: Dept. of Chemistry, University of Notre Dame, Notre Dame, Ind.*

[4]*Pour la préparation de ces cétones, voir (1, 2).*

[5]*La nomenclature est celle en vigueur pour les dérivés du nortropane (aza-8 bicyclo[3,2,1]octane) et les composés apparentés (3). Les formules spatiales III A–VI A et III B–VI B représentées plus loin sont équivalentes aux formules III–VI.*

stériquement purs à la chromatographie sur alumine; chacun donne naissance à un *p*-nitrobenzoate en tous points semblable à celui qui servit à la purification. Chaque alcool fut oxydé par l'acide chromique en homocamphre ou en homoépicamphre, suivant son origine. Il convient de relever que les alcools épimères ne donnent pas de dépression de point de fusion en mélange, alors que leurs dérivés (esters) mentionnés plus haut en donnent. Une observation semblable avait été faite pour les cétones I et II (1).

TABLEAU I

Description des alcools III–VI

Alcools	P.f.	Rendements en alcools	Rendements stériques	$[\alpha]_D$*
Alcool au sodium III	212°	97%	94%	+17.9°±2.0°
Alcool au platine IV	234–235°	93%	90–95%	−29.2°±2.0°
Alcool au sodium V	166°	94%	92%	+35.9°±2.0°
Alcool au platine VI	206°	87%	97%	+43.9°±2.0°

*Benzène.

Le succès de la réduction catalytique dépend de la position du groupe méthyle pontal (position 1 ou 5) par rapport au groupe carbonyle à réduire. Ainsi l'homoépicamphre est aisément réduit par le platine dans l'acide acétique glacial et tout aussi aisément par le platine ou le nickel de Raney dans l'alcool (sans pression et 25°). L'homocamphre, dont le groupe carbonyle est adjacent au méthyle pontal, n'est réduit à une vitesse appréciable que par le platine dans l'acide acétique. Lorsque la réduction a lieu, le rendement stérique est toujours supérieur à 90%. La réduction par le sodium et l'éthanol procède sans difficultés: les rendements en alcools et les rendements stériques sont les mêmes pour la réduction de l'homocamphre et de l'homoépicamphre. Les rendements stériques (Tableau I) ont été déterminés par l'analyse du pouvoir rotatoire des alcools bruts; celui de la réduction de l'homocamphre au platine a dû être estimé, car l'alcool brut contenait des traces de cétone décelées par spectroscopie infrarouge.

Pour déterminer les configurations et les conformations respectives des quatre alcools III à VI, nous avons appliqué plusieurs méthodes. Celles qui font appel aux modes de formation des alcools, à leurs rotations moléculaires et à leurs vitesses d'oxydation chromique seront discutées ici. Les réactions d'élimination des groupes —OH et de leurs esters feront l'objet de mémoires séparés en raison de leur complexité.

Nous appliquerons en premier lieu la méthode des rotations moléculaires de Bose et Chaterjee (4). La règle stipule que si les configurations absolues de deux composés alicycliques épimères peuvent être ramenées aux configurations VII et VIII, l'épimère VII sera plus dextrogyre que l'épimère VIII, pour autant que L, M, S et T représentent l'ordre décroissant de l'encombrement stérique des substituants ou des parties de la molécule adjacents au carbone asymétrique.

Comme la configuration absolue de l'homocamphre (I) et de l'homoépicamphre (II)

(VII) (VIII) (IX)

est connue avec certitude—puisque ces cétones sont dérivées (1, 2) du (+)-camphre (configuration absolue (5, 6), formule IX) par un procédé qui ne saurait provoquer d'inversion de configuration—nous pouvons connaître L et M pour les quatre alcools III à VI en question; L est l'atome de pont et M le groupe méthylène en position 3. En posant: —OH = S et —H = T, nous arrivons aux configurations suivantes:

Série de l'homocamphre: l'alcool au sodium, plus dextrogyre que l'alcool au platine, reçoit la configuration VII et par suite, la formule III. L'alcool au platine sera IV.

Série de l'homoépicamphre: l'alcool au platine, étant le plus dextrogyre, reçoit la configuration VII, donc VI. L'alcool au sodium sera V.

En fait, les formules III à VI peuvent être transposées en formules spatiales, qui se rattachent à deux conformations que nous appelons A et B.

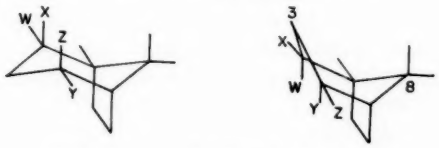

I A	W,X = = O (cétone); Y,Z = —H	I B
II A	Y,Z = = O (cétone); W,X = —H	II B
III A	W = —OH; X,Y,Z = —H	III B
IV A	X = —OH; W,Y,Z = —H	IV B
V A	Y = —OH; W,X,Z = —H	V B
VI A	Z = —OH; W,X,Y = —H	VI B

La conformation B (cyclohexanique bateau) est certainement moins stable que la conformation A (cyclohexanique chaise), en raison principalement de l'interférence prononcée du groupe méthyle en position 8 (flagpole, *fp*) avec l'hydrogène (*fp*) en position 3. Nous avançons ceci en tenant compte de l'analogie qui existe entre les dérivés du triméthyl-1,8,8 bicyclo[3,2,1]octane et les verbanones. Bose a montré (7) que la *cis*-verbanone réagit sous sa conformation X C (analogue à I A et II A) plutôt que X D (analogue à I B et II B); voir aussi (8). Bose laisse toutefois ouverte la question de savoir si le néoisoverbanol a la conformation XI C ou XI D, XI C pouvant être défavorisée en raison des trois substituants axiaux.

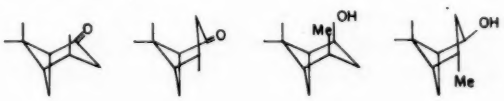

X C X D XI C XI D

Nous ne retenons ainsi pour l'homocamphre (I) et l'homoépicamphre (II) que les conformations I A et II A respectivement, où le groupe carbonyle à réduire se présente comme celui d'une cyclohexanone chaise. De nombreux exemples supportent le fait que la réduction d'un groupe carbonyle par le sodium et l'alcool engendre un groupe —OH équatorial. Les hydroxyles des deux alcools au sodium seraient ainsi équatoriaux et leurs configurations α. Les alcools au platine seraient par conséquent les alcools axiaux, de configuration β, ce qui est conforme à ce que l'on sait de l'hydrogénation catalytique qui conduit, dans des conditions expérimentales ne favorisant pas une isomérisation, à la fixation de l'hydrogène sur le côté le plus dégagé de la molécule: généralement le groupe—OH est axial. Pour de nombreuses références, voir (7, 9, 10, 11, 12).

TABLEAU II
Vitesses d'oxydation chromique et fréquences de vibration C—O des alcools III à VI

Alcools	Vitesses d'oxydation relatives à celle du cyclohexanol	Fréquences de vibration* C—O, cm^{-1}
Cyclohexanol	1	
Alcool au sodium III	5.7	1044 (f), 1033 (f), 1013 (F)
Alcool au platine IV	111.8	1029 (F), 1005 (F)
Alcool au sodium V	6.5	1038 (F)
Alcool au platine VI	125.0	1044 (F)

*Mesurées dans le sulfure de carbone. (F) signifie bande forte, (f) bande plus faible.

À la suite des premiers travaux de Vavon (13) concernant la vitesse de l'oxydation chromique des alcools secondaires en cétones, Barton (14, 15) a fait remarquer que les groupes —OH axiaux étaient oxydés plus rapidement que les hydroxyles équatoriaux. Schreiber et Eschenmoser (16) ont interprété ce fait en termes d'interactions entre atomes non liés et de décompression stérique lors du passage des esters chromiques aux cétones, la décompression stérique, par suite la vitesse d'oxydation, étant plus grande pour une conformation axiale, plus comprimée qu'une conformation équatoriale.

Les résultats[6] rapportés au Tableau II montrent que les deux alcools au platine sont oxydés environ 20 fois plus rapidement que les deux alcools au sodium; ces résultats sont donc bien en accord avec les conformations IV A et VI A pour les alcools au platine (groupes —OH axiaux) et avec les conformations III A et V A pour les alcools au sodium (groupes —OH équatoriaux).

En définitive, l'analyse des modes de formation des alcools III à VI, de leurs pouvoirs rotatoires et de leurs vitesses d'oxydation chromique, contribue à former un faisceau d'indices favorables à l'interprétation suivante: les alcools sont formés à partir des cétones de conformation A (I A et II A, cyclohexanique chaise) et existent sous cette conformation en tant qu'alcools axiaux (IV A et VI A, alcools au platine) et alcools équatoriaux (III A et V A, alcools au sodium).

Nous rapportons au Tableau II les fréquences des vibrations C—O des quatre alcools III à VI; nous les avons mesurées dans le but de les comparer aux valeurs moyennes déduites par Cole, Jones et Dobriner (17) pour les alcools stéroides axiaux (996–1036 cm^{-1}) et équatoriaux (1038–1044 cm^{-1}). Les alcools III et IV issus de l'homocamphre montrent plusieurs bandes et il n'est pas possible d'en choisir une plutôt que l'autre pour appliquer la règle. L'inversion observée pour les triméthyl-5,8,8 bicyclo[3,2,1]-octanols-2α et -2β (V et VI) n'est donc plus significative et ne saurait être retenue pour invalider les conclusions tirées plus haut au sujet de la conformation de ces alcools.

PARTIE EXPÉRIMENTALE[7]

L'homocamphre utilisé dans les sections 1 et 2 a été préparé selon (1).

1. Triméthyl-1,8,8 bicyclo[3,2,1]octanol-2β (IV)

1.1. Préparation de l'alcool brut

(*a*) On procède à l'hydrogénation préalable de 100 mg de PtO_2 dans 10 ml d'acide acétique glacial, puis à l'hydrogénation proprement dite de 2.0 g d'homocamphre dissous

[6]*Nous avons choisi la valeur arbitraire de 1 pour le cyclohexanol; on pourra ainsi rapprocher les vitesses d'oxydation des alcools III à VI de celles données par Schreiber et Eschenmoser pour divers cholestanols (16).*

[7]*Les points de fusion (p.f.) ont été déterminés dans des tubes capillaires dans un bloc chauffé électriquement et en utilisant un thermomètre étalonné avec les standards du Bureau des Standards de Washington. Les spectres infrarouges ont été mesurés à l'aide d'un spectromètre "Perkin–Elmer" modèle 112, à simple faisceau et parcours double, prisme* NaCl. *Les analyses carbone–hydrogène sont de Geller Laboratories, Hackensack, N.J.; celles d'azote sont de M. Lefebvre. Les valeurs des pouvoirs rotatoires* $[\alpha]_D$ *sont à* $\pm 2°$ *près.*

dans 30 ml d'acide acétique glacial. Il y a absorption de 235 ml d'hydrogène en 4½ h (calculé pour $1H_2$: 245 ml; 748 mm, 23°). On reprend le tout par de l'éther, extrait l'acide acétique par des lavages avec une solution aqueuse de soude caustique à 10%. Après les lavages habituels jusqu'à neutralité, séchage et évaporation de l'éther, le résidu est sublimé pour donner 1.89 g (93%) d'alcool brut, p.f. 235°; $[\alpha]_D^{23} = -32.4°$ ($c = 3.93$; benzène).

(*b*) En 8 heures, il n'y eut aucune absorption lorsque 5 g d'homocamphre furent agités en atmosphère d'hydrogène en présence de 5 g de nickel de Raney dans 50 ml d'éthanol 95% et 10 ml de solution alcoolique de soude 10%. De même, en 1 heure, aucune absorption d'hydrogène n'eut lieu ne présence de platine dans l'éthanol 95%.

1.2. Purification de l'alcool brut

L'alcool brut (3.8 g) est chauffé à l'ébullition à reflux durant 2 heures dans 30 ml de pyridine sèche avec 6.5 g de chlorure de *p*-nitrobenzoyle. Après refroidissement, on précipite l'ester par addition d'eau. Le solide est essoré et repris dans de l'éther. On lave (HCl 10%, NaOH 10% puis eau). On sèche, évapore le solvant et cristallise le résidu dans du méthanol jusqu'à point de fusion et pouvoir rotatoire constants. On a 6.5 g (91%) de *p*-nitrobenzoate p.f. 123–124°, $[\alpha]_D^{23} = -96.6°$ ($c = 3.97$; benzène). On en saponifie 4.0 g par chauffage à reflux durant 2 heures avec 4.0 g de NaOH dans 25 ml d'éthanol et 25 ml d'eau. On isole à la manière habituelle 1.3 g de triméthyl-1,8,8 bicyclo[3,2,1]-octanol-2β régénéré. Cet alcool régénéré (2.050 g) est adsorbé sur 60 g d'alumine Merck pour chromatographie. Des élutions de 100 ml chacune ont donné:

(A) Fractions 1–14, éther de pétrole, p.é. 30–40°, 0.685 g, p.f. 234–235°, $[\alpha]_D^{23} = -29.2°$;

(B) Fractions 15–24, éther de pétrole–benzène 1–1, 1.140 g, p.f. 234–235°, $[\alpha]_D^{23} = -28.7°$;

(C) Fractions 25–26, benzène, 0.139 g, p.f. 233–234°, $[\alpha]_D^{23} = -26.4°$. Pour $[\alpha]_D^{23}$: $c = 4.0$; benzène.

Un échantillon de triméthyl-1,8,8 bicyclo[3,2,1]octanol-2β a été sublimé pour l'analyse; p.f. 234–235°, $[\alpha]_D^{23} = -29.2°$ ($c = 4.0$; benzène). Calculé pour $C_{11}H_{20}O$: C, 78.51; H, 11.98%. Trouvé: C, 78.33; H, 12.06%. Spectre infrarouge: bandes à 1029 et 1005 cm^{-1} (CS_2/0.03 *M*).

1.3 p-Nitrobenzoate

L'alcool pur (350 mg) et 420 mg de chlorure de *p*-nitrobenzoyle sont chauffés à reflux durant 2 heures dans 5 ml de pyridine sèche. On isole à la manière habituelle 489 mg de *p*-nitrobenzoate, paillettes incolores, p.f. 125° (éthanol 95%), $[\alpha]_D^{23} = -84.5°$ ($c = 4$; chloroforme). Calculé pour $C_{18}H_{23}O_4N$: C, 68.12; H, 7.30; N, 4.41%. Trouvé: C, 68.19; H, 7.55; N, 4.35%.

1.4. Oxydation chromique

L'alcool (360 mg) et 150 mg d'anhydride chromique sont dissous dans 10 ml d'acide acétique glacial. La solution s'échauffe un peu. On abandonne à température de la pièce pendant 3 heures. On ajoute ensuite 30 ml d'eau et neutralise avec du bicarbonate de sodium (solution aqueuse à 10%). On extrait à l'éther et isole à la manière habituelle 353 mg de cétone brute que l'on traite par 423 mg de dinitro-2,4 phénylhydrazine en solution dans 8 ml de méthanol contenant 4% d'acide chlorhydrique conc. On obtient, après une précipitation lente, 641 mg de dinitro-2,4 phénylhydrazone brute que l'on cristallise dans l'acide acétique glacial. On retrouve 452 mg de dinitro-2,4 phénylhydrazone d'homocamphre, p.f. 238–239° seule ou en mélange avec un échantillon de dinitro-2,4 phénylhydrazone d'homocamphre authentique (1).

2. Triméthyl-1,8,8 bicyclo[3,2,1]octanol-2α (III)

2.1. Préparation de l'alcool brut

Dans un ballon à trois tubulures surmonté d'un agitateur mécanique et d'un réfrigérant, on introduit 9.6 g (0.057 mole) d'homocamphre et 150 ml d'alcool isobutylique. On porte à l'ébullition et ajoute, par portions de 0.5 g environ, 15.0 g (0.65 mole) de sodium. Après l'addition, on chauffe encore 5 heures à reflux, avec agitation. On ajoute de l'eau (30 ml) et distille sous vide. On retrouve 9.36 g (après sublimation) d'alcool brut, à odeur camphrée, p.f. 208–216°, $[\alpha]_D^{23} = +15.1°$ ($c = 4.0$; benzène). Rendement: 97%.

Un essai semblable effectué à partir de 4.0 g d'homocamphre dans 100 ml d'éthanol anhydre et 8 g de sodium a donné 3.9 g (97%) d'alcool brut, après sublimation, p.f. 207.5–209.5°, $[\alpha]_D^{23} = +14.6°$ ($c = 4.00$; benzène).

2.2. Purification de l'alcool brut (*Mode opératoire 1.2*)

Le *p*-nitrobenzoate brut fond à 127–128°, $[\alpha]_D^{23} = +32.9°$ ($c = 4.00$; benzène). Il est saponifié et donne l'alcool régénéré, p.f. 212–213°, $[\alpha]_D^{23} = +16.5°$ ($c = 4.12$; benzène), qui est chromatographié sur alumine; trois fractions principales sont recueillies:

(A) 29%, éther de pétrole–benzène 4–1 (p.é. 30–40°), p.f. 213–215°, $[\alpha]_D^{23} = +15.7°$;

(B) 40%, éther de pétrole–benzène 1–1, p.f. 212°, $[\alpha]_D^{23} = +17.3°$;

(C) 27%, benzène, p.f. 212°, $[\alpha]_D^{23} = +17.9°$. (Pour tous les pouvoirs rotatoires: $c = 4.00$; benzène.)

La fraction (C) fut analysée. Calculé pour $C_{11}H_{20}O$: C, 78.51; H, 11.98%. Trouvé: C, 78.43; H, 12.08%. Le point de fusion de mélange avec l'alcool épimère p.f. 234–235° (voir section 1.2) est de 216.5–220°. Spectre infrarouge: bandes à 1013, 1033 et 1044 cm^{-1} (CS_2/0.03 *M*).

2.3. p-Nitrobenzoate (*Préparation, voir 1.3*)

Aiguilles incolores (méthanol), p.f. 127–128°, $[\alpha]_D^{23} = +35.0°$ ($c = 4$; chloroforme). Calculé pour $C_{18}H_{23}O_4N$: C, 68.12; H, 7.30; N, 4.41%. Trouvé: C, 68.45, 68.03; H, 7.11, 7.31; N, 4.42%.

2.4. Oxydation chromique (*Mode opératoire, voir 1.4*)

La dinitro-2,4 phénylhydrazone obtenue fond à 238–238.5° seule et 237–239° en mélange avec la dinitro-2,4 phénylhydrazone de l'homocamphre (1).

3. Triméthyl-5,8,8 bicyclo[3,2,1]octanol-2β (VI)

3.1. Préparation de l'alcool brut

(*a*) L'homoépicamphre (5.0 g) dissous dans 50 ml d'éthanol 95% est hydrogéné en présence de 5.0 g de nickel de Raney et 10 ml d'une solution alcoolique de NaOH à 5%. En 24 heures, il y a absorption de 725 ml d'hydrogène (calculé pour $1H_2$: 729 ml; 760 mm, 23°). On essore le catalyseur, évapore le filtrat, on reprend le résidu par de l'éther. Après les lavages habituels, on sèche et évapore l'éther; le résidu est sublimé: 4.72 g d'alcool brut (93%), p.f. 207–208.5°, $[\alpha]_D^{23} = +42.8°$ ($c = 4.04$; benzène).

(*b*) L'homoépicamphre (2 g) est hydrogéné en présence de 60 mg de PtO_2, hydrogéné au préalable, dans 40 ml d'acide acétique glacial. Au bout de 3 heures, l'hydrogénation est terminée; absorption: 285 ml (calculé pour $1H_2$: 296 ml; 748 mm, 23°). On essore le catalyseur, reprend la solution par de l'éther, que l'on lave avec une solution aqueuse de NaOH 10%. On extrait à la manière habituelle 1.76 g (87%) d'alcool brut (sublimé), p.f. 205–206°, $[\alpha]_D^{23} = +43.4°$ ($c = 4.0$; benzène).

3.2. Purification de l'alcool brut

Le *p*-nitrobenzoate se présente sous forme de paillettes après cristallisation dans l'éthanol. Il fond à 137–138°, $[\alpha]_D^{23} = +78.5°$ ($c = 4$; chloroforme). Calculé pour

$C_{18}H_{23}O_4N$: C, 68.12; H, 7.30; N, 4.41%. Trouvé: C, 68.24; H, 7.31; N, 4.39%. Après saponification, on retrouve un triméthyl-5,8,8 bicyclo[3,2,1]octanol-2β (VI) homogène à la chromatographie sur alumine: p.f. 206°; $[\alpha]_D^{23} = +43.9°$ ($c = 4.0$; benzène). Calculé pour $C_{11}H_{20}O$: C, 78.51; H, 11.98%. Trouvé: C, 78.27; H, 11.81%. Spectre infrarouge: bande à 1044 cm^{-1} (CS_2/0.03 *M*).

3.3. Oxydation chromique

L'alcool (504 mg) donne 659 mg de dinitro-2,4 phénylhydrazone d'homoépicamphre, p.f. 178–178.5°, seule ou en mélange avec la dinitro-2,4 phénylhydrazone de l'homoépicamphre (1).

4. Triméthyl-5,8,8 bicyclo[3,2,1]octanol-2α (V)

4.1. Préparation de l'alcool brut

Selon le mode opératoire 2.1, 12 g d'homoépicamphre sont réduits par 20 g de sodium dans 200 ml d'éthanol anhydre. On obtient 11.3 g (94%) d'alcool brut sublimé, p.f. 172–173°, $[\alpha]_D^{23} = +36.4°$ ($c = 4.03$; benzène).

4.2. Purification de l'alcool brut (Mode opératoire 1.2)

Le *p*-nitrobenzoate pur fond à 120°, $[\alpha]_D^{23} = +24.5°$ ($c = 4$; chloroforme). Calculé pour $C_{18}H_{23}O_4N$: C, 68.12; H, 7.30; N, 4.41%. Trouvé: C, 68.28; H, 7.39; N, 4.33%. Après saponification, on retrouve un triméthyl-5,8,8 bicyclo[3,2,1]octanol-2α (V) homogène, p.f. 166°, $[\alpha]_D^{23} = +35.9°$ ($c = 4.0$; benzène). Calculé pour $C_{11}H_{20}O$: C, 78.51; H, 11.98%. Trouvé: C, 78.25; H, 11.82%. Le p.f. de cet alcool avec l'épimère p.f. 206° (alcool VI, section 3.2) est de 179–185°. Spectre infrarouge: bande forte à 1038 cm^{-1} (CS_2/0.03 *M*).

4.3. Oxydation chromique (Mode opératoire, voir 1.4)

L'alcool V (504 mg) donne 632 mg de dinitro-2,4 phénylhydrazone d'homoépicamphre, p.f. 177.5°, seule ou en mélange avec la dinitro-2,4 phénylhydrazone de l'homoépicamphre (1).

5. Mesures des vitesses d'oxydation chromique

La mesure de la disparition de l'acide chromique se fait dans un spectrophotomètre Beckman DK1, ajusté à la longueur d'onde de 3500 Å. Une courbe de calibration de la densité optique des solutions de CrO_3, à cette longueur d'onde, a d'abord été tracée en fonction de la concentration. La vitesse d'oxydation a ensuite été mesurée grâce à la variation de la densité optique de la solution en fonctions du temps.

À partir d'une solution mère d'acide acétique aqueux à 90.9% (volume/volume) maintenue à température constante (24.9°±0.1°), on prépare: (*a*) une solution de CrO_3 environ 1.05×10^{-3} *M* que l'on place dans le bain à température constante; (*b*) une solution contenant les alcools à oxyder; cette solution est préparée juste avant l'oxydation. Au temps zéro, on mélange rapidement les solutions (*a*) et (*b*) de manière à obtenir environ 50 ml en tout; on en remplit une cellule en quartz que l'on place dans la chambre de mesures d'un spectrophotomètre Beckman DK1; ces diverses opérations prennent de 20 à 30 secondes depuis le temps zéro. La technique varie ensuite un peu, selon la rapidité de l'oxydation: (1) pour les oxydations lentes, allant jusqu'à 60 minutes, on conserve la solution contenant l'alcool et le CrO_3 dans le bain à température constante; on en prélève des échantillons de temps en temps, que l'on place dans la chambre de mesures du spectrophotomètre et dont on mesure la densité optique; on assure ainsi l'uniformité de la température au cours de l'expérience; (2) pour les oxydations rapides, ne dépassant pas 5 minutes, tous les points de la courbe sont enregistrés automatiquement sur le papier qui se déroule sans interruption; comme la température de la chambre de mesures du spectrophotomètre est voisine de 25°, les variations de température sont négligeables.

Les résultats et les données expérimentales sont rapportés au Tableau III. La vitesse $v = -d\ CrO_3/dt$ a été déterminée par la méthode graphique et les valeurs de v données sont les valeurs de la vitesse extrapolée au temps zéro.

TABLEAU III

Détail des déterminations des vitesses d'oxydation chromique

Alcools	Concentrations molaires des alcools	Concentrations molaires en CrO_3	$v = -d\ CrO_3/dt$ mole×litre^{-1}×min^{-1}
Cyclohexanol	7.136×10^{-4}	10.22×10^{-4}	2.80×10^{-6} (lente)
Alcool au sodium III	7.162×10^{-4}	10.85×10^{-4}	16.0×10^{-6} (lente)
Alcool au platine IV	7.013×10^{-4}	10.76×10^{-4}	330.0×10^{-6} (rapide)
Alcool au sodium V	7.108×10^{-4}	10.76×10^{-4}	18.4×10^{-6} (lente)
Alcool au platine VI	7.111×10^{-4}	10.77×10^{-4}	350.0×10^{-6} (rapide)

REMERCIEMENTS

Nous remercions le Conseil National de Recherches du Canada de son aide financière (subvention de recherche, H.F., et bourse d'études, J-C.R.) et l'Office de Recherches Scientifiques de la Province de Québec d'une bourse d'études, M.L.

BIBLIOGRAPHIE

1. Favre, H., Marinier, B. et Richer, J-C. Can. J. Chem. **34**, 1329 (1956).
2. Favre, H. et Marinier, B. Can. J. Chem. **35**, 278 (1957).
3. Fodor, G. et Nador, K. J. Chem. Soc. 721 (1953).
4. Bose, A. K. Résumé des communications. Tome II. XVIe Congrès international de Chimie pure et appliquée, Paris. juillet 1957. page 141.
5. Fredga, A. et Miettinen, T. K. Acta Chem. Scand. **1**, 371 (1947).
6. Freudenberg, K. et Lwowski, W. Ann. **587**, 213 (1954).
7. Bose, A. K. J. Org. Chem. **20**, 1003 (1955).
8. Kergomard, A. et Geneix, M.Th. Bull. soc. chim. France, (5), 397 (1958).
9. Bose, A. K. J. Org. Chem. **20**, 1010 (1955).
10. Naves, Y.-R. Bull. soc. chim. France, (5), 1020 (1956).
11. Wicker, R. J. J. Chem. Soc. 2165 (1956).
12. Dauben, W. G., Blanz, E. J., Jr., Jiu, J. et Micheli, R. A. J. Am. Chem. Soc. **78**, 3752 (1956).
13. Vavon, G. et Zaremba, C. Bull. soc. chim. France, **49** (4), 1853 (1931).
14. Barton, D. H. R. Experientia, **6**, 316 (1950).
15. Barton, D. H. R. J. Chem. Soc. 1027 (1953).
16. Schreiber, J. et Eschenmoser, A. Helv. Chim. Acta, **38**, 1529 (1955).
17. Cole, A. R. H., Jones, R. N. et Dobriner, K. J. Am. Chem. Soc. **74**, 5571 (1952).

DÉRIVÉS DU TRIMÉTHYL-1,8,8 BICYCLO[3,2,1]OCTANE

IV. DÉTERMINATION DES CONFIGURATIONS DES DEUX DIMÉTHYL-5,5 CYCLOHEXANEDIOLS-1,3[1]

H. FAVRE ET J-C. RICHER[2]

RÉSUMÉ

À la suite de l'analyse des modes de formation et des vitesses d'oxydation chromique des diméthyl-5,5 cyclohexanediols-1,3, les auteurs attribuent la configuration *cis* au diol p.f. 149–151° et la configuration *trans* à l'isomère p.f. 106–107.5°.

Au cours de l'étude de la réduction catalytique de la triméthyl-1,8,8 bicyclo[3,2,1]-octanedione-2,4 (I) (1) nous avons utilisé le dimédon (II) comme substance modèle. Nous avons obtenu avec un rendement de 95% un seul des deux diméthyl-5,5 cyclo-

I

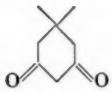

II

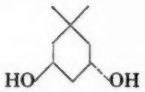

III

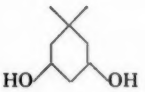

IV

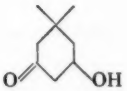

V

hexanediols-1,3 stéréoisomères (p.f. 106–107.5°, III), en opérant à pression atmosphérique et à 25°, en présence de nickel de Raney dans l'éthanol. Les deux diméthyl-5,5 cyclohexanediols-1,3 sont connus à la suite de réductions chimiques ou catalytiques (Tableau I); à notre connaissance, leurs configurations respectives, *cis* et *trans*, ne le sont pas; ce travail a pour but de les déterminer.

TABLEAU I

Réductions du dimédon conduisant aux diméthyl-3,3 cyclohexanediols-1,3

Conditions expérimentales	P.f. et rendements en diméthyl-5,5 cyclohexanediols-1,3	Autres produits de réduction	Références
Ni Raney, 150–200 at., 125°	102–104°+146° (80%)	Diméthyl-3,3 cyclohexanol-1 (3.8%)	(2)
Ni Raney, 100 at., 180°	146°	Diméthyl-3,3 cyclohexanol-1 (75%)	(3)
Ni Raney, 748 mm, 23°, $+CHCl_3$	106–107.5° (95%)		Ce travail
Sodium-éthanol	147° (63–68%)	Diméthyl-3,3 cyclohexanol-1 (7%)	(4)
$LiAlH_4$	102–103.2°+147.6–148° (4%)	Diméthyl-5,5 cyclohexène-2 ol-1 (62%)	(5)

Nous avancerons d'abord quelques considérations concernant le mécanisme de l'hydrogénation catalytique. Dans tous nos essais, l'hydrogénation prenait fin après absorption de deux moles d'hydrogène. En interrompant la réaction après fixation d'une

[1]*Manuscrit reçu le 27 août, 1958.*
Contribution du Département de Chimie de l'Université de Montréal, Montréal, P.Q. Ce mémoire est tiré de la thèse de doctorat de J-C. Richer; il fut présenté au 41e Congrès annuel de l'Institut de chimie du Canada à Toronto, les 26–28 mai, 1958.
[2]*Boursier du Conseil national de Recherches du Canada, 1954–1958. Adresse actuelle: Department of Chemistry, University of Notre Dame, Notre Dame, Ind.*

mole d'hydrogène seulement, nous avons pu mettre en évidence la présence de la diméthyl-5,5 cyclohexanolone-3,1 (V) dans le milieu, à côté du dimédon non réduit et du diol III. En pratique, nous avons isolé le produit de déshydratation du β-cétol V, la diméthyl-5,5 cyclohexène-2 one-1. Cette formation de β-cétol était connue pour la réduction de nombreuses β-dicétones aliphatiques (6). Nous l'avons montrée pour étayer notre raisonnement. Nous formulons ainsi la réaction d'hydrogénation: la réduction catalytique du dimédon conduit d'abord à la diméthyl-5,5 cyclohexanolone-3,1 (V) qui se détache du catalyseur pour s'y fixer à nouveau et se faire réduire en diol. La configuration du diol obtenu dépendra de la conformation du β-cétol V, si aucune isomérisation n'a lieu. Il y a alors une analogie entre la réduction de ce β-cétol et celle de la triméthyl-3,3,5 cyclohexanone-1 (VI A) étudiée en détail par Wicker (7, 8, 9). Cet auteur a montré que dans des conditions douces (température basse, peu de catalyseur alcalin susceptible de provoquer des isomérisations), la cétone VI conduisait principalement à l'alcool *trans* VII (88% de *trans* pour 12% de *cis*); la triméthyl-3,3,5 cyclohexanone serait réduite sous la conformation VI A de préférence à VI B à cause de l'interférence des deux groupes méthyle axiaux 3 et 5; la fixation de l'hydrogène se fait de façon à donner l'alcool axial.

V B R = OH V A R = OH III R = OH IV R = OH
VI B R = CH_3 VI A R = CH_3 VII R = CH_3 VIII R = CH_3

Ainsi, la conformation V A, préférée à V B pour la diméthyl-5,5 cyclohexanolone-3,1,[3] conduira au diol III *trans*, groupes —OH *a*−*e*, à la condition qu'il n'y ait pas d'isomérisation consécutive à la formation du diol. Nous avons mis en oeuvre un nickel de Raney traité par du chloroforme. Cornubert et ses collaborateurs (12, 13, 14, 15) ont montré que le chloroforme et d'autres composés organiques halogénés abaissaient considérablement l'aptitude du nickel de Raney à réduire les groupes carbonyle; l'explication donnée est que le chloroforme engendre avec le nickel de l'acide chlorhydrique qui neutralise la soude fixée par le catalyseur. Comme nous n'avons pas utilisé les quantités prescrites par Cornubert pour contraindre le nickel et l'empêcher de réduire les groupes carbonyle, mais seulement des quantités modérées n'empêchant pas la réduction, nous pensons que notre nickel s'approchait de la neutralité et puisque nous n'avons opéré ni sous pression ni à température élevée, une isomérisation n'était plus à craindre et une configuration *trans* (III) se justifie pour le diol p.f. 106–107.5°. Le diol p.f. 149–151° est alors le diol *cis*.

Nous avons tenté de corroborer ces configurations par deux méthodes:

1. La résolution en antipodes optiques qui fait de l'isomère dédoublable l'isomère *trans*. Nous avons réussi à préparer le bi-phtalate acide de l'isomère p.f. 106–107.5° (*trans*, donc dédoublable, selon nos considérations antérieures), mais nous n'avons pu en cristalliser les sels de strychnine ou de brucine.

2. L'étude infrarouge des ponts hydrogène internes, à la manière de Kuhn (16), qui a montré que le cyclohexanediol-1,3 *cis*, en solution 0.005 *M* dans le tétrachlorure de carbone, présente deux bandes, 3619 et 3544 cm^{-1}, attribuées respectivement aux groupes —OH libres et —OH liés par un pont hydrogène; l'isomère *trans* ne présente qu'une

[3]*Dans son exposé sur la prééminence des formes équatoriales, Cornubert (10) démontre que le diméthyl-3,3 cyclohexanol existe sous la forme* —OH *équatorial. Eliel et Lukach (36) arrivent à la même conclusion. Nous trouvons dans ces travaux la justification de notre avancé.*

bande, 3620 cm^{-1}, la distance séparant les hydroxyles axial et équatorial ne permettant pas la formation d'un pont hydrogène interne. Cette méthode est inappliquable au cas des diméthyl-5,5 cyclohexanols-1 *cis* et *trans*, car les deux isomères ne montrent qu'une bande: 3621 cm^{-1} pour l'isomère p.f. 149–151° et 3627 cm^{-1} pour l'isomère p.f. 106–107.5°.

Nous nous sommes alors tournés vers l'étude cinétique de l'oxydation chromique des deux diols III et IV, en nous inspirant des travaux de Vavon (17) et de Winstein (11) (indiquant que les alcools cyclohexaniques axiaux s'oxydent plus rapidement que les alcools équatoriaux (18, 19)), et de Schreiber et Eschenmoser (20) (montrant que la vitesse d'oxydation est proportionnelle à la compression stérique du système; en particulier, qu'un groupe méthyle axial porté par un carbone en β de celui qui porte le groupe —OH augmente considérablement la vitesse de l'oxydation de l'alcool axial, celle de l'alcool équatorial étant sensiblement la même que s'il n'y avait pas le groupe méthyle: cas des cholestanols-2α et -2β, et -3α et -3β).

Nous avons ainsi commencé par mesurer les vitesses d'oxydation des cyclohexanediols-1,2, -1,3 et -1,4 *cis* et *trans* dont les configurations sont bien connues. Les résultats (Tableau II) appellent les commentaires suivants: (*a*) les diols-1,2 *cis*, -1,3 *trans* et -1,4 *cis* s'oxydent plus rapidement que leur isomère *trans*, *cis* et *trans* respectif; (*b*) les diols qui s'oxydent plus rapidement présentent nécessairement un groupe —OH axial et l'autre équatorial; nous en concluons que les diols qui s'oxydent plus lentement le font sous leur conformation diéquatoriale et non diaxiale.

TABLEAU II

Vitesses d'oxydation chromique des cyclohexanediols

Alcools*	Conformations†	Concentrations molaires en alcool	Concentrations molaires en CrO_3	$v = -d$ CrO_3/dt‡ mole $\times$litre$^{-1}\times$ min^{-1}
Cyclohexanol	$a+e$	7.136×10^{-4}	10.22×10^{-4}	2.8×10^{-6}
Cyclohexanediol-1,2 *cis* (21)	$a-e$	3.542×10^{-4}	10.70×10^{-4}	5.00×10^{-6}
Cyclohexanediol-1,2 *trans* (22, 23)	$e-e$ $a-a$	3.585×10^{-4}	10.70×10^{-4}	1.68×10^{-6}
Cyclohexanediol-1,3 *cis* (24)	$e-e$ $a-a$	3.585×10^{-4}	10.60×10^{-4}	1.76×10^{-6}
Cyclohexanediol-1,3 *trans* (25, 26)	$a-e$	3.539×10^{-4}	10.60×10^{-4}	3.4×10^{-6}
Cyclohexanediol-1,4 *cis* (27, 28, 29, 30, 31, 32)	$a-e$	3.558×10^{-4}	10.60×10^{-4}	2.12×10^{-6}
Cyclohexanediol-1,4 *trans* (27, 33, 34)	$e-e$ $a-a$	3.553×10^{-4}	10.60×10^{-4}	1.72×10^{-6}
Diméthyl-5,5 cyclohexanediol-1,3 *cis*, p.f. 149–151° IV	$e-e$ $a-a$	3.555×10^{-4}	10.60×10^{-4}	2.4×10^{-6}
Diméthyl-5,5 cyclohexanediol-1,3 *trans*, p.f. 106–107.5° III	$a-e$	3.542×10^{-4}	10.60×10^{-4}	20.00×10^{-6}

*On trouve à la suite des diols les références bibliographiques concernant leurs configurations et leurs modes de préparation. Les points de fusion de ces diols sont identiques à ceux décrits dans la littérature.

†Pour les conformations du cyclohexanol, voir (10, 11).

‡Acide acétique aqueux, 90.9% (v/v); $t = 24.9°\pm0.1°$.

Il est clair que ces résultats sont essentiellement approchés. Winstein (11) considère que la réaction d'oxydation est la résultante de plusieurs réactions ayant des vitesses distinctes: (*a*) estérification (réaction d'équilibre, rapide); (*b*) formation de la cétone (réaction lente); (*c*) réactions secondaires, par exemple oxydation de la cétone formée (vitesses inconnues). Dans le cas des diols-1,3 qui nous intéressent, ces réactions secondaires peuvent être extrêmement complexes; les β-cétols issus des diols-1,3 *cis* et *trans*

pouvant (*a*) s'oxyder en dicétone, susceptible elle-même d'être oxydée, (*b*) se déshydrater en cétone α,β-éthylénique, aussi oxydable. De toute façon, nous avons déterminé la vitesse d'oxydation d'une manière simple, en extrapolant graphiquement au temps zéro les vitesses données par l'équation $v = -d\ CrO_3/dt$, et nous ne tirerons de la comparaison des vitesses d'oxydation que des renseignements qualitatifs, d'autant plus que nous prenons pour acquis que l'acide chromique oxydera l'un et l'autre des groupes hydroxyle,[4] ce qui rend toute étude quantitative prématurée. Les cyclohexanediols-1,3, dont l'isomère *trans* s'oxyde 1.9 fois plus rapidement que l'isomère *cis*, nous serviront de point de comparaison pour interpréter les résultats de l'oxydation des diméthyl-5,5 cyclohexanediols-1,3 (III et IV). De ces derniers, l'isomère p.f. 106–107.5° s'oxyde 8.3 fois plus rapidement que l'isomère p.f. 149–151°. Nous interprétons ceci en faisant du premier de ces diols l'isomère *trans*, $a-e$, et du deuxième le diol *cis*, oxidé sous sa forme $e-e$. Nous retrouvons non seulement la différence attendue entre les vitesses d'oxydation, mais encore une accélération notoire de la vitesse du diol diméthylé *trans* (III) par rapport à celle du cyclohexanediol-1,3 *trans*, bien en accord avec la présence d'un groupe méthyle axial sur le carbone en β de celui qui porte le groupe —OH axial. Les configurations déduites de l'oxydation chromique sont donc les mêmes que celles tirées plus haut du mécanisme de l'hydrogénation catalytique.

PARTIE EXPÉRIMENTALE[5]

Le dimédon mis en oeuvre a été cristallisé plusieurs fois dans l'éthanol 95%; il fond à 149–150°.

1. Réduction du dimédon en diméthyl-5,5 cyclohexanediol-1,3 trans (III)

Le dimédon (7.28 g) dissous dans 150 ml d'éthanol 95% est introduit dans un ballon à hydrogéner contenant 7.5 g de nickel de Raney; (préparation voir (37)); on ajoute 50 mg de chloroforme (sous forme d'une solution alcool-chloroforme 90–10) et secoue en atmosphère d'hydrogène. Au bout de 42 heures, la réaction s'arrête d'elle-même. On essore le catalyseur, le lave avec un peu de méthanol, évapore le filtrat à pression ordinaire, puis sous vide de 11 mm. Le résidu est repris par de l'éther et lavé avec une solution aqueuse de NaOH 10% puis à l'eau. On sèche sur sulfate de sodim, évapore l'éther et chromatographie le résidu, dissous dans du benzène, sur 100 g d'alumine Merck pour chromatographie; 300 ml de benzène éluent 3.5 g de composés en partie cristallisés, puis 700 ml de benzène éluent 0.209 g de diol p.f. 105–107°; finalement, 350 ml de méthanol éluent 3.7 g de diol p.f. 106–108°. La fraction partiellement cristalline est reprise dans de l'éther de pétrole et adsorbée sur 100 g d'alumine; l'élution par 600 ml de chloroforme donne 0.256 g de liquide brun, puis 300 ml de méthanol éluent 3.2 g de diol p.f. 106–108°. Le diméthyl-5,5 cyclohexanol pur fond à 106–107.5°, après cristallisation dans l'éther. Calculé pour $C_8H_{16}O_2$: C, 66.63; H, 11.18%. Trouvé: C, 66.99; H, 11.06. Le rendement en diol brut est de 95%.

Si l'on ajoute des quantités de chloroforme représentant 7.5, 14 ou 25% de la quantité de nickel de Raney, il n'y a pas d'absorption d'hydrogène.

[4]*Gallagher et Long (35) ont bien démontré ce fait en étudiant l'oxydation chromique de l'ester méthylique de l'acide cholique; bien que réagissant avec des vitesses différentes, les trois groupes* —OH *sont oxydés, et l'oxydation préférentielle de l'hydroxyle en position 7 ne se fait qu'avec un rendement de 40%.*

[5]*Les points de fusion ont été déterminés en tubes capillaires, le thermomètre étant étalonné avec des substances provenant du Bureau des Standards de Washington. Les spectres infrarouges ont été mesurés à l'aide d'un spectrophotomètre "Perkin–Elmer", modèle 112, à simple passage et double faisceau, optique* LiF.

2. Hydrogénation interrompue: préparation de la diméthyl-5,5 cyclohexène-2 one-1

Le dimédon (5.27 g) est hydrogéné dans 80 ml d'éthanol contenant 90 mg de chloroforme, en présence de 4.5 g de nickel de Raney, jusqu'à fixation de 1.02 mole d'hydrogène; la réaction est interrompue, le catalyseur essoré et lavé avec du méthanol, le filtrat évaporé; le résidu est entraîné par de la vapeur d'eau après adjonction de 50 ml carbonate de sodium (sol. aqueuse 10%). On examine séparément le distillat et les eaux alcalines.

(*A*) *Le distillat.*—Il est saturé par du chlorure de sodium et extrait à l'éther. Les solutions éthérées de plusieurs extractions sont réunies, séchées et évaporées; le résidu est traité par de l'acétate de semicarbazide dans du méthanol. On recueille 125 mg de semicarbazone de diméthyl-5,5 cyclohexène-2 one-1, p.f. 191–192.5° (méthanol) seule ou en mélange avec une semicarbazone de diméthyl-5,5 cyclohexène-2 one-1. Analyse: calculé pour $C_9H_{15}ON_3$: N, 23.19%. Trouvé: N, 23.35%.

(*B*) *Des eaux alcalines.*—On extrait par l'éther le diméthyl-5,5 cyclohexanediol-1,3, p.f. brut 101–103° (1.7 g) et après adjonction d'acide chlorhydrique, le dimédon qui n'a pas réagi (2.1 g).

3. Détermination des vitesses d'oxydation chromique

Le mode opératoire est celui décrit en détail dans la partie III de cette série (37) et les résultats sont rapportés au Tableau II. Les composés ont été préparés selon les travaux antérieurs dont référence est faite au Tableau II.

REMERCIEMENTS

Nous remercions le Conseil National de Recherches du Canada d'une subvention de recherche (H.F.) et d'une bourse d'études (J-C.R.).

BIBLIOGRAPHIE

1. Favre, H. et Richer, J-C. Can. J. Chem. **37**, 417 (1959).
2. Sprague, J. M. et Adkins, H. J. Am. Chem. Soc. **56**, 2669 (1934).
3. Henshall, T. J. Soc. Chem. Ind. London, **62**, 127 (1943).
4. Crossley, A. W. et Renouf, N. J. Chem. Soc. 602 (1915).
5. Dreiding, A. S. et Hartmann, J. A. J. Am. Chem. Soc. **75**, 3723 (1953).
6. Stutsman, P. S. et Adkins, H. J. Am. Chem. Soc. **61**, 3303 (1939).
7. Peppiat, E. G. et Wicker, R. J. Chem. & Ind. 747 (1955).
8. Peppiat, E. G. et Wicker, R. J. J. Chem. Soc. 3122 (1955).
9. Wicker, R. J. J. Chem. Soc. 2165 (1956).
10. Cornubert, R. Bull. soc. chim. France, (5) 996 (1956).
11. Winstein, S. et Holness, N. J. J. Am. Chem. Soc. **77**, 5562 (1955).
12. Cornubert, R. et Kaziz, C. Bull. soc. chim. France, (5) 410 (1952).
13. Cornubert, R. et Phélisse, J. Bull. soc. chim. France, (5) 403 (1952).
14. Cornubert, R. et Réal, M. Bull. soc. chim. France, (5) 407 (1952).
15. Cornubert, R. et Thomas, P. Bull. soc. chim. France, (5) 524 (1954).
16. Kuhn, L. P. J. Am. Chem. Soc. **74**, 2492 (1952).
17. Vavon, G. et Zaremba, C. Bull. soc. chim. France, 1853 (1931).
18. Barton, D. H. R. Experientia, **6**, 316 (1950).
19. Barton, D. H. R. J. Chem. Soc. 1027 (1953).
20. Schreiber, J. et Eschenmoser, A. Helv. Chim. Acta, **38**, 1529 (1955).
21. Clarke, M. F. et Owen, L. N. J. Chem. Soc. 315 (1949).
22. Derx, H. G. Rec. trav. chim. **41**, 312 (1922).
23. Brown, J. B., Henbest, H. B. et Jones, E. R. H. J. Chem. Soc. 3634 (1950).
24. Rigby, W. J. Chem. Soc. 1586 (1949).
25. Rigby, W. J. Chem. Soc. 1588 (1949).
26. Clarke, M. F. et Owen, L. N. J. Chem. Soc. 2103 (1950).
27. Grewe, R., Lorenzen, W. et Vining, L. Chem. Ber. **87**, 793 (1954).
28. Willstatter, R. et Lessing, R. Ber. **34**, 506 (1901).
29. Rothstein, B. Ann. chim. **14**, 461 (1930).
30. Olberg, R. C., Pines, H. et Ipatieff, V. N. J. Am. Chem. Soc. **66**, 1096 (1944).
31. Owen, L. N. et Robins, P. A. J. Chem. Soc. 320 (1949).
32. White, J. N. Z. Krist. **80**, 5 (1931).

33. PERRINE, T. D. et WHITE, W. C. J. Am. Chem. Soc. **69**, 1542 (1947).
34. COOPS, J., DIENSKE, J. W. et SMIT, W. M. Rec. trav. chim. **57**, 637 (1938).
35. GALLAGHER, T. F. et LONG, W. P. J. Biol. Chem. **147**, 131 (1943).
36. ELIEL, E. L. et LUKACH, C. A. J. Am. Chem. Soc. **79**, 5986 (1957).
37. FAVRE, H., LEFEBVRE, M. et RICHER, J-C. Can. J. Chem. **37**, 403 (1959).

DÉRIVÉS DU TRIMÉTHYL-1,8,8 BICYCLO[3,2,1]OCTANE

V. RÉDUCTIONS CATALYTIQUE ET CHIMIQUE DE LA TRIMÉTHYL-1,8,8 BICYCLO[3,2,1]OCTANEDIONE-2,4[1]

H. FAVRE ET J-C. RICHER[2]

RÉSUMÉ

Les auteurs montrent que la triméthyl-1,8,8 bicyclo[3,2,1]octanedione-2,4 est réduite: en triméthyl-1,8,8 bicyclo[3,2,1]octanediol-2β,4β en présence de nickel de Raney et de soude caustique; en triméthyl-1,8,8 bicyclo[3,2,1]octène-3 one-2, ou directement en homocamphre, en présence de nickel de Raney et de très petites quantités de chloroforme, par l'intermédiaire de la triméthyl-1,8,8 bicyclo[3,2,1]octanol-4β one-2; en un mélange de triméthyl-1,8,8 bicyclo[3,2,1]octanediols-2α,4α; -2α,4β et probablement -2β,4α par le sodium dans l'éthanol. Les configurations des diols furent assignées à la suite de l'analyse de leurs modes de formation, de leurs vitesses d'oxydation chromique et des rotations moléculaires de leurs di-*p*-nitrobenzoates.

Rupe et Frey (1) ont hydrogéné la triméthyl-1,8,8 bicyclo[3,2,1]octanedione-2,4 (I) en présence d'un catalyseur de nickel dans l'éthanol aqueux à 50%. A température de 60–70° et sous pression de 90 atmosphères, ils ont obtenu un composé p.f. 276–279° qui n'a pas été étudié, et qui est décrit simplement comme un "dimère". A température et à pression ordinaires, en présence de carbonate de sodium, ces auteurs ont obtenu la triméthyl-1,8,8 bicyclo[3,2,1]octène-3 one-2 (III) avec un rendement de 87.5%; le β-cétol II est postulé comme intermédiaire.

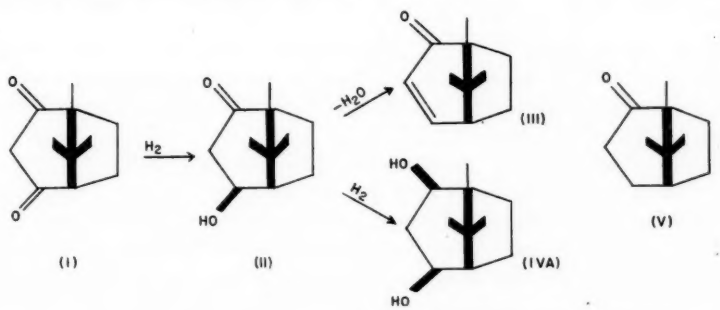

En reprenant les essais du Rupe et Frey, dans le but d'obtenir de l'homocamphre, nous n'avons obtenu que peu ou pas du tout de la cétone α,β-éthylénique III, mais principalement un composé p.f. 279–284°; nous utilisions un catalyseur de nickel de Raney (dans leur mémoire, Rupe et Frey n'indiquent ni la nature ni le mode de préparation de leur nickel). Après avoir caractérisé le composé inconnu, p.f. 279–284°, comme un des 4 triméthyl-1,8,8 bicyclo[3,2,1]octanediols-2,4 stéréoisomères (nous montrons plus loin dans cet article que c'est l'isomère 2β,4β (IV A) répondant à la formule $C_{11}H_{20}O_2$, donnant un di-*p*-nitrobenzoate bien cristallisé, p.f. 213–215°), nous nous sommes attachés à préciser les conditions opératoires pouvant conduire fidèlement soit au diol IV A, soit à la cétone α,β-éthylénique III. On trouve au Tableau I les résultats de cette étude.

Les hydrogénations ont été effectuées dans des conditions contrôlées, le nickel de

[1]*Manuscrit reçu le 27 août, 1958.*
Contribution du Département de Chimie de l'Université de Montréal, Montréal, P.Q. Ce mémoire est tiré de la thèse de doctorat de J-C. Richer.
[2]*Boursier du Conseil National de Recherches du Canada, 1954–1958. Adresse actuelle: Department of Chemistry, University of Notre Dame, Notre Dame, Ind.*

TABLEAU I

Hydrogénations catalytiques de la triméthyl-1,8,8 bicyclo[3,2,1]octanedione-2,4

No. d'ordre	Poids de cétone	Poids de nickel	Adjonction*	H_2 absorbé†	Temps d'absorption	Produits‡
1	12.5 g	12.0 g	0.5 mole NaOH	1.00 mole	25 heures	47% Dicétone I 35% Diol IV A 5.6% Cétones
2	10 g	12 g	1 mole NaOH	0.22 mole	25 heures	91% Dicétone I 5% Diol IV A 2% Cétones
3	5.0	5 g	1.5% Chloroforme	1.02 mole	20 heures	Environ 94% de β-cétol II (selon hydrogénation No. 4)
4	9.85 g	5 g	1.5% Chloroforme	0.97 mole	25 heures	2% Dicétone I 94% Cétone non saturée III
5	20.0 g	12 g	(*a*) 0.9% Chloroforme (*b*) 1 mole NaOH	1.03 mole 0.78 mole	20 heures 30 minutes	92% Homocamphre V 5% Diol IV A
6	5.0 g	3 g	(*a*) Nil (*b*) 1 mole NaOH	1.07 mole 0.72 mole	22 heures 45 minutes	82% Homocamphre V 12% Diol IV A

*La quantité de soude ajoutée est exprimée en mole par mole de dicétone I. Le pourcentage de chloroforme est relatif au poids de nickel de Raney mis en oeuvre.

†Exprimé en mole par mole de dicétone I.

‡Cétones = fractions cétoniques pouvant contenir de l'homocamphre et de la triméthyl-1,8,8 bicyclo[3,2,1]octène-3 one-2 (III) et peut-être d'autres cétones.

Raney mis en oeuvre étant l'objet d'une attention particulière: il fut préparé à partir d'un alliage AN 50 selon le mode décrit dans la partie expérimentale, et fut utilisé rapidement après sa préparation; des échantillons vieux de quelques semaines ne permettent pas de reproduire les résultats.

Delépine et Horeau (2) ont montré que l'activité réductrice du nickel de Raney envers les cétones et l'acétylacétone était accrue par des adjonctions de petites quantités de soude caustique au milieu, tandis que Cornubert et ses collaborateurs (3, 4, 5, 6, 7) ont rapporté l'influence inhibitrice du chloroforme et d'autres dérivés organiques halogénés sur la réduction des groupes carbonyle. Nous nous sommes inspirés de ces observations pour choisir les agents appelés à modifier l'activité du nickel de Raney et à rendre ce catalyseur spécifique et fidèle.

L'addition de soude caustique favorise nettement la formation du diol IV A (essai 1, Tableau I); les rendements en diols dépendent directement de la quantité de soude introduite, car le sel sodé de la dicétone n'est pas réduit comme le montre l'essai 2 (Tableau I).

L'addition massive de chloroforme inhibe complètement la réduction (voir réduction du dimédon (8)); par contre, l'adjonction de quantités ne dépassant pas 2%[3] du poids du catalyseur mis en oeuvre permet la réduction du carbonyle en position 4 et inhibe avec satisfaction celle du carbonyle en position 2. Ce mode opératoire nous a permis d'obtenir:

(1) Le β-cétol intermédiaire II (hydrogénation 3) en évaporant avec précaution le solvant débarrassé du catalyseur lorsque la réduction s'arrête d'elle-même après absorption de 1.0 mole d'hydrogène; ce β-cétol est un composé très instable, p.f. 249–250°,

[3]*Nous avons adopté les termes suivants: nickel "ordinaire", pour le nickel utilisé tel que préparé selon notre méthode; nickel "modéré", lorsque le nickel "ordinaire" est traité par des quantités de chloroforme ne dépassant pas 2% de son poids. Cornubert appelle nickel "contraint" le nickel inapte à réduire les groupes carbonyle.*

spectre infrarouge, bandes à 3455 (—OH) et 1705 (C = 0) cm^{-1}, perdant facilement une molécule d'eau par sublimation ou par entraînement à la vapeur d'eau.

(2) La triméthyl-1,8,8 bicyclo[3,2,1]octène-3 one-2 (III) (hydrogénation 4) avec un rendement de 94% (9, 1).

(3) L'homocamphre (V). Dans ce cas (hydrogénation 5), après absorption d'une mole d'hydrogène et arrêt spontané de la réaction, on introduit dans le milieu réactionnel une mole de soude caustique en solution dans l'éthanol 95%. Il se produit un échauffement de la solution avec élimination d'une molécule d'eau du β-cétol II; l'absorption d'hydrogène reprend aussitôt, et bien que l'absorption ne corresponde alors qu'à 0.78 mole d'hydrogène, on isole l'homocamphre (V) avec un rendement de 94%. Cet homocamphre est très pur et son mode de préparation est le plus simple de tous ceux décrits jusqu'ici (9). L'hydrogénation 6 présente un certain intérêt; elle fut réalisée avec un nickel de Raney "ordinaire" (sans adjonction de soude ou de chloroforme); elle démontre clairement l'influence inhibitrice du chloroforme sur la réduction du carbonyle en position 2 (cf. hydrogénation 5). Elle montre aussi que l'adjonction de soude doit se faire au début de l'hydrogénation si l'on veut obtenir un bon rendement en diol IV A (comme dans l'hydrogénation 1). L'emploi du nickel de Raney "ordinaire" reste cependent fort aléatoire: de nombreux essais ont donné des quantités variables du diol IV A et de la cétone α,β-éthylénique III. Ces essais peu intéressants en raison du manque de fidélité du catalyseur ne sont pas rapportés dans ce mémoire.

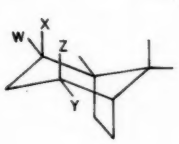

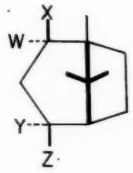

IV A X,Z = OH; W,Y = H
IV B W,Y = OH; X,Z = H
IV C X,Y = OH; W,Z = H
IV D W,Z = OH; X,Y = H

VI X = OH; W,Y,Z = H
VII W = OH; X,Y,Z = H
VIII Y = OH; W,X,Z = H
IX Z = OH; W,X,Y = H

X

Les produits de la réduction de la dicétone I par le sodium dans l'éthanol ont été séparés en produit acide (dicétone I de départ non entrée en réaction) 58.1% et en composés neutres, 39.9%, qu'une chromatographie sur alumine a séparés en:

(1) 4.1% d'un solide jaune non étudié;

(2) 5.5% d'un solide incolore, p.f. 171–173°, $[\alpha]_D^{23} = +23.6°$, correspondant à la formule $C_{11}H_{20}O$. Ce résultat d'analyse et la facilité avec laquelle ce solide s'élue de l'alumine indiquent qu'il doit être un mélange des monoalcools VI–IX;

(3) 20.4% d'un solide incolore, p.f. 250–255°, $[\alpha]_D^{23} = +7.2°$ donnant un di-*p*-nitrobenzoate p.f. 211–212.5°, $[\alpha]_D^{23} = +70.0°$ dont on tire par saponification le diol IV D, p.f. 237–239°, $[\alpha]_D^{23} = -9.0°$;

(4) 68.4% de diol IV B, p.f. 234–236°, $[\alpha]_D^{23} = +32.7°$, dont le di-*p*-nitrobenzoate fond à 221–224°, $[\alpha]_D^{23} = +37°$.

Nous avons en main trois des quatre triméthyl-1,8,8 bicyclo[3,2,1]octanediols-2,4 stéréoisomères; nous les considérons comme stériquement purs; leurs di-*p*-nitrobenzoates donnent des dépressions de point de fusion en mélange. À la suite de l'analyse de leurs modes de formation, de l'application à leurs di-*p*-nitrobenzoates de la méthode des différences de rotation moléculaire et de leurs vitesses d'oxydation chromique, nous leur avons attribué les configurations suivantes:

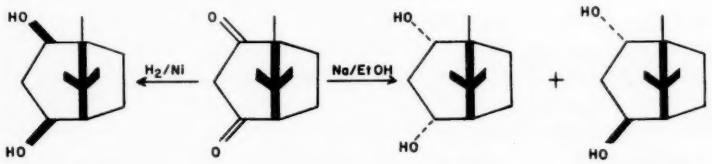

IV A p.f. 279–284° | I | IV B p.f. 234–236° | IV D p.f. 237–239°

Nous pensons aussi avoir en main un mélange des diols IV D et IV C dont le p.f. est de 250–255° (réduction chimique, fraction 3 brute), car le comportement chromatographique de ce mélange semble montrer que l'isomère IV D, qui le constitue en partie, n'est pas accompagné des diols IV A et IV B.

Nous examinerons dans l'ordre les modes de formation, la méthode des différences des rotations moléculaires et les vitesses d'oxydation des diols.

L'hydrogénation catalytique de la triméthyl-1,8,8 bicyclo[3,2,1]octanedione-2,4 (I) est stéréospécifique. Elle rappelle les hydrogénations de l'homocamphre (V) et de l'homoépicamphre (X) qui conduisent aux monols VI et IX de configuration β, —OH axial (10). Il semble raisonnable d'attribuer la configuration -4β au β-cétol intermédiaire (II) et d'envisager que la réduction du groupe C = 0 de ce cétol conduira comme celle de l'homocamphre à un groupe —OH axial. Le diol qui se formera sera ainsi diaxial ou -2β,4β (IV A)[4]; ceci est vrai pour autant qu'il n'y ait pas d'isomérisation des groupes —OH axiaux en groupes équatoriaux; nous voyons l'absence de toute isomérisation dans le fait que nous avons obtenu (voir mémoire antérieur (10)) le même rendement stérique en alcool axial au cours de la réduction de l'homoépicamphre, en mettant en oeuvre le platine dans l'acide acétique et le nickel de Raney en présence de soude.

Nous avançons également par analogie que le diol p.f. 234–236° qui se forme en quantité prépondérante lors de la réduction par le sodium et l'éthanol est le diol-2α,4α (IV B), puisque l'homocamphre (V) et l'homoépicamphre (X) engendrent principalement les monols de configuration α (VII et VIII)(10).

L'examen des rotations moléculaires des di-*p*-nitrobenzoates donne les conclusions suivantes. Utilisant la valeur $[M]_D = +24°$ pour la rotation moléculaire du triméthyl-1,8,8 bicyclo[3,2,1]octane[5] et les valeurs des rotations moléculaires des *p*-nitrobenzoates des triméthyl-1,8,8 et -5,8,8 bicyclo[3,2,1]octanols-2α et -2β décrites dans la partie III de cette série (10), nous pouvons calculer[6] les valeurs des rotations moléculaires des di-*p*-nitrobenzoates des quatre diols (voir Tableau II).

Nous remarquons alors une correspondance convenable entre les valeurs calculées

[4]*Nous ne retenons que la conformation "cyclohexane chaise" pour les diols-2,4 du triméthyl-1,8,8 bicyclo [3,2,1]octane; voir (10).*

[5]*Travaux de notre laboratoire non-publiés. Cet hydrocarbure a été préparé à partir du (+) camphre, sans inversion de configuration.*

[6]*Nous trouvons une justification de cette manière de procéder dans les travaux de Striebel et Tamm (11).*

TABLEAU II

Rotations moléculaires des *p*-nitrobenzoates des monols VI–IX et des di-*p*-nitrobenzoates des diols IV A – IV D

Composés	$[M]_D$ Observées			$[M]_D$ Calc.
	p-Nitrobenzoates	Di-*p*-nitrobenzoates	Δ (O-*p*-Nitrobenzoyle)	Di-*p*-nitrobenzoates
Triméthyl-1,8,8 bicyclo[3,2,1]octane	+24°±3°			
Triméthyl-1,8,8 bicyclo[3,2,1]octanol-2β (VI)	−268°±6°		−292°±9°	
Triméthyl-1,8,8 bicyclo[3,2,1]octanol-2α (VII)	+106°±6°		+82°±9°	
Triméthyl-5,8,8 bicyclo[3,2,1]octanol-2β (IX)	+249°±6°		+225°±9°	
Triméthyl-5,8,8 bicyclo[3,2,1]octanol-2α (VIII)	+78°±6°		+54°±9°	
Triméthyl-1,8,8 bicyclo[3,2,1]octanediol-2β,4β (IV A) (catalytique)		+20°±10°		−43°±15°
octanediol-2β,4α (IV C)				−214°±15°
octanediol-2α,4β (IV D) (Na + EtOH)		+339°±10°		+331°±15°
octanediol-2α,4α (IV B) (Na + EtOH)		+178°±10°		+160°±15°

TABLEAU III

Vitesses d'oxydation chromique comparées des monols et des diols dans les positions 2 et 4 du triméthyl-1,8,8 bicyclo[3,2,1]octane

Composés	Conformations des groupes OH	Concentrations molaires en monol ou diol	Concentrations molaires en CrO_3	$v = -d\ CrO_3/dt$* mole×litre^{-1}×min^{-1}
Triméthyl-1,8,8 bicyclo[3,2,1]octanol-2β (VI)	*a*	7.013×10^{-4}	10.76×10^{-4}	330×10^{-6}
octanol-2α (VII)	*e*	7.162×10^{-4}	10.85×10^{-4}	10×10^{-6}
Triméthyl-5,8,8 bicyclo[3,2,1]octanol-2β (IX)	*a*	7.111×10^{-4}	10.77×10^{-4}	350×10^{-6}
octanol-2α (VIII)	*e*	7.108×10^{-4}	10.76×10^{-4}	18.4×10^{-6}
Triméthyl-1,8,8 bicyclo[3,2,1]octane diol-2β,4β (IV A)	*a*−*a*	3.557×10^{-4}	10.66×10^{-4}	300×10^{-6}
diol-2α,4α (IV B)	*e*−*e*	3.550×10^{-4}	10.58×10^{-4}	12×10^{-6}
diol-2α,4β (IV D)	*a*−*e*	3.550×10^{-4}	10.67×10^{-4}	120×10^{-6}
Mélange, p.f. 250–255°, $[\alpha]_D^{23} = +7.2°$		3.550×10^{-4}	10.69×10^{-4}	110×10^{-6}

*Dans l'acide acétique aqueux 90.9% (v/v); $t = 24.9°\pm0.1°$.

et observées si nous faisons du diol p.f. 234–236° le diol diéquatorial (IV B) et du diol p.f. 237–239° l'isomère 2α,4β (équatorial en 2 et axial en 4) (IV D). La correspondance est encore bonne si l'isomère p.f. 279–284° (catalytique) est le diol-2β,4β (IV A); la différence s'explique par un effet de voisinage.

Finalement, l'étude des vitesses d'oxydation chromique (Tableau III) donne les résultats suivants. Avec Lefebvre (10), nous avons montré que les monols axiaux VI et IX s'oxydent par l'acide chromique plus rapidement que les monols équatoriaux VII et VIII. Nous avons montré également (8) que le cyclohexanediol-1,3 *trans* ($a-e$) s'oxyde plus rapidement que l'isomère *cis* (oxydé sous sa forme $e-e$); malgré son caractère empirique, la méthode est applicable à l'étude des diols-1,3. En l'appliquant à l'élucidation des configurations des diols IV qui font l'object de cette étude, nous n'avions plus affaire à des cyclohexanes convertibles, mais à un système rigide. Théoriquement, donc, nous pouvons prévoir que les diols IV A à IV D se diviseront en trois groupes: (1) diol $a-a$; (2) diol $e-e$ et (3) les deux diols $a-e$ —et que ces trois groupes s'oxyderont avec des vitesses différentes, respectivement grande, petite et moyenne; nous admettons que les deux groupes hydroxyle[7] des diols s'oxydent l'un aussi bien que l'autre.

On remarque (Tableau III) que l'accord est bon, compte tenu de la réduction en concentration molaire des diols, entre les valeurs des monols VI–IX et des 2 diols IV A et IV B et que les configurations assignées sont les mêmes que celles déduites plus haut des modes de formation et des pouvoirs rotatoires. Le diol qui s'oxyde avec la vitesse intermédiaire aura l'un de ses groupes axial et l'autre équatorial; son di-*p*-nitrobenzoate, par son pouvoir rotatoire, en fait le diol-2α,4β (IV D) (voir plus haut).

Nous avons oxydé également le mélange des diols p.f. 250–255°; sa vitesse, semblable à celle du diol axial-équatorial, -2α,4β, nous fait supposer que ce mélange est formé des diols-2α,4β et -2β,4α, comme le comportement chromatographique nous l'avait fait supposer plus haut.

Nous avons mesuré[8] le spectre infrarouge du diol diaxial dans le but de voir à la manière de Kuhn (14) si les groupes —OH pouvaient former un pont hydrogène intramoléculaire; nous n'avons trouvé qu'une bande dans la région caractéristique, à 3630 cm^{-1}; le diol diéquatorial présente également une seule bande à 3627 cm^{-1}.

Nous en concluons que le groupe méthyle axial ne permet pas la formation d'un pont hydrogène intramoléculaire; un tel pont se serait manifesté par une bande de fréquence plus basse que 3630 cm^{-1}. Rappelons qu'un pont hydrogène intramoléculaire ne se forme pas chez le diméthyl-5,5 cyclohexanediol-1,3 *cis* (8). Ces faits nous amènent à considérer un point qui a retenu tout particulièrement notre attention au cours de ce travail. Alors que l'homocamphre n'est pas hydrogénable par le nickel de Raney en présence de soude caustique (10), l'hydroxy-4 homocamphre (II) l'est. La seule explication que nous puissions offrir est que dans l'hydroxy-cétone, l'interaction OH—CH_3 diaxiale modifie la conformation cyclohexanique chaise du squelette au point de rendre l'hydrogénation du groupe cétonique suffisamment rapide pour devenir effective. Nous tentons actuellement de démontrer jusqu'où peut aller cette déformation de conformation dont le stade ultime serait une forme cyclohexanique bateau (voir le IIIe mémoire de cette série (10)).

PARTIE EXPÉRIMENTALE[9]

La (−) triméthyl-1,8,8 bicyclo[3,2,1]octanedione-2,4 (I) a été préparée selon (1, 9).

[7]*L'oxydation chromique de l'acide cholique justifie cet avancé (8, 12).*

[8]*Optique* LiF.

[9]*Les points de fusion (p.f.) ont été déterminés en tubes capillaires, le thermomètre étant étalonné avec des substances de p.f. connu (Bureau des Standards de Washington). Les spectres infrarouges ont été mesurés à l'aide d'un spectromètre Perkin–Elmer, modèle 112, à simple faisceau et parcours double (sauf indication contraire, prisme* NaCl). *Les analyses sont de Geller Laboratories, Hackensack, et de W. Manser, Herrliberg.*

1. Hydrogénation catalytiques

Préparation du nickel de Raney

L'alliage AN 50 (50 g) est ajouté par petites portions à 800 ml de soude caustique 20% à température de 0°–5°. Après l'addition, le tout est chauffé sur un bain-marie durant deux heures. La solution de soude est décantée et remplacée par 400 ml de solution fraîche. Le chauffage au bain-marie est continué pendant une heure. Par décantations successives, le nickel est lavé 20 fois avec l'eau du robinet (portions de 800 ml), trois fois avec de l'éthanol 95% distillé dans un appareil de verre Pyrex. Le catalyseur est conservé dans de l'éthanol 95%.

Nous décrivons les essais dans l'ordre donné au Tableau I (partie théorique).

Hydrogénation No. 1—Nickel de Raney + soude caustique: obtention du triméthyl-1,8,8 bicyclo[3,2,1]octanediol-2β,4β IV A

La dicétone I (12.5 g, 0.0694 mole) et 1.39 g de NaOH (0.0348 mole) en solution dans 150 ml d'éthanol 95% sont hydrogénés en présence de 12.0 g de nickel de Raney. En 25 heures, il y a absorption de 1720 ml d'hydrogène (calculé pour $1H_2$: 1710 ml, pour 750 mm et 23°). Le catalyseur est essoré; la solution alcoolique est évaporée et le résidu soumis à l'action de la vapeur d'eau.

La fraction volatile, extraite à l'éther, représente 700 mg (5.6%); il s'agit de cétones qui n'ont pas été étudiées.

La solution alcaline qui contient les composés non volatils est extraite par de l'éther, puis acidifiée par HCl (rouge Congo); une extraction au chloroforme permet de retrouver 5.9 g de dicétone (47%) qui n'a pas réagi. La solution éthérée contient les composés neutres dont on retire par chromatographie sur alumine et élution par le chloroforme 81% de triméthyl-1,8,8 bicyclo[3,2,1]octanediol-2β,4β (IV A) très pur; les fractions éluées par le benzène et le mélange benzène-chloroforme 1-1, précédant l'élution par le chloroforme pur, n'ont pas été étudiées. Le diol pur présente les constantes suivantes: p.f. 279–284°, $[\alpha]_D^{22} = -17.4°$ ($c = 4.09$; éthanol/95%).

Calculé pour $C_{11}H_{20}O_2$: C, 71.69; H, 10.94%. Trouvé: C, 71.87; H, 10.94%. En chauffant le diol avec du chlorure de *p*-nitrobenzoyle dans de la pyridine sèche le di-*p*-nitrobenzoate précipite sous forme d'aiguilles qui se transforment en paillettes par cristallisation dans le chloroforme-éthanol: p.f. 213–215°, $[\alpha]_D^{23} = +4.16°$ ($c = 2.97$; chloroforme). Calculé pour $C_{25}H_{26}O_8N_2$: C, 62.23; H, 5.43; N, 5.81%. Trouvé: C, 62.34; H, 5.46; N, 5.52, 5.80%. Poids moléculaire du di-*p*-nitrobenzoate, déterminé dans le camphre, 432; valeur théorique: 482.

Hydrogénation No. 2—Nickel de Raney + soude caustique

Si l'on hydrogène 10.0 g de dicétone I (0.055 mole) en présence de 2.22 g de NaOH (0.055 mole) et de 12 g de nickel de Raney, dans 85 ml d'éthanol 95%, en 25 heures, il y a absorption de 310 ml d'hydrogène. On retrouve, selon le mode opératoire de l'hydrogénation No. 1, 91% de cétone qui n'a pas réagi, 5% de diol IV A brut p.f. 267–276° et 2% de cétones (non étudiées).

Hydrogénation No. 3—Nickel de Raney + chloroforme: obtention de la triméthyl-1,8,8 bicyclo[3,2,1]octanol-4β one-2 (II)

Dans un ballon à hydrogéner on introduit 5.022 g de dicétone I, 50 ml d'éthanol 95% et 5 g de nickel de Raney; on ajoute alors 0.75 ml d'une solution éthanolique de chloroforme à 10% (soit 75 mg de chloroforme) et on procède à l'hydrogénation. En 20 heures il y a fixation de 710 ml d'hydrogène (calculé pour $1H_2$: 698 ml; 774 mm et 26°). On essore le catalyseur et sépare la solution alcoolique en deux portions égales.

La première portion est évaporée sur un bain-marie; le résidu est rendu alcalin et

entrainé à la vapeur d'eau; on recueille la triméthyl-1,8,8 bicyclo[3,2,1]octène-3 one-2 p.f. 174–176° (pour la caractérisation de ce composé voir (9) et dans ce travail l'hydrogénation No. 4).

La deuxième portion est évaporée à 25°, puis séchée sous vide poussé à cette température. La triméthyl-1,8,8 bicyclo[3,2,1]octanol-4β one-2 se présente sous la forme d'un solide incolore et amorphe, p.f. 249–250°. L'analyse centésimale est satisfaisante en raison des conditions rudimentaires d'isolement du composé: calculé pour $C_{11}H_{18}O_2$: C, 72.52; H, 9.96%. Trouvé: C, 71.05; H, 9.85%. Ce β-cétol perd une molécule d'eau si on le sublime; les fractions de tête de la sublimation fondent à 180–182° et leur spectre infrarouge présente une bande à 1678 cm^{-1}, caractéristique d'une cétone α,β-éthylénique. Les fractions de queue de la sublimation fondent à 242–244°: leur spectre infrarouge montre la présence du groupe —OH (3455 cm^{-1}) et de la cétone saturée (1705 cm^{-1}), dans le Nujol.

Hydrogénation No. 4—Nickel de Raney + chloroforme: obtention de la triméthyl-1,8,8 bicyclo[3,2,1]octène-3 one-2 (III)

La dicétone I (9.854 g) est hydrogénée, en présence de 5 g de nickel de Raney modéré par adjonction de 0.7 ml d'une solution de chloroforme-éthanol 10–90, dans 100 ml d'éthanol 95%. En 25 heures il y a absorption de 1265 ml d'hydrogène (calculé pour $1H_2$: 1300 ml; 745 mm et 25°). On essore le catalyseur, distille l'alcool à pression ordinaire, ajoute 100 ml d'une solution de Na_2CO_3 10% au résidu et entraîne à la vapeur d'eau. Le solide qui est entraîné est repris par de l'éther qui après séchage est évaporé. Le résidu (8.22 g, 94%) est sublimé. La triméthyl-1,8,8 bicyclo[3,2,1]octène-3 one-2 (III) fond à 176.5–178°, $[\alpha]_D^{23} = -54.9°$ ($c = 3.93$; benzène). Calculé pour $C_{11}H_{16}O$: C, 80.44; H, 9.82%. Trouvé: C, 80.37; H, 9.84%. La dinitro-2,4 phénylhydrazone fond à 191–192.5°. L'homocamphre qui résulte de la réduction de la double liaison fond à 191–191.5°, $[\alpha]_D^{23} = -111.4°$ ($c = 4.32$; benzène). Pour fins de comparaison, voir (9, 1). Les composés non volatils avec la vapeur d'eau ont été séparés en: (*a*) triméthyl-1,8,8 bicyclo[3,2,1]-octanediol-2β,4β (IV A), p.f. 280–281.5° (rendement 4%); (*b*) dicétone I qui n'a pas réagi (2%).

Hydrogénation No. 5—Nickel de Raney + chloroforme: obtention de l'homocamphre

La dicétone I (20 g) est hydrogénée dans 200 ml d'éthanol 95%, en présence de 12 g de nickel de Raney modéré par adjonction de 1.08 ml d'une solution à 10% de chloroforme dans l'éthanol 95% (soit 108 mg de chloroforme). En 20 heures il se fixe 2825 ml d'hydrogène (calculé pour $1H_2$: 2750 ml; 749 mm et 23°). Lorsque l'absorption s'arrête, on indroduit dans le milieu 44.4 ml d'une solution à 10% de NaOH dans l'éthanol 95% (1 mole de NaOH par mole de dicétone I). Il y a dégagement de chaleur et le tout, remis en présence d'hydrogène, absorbe alors 2140 ml d'hydrogène en 30 minutes. On essore le catalyseur, évapore lentement l'éthanol du filtrat à travers une colonne de Widmer. Le résidu est repris dans de l'éther qui est séché sur sulfate de sodium et évaporé (colonne de Widmer). L'homocamphre brut pèse 17.92 g. On le chromatographie sur alumine Merck pour chromatographie. Pour 41 g on utilise 300 g d'alumine; l'élution par 2250 ml de benzène donne 38.54 g d'homocamphre pur, p.f. 191–192°, $[\alpha]_D^{23} = -112.2°$ ($c = 2.97$; benzène) et 2.22 g de triméthyl-1,8,8 bicyclo[3,2,1]octanediol-2β,4β (IV A), p.f. 275–280°.

Hydrogénation No. 6—Nickel de Raney sans adjonction

La dicétone I (5.0 g; 0.0275 mole) est hydrogénée dans 50 ml d'éthanol 95% en présence de 3 g de nickel de Raney. En 22 heures il se fixe 740 ml d'hydrogène (calculé pour $1H_2$:

686 ml; 754 mm et 25°). Ce temps écoulé, on introduit dans le milieu 1.11 g de NaOH (0.0227 mole) sous forme d'une solution alcoolique) et l'on reprend l'hydrogénation. Il y a alors absorption de 495 ml d'hydrogène. On essore le catalyseur, évapore l'alcool du filtrat, reprend par de l'éther que l'on sèche sur sulfate de sodium anhydre. On recueille après distillation de l'éther 4.458 g de composés neutres que l'on chromatographie sur 130 g d'alumine Merck pour chromatographie. L'élution par 600 ml de benzène donne 3.658 g d'homocamphre, $[\alpha]_D^{23} = -114°$ ($c = 4.95$; éthanol); 40 mg sont élués ensuite des mélanges benzène-chloroforme; le triméthyl-1,8,8 bicyclo[3,2,1]octanediol-2β,4β (IV A) est finalement élué par 300 ml de méthanol: 517 mg, p.f. 276–280°.

2. Réduction chimique (sodium et éthanol) de la dicétone I

À une solution de 20.78 g (0.1156 mole) de dicétone I dans 500 ml d'éthanol anhydre, on ajoute par petites portions 36 g (1.564 mole) de sodium. Lorsque le sodium a fini de réagir, on ajoute 40 ml d'eau et distille l'éthanol à travers une colonne de Widmer. Le résidu est repris par de l'eau et extrait par du chloroforme. Les fractions chloroformiques réunies sont séchées sur du sulfate de sodium et évaporées à travers une colonne de Widmer: on recueille 8.455 g de composés neutres, que l'on met en suspension dans 850 ml d'un mélange benzène-chloroforme 1-1 et que l'on introduit dans un tube à chromatographie contenant 250 g d'alumine Merck pour chromatographie. La partie insoluble du mélange se trouve reposer au sommet de la colonne d'alumine; on procède alors à l'élution par des portions de 850 ml de solvant.

Chromatographie I

Fractions	Eluant	Quantité éluée	P.f.
1	Benz-chlor 1-1	0.025 g	
2	Benz-chlor 1-2	0.225 g	
3	Benz-chlor 1-4	0.738 g	184–186°
4	Chloroforme	1.034 g	265–267°
5	Chloroforme	1.260 g	235–238°
6–12	Chloroforme	5.175 g	236–238°

Les fractions 6–12 sont sublimées et constituent le triméthyl-1,8,8 bicyclo[3,2,1]-octanediol-2α,4α (IV B), p.f. 234–236°, $[\alpha]_D^{23} = +32.7°$ ($c = 3.82$; éthanol 95%). Calculé pour $C_{11}H_{20}O_2$: C, 71.69; H, 10.94%. Trouvé: C, 71.49; H, 10.80%. On en prépare un di-*p*-nitrobenzoate, p.f. 221–224°, $[\alpha]_D^{23} = +37.0°$ ($c = 2.91$; chloroforme). Calculé pour $C_{25}H_{26}O_8N_2$: C, 62.23; H, 5.43; N, 5.81%. Trouvé: C, 62.37; H, 5.38; N, 5.67%.

Les fractions 3, 4 et 5 de la chromatographie I sont mises en solution dans 300 ml de benzène et adsorbées sur 90 g d'alumine. L'élution par des portions de 300 ml de solvent donne:

Chromatographie II

Fractions	Eluant	Quantité éluée	Caractéristiques
1–2	Benzène	0.085 g	
3–5	Benz-chlor Jusqu'à 1-1	0.438 g	$[\alpha]_D^{23} = +22.1°$ ($c = 3.6$; benz)
6–12	Benz-chlor 1-1	1.265 g	$[\alpha]_D^{23} = +8.36°$ ($c = 3.7$; EtOH)
13–17	Benz-chlor Jusqu'à 1-9	0.410 g	$[\alpha]_D^{23} = +4.93°$ ($c = 3.5$; EtOH)
18–21	Chloroforme	0.373 g	$[\alpha]_D^{23} = +34.2°$ ($c = 4$; EtOH)
22–23	Chloroforme	0.156 g	$[\alpha]_D^{23} = +36.9°$ ($c = 3.4$; EtOH)
24	Chloroforme	0.057 g	

Les fractions 3–5 de la chromatographie II sont sublimées: p.f. 171–173°, $[\alpha]_D^{23} = +23.6°$ ($c = 3.6$; benzène). Calculé pour $C_{11}H_{20}O$: C, 78.51; H, 11.98%. Trouvé: C, 78.56; H, 11.95%. Il s'agit d'un mélange de triméthyl-1,8,8 et -5,8,8 bicyclo[3,2,1]-octanols-2α et -2β (VI–IX) qui n'a pas été étudié plus à fond.

Les fractions 6–12 sont réunies et sublimées: p.f. 250–255°, $[\alpha]_D^{23} = +7.2°$($c = 4.2$; EtOH). Calculé pour $C_{11}H_{20}O_2$: C, 71.69; H, 10.94%. Trouvé: C, 71.57; H, 11.07%. On en prépare un di-*p*-nitrobenzoate brut, qui après 8 cristallisations dans le nitrométhane fond à 211–212.5°, $[\alpha]_D^{23} = +70.0°$($c = 2$; chloroforme). Calculé pour $C_{25}H_{26}O_8N_2$: C, 62.23; H, 5.43; N, 5.81%. Trouvé: C, 62.24; H, 5.42; N, 5.91%. Il s'agit du di-*p*-nitrobenzoate du triméthyl-1,8,8 bicyclo[3,2,1]octanediol-2α,4β. Une fraction (432 mg) légèrement moins pure de cet ester a été saponifiée par 500 mg de NaOH dans 20 ml d'éthanol et 5 ml d'eau par chauffage à reflux durant 3 heures. Le triméthyl-1,8,8 bicyclo[3,2,1]octanol-2α,4β (IV D) fut isolé à la manière habituelle; après chromatographie sur alumine et sublimation (152 mg) il fondait à 237–239°, $[\alpha]_D^{23} = -9.0°$ ($c = 1.4$; éthanol 95%).

3. Vitesses d'oxydation chromique

Elles ont été déterminées selon le mode opératoire décrit dans la partie III de cette série (8) et sont rapportées au Tableau III (partie théorique).

REMERCIEMENTS

Nous remercions le Conseil National de Recherches du Canada de son aide financière: subvention de recherche (H.F.), et bourse d'études (J-C. Richer). Nous remercions également M. le Professeur C. Sandorfy de son aide dans l'étude des spectres infrarouges.

BIBLIOGRAPHIE

1. Rupe, H. et Frey, C. Helv. Chim. Acta, **27**, 627 (1944).
2. Delépine, M. et Horeau, A. Bull. soc. chim. France, **4** (5), 31 (1937).
3. Cornubert, R. et Phélisse, J. Bull. soc. chim. France, **19** (5), 403 (1952).
4. Cornubert, R. et Réal, M. Bull. soc. chim. France, **19** (5), 407 (1952).
5. Cornubert, R. et Kaziz, C. Bull. soc. chim. France, **19** (5), 410 (1952).
6. Cornubert, R. et Eggert, H. G. Bull. soc. chim. France, 522 (1954).
7. Cornubert, R. et Thomas, P. Bull. soc. chim. France, 524 (1954).
8. Favre, H. et Richer, J-C. Can. J. Chem. **37**, 411 (1959).
9. Favre, H., Marinier, B. et Richer, J-C. Can. J. Chem. **34**, 1329 (1956).
10. Favre, H., Lefebvre, M. et Richer, J-C. Can. J. Chem. **37**, 403 (1959).
11. Striebel, P. et Tamm, Ch. Helv. Chim. Acta, **37**, 1094 (1954).
12. Gallagner, T. F. et Long, W. P. J. Biol. Chem. **147**, 131 (1943).
13. Schreiber, J. et Eschenmoser, A. Helv. Chim. Acta, **38**, 1529 (1955).
14. Kuhn, L. P. J. Am. Chem. Soc. **74**, 2492 (1952).

A NEW MOLECULAR REARRANGEMENT

IV. FURTHER OBSERVATIONS ON THE CHEMISTRY OF 1-NITRO-2,3,5,6-TETRAHYDRO-1(H)-IMIDAZ(1,2-a)IMIDAZOLE AND 1-(β-CHLOROETHYL)-2-IMIDAZOLIDONE[1]

A. F. McKay and M.-E. Kreling

ABSTRACT

Chlorination of 1-(β-hydroxyethyl)-2-nitriminoimidazolidine gives a mixture of 1-(β-chloroethyl)-2-nitriminoimidazolidine and 1-nitro-2,3,5,6-tetrahydro-1(H)-imidaz(1,2-a)imidazole hydrochloride. The other products, 1-(β-aminoethyl)-3-nitro-2-imidazolidone hydrochloride and 1-(β-nitraminoethyl)-2-imidazolidone, isolated during the original study of the chlorination of 1-(β-hydroxyethyl)-2-nitriminoimidazolidine are formed by the action of ethanol on 1-nitro-2,3,5,6-tetrahydro-1(H)-imidaz(1,2-a)imidazole hydrochloride. Amines add to 1-nitro-2,3,5,6-tetrahydro-1(H)-imidaz(1,2-a)imidazole nitrate to give the corresponding 1-(β-nitraminoethyl)-2-substituted amino-2-imidazoline nitrates. These reactions and the aminolysis of 1-(β-chloroethyl)-2-imidazolidone are described in detail.

INTRODUCTION

The present work was directed to a comparison of the chemical properties of 1-(β-chloroethyl)-2-nitroguanidine (1) with 1-(β-chloroethyl)-2-nitriminoimidazolidine (2) and to an attempt to find an explanation for the origin of the products isolated from the reaction of thionyl chloride with 1-(β-hydroxyethyl)-2-nitriminoimidazolidine (2).

The cyclization of 1-(β-chloroethyl)-2-nitroguanidine to 1-nitro-2-iminoimidazolidine hydrochloride (or its tautomer, 1-nitro-2-amino-2-imidazolinium chloride) was described first in 1950 (1). This cyclization occurred at the melting point of the compound or it could be effected by heating the compound with an inert solvent. A carbonium ion mechanism was suggested (3, 4) for this cyclization reaction but it was noted that this suggestion was premature owing to the absence of kinetic data. Later the kinetic data were supplied by the work of Boyars, Sager, and Skolnik (5). They found that the relative rates of cyclization of the 1-β-substituted-2-nitroguanidines were 1-β-bromoethyl- > 1-β-chloroethyl- > 1-β-nitroxyethyl-. These relative rates of reaction are in agreement with the bond energies for C–Br, C–Cl, C–O covalent links which would be expected in a carbonium ion mechanism. However, since the rate of cyclization of 1-(β-nitroxyethyl)-2-nitroguanidine was greater than the cyclization rate of 1-(β-nitroxypropyl)-2-nitroguanidine, an internal Sn_2 mechanism rather than a carbonium ion mechanism was favored. Further evidence for the internal Sn_2 mechanism was established by a demonstration (6) of the lack of salt effect on the cyclization rate. Thus the cyclization of 1-(β-chloroethyl)-2-nitroguanidine is considered to occur by a backside approach of the nitrimino group to the substituted side chain as follows:

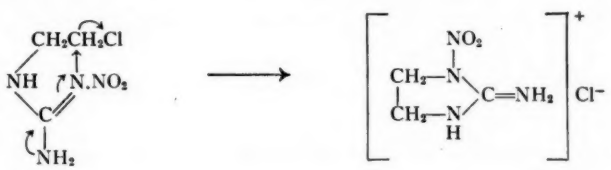

[1]*Manuscript received May 14, 1958.*
Contribution No. 21 from the L. G. Ryan Research Laboratories of Monsanto Canada Limited, Montreal, Quebec.

If cyclization of 1-(β-chloroethyl)-2-nitriminoimidazolidine to 1-nitro-2,3,5,6-tetrahydro-1(H)-imidaz(1,2-a)imidazole hydrochloride occurred in a similar manner, it would provide an explanation for some of the products obtained in the reactions (2, 7) of the former compound.

DISCUSSION

A study of the chemical properties of 1-(β-chloroethyl)-2-imidazolidone (III), 1-(β-aminoethyl)-3-nitro-2-imidazolidone hydrochloride (V), and 1-(β-nitraminoethyl)-2-imidazolidone (VI) obtained (2) from the reaction of thionyl chloride with 1-(β-hydroxyethyl)-2-nitriminoimidazolidine has indicated that the origin of these products may be represented as shown in Chart I. The mechanism for the chlorination of 1-(β-hydroxyethyl)-2-nitriminoimidazolidine (I) to 1-(β-chloroethyl)-2-nitriminoimidazolidine (III) is assumed to be similar to that suggested (8) for the chlorination of alcohols with thionyl chloride.

CHART I

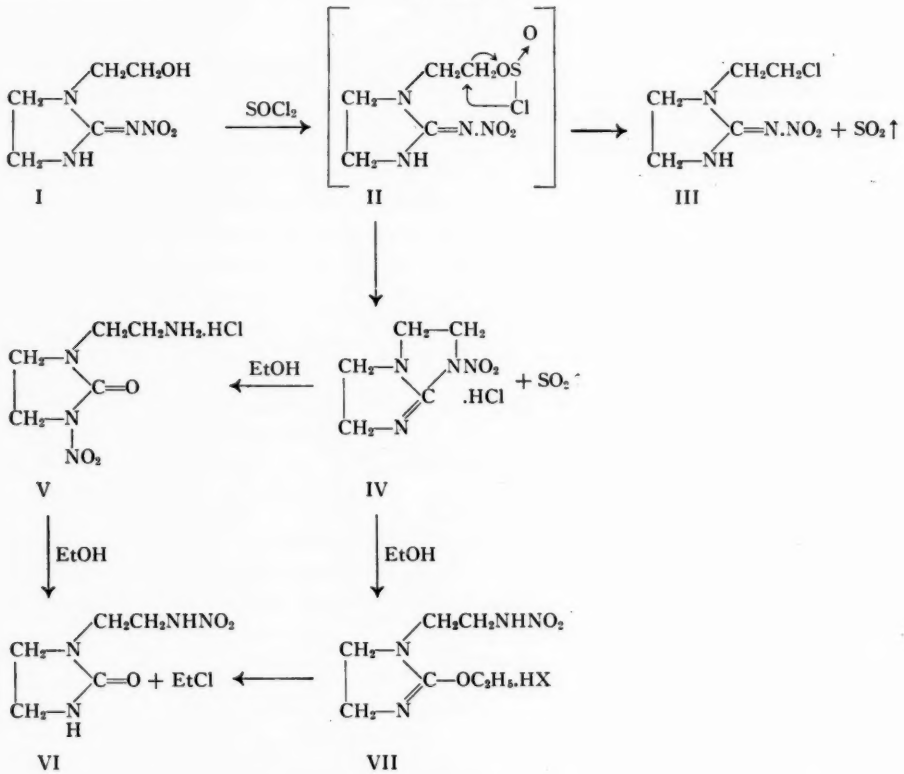

Since 1-(β-chloroethyl)-2-nitriminoimidazolidine (III) was recovered unchanged in 90% yield after it was heated under reflux for 4 hours in benzene containing dry hydrogen chloride and thionyl chloride, it cannot be considered the precursor of 1-nitro-2,3,5,6-tetrahydro-1(H)-imidaz(1,2-a)imidazole hydrochloride (IV) or 1-(β-aminoethyl)-3-nitro-2-imidazolidone hydrochloride (V). We could find no evidence for the cyclization of 1-(β-chloroethyl)-2-nitriminoimidazolidine (III) under the conditions (1) used successfully in the cyclization of 1-(β-chloroethyl)-2-nitroguanidine. Thus the bicyclic compound

IV would have to arise from II or an active intermediate in the chlorination of I to III.

1-Nitro-2,3,5,6-tetrahydro-1(H)-imidaz(1,2-a)imidazole nitrate was converted into 1-(β-aminoethyl)-3-nitro-2-imidazolidone hydrochloride by heating with moist benzene containing hydrogen chloride. Therefore the bicyclic compound (IV) could give rise to 1-(β-aminoethyl)-3-nitro-2-imidazolidone hydrochloride (V). Moreover, 1-(β-nitraminoethyl)-2-imidazolidone (VI) also must arise from one of the products of the thionyl chloride reaction during their isolation because primary nitramines are unstable in the presence of acid chlorides even under anhydrous conditions (9, 10, 11, 12, 13, 14, 15). It has been shown that both 1-nitro-2,3,5,6-tetrahydro-1(H)-imidaz(1,2-a)imidazole nitrate (16) and 1-(β-aminoethyl)-3-nitro-2-imidazolidone nitrate (7) on refluxing with ethanol give good yields of 1-(β-nitraminoethyl)-2-imidazolidone (VI). 1-Nitro-2,3,5,6-tetrahydro-1(H)-imidaz(1,2-a)imidazole nitrate in the presence of warm ethanol (50° C) gives a new compound whose analysis and properties agree with the structure, 1-(β-nitraminoethyl)-2-ethoxy-2-imidazolinium nitrate (VII, X = NO_3). The latter compound VII on heating under reflux in absolute ethanol is converted in good yield into 1-(β-nitraminoethyl)-2-imidazolidone (VI). On heating 1-(β-aminoethyl)-3-nitro-2-imidazolidone hydrochloride (V) with ethanol, ethyl chloride forms and the unstable free base rearranges to the more stable compound (VI).

When 1-nitro-2,3,5,6-tetrahydro-1(H)-imidaz(1,2-a)imidazole nitrate was heated in benzene containing hydrogen chloride and thionyl chloride it was converted into 1-nitro-2,3,5,6-tetrahydro-1(H)-imidaz(1,2-a)imidazole hydrochloride. Thus the hydrochloride salt of the bicyclic compound (IV) is stable under the conditions previously (2) used in the chlorination of 1-(β-hydroxyethyl)-2-nitriminoimidazolidine. Since both the 1-(β-chloroethyl)-2-nitriminoimidazolidine and the bicyclic compound IV are stable under these conditions, a method was developed for their isolation from the reaction of 1-(β-hydroxyethyl)-2-nitriminoimidazolidine with thionyl chloride. The crude crystalline product from the chlorination reaction was washed with water leaving behind the water insoluble 1-(β-chloroethyl)-2-nitriminoimidazolidine (59% yield). The aqueous filtrate on treatment with aqueous picric acid solution gave a crystalline picrate of 1-nitro-2,3,5,6-tetrahydro-1(H)-imidaz(1,2-a)imidazole (41% yield). It is now apparent that the products produced directly in the reaction of 1-(β-hydroxyethyl)-2-nitriminoimidazolidine with thionyl chloride are 1-(β-chloroethyl)-2-nitriminoimidazolidine (III) and 1-nitro-2,3,5,6-tetrahydro-1(H)-imidaz(1,2-a)imidazole hydrochloride (IV). The other products, 1-(β-aminoethyl)-3-nitro-2-imidazolidone hydrochloride and 1-(β-nitraminoethyl)-2-imidazolidone, isolated during the original (2) study of this chlorination reaction, were formed by the reaction of the bicyclic compound with ethanol.

1-(β-Chloroethyl)-2-nitriminoimidazolidine (III) has been converted (7) into 1-(β-nitraminoethyl)-2-benzylamino-2-imidazolinium chloride (VIII) by heating with benzylamine in the presence of water.

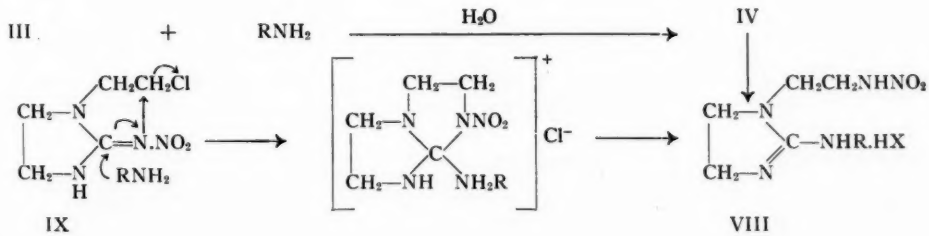

A carbonium ion mechanism giving a bicyclic intermediate was suggested for this reaction. On the basis of this proposal it was considered that 1-nitro-2,3,5,6-tetrahydro-1(H)-imidaz(1,2-a)imidazole might provide a more favorable starting material for the preparation of 1-(β-nitraminoethyl)-2-substituted amino-2-imidazoline salts (VIII). This proved to be the case and the compounds prepared by this method are described in Table I. However the successful use of a proposed bicyclic intermediate in a reaction does not provide unequivocal proof of its importance in the reaction mechanism. The concerted mechanism with ring opening (IX → VIII) offers an equally plausible mechanism for this reaction.

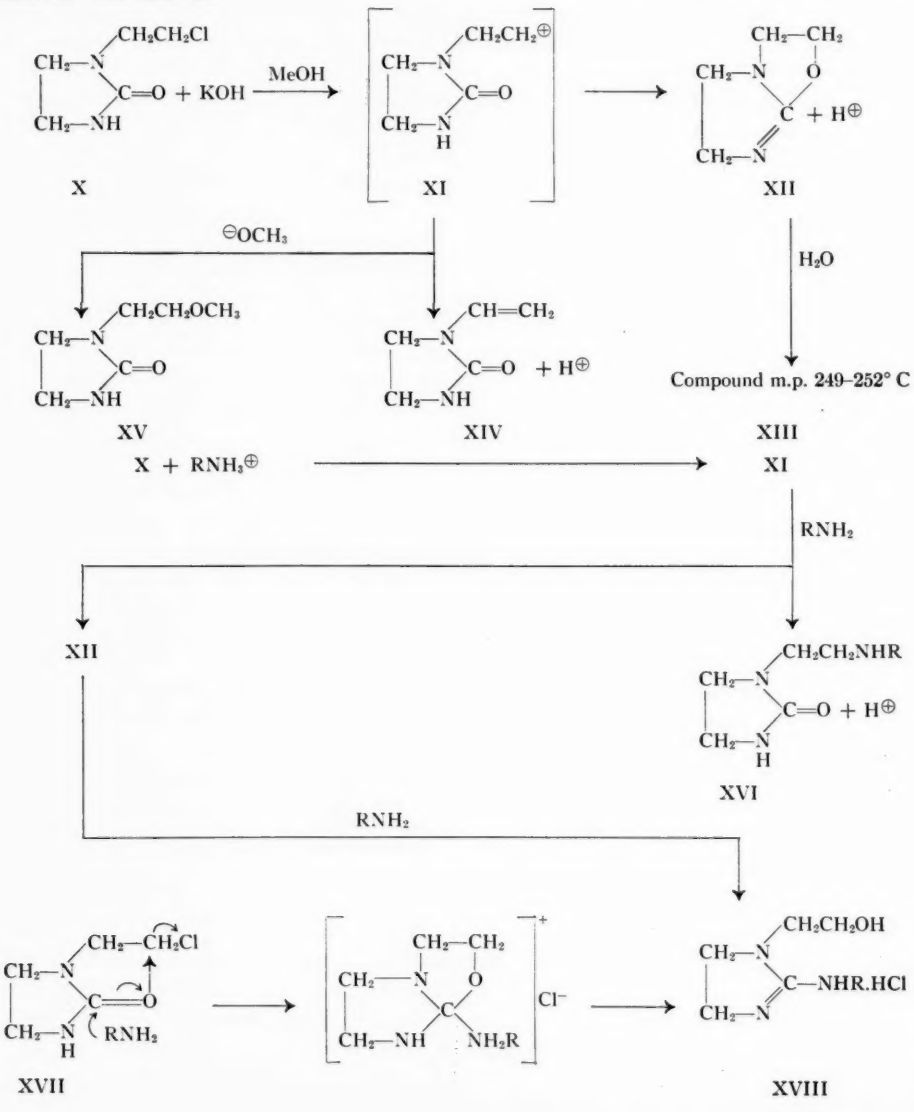

A further study was made of the reaction between methanolic potassium hydroxide and 1-(β-chloroethyl)-2-imidazolidone (X). This reaction gives several products, which is considered typical (17) of reactions involving carbonium ion intermediates. However, the number of products produced in a reaction involving a carbonium ion intermediate depend to some extent on the concentration of reactants and reaction conditions. The products identified from the reaction of 1-(β-chloroethyl)-2-imidazolidone with methanolic potassium hydroxide were Δ^7-1-oxa-4,7-diazabicyclo(3.3.0)octene (XII), 1(-β-methoxyethyl)-2-imidazolidone (XV), and 1-vinyl-2-imidazolidone (XIV).

Freshly distilled samples of Δ^7-1-oxa-4,7-diazabicyclo(3.3.0)octene (XII) on standing deposited crystals (XIII), which melted at 249–252° C. It appears that the bicyclic compound is converted slowly into the latter compound by absorbed moisture. Δ^7-1-Oxa-4,7-diazabicyclo(3.3.0)octene (XII) was considered (18) a possible intermediate in the formation of 1-(β-hydroxyethyl)-2-iminoimidazolidine (or its tautomer, 1-(β-hydroxyethyl)-2-amino-2-imidazoline) from 1-(β-chloroethyl)-2-imidazolidone (X). The bicyclic compound XII could arise from a carbonium ion intermediate (XI). This intermediate XI would also explain the formation of 1-(β-aminoethyl)-2-imidazolidone in the reaction of X with ammonia. If, however, we considered the concerted mechanism with ring opening (XVII → XVIII) for the formation of 1-(β-hydroxyethyl)-2-amino-2-imidazoline (XVIII, R = H) from the reaction of ammonia with XI, then another mechanism[2] must be operative in this reaction to produce the second product 1-(β-aminoethyl)-2-imidazolidone (XVI, R = H).

Δ^7-1-Oxa-4,7-diazabicyclo(3.3.0)octene (XII) on treatment with benzylamine gave 1-(β-hydroxyethyl)-2-benzylamino-2-imidazoline (XVIII, R = benzyl).

EXPERIMENTAL[3]

1-(β-Nitraminoethyl)-2-ethoxy-2-imidazolinium Nitrate

A freshly prepared sample of 1-nitro-2,3,5,6-tetrahydro-1(H)-imidaz(1,2-a)imidazole nitrate (7) (10 g, 0.046 mole) was dissolved in absolute ethanol (500 ml) at 50° C. Although this solution was cooled immediately in freezing mixture only 2.2 g (22%) of 1-nitro-2,3,5,6-tetrahydro-1(H)-imidaz(1,2-a)imidazole nitrate (m.p. 149–151° C with decomposition) was recovered. After the filtrate was concentrated to a volume of 200 ml, a second crystalline compound (m.p. 116–119° C with decomposition) was obtained, yield 5.1 g (42%). The melting point was raised to 124–125.5° C with decomposition by one crystallization from ethanol–ether (2:1) solution. Anal. Calc. for $C_7H_{15}N_5O_6$: C, 31.70; H, 5.70; N, 26.42%. Found: C, 31.90; H, 5.75; N, 26.41%.

1-(β-Nitraminoethyl)-2-imidazolidone from 1-(β-Nitraminoethyl)-2-ethoxy-2-imidazolinium Nitrate

1-(β-Nitraminoethyl)-2-ethoxy-2-imidazolinium nitrate (215 mg, 0.81 mm) was heated under reflux in absolute ethanol (5 ml) for 2 hours. Removal of the ethanol *in vacuo* gave a crystalline product melting at 176–180° C with decomposition. One crystallization from absolute ethanol (7 ml) raised the melting point to 180–182.5° C with decomposition, yield 133 mg (94%). A mixture melting point determination with a known sample of 1-(β-nitraminoethyl)-2-imidazolidone (7) was not depressed.

[2] *The Referee has suggested that the reaction between ammonia and 1-(β-chloroethyl)-2-imidazolidone represents a competition between* S_{N2} *and elimination reactions. This is certainly a possibility.*

[3] *All melting points are uncorrected. Microanalyses were performed by Micro-Tech Laboratories, Skokie, Illinois.*

TABLE I

1-(β-Nitraminoethyl)-2-substituted amino-2-imidazolines

Substituents	Yield, m.p.		Formula	C		H		N	
	%	°C		Calc.	Found	Calc.	Found	Calc.	Found
Benzyl	86.4	115.5–116.5	$C_{12}H_{18}N_6O_5$*	44.17	43.90	5.56	5.54	25.76	25.75
	78.0	151.5–152.5	$C_{18}H_{20}N_6O_9$†	43.90	43.86	4.09	4.27	22.76	22.42
Phenyl	90.4	139–140	$C_{17}H_{18}N_6O_9$†	42.68	42.81	3.79	4.08	23.42	23.15
p-Methoxyphenyl	96.4	118.5–120‡	$C_{12}H_{18}N_6O_6$*	42.10	42.49	5.30	5.47	24.55	24.26
	78.0	121–122	$C_{18}H_{20}N_6O_{10}$†	42.52	42.69	3.97	4.18	22.04	22.35
p-Ethoxyphenyl	81.8	125.5–127‡	$C_{13}H_{20}N_6O_6$*	43.82	43.76	5.66	5.80	23.58	23.58
p-Hydroxyphenyl	80.6	189.5–190.5‡	$C_{11}H_{16}N_6O_6$*	40.24	40.40	4.91	5.13	25.60	25.57
5-(1-Hydroxynaphthyl)	32.3	198.5–199.5‡	$C_{15}H_{18}N_6O_6$*	47.61	47.50	4.79	5.15	22.21	21.89

*Nitrate salt. †Picrate. ‡Melts with decomposition.

1-(β-Nitraminoethyl)-2-substituted Amino-2-imidazolines

The properties of the 1-(β-nitraminoethyl)-2-substituted amino-2-imidazoline salts prepared by the reaction of amines with 1-nitro-2,3,5,6-tetrahydro-1(H)-imidaz(1,2-a)-imidazole nitrate are described in Table I. Since the conditions for these reactions are very similar, only the preparation of 1-(β-nitraminoethyl)-2-(*p*-anisidino)-2-imidazoline nitrate is described below in detail.

1-Nitro-2,3,5,6-tetrahydro-1(H)-imidaz(1,2-a)imidazole nitrate (657.5 mg, 0.003 mole) and *p*-anisidine (369 mg, 0.003 mole) in absolute ethanol (8 ml) were heated under reflux for 3 hours. After removal of the solvent *in vacuo*, a hard gum was obtained, yield 1.025 g (100%). Trituration with acetone gave 984 mg (96%) of crystalline product melting at 115–118° C with decomposition. Four crystallizations from ethanol–ether (5:3) solution raised the melting point to 118.5–120° C with decomposition.

An oily picrate, which crystallized slowly on standing in the refrigerator for 2 weeks, was obtained in the usual way from water in 78% yield. Two recrystallizations from water raised the melting point from 120 to 122° C to a constant value of 121–122° C.

Stability of 1-(β-Chloroethyl)-2-nitriminoimidazolidine

1-(β-Chloroethyl)-2-nitriminoimidazolidine (235 mg) in absolute ethanol (7 ml) was heated under reflux for 7 hours. The solution on cooling deposited crystals melting at 142–144° C with decomposition, yield 178 mg (76%). The crystals were identified as unchanged starting material by a mixed melting point determination.

1-(β-Chloroethyl)-2-nitriminoimidazolidine (188 mg) was also recovered in 90% yield after it was refluxed for 4 hours in a benzene solution containing dry hydrogen chloride (200 mg) and thionyl chloride (150 mg).

1-(β-Aminoethyl)-3-nitro-2-imidazolidone Nitrate from 1-Nitro-2,3,5,6-tetrahydro-1(H)-imidaz(1,2-a)imidazole Nitrate

1-Nitro-2,3,5,6-tetrahydro-1(H)-imidaz(1,2-a)imidazole nitrate (1 g, 0.0046 mole) in benzene (50 cc) saturated with hydrogen chloride was heated under reflux for 8.5 hours. After the solvent was decanted from the insoluble oil (0.76 g) the oil was triturated with warm (40° C) ethanol. The crystals (m.p. 155–159° C with decomposition) were recovered by filtration, yield 0.36 g (38%). The crystals were purified by solution in water and precipitation with ethanol. The pure product melted at 160.5° C with decomposition alone and on admixture with a known (7) sample of 1-(β-aminoethyl)-3-nitro-2-imidazolidone nitrate.

The picrate (m.p. 198° C decomposition) was prepared in the usual manner from water. It did not depress the melting point of a known (7) sample of the picrate of 1-(β-aminoethyl)-3-nitro-2-imidazolidone.

Stability of 1-Nitro-2,3,5,6-tetrahydro-1(H)-imidaz(1,2-a)imidazole Hydrochloride in Benzene – Thionyl Chloride Medium

Thionyl chloride (5 ml) was added to dry benzene (15 ml) and then 1-nitro-2,3,5,6-tetrahydro-1(H)-imidaz(1,2-a)imidazole nitrate (0.57 g, 0.0026 mole) was added portionwise at room temperature. A vigorous reaction occurred and brown fumes were evolved. Although the reaction was complete in 15 minutes, the solution was held at 55° C for a further 6 hours. At the end of this time the solution was cooled and the crystalline precipitate was recovered by filtration, yield 0.49 g (98% based on 1-nitro-2,3,5,6-tetrahydro-1(H)-imidaz(1,2-a)imidazole hydrochloride). The melting point was raised from 130–135° C with decomposition to 137–139° C with decomposition by solution in ethanol

at room temperature and precipitation with ether. This sample gave low chlorine values on analysis so it was characterized as its picrate.

The picrate was formed in 50% yield in the usual manner from aqueous solution. It melted at 150–151° C alone and on admixture with a known (16) sample of 1-nitro-2,3,5,6-tetrahydro-1(H)-imidaz(1,2-a)imidazole picrate.

Chlorination of 1-(β-Hydroxyethyl)-2-nitriminoimidazolidine

1-(β-Hydroxyethyl)-2-nitriminoimidazolidine (2, 19) (1.74 g, 0.01 mole) was chlorinated with thionyl chloride in benzene under the conditions previously (2) described. At the end of the reaction period the crystalline starting material had been transformed into a colorless oil which crystallized after a small amount of benzene had been evaporated *in vacuo* at 50° C. The hygroscopic crystals were collected by filtration and dried *in vacuo*, yield 1.87 g (98%). A sample (0.74 g) of the crude product was suspended in water. The water insoluble crystalline product (m.p. 142–143° C) was collected by filtration and dried, yield 0.44 g (59%). A mixed melting point determination with a known (2) sample of 1-(β-chloroethyl)-2-nitriminoimidazolidine (m.p. 142.5–143.5° C) gave no depression.

The filtrate from 1-(β-chloroethyl)-2-nitriminoimidazolidine on treatment with aqueous picric acid yielded a crystalline picrate (m.p. 150–151.5° C). A mixture melting point with a known sample of 1-nitro-2,3,5,6-tetrahydro-1(H)-imidaz(1,2-a)imidazole picrate (m.p. 151° C) was not depressed.

The yield of picrate was 306 mg. Since pure 1-nitro-2,3,5,6-tetrahydro-1(H)-imidaz-(1,2-a)imidazole hydrochloride under the same conditions gives a 50% yield of picrate, this yield of picrate corresponds to the presence of 304 mg (41%) of bicyclic hydrochloride.

Δ^7-1-Oxa-4,7-diazabicyclo(3.3.0)octene

A methanolic solution of potassium hydroxide (533 ml of 1.69 *N* solution) was added dropwise over a period of 1.5 hours to a solution of 1-(β-chloroethyl)-2-imidazolidone (18) (133 g, 0.9 mole) in absolute methanol (300 ml). This reaction mixture was heated under reflux for 5 hours after which it was worked up as previously (18) described. The volume of the final chloroform solution was 265 ml. A portion (29.4 ml) of the chloroform extract on evaporation gave 11.9 g of yellowish oil. This oil on treatment with aqueous picric acid solution yielded 6.7 g (18.5%) of crude (m.p. 134–138° C) Δ^7-1-oxa-4,7-diazabicyclo(3.3.0)octene picrate. One crystallization from acetone–ether (3:1) solution raised the melting point to 145–146.5° C. This picrate did not depress the melting point of a known (18) sample of Δ^7-1-oxa-4,7-diazabicyclo(3.3.0)octene picrate (m.p. 144.5–145.5° C).

The residual oil (21.8 g) from another portion (55 ml) of the chloroform extract was distilled *in vacuo*. The following four fractions were obtained: (1) 1.69 g of crystals (b.p. 78–80° C/0.07 mm), (2) 0.9 g of liquid containing some crystals (b.p. 82–88° C/0.06 mm), (3) 2.18 g of turbid liquid (b.p. 92–95° C/0.06 mm), and (4) 15.26 g of a low melting crystalline material (b.p. 98–100° C/0.06 mm).

A small sample of fraction 1 on treatment with a saturated aqueous picric acid solution gave Δ^7-1-oxa-4,7-diazabicyclo(3.3.0)octene picrate (m.p. 145–146° C) in 86% yield. Two samples (1.3 g) of Δ^7-1-oxa-4,7-diazabicyclo(3.3.0)octene (both samples originally contained 86–87% bicyclic compound by picrate analyses), which had been standing for 2 weeks, were combined and redistilled *in vacuo*. It was noted that most of the originally low melting solid had been converted into a high melting solid which was no longer distillable. Only 0.3 g (b.p. 76–78° C/0.07 mm) of distillate was obtained. This small

sample of Δ^7-1-oxa-4,7-diazabicyclo(3.3.0)octene was redistilled for analysis. Anal. Calc. for $C_5H_8N_2O$: C, 53.55; H, 7.19; N, 24.99%. Found: C, 53.25; H, 7.09; N, 24.63%.

The residue from the distillation of bicyclic compound was crystallized from chloroform–hexane solution, yield 0.35 g (27% by weight). The melting point was increased from 237–241° C to 249–252° C by two crystallizations from chloroform–hexane solution. Anal. Calc. for $C_{10}H_{18}N_4O_3$: C, 49.57; H, 7.49; N, 23.13%. Found: C, 49.90; H, 7.38; N, 23.45%.

Iodometric titrations of fractions 3 and 4 indicated that they contained 58.7 and 50.8% respectively of the 1-vinyl-2-imidazolidone compound. Fractions 3 and 4 on treatment with dinitrophenylhydrazine in acid solution gave 56% and 47.2% yields respectively of the dinitrophenylhydrazone of acetaldehyde. The dinitrophenylhydrazone melted at 151–152° C with sintering at 149° C after several crystallizations from aqueous methanol. Anal. Calc. for $C_8H_8N_4O_4$: C, 42.86; H, 3.60; N, 24.99%. Found: C, 43.32; H, 3.51; N, 25.13%. The formation of the dinitrophenylhydrazone of acetaldehyde from fractions 3 and 4 agrees with the observation of Reppe (20) that vinyl groups attached to nitrogen are split off as acetaldehyde under the influence of weak acids.

Reaction of Δ^7-1-Oxa-4,7-diazabicyclo(3.3.0)octene with Benzylamine

Benzylamine (0.086 g, 0.008 mole) was added to Δ^7-1-oxa-4,7-diazabicyclo(3.3.0)-octene (0.09 g, 0.008 mole) in absolute ethanol (5 ml). The mixture was allowed to stand at room temperature overnight after which it was evaporated to dryness *in vacuo* at 40° C. A pink-colored semicrystalline oil was obtained, yield 120 mg.

A portion (40 mg) of this oil on treatment with aqueous picric acid solution gave a 68% yield of crystalline picrate (m.p. 116–119° C). Crystallization from ethanol raised the melting point to 122.5° C. This picrate did not depress the melting point of a known sample of 1-(β-hydroxyethyl)-2-benzylamino-2-imidazoline picrate (21).

REFERENCES

1. McKay, A. F. and Milks, J. E. J. Am. Chem. Soc. **72**, 1616 (1950).
2. McKay, A. F. and Gilpin, J. R. J. Am. Chem. Soc. **78**, 486 (1956).
3. McKay, A. F. and Braun, R. O. J. Org. Chem. **16**, 1829 (1951).
4. McKay, A. F. Chem. Revs. **51**, 301 (1952).
5. Boyars, C., Sager, W. F., and Skolnik, S. J. Am. Chem. Soc. **78**, 4590 (1956).
6. Boyars, C., Cary, H., and Stark, V. J. Org. Chem. **22**, 716 (1957).
7. McKay, A. F., Hatton, W. G., and Braun, R. O. J. Am. Chem. Soc. **78**, 6144 (1956).
8. Cowdrey, W. A., Hughes, E. D., Ingold, C. K., Masterman, S., and Scott, A. D. J. Chem. Soc. 1267 (1937).
9. Hall, R. H., McKay, A. F., and Wright, G. F. J. Am. Chem. Soc. **73**, 2205 (1951).
10. McKay, A. F. and Hatton, W. G. J. Am. Chem. Soc. **75**, 963 (1953).
11. McKay, A. F., Hatton, W. G., and Taylor, G. W. J. Am. Chem. Soc. **75**, 1120 (1953).
12. McKay, A. F. J. Am. Chem. Soc. **77**, 1057 (1955).
13. Barrott, J., Denton, I. N., and Lamberton, A. H. J. Chem. Soc. 1998 (1953).
14. Denton, I. N. and Lamberton, A. H. J. Chem. Soc. 1655 (1955).
15. Bruck, P., Denton, I. N., and Lamberton, A. H. J. Chem. Soc. 921 (1956).
16. McKay, A. F., Kreling, M.-E., Paris, G. Y., Braun, R. O., and Whittingham, D. J. Can. J. Chem. **35**, 843 (1957).
17. Burton, H. and Praill, P. F. G. Quart. Revs. (London), **6**, 302 (1952).
18. McKay, A. F., Paris, G. Y., and Kreling, M.-E. J. Am. Chem. Soc. **79**, 5276 (1957).
19. McKay, A. F., Bryce, J. R. G., and Rivington, D. E. Can. J. Chem. **29**, 382 (1951).
20. Reppe, W. Ann. **601**, 208 (1956).
21. McKay, A. F. and Vavasour, G. R. Can. J. Chem. **32**, 59 (1954).

CO-ORDINATION COMPOUNDS OF NICKEL(II)

PART I. THE SPECTRA OF SALICYLALDIMINE DERIVATIVES OF NICKEL(II) IN SOME ORGANIC SOLVENTS[1]

H. C. Clark and R. J. O'Brien

ABSTRACT

Measurements of the ultraviolet and visible absorption spectra of bis-N-methyl-salicylaldimine nickel(II) and its 5-chloro and 5-bromo derivatives in benzene, chloroform, carbon tetrachloride, and cyclohexane solutions at temperatures between 15° and 45° C are reported. The results confirm the occurrence of a temperature dependent equilibrium between dia- and para-magnetic forms. The nature of the paramagnetic form is discussed in terms of the recent developments of the ligand field theory. The effect on the equilibrium of substitution of chlorine or bromine in the five position of the salicylaldehyde molecule is also discussed.

INTRODUCTION

The co-ordination compounds formed between nickel and various salicylaldimines are generally highly colored, diamagnetic solids with square planar configurations. Willis and Mellor (1) found that the addition to these complexes of organic solvents such as pyridine, dioxan, benzene, and chloroform caused changes to paramagnetism, magnetic moments of between 1 and 3 Bohr magneton being observed at room temperature. These magnetic moments are independent of concentration, but measurements over a wide temperature range have shown (2, 3) that in many of these solutions, a temperature dependent equilibrium occurs between dia- and para-magnetic forms, the latter being favored at low temperatures. The paramagnetic species may be (1) octahedral with two co-ordination sites occupied by solvent molecules, (2) tetrahedral, or (3) square planar but with unpaired electrons. Tetrahedral nickel(II) complexes, although long postulated theoretically, have only recently been isolated (4) and the existence of such complexes in solution now seems more probable. Square planar paramagnetic complexes can be predicted only from ligand field theory and have not been isolated as yet.

Later work on the absorption spectra of nickel–salicylaldimine complexes in organic solvents (5) generally supported the magnetic evidence of a temperature dependent equilibrium between dia- and para-magnetic forms, but there were several important exceptions. Further spectral measurements as reported below, and also by Sacconi, Paoletti, and Del Re (6) provide assistance in explaining these exceptional cases.

EXPERIMENTAL

The complexes were prepared by the method described previously (3, 7) in which bis-salicylaldehyde nickel(II) or its 5-chloro or 5-bromo derivative was gradually added to a saturated alcoholic solution of methylamine. It was interesting to note that in the early stages of the preparation, when a large excess of methylamine was present, a light green flocculent precipitate was formed. As more of the salicylaldehyde complex was added, this precipitate was converted to the more familiar, dark green crystals of the desired product. This light green precipitate is possibly an octahedral nickel complex containing two methylamine molecules linked directly to the nickel atom. In the presence of larger amounts of bis-salicylaldehyde nickel(II), these two molecules are readily lost. The final dark green products were recrystallized from either chloroform or carbon

[1]*Manuscript received October 2, 1958.*
Contribution from the Chemistry Department, University of British Columbia, Vancouver 8, B.C.

tetrachloride, and identities of the new compounds confirmed by determinations of the nickel content by precipitation with dimethylglyoxime.

Bis-N-methyl-5-chloro-salicylaldimine nickel(II): Found: Ni, 14.76. Calc. for Ni-$(C_8H_7ONCl)_2$ 14.84%.

Bis-N-methyl-5-bromo-salicylaldimine nickel(II): Found: Ni, 12.25. Calc. for Ni-$(C_8H_7ONBr)_2$ 12.11%.

All solvents used were carefully dried and purified by standard procedures. The spectral measurements were made with a Cary recording spectrophotometer, model 14, with 10-mm sample cells. These cells were contained in a thermostated tank which was controlled to ±0.5° at 15°, 25°, 35°, or 45° C. The following tables (I and II) give values of the molecular extinction coefficients at the above temperatures, in chloroform, benzene, carbon tetrachloride, cyclohexane, and ethyl alcohol.

The tables in many cases show a slight decrease in the extinction coefficient with

TABLE I

Molecular extinction coefficients for the 325 mμ bands

Compound	Solvent	Concentration (molar)	15°	25°	35°	45°
Bis-N-methylsalicyl-aldimine nickel(II)	Chloroform	4.89×10^{-3}	9940	9910	9780	9670
	Benzene	1.11×10^{-2}	9210	8850	8790	8650
	Carbon tetrachloride	3.41×10^{-3}	9670	9520	9430	9060
	Cyclohexane					
Bis-N-methyl-5-chlorosalicylaldimine nickel(II)	Chloroform	5.66×10^{-4}	9770	9740	9740	9500
	Benzene	3.64×10^{-4}	8950	8870	8770	8680
	Carbon tetrachloride	8.11×10^{-4}	7950	7800	7830	7800
	Cyclohexane	1.01×10^{-4}	7810	7840	8000	7940
Bis-N-methyl-5-bromosalicylaldimine nickel(II)	Chloroform	3.05×10^{-3}	8960	8970	9070	9390
	Benzene	2.31×10^{-3}	8880	8880	9060	9060
	Carbon tetrachloride	9.09×10^{-4}	8250	8250	7900	8090
	Cyclohexane	6.48×10^{-5} (approx.)	6940	6940	6630	6700
Molecular extinction coefficients for the 415 mμ bands						
Bis-N-methylsalicyl-aldimine nickel(II)	Chloroform	1.96×10^{-4}	3990	4010	4020	4030
	Benzene	1.78×10^{-4}	4280	4220	4170	4130
	Carbon tetrachloride	1.36×10^{-4}	4230	4170	4110	4070
	Cyclohexane					
Bis-N-methyl-5-chlorosalicylaldimine nickel(II)	Chloroform	2.25×10^{-4}	3690	3690	3700	3700
	Benzene	1.82×10^{-4}	4070	4070	4020	3990
	Carbon tetrachloride	1.62×10^{-4}	3050	3080	3130	3200
	Cyclohexane	1.01×10^{-4}	3370	3380	3520	3520
Bis-N-methyl-5-bromosalicylaldimine nickel(II)	Chloroform	1.22×10^{-4}	3090	3130	3250	3350
	Benzene	2.31×10^{-3}	3660	3680	3720	3720
	Carbon tetrachloride	3.64×10^{-5}	3380	3380	3350	3350
	Cyclohexane	6.48×10^{-5}	2140	2240	2240	2140
Molecular extinction coefficients for the 620 mμ bands						
Bis-N-methylsalicyl-aldimine nickel(II)	Chloroform	1.84×10^{-2}	58.1	61.2	65.5	68.5
	Benzene	1.25×10^{-2}	64.6	67.2	68.9	69.5
	Carbon tetrachloride	3.41×10^{-3}	74.9	76.3	77.7	78.4
Bis-N-methyl-5-chlorosalicylaldimine nickel(II)	Chloroform	6.50×10^{-3}	49.3	60.9	69.7	75.7
	Benzene	2.54×10^{-3}	78.0	94.3	110.0	124.0
	Carbon tetrachloride	8.11×10^{-4}	81.4	91.2	94.5	97.3
Bis-N-methyl-5-bromosalicylaldimine nickel(II)	Chloroform	3.05×10^{-3}	71.2	78.0	83.3	86.6
	Benzene	1.93×10^{-3}	75.7	79.3	81.3	
	Carbon tetrachloride	9.09×10^{-4}	105.0	110.0	114.0	117.0

TABLE II

Molecular extinction coefficients of ethyl alcohol solutions

Compound	Concentration (molar)	max (mμ)	15°	25°	35°	45°
Bis-N-methylsalicylaldimine nickel(II)	3.53×10^{-5}	325	6515	6660	6855	7050
		378	4530	4250	3995	3770
		410	2550	2775	2890	3005
Bis-N-methyl-5-chlorosalicylaldimine nickel(II)	1.60×10^{-4}	325	3560	4120	4570	5070
		378	8480	7580	6840	6100
		410	2440	2580	2910	3010
Bis-N-methyl-5-bromosalicylaldimine nickel(II)	8.00×10^{-5}	325	3630	4000	4570	4640
		378	8000	7300	6660	5970
		410	2290	2560	2690	2880

increasing temperature. This is attributed to the change in concentration that is due to the expansion of the solvent, and a suitable correction would show the extinction coefficient to remain constant.

DISCUSSION

It should first be pointed out that these results differ from those of Sacconi *et al.* (6), who found a slight temperature variation in the intensities of the 325 mμ and 415 mμ bands of bis-N-methylsalicylaldimine nickel(II) in benzene solution. The present results are, however, in good agreement with others previously reported (5). Sacconi also reported that the "620 mμ" band is actually located at 615 mμ in chloroform, 630 mμ in dioxan, and 635 mμ in benzene. We could find no definite indication of such a shift.

The temperature dependent equilibrium observed both magnetically and spectrophotometrically in solutions of these complexes is unusual, and has otherwise been observed only in solutions of bis-formylcamphorethylenediimine nickel(II) (8). The addition to a planar nickel complex of an organic solvent may produce one of several effects: (*a*) the co-ordination of two solvent molecules to the nickel atom to form an octahedral, or more accurately, tetragonal paramagnetic complex; (*b*) conversion to a tetrahedral configuration; (*c*) a reduction in the splitting of the 3*d* energy levels by the ligand to produce a square planar, paramagnetic complex. Solvation of the resultant complex is possible in all cases and must be carefully distinguished from co-ordination occurring only in case (*a*). The first effect will be expected in basic solvents such as pyridine; thus bis-N-methyl-salicylaldimine nickel(II) forms a stable paramagnetic dipyridine adduct. Conversion to a tetrahedral configuration may possibly occur when the intermolecular forces of the crystalline solid are removed by the addition of a non-co-ordinating solvent such as cyclohexane, thus allowing the isolated molecule to assume the shape of lowest potential energy (9). The energy difference between the planar and tetrahedral configurations must be small allowing a thermal equilibrium; at low temperatures the more stable tetrahedral form will predominate, while at higher temperatures, where thermal distortion of the complex molecule becomes appreciable, the diamagnetic planar form will exist. Hence, in agreement with observation, the magnetic moment will decrease with increasing temperature. Alternatively, the removal of intermolecular crystalline forces may merely reduce the splitting of the 3*d* levels so that it is energetically preferable for the electrons to remain unpaired. However, it is less easy to determine the cause of this transition, as compared with the planar–tetrahedral change. That diamagnetism may be peculiar to the solid state, and that the change to paramagnetism

may occur in the absence of a solvent, is further shown by the observation that certain nickel–salicylaldimine complexes are paramagnetic in the molten state (10). In particular, the transition to paramagnetism of bis-N-methyl-salicylaldimine nickel(II) above 180° has been interpreted (11) as being due to the formation of a polymeric octahedral complex, but these results can with equal validity be interpreted as resulting from either effect (*b*) or effect (*c*) discussed above.

Previously (5) the relationships between the magnetic and spectral properties of nickel–salicylaldimine complexes in pyridine, alcohol, and dioxan solutions have been discussed. In these cases, octahedral paramagnetic adducts appear to be formed. This paper is concerned with the spectra of the benzene, methylbenzene, chloroform, carbon tetrachloride, and cyclohexane solutions. These spectra consist of four bands located at approximately 270 mμ, 325 mμ, 415 mμ, and 620 mμ, and in many cases a "shoulder" in the 360–370 mμ region is also apparent. The first of these bands at 270 mμ is produced by a transition in the benzenoid ring of the salicylaldehyde molecule (12). Similarly, the 325 mμ band must result from internal transitions within the conjugated system of the free ligand since it also occurs in the spectra of the free organic ligands. The band at 415 mμ is observed only in the spectra of the complexes, and from its high intensity must be considered a charge transfer band due to electron transfer in the new conjugated system present only in the complex.

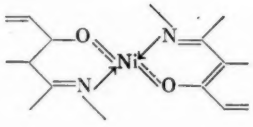

The fourth band at 620 mμ (for which $\log \epsilon < 2$) is due to a so-called "forbidden" *d–d* transition of the nickel atom.

Bis-N-methylsalicylaldimine nickel(II) has been shown to exist in pyridine solution as the tetragonal dipyridine adduct, which shows absorption at 270 mμ and 378 mμ. After allowance is made for the shift of up to 20 mμ to longer wavelengths which is observed in all these pyridine solutions, the latter of these two bands may be considered the enhancement of the "shoulder" at 360–370 mμ. Certainly, high intensities of this band are characteristic of an octahedral configuration of these complexes. Also, in appropriate cases where an equilibrium between diamagnetic and paramagnetic forms occurs, its intensity is related in an inverse manner to the intensities of the 325 mμ and 415 mμ band. The relative intensities of these three bands may therefore allow conclusions to be drawn concerning the extent of solvent–solute interaction. The ethyl alcohol solution of this nickel complex absorbs at 325 mμ, 378 mμ, and 415 mμ, and the effect of increasing temperature is to increase the intensity of the first and last of these bands at the expense of the 378 mμ band. Hence, a temperature-dependent equilibrium exists in this solution between a diamagnetic planar form characterized by the 325 and 415 mμ bands, and a paramagnetic tetragonal species characterized by the 378 mμ band, since there is clearly sufficient interaction between the complex and the solvent to greatly enhance this last charge transfer band. It also may be noted that the spectra of the 5-chloro and 5-bromo derivatives show that the equilibrium has shifted in favor of the paramagnetic species. For the dioxan solution of this complex, the bands at 325 mμ and 410 mμ show only very small changes with temperature, and

only a slight shoulder is apparent at 360 mμ. Hence solute–solvent interaction is weak and any resultant tetragonal product must retain its fifth and sixth groups very weakly.

For solutions in benzene, the methylbenzenes, and chloroform, magnetic measurements again showed the occurrence of an equilibrium, but absorption bands are apparent only at 325 mμ and 415 mμ, and the intensities of these bands are temperature independent. Hence in these solvents, there can be no strong interaction between solvent and solute, since there is no enhancement of the 360–370 mμ charge transfer band. The paramagnetic form must therefore be either tetrahedral or square planar (paramagnetic). Basolo and Matoush (8) have previously concluded that the paramagnetic form of bis-formylcamphorethylenediimine nickel(II) in methyl benzene solutions is tetrahedral, since no direct correlation could be found between the magnetic susceptibilities of these solutions and the base strengths of the solvents. Whatever the configuration of the paramagnetic form, it is remarkable that there are no changes in the charge transfer bands, since the change from dia- to para-magnetism must result from changes in the splittings of the 3*d* levels and these levels are almost certainly involved in several of the charge transfer processes.

From the present results, similar conclusions regarding the configuration of the paramagnetic form may now be drawn for solutions in carbon tetrachloride and cyclohexane, for solutions of the 5-chloro derivative in benzene, chloroform, carbon tetrachloride, and cyclohexane, and of the 5-bromo derivative in carbon tetrachloride and cyclohexane. In all these solutions, the 325 mμ and 415 mμ bands are unaffected by temperature changes, so that solvent–solute interaction must be negligibly weak, and again the paramagnetic form can only be four-co-ordinated. A list of the solvents arranged in order of decreasing effect on these charge transfer bands further supports this deduction regarding the nature of the paramagnetic form, the order being pyridine > alcohol > dioxane > benzene > chloroform ~ methylbenzenes ~ carbon tetrachloride ~ cyclohexane. This order is that of decreasing basic strength, or decreasing co-ordinative ability of these solvents.

Since the 620 mμ band results from forbidden *d–d* transitions and is hence directly concerned with the configuration of the 3*d* electrons of the nickel atom, a direct relationship must exist between the intensity of this band and the concentration of the paramagnetic form. The above results show that without exception, the 620 mμ band increases in intensity with increasing temperature as compared with the observed decrease in magnetic moment. Unfortunately, the solubilities in cyclohexane were too low for accurate measurement of the optical densities in this region. It is noticeable that the intensity changes are much greater in certain cases than in others; thus the intensity of the 620 mμ band of the benzene solution of the 5-chloro compound shows much greater changes than that of the carbon tetrachloride solution. This is probably due to the fact that in this latter solvent the equilibrium lies very much more on the diamagnetic side, so that much smaller changes in the extinction coefficient can occur.

The effect of varying the solvents in the order of decreasing co-ordinative power is thus to change the configuration of the paramagnetic form from almost regularly octahedral for pyridine solutions, through more tetragonal configurations in alcohol and dioxan solutions, to either tetrahedral or planar paramagnetic configurations in chloroform, carbon tetrachloride, and cyclohexane. It is not reasonable to conclude that in these latter solvents, solvent interaction with the complex molecule is strong enough to produce paramagnetism (and hence a tetragonal configuration) and yet on the other hand, is so weak that the charge transfer bands are not affected. For such non-co-ordinating

solvents as carbon tetrachloride and cyclohexane, the resultant paramagnetic product can contain no solvent molecules and hence can only be tetrahedral or square planar. The point in the above solvent series at which co-ordination of solvent molecules ceases is difficult to determine, and may depend on the balance between the co-ordinating power of the solvent, and the tendency of the complex molecule to attain a more energetically favorable configuration. Certainly in pyridine, ethyl alcohol, and probably in dioxan, these salicylaldimine complexes form tetragonal species, while in carbon tetrachloride and cyclohexane no co-ordination of solvent molecules occurs.

Assignment of the 620 mμ band is best made in terms of ligand field theory. The splittings of the 3*d* energy levels for different geometries of the ligand field are shown below together with the arrangement within these levels of the eight 3*d* electrons of the nickel(II) atom.

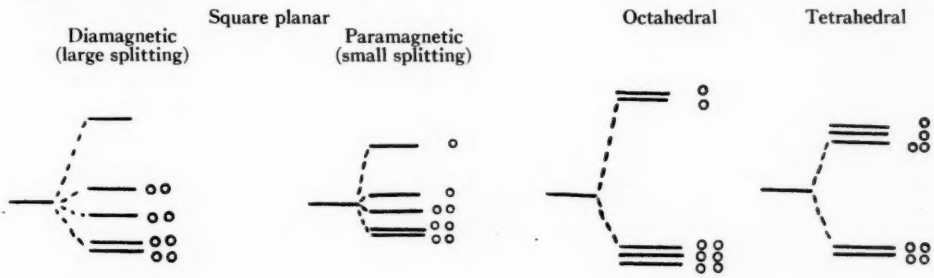

Hence, for the planar configurations, three "forbidden" *d–d* transitions are possible, which may be named ω_1, ω_2, and ω_3 according to the scheme of Belford, Calvin, and Belford (13). Only one transition is possible for the tetrahedral form, although the removal of the degeneracy of the upper triplet as a result of the Jahn–Teller effect will produce several transitions which differ only very slightly in energy content. For an octahedral form, only one transition is possible since the Jahn–Teller effect does not apply. Analysis of a typical 620 mμ band (Fig. 1) shows that after allowance is made

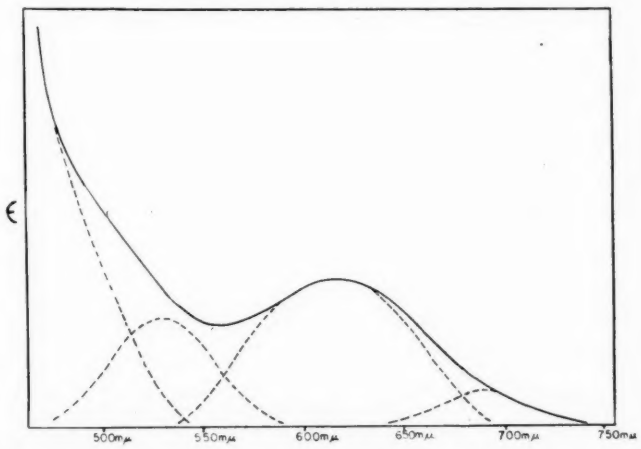

FIG. 1.

for the tail of the intense 415 mμ band, there remains a broad asymmetric peak which may be separated into three gaussian components. This closely resembles the spectra of planar copper complexes in the 650 mμ band region (13). Moreover, this 620 mμ band is also observed in ethyl alcohol solutions for which the paramagnetic form is tetragonal, while for pyridine solutions there is no absorption band in 600–650 mμ region. Hence this 620 mμ band must be produced by the diamagnetic complex, and as the proportion of this form increases with increasing temperature the intensity of this band will also increase in agreement with observation.

Sacconi, Paoletti, and Del Re (6) have previously suggested that the paramagnetic forms in these non-co-ordinating solvents are of the "outer" sp^2d type, this being the valence bond description of paramagnetic square planar complexes. This conclusion is based on the observation that bis-N-alkyl-salicylaldimine – nickel(II) complexes in benzene and dioxan solutions at 25° have a very low, almost zero, dipole moment; hence the paramagnetic form must still be planar. However, magnetic measurements (3) have shown that at this temperature and in these solvents, more than half of the complex is already in the diamagnetic planar form which has a zero moment. Thus, bis-N-methyl-salicylaldimine nickel(II) exists in benzene solution at 25° to the extent of 64% in the diamagnetic, trans-planar form. Hence, assuming a tetrahedral nickel(II) complex to have a moment of approximately 5 D, the observed value of 1 to 2 D is to be expected and may still be consistent with a tetrahedral configuration of the paramagnetic form. Moreover, if as suggested above, the paramagnetic form in dioxan is actually tetragonal, with two trans-solvent molecules, the dipole moment will in any case be zero. Only in solvents such as chloroform, carbon tetrachloride, and cyclohexane and at low temperatures, can an appreciable dipole moment be expected. Such measurements are now in progress, and it is hoped the results will make it possible to distinguish between tetrahedral and square planar paramagnetic forms.

These present results also show the effect on the equilibrium of differences in the solvent, and also differences in the complex itself. From a consideration of the intensity of the 620 mμ band at say 15°, it would appear that the proportion of diamagnetic form increases as the solvent is changed from chloroform to benzene to carbon tetrachloride, although this effect is less apparent at higher temperatures. The spectra of the alcohol solutions shows the effect of substitution on the aromatic ring. The halogen atom, substituted in the five position and acting through the conjugated system of the Schiff's base, will reduce the donor properties of the nitrogen atom. In other words, the ligand field strength will be reduced, thus facilitating the formation of a species in which the electrons remain unpaired. Thus the spectra of the alcohol solutions show that the intensity of the 378 mμ band which is characteristic of the tetragonal form is markedly greater for the 5-chloro and 5-bromo derivatives. The secondary effect of increased acidity of the phenolic group by this substitution is apparently of secondary importance to the reduced donor properties of the nitrogen atom in determining the strength of the ligand field.

Further substituted derivatives are being examined to determine more extensively the factors which control the equilibrium.

ACKNOWLEDGMENTS

The authors thank Dr. T. N. Waters of A.E.R.E., Harwell, England, and Dr. J. Halpern for much valuable discussion and advice.

REFERENCES

1. WILLIS, J. B. and MELLOR, D. P. J. Am. Chem. Soc. **69**, 1237 (1947).
2. FUJII, S. and SUMITANI, M. Sci. Repts. Research Insts., Tohoku Univ., Ser. I, **37**, 49 (1953).
3. CLARK, H. C. and ODELL, A. L. J. Chem. Soc. 3431 (1955).
4. VENANZI, L. M. J. Chem. Soc. 719 (1958).
5. CLARK, H. C. and ODELL, A. L. J. Chem. Soc. 520 (1956).
6. SACCONI, L., PAOLETTI, P., and DEL RE, G. J. Am. Chem. Soc. **79**, 4062 (1957).
7. PFEIFFER, P. Ann. **503**, 84 (1933).
8. BASOLO, F. and MATOUSH, W. R. J. Am. Chem. Soc. **75**, 5663 (1953).
9. NYHOLM, R. S. Chem. Revs. **53**, 263 (1953).
10. SACCONI, L., CINI, R., and MAGGIO, F. J. Am. Chem. Soc. **79**, 3933 (1957).
11. SACCONI, L., PAOLETTI, P., and CINI, R. J. Am. Chem. Soc. **80**, 3583 (1958).
12. LEMON, H. W. J. Am. Chem. Soc. **69**, 2998 (1947).
13. BELFORD, R. L., CALVIN, M., and BELFORD, G. J. Chem. Phys. **26**, 1165 (1957).

NOTE ADDED IN PROOF: Since this paper was submitted, Maki (J. Chem. Phys. **29**, 1129 (1958)) has made a more elegant assignment of the spectra of bis-N-methylsalicylaldimine nickel(II), as a solid and in pyridine and chloroform solutions. The conclusion is reached that for a complex with this *trans*-planar symmetry, only a small axial perturbation is sufficient to cause a change from dia- to para-magnetism. However, the charge transfer bands are not mentioned and from the above results it would seem more a matter of definition to determine whether the small axial perturbation produced by a solvent such as carbon tetrachloride can be termed "co-ordination", or whether it is sufficient to term the product a paramagnetic planar complex. Maki's work is certainly opposed to any possibility of tetrahedral configurations.

THE REACTIVITY OF CELLULOSE

III. THE NITRATION OF COTTON LINTERS ALTERNATELY WETTED WITH WATER AT VARIOUS TEMPERATURES AND DRIED, AND THE PROBABLE DISTRIBUTION OF THE NITRATE GROUPS[1,2]

T. P. YIN[3] AND R. K. BROWN

ABSTRACT

Cotton linters alternately wetted at 0° or 25° and dried show progressively greater ease of nitration paralleling the number of wetting–drying cycles. The reverse is found to be true for linters wetted at 50°, 75°, or 100°. Analysis of the data obtained from lead tetraacetate oxidation of the nitrates favors the depressive concept of nitration and indicates that the observed changes in reactivity occasioned by the wetting–drying treatments are largely due to greater alterations in the accessibility of the primary rather than the secondary hydroxyl groups.

INTRODUCTION

It is known that the physical treatment and moisture history of cellulose has a definite effect upon its reactivity (1, 2, 3). Highly swollen cotton linters nitrate to a significantly greater extent than do the same linters "collapsed" by drying from a water-soaked state (3). Furthermore, repeated experiments have shown that dewaxed cotton linters, alternately wetted with water at 25° and dried, exhibit a small increase in accessibility to thallous ethylate in ether, to a nitration mixture of sulphuric acid, nitric acid, and water, and to deuterium exchange with heavy water (4, 5). Thus the extent of reaction and doubtless the distribution of the reacted hydroxyl groups are determined to some extent by the treatment the cellulose has received prior to reaction.

The present work attempts to gain more information concerning the effects of the wetting–drying process on the reaction proclivities of the primary and secondary hyrodxyl groups of cellulose as well as to verify and extend the observation that linters wetted at 80° and dried become *less* rather than *more* reactive (5).

Accordingly, cotton linters were repeatedly subjected to alternate wetting and drying cycles, the wetting temperature ranging from 0° to 100°. The dried samples were nitrated and the nitrates examined by lead tetraacetate oxidation for glycol content. The data from the nitration and oxidation reactions were analyzed and certain conclusions made concerning the probable course of the nitration reaction.

EXPERIMENTAL

Preparation of the Cotton Linters

High grade cotton linters[4] were dewaxed (5) and air-dried. A quantity of the dried linters was divided into five 20- to 30-gram portions, each one of which was given 15 cycles of alternate wetting and drying, the wetting temperatures being, for the five portions respectively, 0° (a mixture of ice and water), 25°, 50°, 75°, and 100° (wet steam). Each wetting involved immersion of the linters in water at the specified temperature for a 3-hour period while the mixture was occasionally stirred. The 100° wetting was

[1]*Manuscript received September 15, 1958.*
Contribution from the Department of Chemistry, University of Alberta, Edmonton, Alberta, Canada. This paper was presented in part at the Fourth Regional Conference of the Chemical Institute of Canada at Winnipeg, Manitoba, on September 4–6, 1958.
[2]*Taken in part from the thesis submitted by T. P. Yin in partial fulfillment of the requirements for the degree of M.Sc.*
[3]*Present address: Department of Chemistry, University of Wisconsin, Madison, Wis., U.S.A.*
[4]*Generously donated by the Hercules Powder Company.*

accomplished by passing wet steam (at 100°) through a mass of loosely packed linters held in a wide tube with smaller openings at either end. The water was then separated from the linters by mild suction and the moist fibers spread out to dry in air. This preliminary drying was followed by one of greater intensity with phosphorus pentoxide as previously described (5). A sample (1.5–2 g) was retained while the bulk of the linters was again wetted and dried. In this way a number of samples of linters were obtained and all were kept in a large desiccator over phosphoric anhydride for 2 weeks before further treatment.

Nitration of the Dried Cotton Linters

Standard tables (6, 7) facilitated the preparation of a nitration mixture which would produce 10–11% nitrogen in the cellulose nitrate. A quantity of this reagent, sufficient for the whole series of experiments, was kept in a refrigerator and found to maintain its strength. The details of the nitration followed the published directions (3, 4) but with the modification that during the ½-hour nitration, the linters and mixed acid were constantly though gently stirred to facilitate diffusion of the liquid.

Nitrogen Estimation

Analysis for nitrogen by the Du Pont semimicronitrometer (8) followed the procedure adopted previously (5).

Lead Tetraacetate Oxidations

Glacial acetic acid was freed from aldehyde by heating for 3 hours under reflux with chromic anhydride (2.5 g per liter of acid) added in small quantities at suitable intervals to avoid violent reaction. The acid was then fractionated in an all-glass apparatus.

Acetic anhydride was purified by fractionation.

The nitrocellulose (0.5 g corrected for moisture absorption) was weighed to 4 figures in a capped weighing bottle and transferred to a 200-ml glass-stoppered volumetric flask. The sample was covered with 125 ml purified anhydrous ethyl acetate (9) and slowly dissolved by agitation in a mechanical shaker for 2–3 days. Fifty milliliters of 0.1 *N* lead tetraacetate (10) in glacial acetic acid was added followed by enough ethyl acetate to bring the total volume to the 200-ml mark. The flask was well shaken again and placed in a constant temperature bath at 25°±0.1°. Two blanks were prepared simultaneously and duplicate runs were made for each sample.

Consumption of lead tetraacetate by the cellulose nitrate was followed by amperometric titration (11) with 0.02 *N* sodium thiosulphate added from a microburette. The

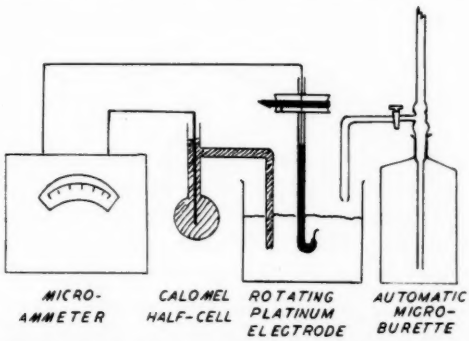

FIG. 1. Amperometric titration apparatus for the lead tetraacetate analyses.

apparatus is shown in Fig. 1 and consists of a rotating platinum electrode operating at 60 r.p.m., a saturated calomel half-cell, and a microammeter connected to the two electrodes. At suitable intervals the volumetric flasks were removed from the bath and briskly shaken. Suspended, undissolved material, if any, was allowed to settle and then a 10-ml aliquot was pipetted into 30 ml of potassium iodide – sodium acetate solution (12) in a 300-ml electrolysis beaker. The pipette was flushed with 10 ml of pure ethyl acetate and the washings added to the beaker. This is important, since the viscosity of the solutions of the cellulose nitrate in ethyl acetate varies with the nitrogen content of the nitrates producing variable delivery from the pipette. After the addition of 100 ml of distilled water the contents of the beaker was titrated with the two electrodes well-immersed in the liquid. The course of the titration was followed by the

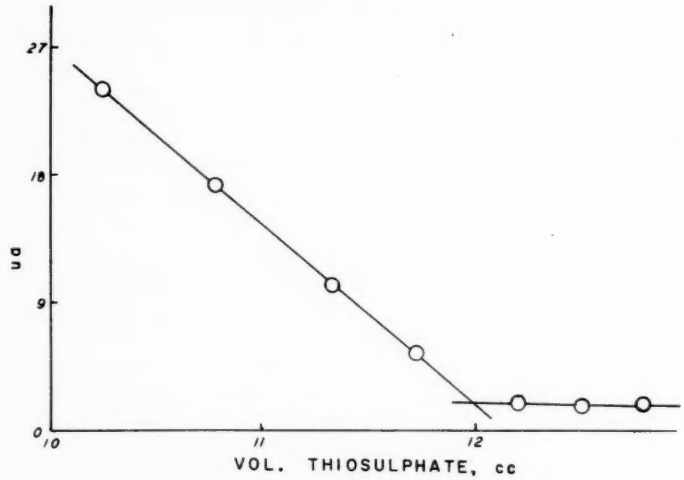

FIG. 2. Sample titration graph using the amperometric method.

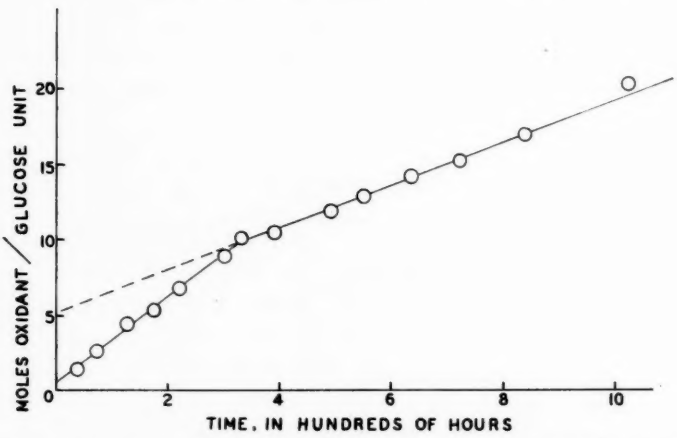

FIG. 3. Lead tetraacetate oxidation of the nitrate obtained from cotton linters which had received eleven cycles of immersion in water at 25° followed by drying.

scale readings of the microammeter. Usually 6–7 readings were recorded, three or four before and three after the equivalence point. This point was determined by plotting the volume of thiosulphate against the corresponding microammeter readings. A typical plot is shown in Fig. 2. Consumption of oxidant is expressed as the difference in titrations between blank and sample, and calculated as moles of oxidant consumed per glucose unit. One can add starch indicator to act as a visual check on the end point, but since the iodine is absorbed by the cellulose and the ethyl acetate layer, colorimetric end points are not reliable.

RESULTS AND DISCUSSION

Table I contains the data obtained from duplicate or triplicate nitrometer nitrogen analyses of the five series of nitrates. For convenience, the degree of substitution (D)[5] per glucose unit is listed along with the percentage of nitrogen. In addition the nitrogen analyses for the dewaxed but unwetted linters, nitrated by the same stock mixture, are noted in the same table. The decreased nitratability occasioned by one wetting at 0° or 25° (e.g. from 10.36% N to 10.20% N or 10.29% N) has been observed before (4, 5) and ascribed to a general collapse of the accessible cellulose from the partly swollen state which might have been attained during the dewaxing process. However, a similar single wetting–drying treatment at the higher temperatures (50°–100°) either maintains the same state or produces more reactive linters as in the case of the 75° series (an increase from 10.36% N to 10.63% N).

Examination of the data in Table I shows unmistakably that linters repeatedly wetted at 0° or 25° show enhanced nitration while those wetted at 50°, 75°, or 100° become less inclined to react as the number of wetting–drying cycles is increased. The differences are small, but several repetitions of this work show that the trend, though not the figures, is quite reproducible. The division between increasing and decreasing ease of nitration occurs somewhere in the region of 25° to 50°.

It should also be noted that the greatest over-all enhancement of reactivity caused by the wetting processes is found in the 0° series (0.41% N increase), while the most marked change in reactivity due to the first wetting is found in the 75° series (0.27% N increase). These observations *may* be significant.

Furthermore, of the five series of treated linters, only that exposed to steam at 100° gave a product which was non-uniform in physical appearance. It was somewhat more brittle and contained many small "nodules" which no doubt gave rise to the greater variability observed in the nitrogen analyses of the nitrates. At least three analyses were made on each nitrate of the 100° series in order to obtain a reasonable average value for the nitrogen content. These observations and the figures for the 100° series in Table I suggest that linters wetted by steam at 100° and dried, in addition to becoming less homogeneous, suffer a general reduction of accessibility to a technical nitration mixture.

The lead tetraacetate oxidations of the nitrates of these five series were carried out with the same stock solutions of the tetraacetate in acetic acid (normality, 0.0969). Although the nitrates in the ethyl acetate – acetic acid gave transparent, gel-like solutions, they were considered suitable for reaction and apparently presented no difficulties during the oxidations. Analyses were made by amperometric titration, since in several trials it was found that even though the blue-violet coloration of the starch–iodine complex disappeared, indicating complete reaction of the iodine with thiosulphate, the thin

[5]*The usual abbreviation is* D.S. *Here* D *is used for the sake of brevity.*

TABLE I

Nitrogen analyses (% N)[b] and degree of substitution (D)[c] of nitrocelluloses

No. of[a] wetting–drying cycles	0° Series		25° Series		50° Series		75° Series		100° Series	
	% N	D	% N	D	% N	D	% N	D	% N	D
1	10.20	1.76	10.29	1.78	10.41	1.81	10.63	1.87	10.30	1.79
3	10.49	1.83	10.54	1.85	10.29	1.78	10.52	1.84	10.29	1.78
5	10.46	1.83	10.39	1.81	10.22	1.76	10.49	1.83	10.24	1.77
7	10.51	1.84	10.44	1.82	—	—	—	—	10.25	1.77
9	10.54	1.85	10.46	1.83	—	—	—	—	10.20	1.76
11	10.59	1.86	10.51	1.84	—	—	—	—	10.19	1.76
13	10.63	1.87	10.53	1.84	—	—	—	—	10.22	1.76
15	10.61	1.87	10.52	1.84	—	—	—	—	10.16	1.75
0			10.36	1.80						

[a]Each wetting consisted of 3-hour immersion in water at the specified temperature, followed first by air-drying, then thorough drying over P_2O_5 under vacuum. The 100° series was exposed to wet steam at 100° for the 3-hour period.

[b]Average of duplicate or triplicate Dupont nitrometer analyses generally agreeing very well. Those for the 100° series gave somewhat poorer reproducibility, hence the percentage of nitrogen values shown are the averages of *at least three* analyses per sample.

[c]Obtained from the relation: (D×atomic wt. nitrogen)/(submolar wt. of cellulose) = 14D/(162.2−45D) = %N /100.

TABLE II

Comparison of glycol content (G) of cellulose nitrates with their unnitrated hydroxyl content (F)

Wetting–drying cycle	0° Series		25° Series		50° Series		75° Series		100° Series	
	G[a]	F[b]	G[a]	F[b]	G[a]	F[b]	G[a]	F[b]	G[a]	F[b]
1	0.057	1.24	0.045	1.22	0.039	1.19	0.052	1.13	0.049	1.21
5	0.050	1.17	0.052	1.19	0.043	1.24	0.053	1.17	0.050	1.23
11	0.049	1.14	0.055	1.16	—	—	—	—	0.051	1.24
15	0.047	1.13	0.058	1.16	—	—	—	—	0.051	1.25
0	0.033	1.20							0	

[a]Moles of 2,3-glycol per glucose unit as measured by consumption of lead tetraacetate in moles per anhydroglucose unit.

[b]Total unnitrated hydroxyl content per anhydroglucose unit obtained from the degree of nitrate substitution D (Table I) subtracted from 3, the number of hydroxyl groups per anhydroglucose unit in cellulose.

organic layer of ethyl acetate still showed a faint yellow color of iodine. The starch was used, if at all, only as a visual aid for the determination of the approaching end point, and the exact equivalence point obtained amperometrically.

The consumption of lead tetraacetate by cellulose nitrate should reach a maximum when all free glycol groups in the anhydroglucose unit have reacted. However, in the present work, consumption continued to rise in all cases even after a period of 1200 hours. This phenomenon has been reported by other workers (12, 13). The glycol estimation, however, was obtained in the usual manner by extrapolation of the slower reaction curve to zero time. Figure 3 is typical of the results obtained in all cases and shows that a definite and unambiguous break occurs in the line. Duplicates were generally in very good agreement. The break in the oxidation curve usually occurred at about 300 hours. Confidence that the break did indicate completion of the glycol oxidation was obtained from the observation that cellulose trinitrate under similar conditions showed no evidence of oxidation (14).

Table II summarizes the oxidation data for the samples of nitrocelluloses from the five series of linters. It is unfortunate that for the series 50° and 75° only two sets of values are available. This was unavoidable at the time, since a choice was necessary because only a limited number of oxidations could be carried on simultaneously. Nevertheless, the information in Table II reveals that lead tetraacetate consumption (and therefore glycol content), *decreases* in the 0° series, but *increases* for the 50°, 75°, and 100° groups with the number of cycles. Since the capacity for reaction with the nitration mixture employed was found to follow the directly opposite trend in these four cases, one infers that the augmented ease of reaction for the 0° linters is at least partly due to *greater accessibility and reactivity* of the secondary hydroxyl units, whereas the lowered nitratability for the 50°–100° series is due, in part, to the *diminishing accessibility and reactivity* of the secondary hydroxyl groups developed by the repeated wetting and drying.

Cyclic treatment at 25°, however, yields linters whose accessibility to nitration, *and* glycol content of the resulting nitrate, increases with the number of wettings. One must infer, therefore, that the rising nitration is due to the greater availability of the primary hydroxyl groups, outweighing the fall in accessibility of those on carbons 2 and 3 of the glucose unit.

The region of 25° in wetting temperature appears to constitute a dividing line between high and low temperature wetting effects, the former increases while the latter decreases the accessibility of the secondary hydroxyl groups to technical nitration.

It is also to be noted that the glycol content of the unwetted but dewaxed and nitrated linters is lower than that of any of the singly wetted and dried samples, even though the nitrogen content exceeds that found for the 0° and 25° series.

In attempting to understand the causes of the changes in reactivity noted above and the resulting distribution of reacted hydroxyl groups, one must consider both the kinetics and the nature of the nitration reaction. Since the over-all rate of nitration is fairly rapid and the reaction is essentially complete within 10 minutes (15), the $\frac{1}{2}$-hour allowed for the nitration should give ample time for the equilibrium to be well established for both primary and secondary hydroxyl groups. Thus the differences in reaction rates between these two types of hydroxyls should not be a determining factor in the distribution of the reacted positions. It is true, however, that reaction at one hydroxyl of the glycol pair might somehow inhibit reaction at the second hydroxyl of the pair. What seems to be important is the position of equilibrium and the accessibility of the hydroxyl groups in determining the extent of reaction and the distribution of affected sites.

Because the nitration mixture is of constant composition, the equilibrium position

reached (16) at the completion of the reaction should be the same in all cases. Two factors might interfere with the attainment of this equilibrium. The first is the "bound water" content in the linters. Previous work (5) has shown that a series of linters wetted at 25° shows progressively greater water content, measured by Karl Fischer titration, as the number of cycles of wetting and drying increase. A stock nitration mixture should then, upon reaching equilibrium, have a slightly larger water content for the more frequently wetted and dried linters than is found in the case of the singly wetted and dried sample. The extent of nitration determined by the final composition of the nitration solution (16) should then be less. But, since the reverse was found true (5), small differences in the "bound water" content do not cause the regular variation in nitratability observed. The second factor, that of diffusion of the reagent to the reaction site, probably involving reaction with more resistant "hydrogen bonded" hydroxyls, appears to be important, since it has been shown that extension of the reaction time of nitration from 30 to 90 minutes obliterated the differences observed (5).

Some assistance in the clarification of this problem might be gained by a consideration of the three proposed concepts of the manner in which nitration occurs in the cellulose fiber. The most popular one, the *homogeneous* or *permutoid* method, considers that the fibrous structure of the cellulose is sufficiently swollen by the reaction environment that all portions of the macromolecule are uniformly exposed to the reagent and the hydroxyl groups are randomly substituted. This method is also referred to in this paper as the *random* method. The *heterogeneous* concept considers that the readily accessible regions of the fiber are extensively substituted and the hydrophobic shell so formed hinders the progress of the reagent to the interior of the micelles. There is thus produced a nitrate in which the glucose units are either completely substituted or entirely unsubstituted. The third concept of interest is termed the *depressive* method wherein a permutoid-like reaction occurs. The C_6 hydroxyl reacts without difficulty but substitution at either the C_2 or C_3 hydroxyl depresses the reactivity of the remaining member of the glycol pair (13, 17, 18).

Considerable evidence is available which discounts the heterogeneous viewpoint (18). The homogeneous or permutoid (random) theory agrees with a large mass of information available (18). However, the depressive mode of reaction has been postulated to account for the observation that in partly xanthated cellulose, the xanthate groups occupy the C_3 and C_6 but not the C_2 position (19), and the same concept may explain the presence of approximately half the nitrate groups in the primary position with the other half "distributed between" the two available secondary positions in cellulose nitrates containing from 2.5% to 7.5% nitrogen (20).

Expressions may be obtained for the coincidence of glycol groups for these three concepts of nitration and have been used in conjunction with data from tosylation, iodination, and oxidation experiments to estimate the probable distribution of substituents between the three available hydroxyl groups of cellulose (12, 13, 17, 21).

Setting H equal to the total molar value of the secondary hydroxyl groups unnitrated, and X as the concentration of the unreacted C_2 hydroxyl per anhydroglucose unit, the probability of glycol occurrence based on the assumption of random or homogeneous nitration is (X) (H−X) whose value is maximum when $X = H-X = H/2$. Thus $H^2/4$ estimates the glycol occurrence. The depressive concept, permitting in the ideal case reaction at only one of either the C_2 or C_3 hydroxyls, would exhibit the presence of glycol only when the total degree of substitution in the secondary positions falls below one hydroxyl per glucose unit. The probability for glycol occurrence is then $[(H-X)+X]-1$

TABLE III

Total number of reacted (nitrated) secondary (2−H) and primary (D−2+H) hydroxyl groups per glucose unit in the nitrate

Based on assumption of:	No. of cycles	0° Series		25° Series		50° Series		75° Series		100° Series	
		Secondary	Primary	Secondary	Primary	Secondary	Primary	Secondary	Primary	Secondary	Primary
A. Random substitution	1	1.52	0.24	1.58	0.20	1.61	0.20	1.54	0.33	1.56	0.23
	5	1.55	0.28	1.54	0.27	1.59	0.17	1.54	0.29	1.55	0.22
	11	1.56	0.30	1.53	0.31	—	—	—	—	1.55	0.21
	15	1.57	0.30	1.52	0.32	—	—	—	—	1.55	0.20
	0	1.64	0.16	—	—	—	—	—	—	—	—
Over-all change*		+0.05	+0.06	−0.06	+0.12	−0.02	−0.03	0.00	−0.04	−0.01	−0.03
B. Depressed substitution	1	0.94	0.82	0.96	0.83	0.96	0.85	0.95	0.92	0.95	0.84
	5	0.95	0.88	0.95	0.86	0.96	0.80	0.95	0.88	0.95	0.82
	11	0.95	0.91	0.95	0.90	—	—	—	—	0.95	0.81
	15	0.95	0.92	0.94	0.90	—	—	—	—	0.95	0.80
	0	0.97	0.83	—	—	—	—	—	—	—	—
Over-all change*		+0.01	+0.10	−0.02	+0.07	0.00	−0.05	0.00	−0.04	0.00	−0.04
C. Heterogeneous substitution	1	1.89	−0.13	1.91	−0.13	1.92	−0.11	1.89	−0.02	1.90	−0.11
	5	1.90	−0.07	1.90	−0.09	1.91	−0.15	1.89	−0.06	1.90	−0.13
	11	1.90	−0.04	1.89	−0.05	—	—	—	—	1.90	−0.14
	15	1.91	−0.04	1.88	−0.04	—	—	—	—	1.90	−0.15
	0	1.93	−0.13	—	—	—	—	—	—	—	—
Over-all change*		+0.02		−0.03		−0.01		0.00		0.00	

* + indicates increase; − indicates decrease in extent of nitration.

or H−1. Finally, the heterogeneous viewpoint allows either 100% glycol or 0% glycol per glucose unit and the estimate for glycol occurrence is obviously H/2 if it occurs at all.

Equating in turn these three expressions to the glycol content measured by lead tetraacetate oxidations, one obtains a figure for H representing the probable occurrence of *unreacted* secondary hydroxyl groups for each of the three modes of nitration. By subtracting this value from the total unnitrated hydroxyl content (F) per glucose unit (Table II), one arrives at probable values for unreacted primary hydroxyls (F−H). From this can be obtained the probable extent of nitration of the primary and secondary positions. For example, the equation for the sample isolated after one wetting–drying cycle at 0° is $0.057 = H^2/4$, or H/2 or H−1, according to the three assumptions, yielding values for the unnitrated secondary hydroxyl groups of H = 0.48, 1.06, and 0.11, respectively. Subtraction from the total amount of unnitrated hydroxyl groups (F in Table II) then gives values for the primary hydroxyl group as (1.24−0.48) = 0.76, etc. The probable extent of nitration in the two secondary positions is then (2−0.48) or 1.52, and that in the single primary position (1−0.76) or 0.24. All the nitrate substitutions calculated on the three assumptions are recorded in Table III.

The negative values for primary nitration shown in the lower section of Table III immediately eliminate heterogeneous nitration as a reasonable process. The figures for the probable reaction on the basis of random substitution suggest that the secondary positions react to a five- to seven-fold greater extent than do the primary positions. However, many examples can be quoted from the literature which clearly show that the primary hydroxyl in cellulose reacts more readily than do the secondary hydroxyl groups (22). In view of this, and the implication in the concept of random substitution that all hydroxyls are equally exposed to reaction and at equilibrium the extent of their reaction should be roughly the same, one would not expect this great preponderance of secondary over primary positions esterified. On the other hand, the depressive type of reaction, if permutoid-like, might be expected to yield after equilibrium is attained, a nitrate with the primary, and one of the two secondary positions more or less equally affected. This agrees with the analysis of the oxidation data on the basis of the depressive reaction theory. The observation by Murray and Purves (20) that half the nitrate groups in a nitrocellulose containing less than 8% nitrogen are found in the primary position lends support to the acceptance of the depressive permutoid-like reaction process as a reasonable mode for nitration. Although the homogeneous concept is favored for esterifications and etherifications in general, the suggestion has been made that nitration may not follow the course of most esterifications (23).

A further conclusion can be drawn from the data in Table III. The over-all change in primary and secondary nitrate substitution was obtained by subtracting the value after the first wetting–drying cycle from that obtained after the last, e.g. 1.57–1.52 or +0.05, in the case of the secondary nitrates in the 0° series assuming random substitution. The figures reveal that, except in the case of the 50° series, the differences in ease of nitration observed are largely due to the two- to three-fold greater change in reactivity of the primary over the secondary hydroxyl groups.

ACKNOWLEDGMENTS

The authors express their appreciation for the financial support given to this project by the National Research Council of Canada. One of us, T. P. Yin, wishes to thank the Shell Oil Company for the award of a scholarship which permitted him to carry out this work.

REFERENCES

1. JAYME, G. Cellulosechemie, **21**, 73 (1943).
2. SCHUR, M. O. and HOOS, B. G. Ind. Eng. Chem. **29**, 26 (1937).
3. BROWN, R. K. and PURVES, C. B. Pulp & Paper Mag. Can. **48** (6), 100 (1947).
4. ROSENTHAL, A. and BROWN, R. K. Pulp & Paper Mag. Can. **51** (6), 99 (1950).
5. BRICKMAN, W. J., DUNFORD, H. B., TORY, E. M., MORRISON, J. L., and BROWN, R. K. Can. J. Chem. **31**, 550 (1953).
6. DOREE, C. The methods of cellulose chemistry. Chapman & Hall, Ltd., London. 1933. p. 223.
7. OTT, E. and SPURLIN, H. M. *Editors* Cellulose and cellulose derivatives. Interscience Publishers, Inc., New York, 1954. pp. 718–722.
8. ELVING, P. T. and MCELROY, W. R. Ind. Eng. Chem. Anal. Ed. **14**, 84 (1942).
9. FIESER, L. E. Experiments in organic chemistry. 3rd ed. D. C. Heath & Co., New York. 1955, p. 287.
10. WALTON, H. F. Inorganic preparations. Prentice-Hall, Inc., New York. 1953. p. 138.
11. EWING, G. W. Instrumental methods of chemical analysis. McGraw-Hill Book Co., Inc., New York. 1954. p. 80.
12. CRAMER, F. B., HOCKETT, R. C., and PURVES, C. B. J. Am. Chem. Soc. **61**, 3463 (1939).
13. MAHONEY, J. F. and PURVES, C. B. J. Am. Chem. Soc. **64**, 9 (1942).
14. BROWN, R. K. Thesis submitted to the Faculty of Graduate Studies at McGill University, Montreal, Quebec. 1946. p. 102.
15. OTT, E. and SPURLIN, H. M. *Editors* Cellulose and Cellulose derivatives. Interscience Publishers, Inc., New York. 1954. pp. 722–723.
16. OTT, E. and SPURLIN, H. M. *Editors* Cellulose and cellulose derivatives. Interscience Publishers, Inc., New York. 1954. p. 730.
17. HONEYMAN, J. J. Chem. Soc. 168 (1947).
18. OTT, E. and SPURLIN, H. M. *Editors* Cellulose and cellulose derivatives. Interscience Publishers, Inc., New York. 1954. pp. 733–736.
19. SWAN, E. P. and PURVES, C. B. Can. J. Chem. **35**, 1522 (1957).
20. MURRAY, G. E. and PURVES, C. B. J. Am. Chem. Soc. **62**, 3194 (1940).
21. SPURLIN, H. M. J. Am. Chem. Soc. **61**, 2222 (1939).
22. CRAMER, F. B. and PURVES, C. B. J. Am. Chem. Soc. **61**, 3458 (1939).
23. TIMELL, T. E. Chem. Eng. News, 4036 (1955).

THE DETERMINATION OF ATOMIC RATIOS IN THE URANIUM–OXYGEN SYSTEM BY A THERMOGRAVIMETRIC METHOD[1]

L. G. STONHILL

ABSTRACT

A description is given of a thermogravimetric oxidation–reduction method for determining U–O ratios, especially suited to oxygen-sensitive materials of undetermined purity, and equally applicable to pure stoichiometric and non-stoichiometric oxides and their mixtures with each other and with uranium metal.

Provided that no uncombined base metals other than uranium, and no oxidizable or reducible matter other than its oxides, are present, it is not essential to know the detailed composition of the sample, since the assay is based on interconversion of the stoichiometric oxides UO_2 and U_3O_8 within that sample.

Incidental advantages of this method are: the avoidance of manipulation of the sample during the determination, precise reaction control, and immediate recording of the completion or otherwise of the required reaction.

INTRODUCTION

One of the chief characteristics of the uranium–oxygen system is the extent to which excess oxygen can be absorbed into the crystal lattice to form non-stoichiometric oxides. By far the most important of the oxides which has this ability is the dioxide, UO_2, often termed "brown oxide". In view of its function as an intermediate in the production of the metal, and being itself a potentially valuable reactor fuel, a knowledge of its exact U–O atomic ratio is often necessary. Current research into new methods of production has extended this need to materials, such as freshly precipitated oxide, which are extremely sensitive to oxidation by exposure to air and may contain inert impurities besides a large percentage of water.

It appeared likely that thermogravimetry offered a solution to the problems connected with this type of product, and would also provide a convenient general method for U–O ratios. A controlled-atmosphere apparatus (1) incorporating a Stanton milligram recording thermobalance was used in the investigation: the advantages of exact control over reaction conditions and a visible continuous record of the weight changes associated with a reaction make it possible to carry out a complete analytical operation within the assembly, thereby avoiding excessive manipulation of sensitive samples.

The standard chemical methods for determining atomic ratios, namely oxidation to U_3O_8 (2) or reduction to UO_2 (3), have been evaluated and refined by Bright *et al.* (4): these latter investigators point out the necessity of preparation and weighing in an oxygen-free atmosphere and recommend the use of an argon-filled dry box for these operations. Assumptions are usually made that the material under investigation contains only uranium oxide after a preliminary heat treatment to drive off water, etc. Though justifiable with familiar samples, such assumptions could not be made in the case of unusual products, and preliminary assays of material subject to aging should be avoided. The method to be described postulates only that oxidizable and reducible matter other than uranium and its oxides shall be absent, and uses interconversion of stoichiometric UO_2 and U_3O_8 as an internal standard on which to base the assay.

Composition of Oxides UO_x

The empirical formula UO_x may represent a homogeneous oxide species or, alternatively, a mixture of various oxidation states from UO_3 down to the uncombined metal.

[1]*Manuscript received September 30, 1958.*
Contribution from the Metallurgical Laboratories, Eldorado Mining and Refining Ltd., Ottawa, Canada.

Thus, UO may be the true monoxide, or mixed uranium metal and other oxides, and partial reduction of UO_3 with hydrogen results in a product UO_{2+x} containing UO_3, U_3O_8, and the dioxide, as evinced by its behavior in the thermobalance and also by analysis (5). The importance of these alternative possibilities in the development of a general procedure for determining formulae will be considered below.

Thermogravimetric Behavior of Uranium Oxides

In view of the preceding observations it will be clear that a knowledge of the behavior of uranium in various oxidation states towards heat, and oxidizing and reducing atmospheres, is required. Figure 1 shows the effect of these factors on the pure oxides and also on the metal. Between UO_2 and U_3O_8 several phases have been detected by X-ray study: these tend to disproportionate on being heated (6), presumably without loss of oxygen from the system (7).

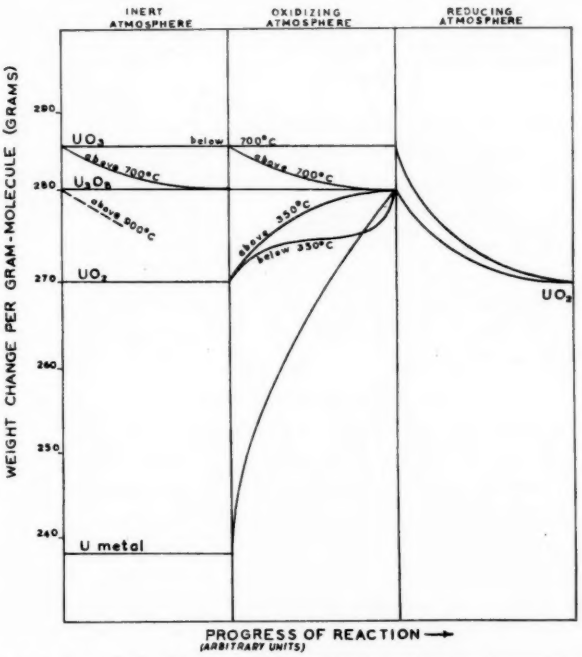

FIG. 1. Behavior of uranium and its principal oxides in various environments (temperatures approximate).

In the case of mixtures, the observed behavior depends on circumstances: in an inert atmosphere UO_3 will oxidize UO_2 with little or no evolution of oxygen until the rest of the uranium has been converted to U_3O_8; but if the material be oxidized by heating gradually in air from cold, the UO_3, which is unaffected by such treatment, will decompose on reaching a temperature of about 700° C, and the material will undergo a loss in weight.

The experimental observations on which Fig. 1 is based show (*a*) that for complete conversion of the uranium of any mixture to pure U_3O_8, it should be heated to 800° C to constant weight in air to ensure decomposition of UO_3, then cooled somewhat to compensate for a tendency of U_3O_8 to lose oxygen at that temperature; (*b*) that for

similarly complete reduction to UO_2, temperature is not a critical factor but can be chosen so as to give a suitable reaction velocity; (*c*) that to ensure decomposition of hydrates, particularly of UO_3, and to volatilize traces of nitric acid, preliminary heating to at least 550° C is advisable.

Derivation of U–O *Molecular Formulae*

Suppose that a sample contains oxygen combined with uranium to an extent giving a general formula UO_x, and that the following reactions are made to occur in such a way that the whole of the uranium present is converted to the appropriate stoichiometric compound, either UO_2 or U_3O_8, thus

$$UO_x \rightarrow U_3O_8 \rightarrow UO_2,$$

or alternatively

$$UO_x \rightarrow UO_2 \rightarrow U_3O_8.$$

The weight changes accompanying these reactions can be obtained directly from the thermogravimetric record. For any given weight of uranium, let these weights be *a*, *b*, and *c* as shown diagrammatically:

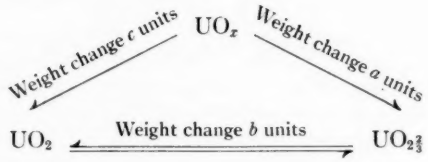

The weight change in each reaction step will be proportional to the amount of uranium taking part (a constant, *k*) and the change in its level of oxidation: therefore, for the conversion UO_x to U_3O_8 to UO_2:

$$a = k(2\tfrac{2}{3}-x)$$

and

$$b = k(2\tfrac{2}{3}-2),$$

therefore

$$a/b = (2\tfrac{2}{3}-x)/\tfrac{2}{3} = 4-(3x/2).$$

Similarly for the alternative route UO_x to UO_2 to U_3O_8:

$$c = k(x-2)$$

therefore

$$c/b = (3x/2)-3.$$

Obviously the value of *x* is obtainable from either of these reaction cycles independently of the actual sample weight employed. In practice, however, several limiting possibilities should be distinguished.

Case *a*: $2\tfrac{2}{3} < x \leqslant 3.$

This arises when oxygen is present beyond the proportion required to give U_3O_8, and, therefore, presumably the material contains some UO_3. When the material is heated in air there will be a net *loss* in weight owing to the decomposition of this UO_3, but the general equations deduced above still apply.

Case *b*: $x = 2\tfrac{2}{3}.$

Stoichiometric U_3O_8 is of course not further oxidizable by heating in air, but net weight changes associated with reduction followed by reoxidation will be equal.

Case *c*: $2 < x < 2\frac{2}{3}$.

This covers the range of oxides usually met. Either sequence of reactions may be employed.

Case *d*: $x = 2$.

The true dioxide is not often encountered, since, once it has been exposed to air, an excess of oxygen is always present (3), but it could be simulated by a mixture of metal with other oxides.

Case *e*: $0 \leqslant x < 2$.

In this case metal is most probably present in view of the uncertainties surrounding the monoxide UO (8, 9). Only the procedure involving a preliminary oxidation is applicable, as explained below.

Material Containing Uranium Metal

The presence of uncombined uranium metal invalidates the use of the equation derived above for reduction followed by oxidation, since the supposition that the whole of the uranium present takes part in the full cycle of reaction would not be true. However, the alternative preliminary oxidation procedure would be reliable, because the metal begins to oxidize at about 400° C (depending on its state of subdivision) and gives a final product of U_3O_8 in the same way as the oxides.

Samples containing uranium metal show a gain in weight during initial heating in nitrogen (see method, below) owing to nitride formation. On the admission of air, this nitride is converted to oxide.

ANALYTICAL PROCEDURE

Air is first displaced from the reaction chamber of the thermobalance by passing in oxygen-free nitrogen for about 10 minutes at a rate of 1 l. per minute. A sample of the material under test, weighing approximately 10 g (or, in the case of precipitated oxide, sufficient to contain that weight of UO_2), is then placed in the sample holder and the furnace lowered into position.

The material is thereby protected from oxidation, and may be subsequently balanced; the tare weight being known, this gives the weight of sample actually taken. Nitrogen is fed into the seal compartment at a rate of 0.75 l. per minute and the exhaust system, calibrated for an extraction rate of 1.5 l. per minute, set in operation.

The furnace is then heated to 600° C and held at this temperature until the sample has maintained a constant weight for about 5 minutes. If reduction is to be employed, the nitrogen flow rate is reduced to 0.25 l. per minute and 0.75 l. per minute hydrogen added to the gas stream; if oxidation, then the seal nitrogen flow is cut off and the gas input line disconnected to allow the entry of air. For faster oxidation a mixture of air and oxygen may be introduced. During this oxidation the furnace temperature is allowed to rise to 900° C, by which time the reaction should be complete (it is not essential to reach this temperature in the reduction stage—cooling can be commenced when reaction ceases) and the furnace is allowed to cool back to 600° C.

The reaction chamber is next purged with nitrogen under the same conditions used at the start of the operation; after 10 minutes the weight change accompanying the reaction

may be noted. The reverse operation, either reduction or oxidation, can then be carried out, and on its completion the standard conditions of nitrogen flush and temperature are restored so that each weight change is measured under as nearly as possible identical conditions, thereby avoiding spurious changes due to buoyancy, etc. The uranium–oxygen ratio is calculated from the formulae deduced above. Incidentally it is worth noting that the thermogravimetric record, by showing the actual weight change involved in the interconversion of UO_2 and U_3O_8, gives data from which the total uranium content of the sample may be calculated.

Certain special problems require a slight modification of the above procedure; thus, if a loss on ignition determination is to be carried out, the furnace temperature is initially raised to the necessary extent, then brought back to 600° C. Any weight loss commencing near 700° C would then require especial notice if the presence of UO_3 were possible. In the case of samples containing uranium metal, argon is used as the flushing gas in place of nitrogen.

RESULTS

A sample of U_3O_8 (99.9% pure) used as a reference standard in these laboratories was employed in the evaluation of the reduction–oxidation technique. In five consecutive runs the number of oxygen atoms per uranium atom was found to be 2.669, 2.672, 2.665, 2.665, and 2.668, giving an average value close to 2.668 compared with a theoretical 2.667 for 100% pure U_3O_8. It therefore appears that a good degree of accuracy is obtainable.

In order to test the procedure through both possible reaction cycles, and over a wide range of sample types, a number of materials which could be met in practice were taken. These are listed in Table I, together with the results obtained.

TABLE I

Atomic ratios obtained by the thermogravimetric procedure

Material	Atoms of oxygen per atom of uranium as determined by:	
	Oxidation followed by reduction	Reduction followed by oxidation
UO_3 (technical)	3.003	3.005
UO_3 (partly reduced with hydrogen):		
Sample *a**	2.873	2.878
b	2.412	2.410
c	2.277	2.274
d	2.147	2.150
e	2.082	2.083
f	2.035	2.038
UO†	0.99	Not applicable
U (metal, 99.4% pure)	0.008	Not applicable

*Microscopic examination shows presence of UO_3.

†Prepared by oxidizing uranium metal in the thermobalance, followed by cooling in argon. Microscopic examination shows presence of uncombined metal.

The data recorded above indicate that the present method can be used over the full range U to UO_3 with an accuracy suitable for all practical purposes.

DISCUSSION

The need for caution in applying the method in the presence of uranium metal has already been noted, and the absence of oxidizable or reducible foreign matter presupposed.

Apart from independent tests, these complications would normally manifest themselves in inconsistent results if both oxidation and reduction procedures were to be applied to the same material, and this might be used as a distinguishing criterion. Substantial quantities of free metals other than uranium, oxides of transitional metals, and certain compounds of uranium apart from the oxides would be expected to interfere.

From the point of view of accuracy this method compares favorably with earlier procedures with which, according to Bright (4), the number of oxygen atoms per atom of uranium can be determined to a precision of ± 0.005.

In conclusion, it is suggested that the general procedure is adaptable to the study of other metal–oxygen systems, as, for example, those involving molybdenum and tungsten, lead, etc., for which comparable reaction schemes might be devised.

REFERENCES

1. STONHILL, L. G. J. Inorg. & Nuclear Chem. To be published.
2. RODDEN, C. J. Analytical chemistry of the Manhattan project. 1st ed. McGraw-Hill Book Co., Inc., New York. 1950. p. 46.
3. ROBERTS, L. E. J. and HARPER, E. A. The determination of oxygen in uranium oxides. Atomic Energy Research Establ., Gt. Brit. A.E.R.E. C/R 885 (1952).
4. BRIGHT, N. F. H., RIPLEY, L. G., ROWLAND, J. F., and LAKE, R. H. Department of Mines & Technical Surveys, Mines Branch (Canada), MD-207 (1956).
5. STONHILL, L. G. Can. J. Chem. **36**, 1487 (1958).
6. ALBERMAN, K. B. and ANDERSON, J. S. J. Chem. Soc. 303 (1949).
7. ROBERTS, L. E. J. Uranium dioxide as a fuel element. Atomic Energy Research Establ., Gt. Brit. A.E.R.E. C/M 268, 2 (1956).
8. WILLIAMS, J. and WESTMACOTT, K. H. Atomic Energy Research Establ., Gt. Brit. A.E.R.E. M/R 1235 (1953).
9. VAUGHAN, D. A., MELTON, C. W., and GERDS, A. F. Battelle Memorial Institute, B.M.I. Rept. 1175 (1957).

ORBITAL CONSTRUCTIONS AND ELECTRON POPULATIONS IN THE TRANSITION ELEMENTS[1]

W. R. TROST

ABSTRACT

Orbital constructions and electron populations for the bands in the transition elements have been worked out. With the assumption of uniform density of states in delocalized bands among nearest neighbors, it is possible to predict correctly the lattice elected by the elements. Manganese and iron are exceptions. Numerical values for electron populations in the several *s*, *p*, *d*, and hybrid bands, including their bonding, antibonding, and non-bonding levels, are obtained.

INTRODUCTION

Though molecular orbitals were first proposed for metals by Bloch (1) in 1928, the orbital constructions and hence the electron populations for the bands in metals, particularly for the transition metals, are still lacking. In simple cases, such as the alkali metals, detailed calculations of the binding energy have been made and reasonable agreement with experimentally determined binding energies obtained (2). Even in the case of atoms with one valence electron, however, the definition in space of the atomic orbitals comprising the bands is missing. In the more complicated case of the transition metals, where up to 12 valence electrons and 9 atomic orbitals are to be counted for each atom, the binding energy calculations are more difficult, and the problem of locating the orbitals and electrons is also more complex. It is perhaps correct to say that as yet no general success has been met with here. Indeed in many cases, as a simplification, the *d* orbitals have been ignored. It is true that Pauling counted *d* electrons when he proposed metallic valences for the transition metals (3). However, the spatial constructions and the electron populations of the bands were not offered. Indeed, precisely because of a general lack of emphasis on the directive properties of the orbitals it has not been possible up till now to answer the simple structural question, "Why should a particular metal have one lattice rather than another?"

It would seem that a solution to the problem is implicit in the molecular orbital theory, particularly in view of recent developments in the ligand-field theory (4), and the work of Jaffe (5) and of Craig, Maccoll, Nyholm, Orgel, and Sutton (6, 7) on orbital pairs.

THE TRANSITION METALS

In the transition metals nine orbitals (one ns, three np, and five $(n-1)d$) are to be counted for each atom. To make a metal it is necessary to locate in space the nine orbitals of each of an infinite number of atoms in such a way that the orientations and the overlaps of every orbital become specified. The orbital constructions are to place the nuclei on lattice points. At the same time, through the overlap property, the orbital interactions that stabilize the lattice are established.

The number of valence electrons in the transition elements varies from 3 (s^2d^1) to 12 (s^2d^{10}). As bonding, antibonding, and non-bonding bands are, in general, to be expected from the orbital constructions, the net binding energy and hence the stability of the lattice will also be a reflection of the changing electron populations in these bands. It therefore becomes necessary to classify the energy levels of the several bonding, antibonding, and non-bonding bands, relative to each other, so that the valence electrons

[1]*Manuscript received July 31, 1958.*
Contribution from the Chemistry Department, Dalhousie University, Halifax, Nova Scotia.

can be placed and the populations in the bands calculated. That is, electron density and orbital overlap both become criteria for lattice stability.

THE ORBITAL CONSTRUCTIONS OF THE BANDS

The overlaps and symmetry relationships as between pairs of s, p, and d orbitals have been worked out in detail by several authors (5, 6, 7) and are summarized in Fig. 1. Removal of the restriction that the number of orbitals in overlap be limited to two permits more closely packed assemblies of these orbitals to be sought. When all orbitals have been so arranged, and consideration given to the numbers of electrons involved, lattice systems that reproduce the metallic lattices are obtained. The d, p, and hybrid orbitals become the orbitals that determine structure. The spherical s orbital, having no directional dependence, offers no choice between alternative close-packed structures. The results are summarized in Table I.

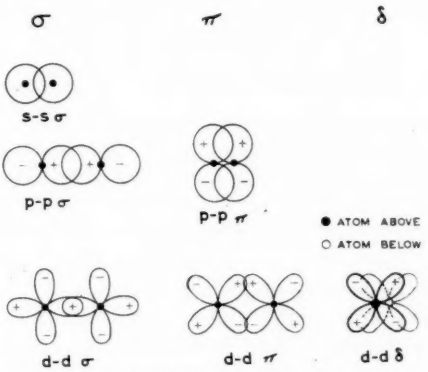

FIG. 1. Overlaps among orbital pairs.

TABLE I

Lattice systems and orbital assignments

Structure type	Orbital type	
	Bonding	Antibonding
1. *bcc*		
Nearest neighbors	s, p^3, $d\epsilon$	s'
Next to nearest	$d\gamma$	
2. *hcp*		
Nearest neighbors	s, d^5p, p^2 (or) sp^2, d^5p (or) sd^4p, p^2	
Next to nearest	d_z	d_z'
3. *ccp*		
Nearest neighbors	s, p^3, $d\epsilon$	$d\epsilon'$
Next to nearest	$d\gamma$	$d\gamma'$
4. Distorted *hcp*		
Nearest neighbors	sp^2, p	

1. *The p Orbitals*

The shape and the degeneracy of the orbitals provides a basis for choosing among alternative close-packed schemes. The p orbital construction shown in Fig. 2, in which each p orbital overlaps eight others, has three advantages. The arrangement can be

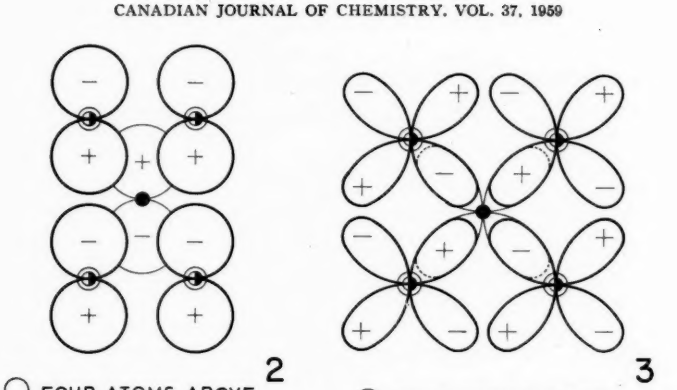

FIG. 2. The body-centered cubic p band.
FIG. 3. The body-centered cubic $d\epsilon$ band.

indefinitely and smoothly expanded, as more orbitals are added, to produce an indefinitely large and perfect body-centered cube. The arrangement has a threefold degeneracy, as the three mutually perpendicular directions are equivalent with $p_x(p_x)_8 = p_y(p_y)_8 = p_z(p_z)_8$. That is, the three p orbitals on each atom overlap the corresponding orbitals on the adjacent eight atoms in the same way. Finally, as an assurance that the overlap factor for the arrangement is favorable, the distance between the axes of the overlapping lobes is 0.81 the internuclear distance.

The result is that what will be called the *bcc p* band has cubic symmetry, is perfectly degenerate in the three p orbitals, is delocalized over all atoms in the lattice, and constitutes a close-packed assembly of p orbitals.

2. The d Orbitals

Turning to the d orbitals, it at once becomes evident that the degeneracy of the subshell cannot be retained in metallic bonding unless hybridization occurs, as all d orbitals cannot achieve the same overlap at the same time in any one lattice. The symmetry relationships for space-packing, however, separate the subshell into two groups of orbitals, the diagonal (d_{xy}, d_{xz}, d_{yz}) and the axial ($d_{x^2-y^2}$, d_{z^2}). Two different close-packed structures are possible for the diagonal orbitals. In the first of these, shown in Fig. 3, one orbital overlaps eight others. This configuration has the merit that each diagonal orbital becomes identically engaged, so that $d_{xy}(d_{xy})_8 = d_{xz}(d_{xz})_8 = d_{yz}(d_{yz})_8$, thereby preserving the degeneracy of the three orbitals and establishing a body-centered cubic lattice. In it the d band is delocalized over all atoms. The interlobar distance,[2] in this construction, is 0.58 the internuclear distance, a favorable feature for overlaps that is at least partly counterbalanced by the manner of approach of the orbitals. This is through the thickness of the lobes, much as in the d–$d\delta$ bonding of Fig. 1, which is not in the direction of maximum extension. The band will be called the *bcc* $d\epsilon$ band to conform with usage in the ligand-field theory (4). (The $d\epsilon$ level has also been called t_{2g} and γ^5.) The two remaining orbitals, $d_{x^2-y^2}$ and d_{z^2}, constitute the $d\gamma$ level.

A second way to close-pack d orbitals, shown in Fig. 4, places four orbitals around a central one. When the 3 diagonal orbitals on a central atom are so engaged, 12 atoms

[2]*The interlobar distance is the distance between the principal axes of the lobes.*

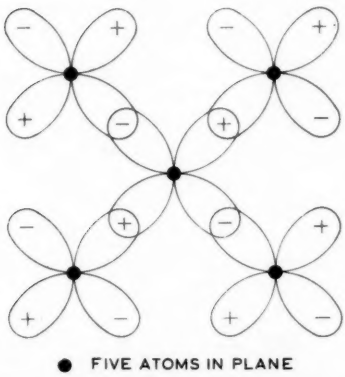

FIG. 4. The cubic close-packed $d\epsilon$ band.

surround the central one, in a cubic close-packed arrangement. That is, $d_{xy}(d_{xy})_4 = d_{xz}(d_{xz})_4 = d_{yz}(d_{yz})_4$, so the cubic close-packed $d\epsilon$ band, like the body-centered cubic $d\epsilon$ band, has cubic symmetry and is delocalized over all atoms. In each arrangement (i.e. *bcc* $d\epsilon$ and *ccp* $d\epsilon$) 2 *d* orbitals are still to be located. In both lattices, the direction of maximum extension of the $d\gamma$ orbitals ($d_{x^2-y^2}$, d_{z^2}) is identical with an octahedral arrangement of next nearest neighbors. The distance between the next nearest neighbors, as compared to the nearest neighbor distance, is 1.15 in *bcc* and 1.42 in *ccp*. In orbital constructions like that of Fig. 4 (for $d_{x^2-y^2}$, d_{z^2} has its maximum extension on the *z*-axis) these internuclear distances enable *bcc* $d\gamma$ to make a substantial minor contribution to the bonding,[3] whereas *ccp* $d\gamma$ is virtually non-bonding. The *bcc* $d\gamma$ will therefore support *bcc* $d\epsilon$ when fewer than five *d* electrons are present, but will weaken *bcc* $d\epsilon$ when more than five electrons are present. In the latter case, as antibonding levels in *bcc* $d\gamma$ become occupied, the cubic close-packed lattice with a *ccp* $d\epsilon$ band becomes preferred.

3. Hybrid Orbitals

Two hybrid orbital constructions lead to close-packed lattices. One of these applies to ground states between d^3 and d^7, which is just the gap left when orbital constructions based on the $d\epsilon$–$d\gamma$ split are employed. The second hybrid construction becomes relevant when the *d* subshell becomes non-bonding, as in s^2d^{10}.

The only hybrid sets that use four and five *d* orbitals and lead to close-packed structures are sd^4p and d^5p. In both of these 1×6 configurations, the bonding directions are towards the corners of a trigonal prism (8). When a set of identical atoms in this state are brought together a hexagonal close-packed lattice results, in which each atom is bonded to 6 neighbors through localized bonds, but is equidistant from 12, as shown in Fig. 5. The orbitals remaining after sd^4p or d^5p is chosen are accordingly to be placed with reference to the *hcp* system.

The last arrangement to be described is an sp^2 construction. The packing of sp^2 orbitals as in Fig. 6 sets up close-packed layers of atoms. The layers are bonded to each other

[3] *In view of the somewhat different shapes of the 2 orbitals it is possible that* $d\gamma$ *is not perfectly degenerate. A detailed analysis shows, however, that these orbitals also have small overlaps with nearest neighbors (the overlaps are small because of the orientations and shapes of the orbitals) that tend to make the two bonding functions equivalent. Therefore, although the band cannot be considered solely a next nearest neighbor band, it is possibly correct to describe it as a weakly bonding band with twofold degeneracy. It is also assumed in ligand-field theory (4) that* d_{z^2} *and* $d_{x^2-y^2}$ *remain degenerate in the* $d\gamma$ *level.*

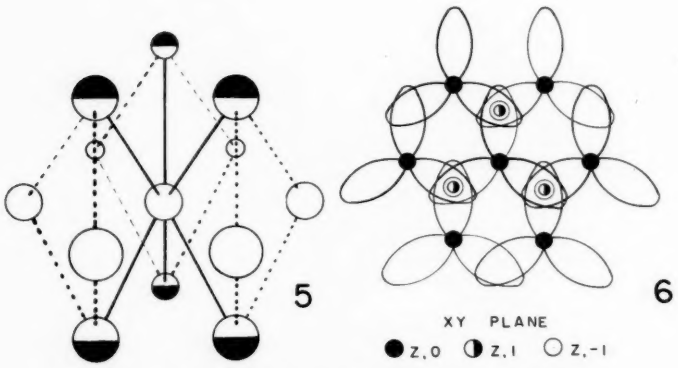

FIG. 5. The hexagonal close-packed hybrid band (sd^4p or d^5p).
FIG. 6. The distorted hexagonal close-packed sp^2 band.

through the p_z orbital, which provides a $p_z(p_z)_6$ band, and by a perpendicular delocalization in the three-center sp^2 molecular orbitals. A distorted hexagonal close-packed lattice appears, with six nearest neighbors in a layer, and three more distant ones above and three below. The electron cloud of the p_z band extends over the lattice but contains regularly spaced vacancies that have a definite shape. The superimposed sp^2 molecular orbitals through delocalization attain the shape of an endlessly repeated hour glass, with the thin part of the electron cloud between the layers and the thick part in the layer. The sp^2 band consists of an indefinite array of these, in parallel extension in a 1×6 packing, with each endless hour glass precisely occupying a vacancy in the electron cloud of the p_z band.

THE ATOMIC ORBITAL ENERGY LEVELS

An explanation of the properties of the transition metals should take account of both the spatial and the energy level properties of the orbitals. The foregoing consideration of the spatial problem gave rise to specific band systems with orbital constructions requiring one or another of four lattices, the body-centered cubic, the hexagonal close-packed, the cubic close-packed, and the distorted hexagonal close-packed. The energy level problem involves a consideration of both the atomic and molecular orbital energy levels. Complications arise here because of the likelihood that these levels change as the d subshell fills; as the principal quantum number varies; and in the molecular orbitals, as the band systems change. The atomic orbitals will be dealt with first.

An inspection of the ground states of the transition elements shows that the energy level of the $(n-1)d$ orbitals, which at first is above that of the ns orbital, as in s^2d^0, changes value until it is the stabler orbital, as in s^0d^9 and s^0d^{10}. This cannot be thought of as simply a regular increase in the stability of the d orbital as the d subshell fills, for energy is also contributed to the system in a non-linear way. Because of a lower electrostatic repulsive energy and a more favorable exchange energy among single electrons with parallel spins, states with the maximum number of singly filled orbitals are favored, as is well known from Hund's rule (4). As the magnitude of this energy term depends directly on the number of singly filled states, the d orbitals will be stabilized by increasing amounts as the number of valence electrons increases from one to six. Such a change is shown in the ground states of these atoms.

Valence electrons	Ground states
1	s^1d^0
2	s^2d^0
3	s^2d^1
4	s^2d^2
5	s^2d^3, s^1d^4
6	s^2d^4, s^1d^5

The number of single electrons, and hence the magnitude of the exchange energy contribution, must necessarily diminish upon the addition of further electrons. This will make the *d* levels fall more slowly after the six-electron atom than before it. However, the linear factor, associated with the increasing positive charge on the nucleus, still persists. The *d* levels are stabilized more than *s* because the $(n-1)d$ electrons are on the average closer to the nucleus than the *ns*. The *d* levels are therefore more directly affected by the increasing electrostatic field of the nucleus. At the same time, the $(n-1)d$ electrons intervene between the nucleus and the spherical electron cloud of the *ns* orbital. A screening effect occurs that tends to make the *s* electrons somewhat unresponsive to an increase in the charge on the nucleus. Both affects foresay a steadily increasing relative stability in the *d* orbitals as the subshell fills. This can also be seen in the ground states of the elements.

Valence electrons	Ground states
7	s^2d^5, s^1d^6
8	s^2d^6, s^1d^7
9	s^2d^7, s^1d^8, s^0d^9
10	s^2d^8, s^1d^9, s^0d^{10}
11	s^1d^{10}
12	s^2d^{10}

It is to be noticed that the *d* levels are unambiguously below the *s* level for the first time in the ground state, s^0d^9.

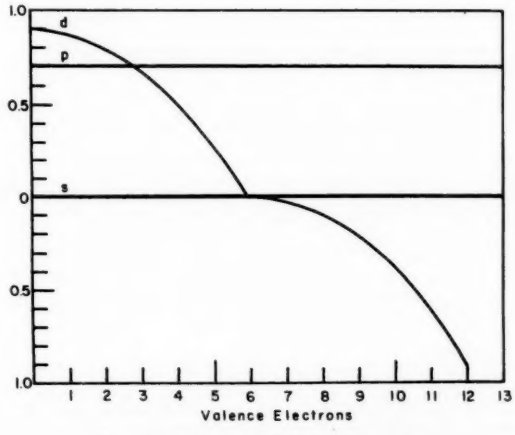

FIG. 7. Atomic orbital energy levels.

When the effects of filling the subshell are combined with the stabilizing property of single electrons in the subshell, a two-part curve as in Fig. 7 is forecast, which shows the change in the relative values of the energy levels as the number of valence electrons increases. When Fig. 7 was drawn, it was assumed that the d passes through the s level at six valence electrons (s^1d^5), and that d is just below p at three valence electrons (s^2d^1). As a simplification the two parts of the d curve were drawn to repeat each other.[4]

THE METALLIC BANDS

For an adequate description of the bands in a metal, in addition to the energy levels of the atomic orbitals and the orbital construction of the bands, it is necessary to know the binding energy and the density of states in the molecular orbitals that comprise the bands. Delocalized, localized, antibonding, and non-bonding bands are to be considered.

TABLE II

Electron populations in the bands of the transition elements

Element		Band populations							
		Bonding							Valence, net-bonding electrons
Valence electrons	Lattice system	s band	p band*	$d\epsilon$ band	$d\gamma$ or d_z band†	hybrid bands‡	Anti-bonding bands§	Non-bonding bands‖	
1	*bcc*	0.775	0.225						1.0
3	*bcc*	1.00	0.96	1.02			0.02		2.96
4	*bcc*	1.00	1.02	1.69	0.24		0.05		3.90
5	*bcc*	1.00	0.92	2.18	0.90				5.00
6	*bcc*	0.92	0.66	2.76	1.68				6.00
6	*hcp*	0.12				5.88			6.00
7	*hcp*		0.37		0.63	6.0			7.00
8	*hcp*		0.50		1.0	6.0	0.50		7.00
9	*ccp*	0.97	0.81	3.0	2.0		2.21		4.57
10	*ccp*	0.99	0.89	3.0			1.12	4.0	3.76
11	*ccp*	1.0	1.00	3.0			2.00	4.0	3.00
12	dis. *hcp*		0.33			1.67		10.0	2.00

*Threefold degeneracy in cubic lattices; twofold in *hcp*; onefold in distorted *hcp*.
†$d\gamma$ and d_z are next nearest neighbor bands in cubic and hexagonal systems respectively.
‡sd^5p for 6 electrons; d^5p for 7 and 8; sp^3 for 12.
§s' for 3 and 4 valence electrons; d_z' for 8; $d\epsilon'$ and $d\gamma'$ for 9 (see Fig. 9).
‖$d\gamma$ for 10 and 11 valence electrons; d^{10} for 12.

1. *The Delocalized Bands*

Bands in which electrons are delocalized over all atoms have been constructed from s, p, and d orbitals and, with a more limited delocalization, from sp^2 orbitals. These delocalized bands are specific cases satisfying the principal conditions for the classic Bloch molecular orbitals (1). The width of the bands, which is the separation between the lowest and the highest state in the band, and the level of the lowest lying state are to be obtained.

[4]*It is to be noted that Fig. 7 has been drawn independently of the principal quantum number. The assumption that the relative levels of the ns, np, and (n−1)d atomic orbitals are independent of n is certainly not correct. Figure 7 therefore becomes an average curve that need not be precisely correct for any element. The electron population values in Table II depend on Fig. 7 and therefore contain a substantial probable error. They are given to three significant figures, however, as this helps to keep the adding neat.*

It is convenient, though not entirely correct (see later for a rule of thumb), to assume that the density of states is uniform in delocalized bands made up of overlaps from among nearest neighbors. The phenomena of width in the band arises from the delocalization property. As the wave function for each electron extends over all nuclei incorporated in the delocalized wave function, and as no two electrons can be identical, successive electrons must lie in states that are distinguishable in the energy parameter. Consequently the density of states has a relation to the effectiveness of the delocalization property. In the multiple overlaps encountered in the prescribed orbital constructions, delocalization is measured by both the number of overlaps an orbital has, and by the magnitude of the overlap volume. The bands made up from orbitals in close-packed arrangements can be expected to be somewhat similar in both these regards. For the d orbitals it may be recalled that delocalized bands were found among both nearest neighbors (*bcc* $d\epsilon$ and *ccp* $d\epsilon$) and next nearest neighbors (*bcc* $d\gamma$ and *ccp* $d\gamma$). In these cases of nearest and next nearest neighbor bands, both the density of states and the binding energy must vary, with internuclear distance as the most direct parameter.

In detailed calculations (2) for the alkali metals it has been shown that both s and p states are populated in Li and Na. As there is only one valence electron in these metals it is necessary to conclude that upper states in the s band lie above lower states in the p band. Using the assumption of uniform density of states and remembering the threefold degeneracy of the *bcc* p band, an electron population chart as in Fig. 8 can at once be drawn. The separation between the s and p band heads, which is the only independent adjustment, has been arbitrarily chosen so that the s and p band populations become 0.775 and 0.225 electrons respectively.[5] Counting the degeneracy, this amounts to 0.775 and 0.075 electrons per orbital for the s and p orbitals respectively. This arbitrary decision is not unimportant. For it, along with the assumption of uniform density of states, at once defines the energy separation between s and p atomic orbitals in units of the width of a nearest neighbor delocalized band. This can be seen by comparing the ordinates of Figs. 7 and 8. Specific population figures did not appear in the calculations for the alkali metals referred to above. Pauling (9) has used the value 0.1 for the p orbital population in Li. A somewhat larger value was chosen here in the expectation that the energy separation between the atomic orbitals decreases as the principal quantum number increases. Such a trend would require a more important p orbital participation in the heavier alkali metals than in Li.

2. The Localized Bands

Band systems that retain more than a threefold degeneracy in the d orbitals set up an hexagonal close-packed lattice. In this lattice, both the d^4sp and d^5p hybrid configurations gave rise to orbital-pair overlaps between nearest neighbors, with the result that the bonding electrons became localized on pairs of nuclei. As in the ordinary convention for electron-pair covalent bonds, these spatially independent states are here assumed to be without appreciable effect on each other. That is, all such states exist at the same energy level. For purposes of definiteness, the discrete energy levels of the d^5p and of the sd^4p bands have been taken from the weighted average of the energy levels of the band heads of the delocalized s, p, and d bands. The decision, in so far as its correctness is concerned, could affect electron population calculations only in the case of one modification of the six-electron atom, Table II.

It should perhaps be mentioned that in another hybrid construction, that of the sp^2

[5] *See footnote 4.*

configuration in a distorted hexagonal close-packed lattice, a localization property also appears when the electron population is equal to or in excess of 0.66 electrons per orbital. Then bonding electron pairs can be associated with nuclear triads. The electron population was less than 0.66 per orbital in the 12 (or 2) valence electron atoms considered here.

3. The Antibonding and the Non-bonding Bands

The antibonding bands are identified with the corresponding bonding bands through the assumption of uniform density of states, and through the requirement that the binding energies of the bonding and antibonding states be equal and opposite. For electron population purposes, the bonding and antibonding bands then become a single

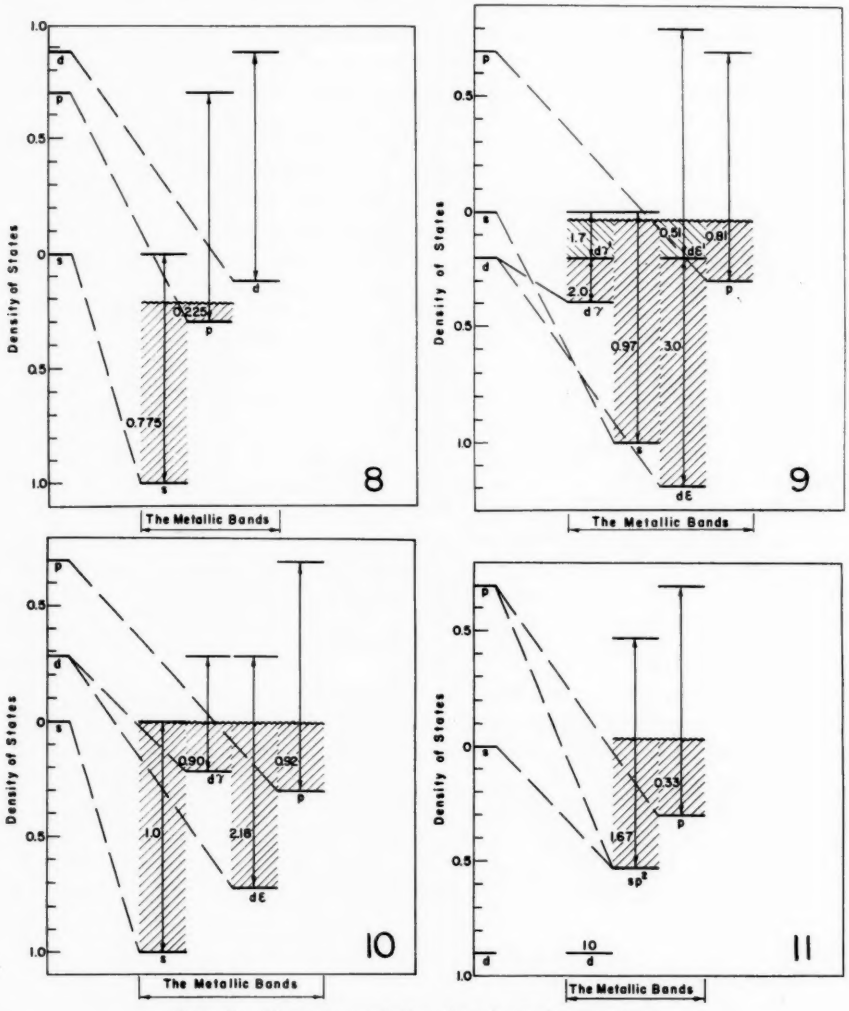

FIG. 8. Electron population chart for 1-electron atoms.
FIG. 9. Electron population chart for 9-electron atoms.
FIG. 10. Electron population chart for 5-electron atoms.
FIG. 11. Electron population chart for 12-electron atoms.

system of uniformly separated states, divided into equivalent bonding and antibonding portions by the energy level of the (non-bonding) atomic orbital. This can be seen in the electron population chart, Fig. 9, where bonding ($d\epsilon$, $d\gamma$) and antibonding ($d\epsilon'$, $d\gamma'$) bands are shown.

The symmetrical disposition of the bonding and antibonding states about the level of the non-bonding atomic orbital includes two variations that have a general significance. One points up the distinction to be made between nearest and next nearest neighbor bands; the other corresponds with a transition from localized to delocalized bands. Either the binding energy can decrease, which tends to compress the bonding and antibonding bands into a narrower region about the non-bonding level; or, if a decrease in delocalization occurs, both bonding and antibonding bands are compressed away from the non-bonding level towards their own lower and upper states, respectively. In each of these cases, the density of states is altered, though in the same way in both bonding and antibonding bands.

The next nearest neighbor bands, *bcc* $d\gamma$, *ccp* $d\gamma$, and *hcp* d_z, with internuclear distances of 1.15, 1.41, and 1.62 respectively, provide an example in which binding energies progressively decrease, compared to nearest neighbor bands like *bcc* $d\epsilon$ and *ccp* $d\epsilon$ where the internuclear distance is unity. In view of the proximity (overlap) there is a decrease in the resonance integral. The density of states must therefore necessarily increase as the internuclear distance increases conceivably until, when the internuclear distance is large enough, the atomic orbital is non-bonding and single states are achieved. By associating the levels of the band heads with the internuclear distance,[6] the density of states in *bcc* $d\gamma$ becomes twice, in *ccp* $d\gamma$ 5, and in *hcp* d_z 10 times that in nearest neighbor bands. As *bcc* $d\gamma'$ attains no antibonding population, for the lattice becomes unstable before antibonding electrons appear, the decision affects antibonding electron populations only in the eight and nine valence electron elements. The first antibonding electrons are absorbed by *hcp* d_z' and *ccp* $d\gamma'$. Once these bands are filled, creating in conjunction with *hcp* d_z or *ccp* $d\gamma$ the equivalent of one or two filled non-bonding d orbitals respectively, the question of the density of states in bands with different binding energies no longer affects the population figures.

A change in the delocalization factor may also occur more gradually than is implied in the assumption of the two extremes of delocalized and localized bonds. This is already indicated in the appearance of orbital constructions in which single orbitals overlap varying numbers of others (as for example eight in *bcc* $d\epsilon$, six in the distorted *hcp* p band, and four in *ccp* $d\epsilon$, compared with one in a localized bond) while still retaining the delocalized property. If delocalization were subject to such a continuous diminishment, its effect on the electron population figures would be real, though small, and found mostly in the 8-, 9-, and 10-electron atoms. If, for example, *ccp* $d\epsilon$ and *ccp* $d\epsilon'$ (because of the four co-ordination in their orbital constructions) were to some extent compressed away from the non-bonding level while *bcc* $d\epsilon$ and *bcc* $d\epsilon'$ (with eight co-ordination) were not, minor changes in the population of the antibonding *ccp* $d\epsilon'$ would result. The largest effect occurs when the *ccp* $d\epsilon'$ band is just beginning to be occupied, as in atoms with nine valence electrons, the correction tending to eliminate itself as more electrons are added.

The antibonding levels associated with the localized bonding orbitals achieve no significant population. It is therefore not necessary to specify them closely at this time.

THE FOUR LATTICES

The methods that have been outlined assume to predict both the lattice a transition

[6] *Approximately inversely proportional to the third power of the internuclear distance.*

element elects, and the electron population of the bands in that lattice. The predicted and the known lattices can be compared at once. Experimental values for electron populations are, however, not available, so the validity of the calculated populations cannot be properly assessed. In what follows a few words will be said about each metallic lattice.

1. The Body-centered Cubic Lattice

The band system for the body-centered cubic lattice consists of an *s* band, a *p* band (Fig. 1), and two *d* bands. The *bcc* $d\epsilon$ band has threefold degeneracy, and begins at a lower level than the *bcc* $d\gamma$ band which is a next nearest neighbor band, with twofold degeneracy.

In atoms with one valence electron, the electron population is confined to the *s* and *p* bands, Fig. 8. With an increase in the number of valence electrons, not only must more electrons be placed, but the energy level of the *d* orbitals falls relative to the *s* and *p* as shown in Fig. 7. In atoms with five valence electrons, the *d* orbitals may be fairly said to dominate the structure, holding 3.08 of the five electrons, Table II and Fig. 10. The important changes that occur in the band system as the valence electron count increases from three to six are the disappearance of a small antibonding population, a regular increase in the $d\epsilon$ population, and a relatively more rapid increase of the electron density in the $d\gamma$ band. These features combine to give the lattice its limited stability range.

It is evident that in any band system the upper levels make a smaller contribution to the binding energy than do the lower states. Moreover, in systems in which the band pattern changes because of changes in the symmetry of the orbital constructions, it follows that maximum binding energy and consequently a stable lattice corresponds with those constructions that provide a maximum population in the low-lying states. It is suggested as a rule of thumb for these multiple overlap systems that a stable lattice corresponds with an electron density of $2/m$ in the bonding orbitals. Here m is the number of lobes (not orbitals) in mutual overlap.

The rule of thumb may have some validity as a delocalization factor, though it is not in this sense that it will be applied. It is taken as a generalization of the delocalization observed in lone pairs and covalent bonds where m, the number of lobes that overlap, is 1 and 2 respectively, the electron density is 2 and 1 as is in each case required by the rule of thumb. In application to the multiple overlap systems, with m equal to 5 in the *p* band, 3 in the *bcc* $d\epsilon$ band, and 2 in the *ccp* $d\epsilon$ band, the rule of thumb electron densities become 0.4, 0.66, and 1.0 respectively. In so far as it has significance as a delocalization factor, the rule of thumb implies that the density of states in the respective bands differs in such a way as to make their lattice constructions stable, compared to alternate arrangements, at the prescribed electron density. If this is the case, the rule of thumb describes a limitation to the assumption of uniform density of states in the delocalized bands. It will actually be used, however, in a rather more rough and ready sense than this in what follows. In any event it should be noted that the rule of thumb does not apply, as an indicator of lattice stability, to the *s* orbitals, for this band does not determine structure.

Both the *bcc* $d\epsilon$ and the *ccp* $d\epsilon$ orbital constructions can be applied to atoms with three, four, five, or six valence electrons. The differences in the electron population charts for the two lattice systems, at any rate under the present assumptions, are entirely due to the difference, not in *bcc* $d\epsilon$ and *ccp* $d\epsilon$, but in *bcc* $d\gamma$ and *ccp* $d\gamma$. As *bcc* $d\gamma$ (at 1.15 the internuclear distance) provides more binding energy than *ccp* $d\gamma$ (at 1.41 the internuclear distance) the *bcc* $d\gamma$ band begins at a lower level. The effect of this is to increase the total number of *d* electrons lying at low and intermediate levels in the *bcc* bands, as compared with *ccp*, where the uppermost energy levels would have to be occupied as well. The concentration of electrons in the stabler states occurs whenever the *bcc* $d\gamma$

band shows a population, which is in the four-, five-, and six-valence electron atoms, Table II. Consequently, the *bcc* lattice can be chosen over the *ccp* lattice unambiguously only for the four-, five-, and six-electron atoms. The over-all result is that the *bcc* $d\gamma$ band keeps the electron density of the *bcc* $d\epsilon$ band in the vicinity of 0.66, which is the rule of thumb density for *bcc d* (0.34, 0.56, 0.73, and 0.92 are the calculated values for the three-, four-, five-, and six-electron atoms respectively). The electron density in the *p* band is also close to the 'best' value, 0.4, except in the six-electron atom (0.32, 0.34, 0.31, and 0.22 in the three-, four-, five-, and six-electron atoms respectively).

There is no $d\gamma$ population in the three-electron atom. It is therefore not possible to make a choice between the *bcc* and *ccp* lattices for this element on the proffered grounds. Moreover, the antibonding population appearing when *bcc* is elected (Table II) and the relatively small *d* population, together indicate that the band system for the three-electron atom is apt to be different in detail from those of the other transitional elements. However, a close-packed metal can evidently be obtained.

A *d* band population of 4.54 electrons is calculated for the *bcc* system for the six-electron atom. Of this, 1.68 electrons are in the relatively weakly binding $d\gamma$ band. The result is that at this stage a concentration of electrons is beginning to build up in the less stable upper levels of the *d* band. This is to be expected as the principal *d* band has only threefold degeneracy, and at least four *d* electrons are available for bond formation. Instability features are also shown in the deviation of the *p* and *d* electron densities from the rule of thumb values. However, when the alternate band system for the six-electron atom, which employs a hexagonal close-packed lattice, is charted, an instability feature also appears in it. The d^5p band, a system of localized electrons, is incompletely occupied, Table II. It is therefore necessary to predict that an atom with six valence electrons will show two forms, one with a *bcc*, the other with an *hcp* lattice. The predictions therefore are that transition elements with four, five, and six valence electrons have a *bcc* lattice, as is in fact the case for βTi, βZr, V, Cb, Ta, αCr, Mo, and αW.

2. The Hexagonal Close-packed Lattice

The hexagonal close-packed lattice emerges as a consistent choice for elements with six, seven, or eight valence electrons, although the band systems that establish the lattice are subject to minor variations within this group. With both sd^4p and d^5p providing trigonal hybrids, either configuration will establish an *hcp* lattice. The difference between the two will therefore be small depending for the most part on whether an *s* band (with d^5p) or a d_z band (with sd^4p) is to be found in the lattice. The *p* band is doubly degenerate in either case, though a third alternative, that of a delocalized sp^2 band (in connection with d^5p), is also possible. These three alternatives correspond to rather slight changes in the over-all electron population picture, being confined to minor variations in the electron density and direction dependence property of the conductivity bands. In no case is the lattice affected, at any rate with respect to its classification as *hcp*. The electron population calculations, Table II, were made for d^5p in the case of the six-electron atoms, and for sd^4p for the seven- and eight-electron atoms.

In addition to the appearance of localized bonds, an important antibonding population also appears for the first time in this group of elements. The precise value of this population depends on the level selected for the d_z band which, like *bcc* $d\gamma$ and *ccp* $d\gamma$, is a next nearest neighbor band. The distance in d_z is 1.6 the nearest neighbor distance, so that the band would be expected to be less effective than either of the $d\gamma'$. The antibonding population is confined to the *d* orbitals and, under the assumptions used, is not quite equivalent to having an electron pair in a non-bonding d_{z^2} orbital in the eight-electron atom. In the latter case, the net-bonding electrons would be lowered from 7.0 to

6.0. The prediction of an *hcp* lattice for the six-, seven-, and eight-electron atoms is borne out in the elements Mo, Tc, Re, Ru, and Os. Manganese and iron are exceptions and will be referred to again.

3. The Cubic Close-packed Lattice

Atoms with 9, 10, and 11 valence electrons satisfy the conditions for the *ccp* band system, Fig. 9. The transformation to the *ccp* lattice occurs when an extra electron is added to the *hcp* system. The ninth electron, going into the antibonding *d* levels of the *hcp* system would produce the near equivalent of two filled non-bonding *d* orbitals in that system. As a result, neither d^5p nor sd^4p can be constructed, and the *hcp* lattice is destroyed. At 9 electrons in the *ccp* system the $d\gamma$ band is nearly non-bonding, and becomes so at 10 electrons. The *ccp* $d\epsilon$ remains, and with an electron density of one electron per orbital provides the *d* orbital contribution to the binding energy and determines the structure.

The antibonding levels that are occupied as electrons are added to the *ccp* system are altogether in the *d* orbitals, with the increase for the most part to be found in the triply degenerate *ccp* $d\epsilon'$ band. That is to say, the bonding *s* and *p* and the antibonding *d* levels have approximately the same energy throughout this triad. The over-all result, going from 9 to 11 electrons in the *ccp* system, is to steadily diminish the net contribution of the *d* orbitals to the binding energy and the lattice. At 12 electrons the *d* orbitals have become altogether non-bonding, with 3 electrons in $d\epsilon'$ balancing 3 electrons in $d\epsilon$. Counting the non-bonding $d\gamma$, the non-bonding $d\epsilon$ now restore a fivefold degeneracy to the *d* orbitals. That is to say, at 12 electrons, the *d* subshell has become a part of the inner core. The prediction of a cubic close-packed lattice for 9-, 10-, and 11-electron atoms is observed without exception in these elements, namely Co, Rh, Ir, Ni, Pd, Pt, Cu, Ag, Au. The fact that αCo is *hcp* will be mentioned again.

4. The Distorted Hexagonal Close-packed Lattice

As described above, the 12-electron atom (speaking in valence terms) becomes a 2-electron atom, as the *d* levels are fully occupied and non-bonding. The band system projected for the 12-electron atom, Fig. 11, is therefore in principle also applicable to the 2-electron elements, Be and Mg. The only differences to be expected are those that can be associated with the principal quantum number. This band system is, however, incompatible with the two-electron elements, Ca, Ba, and Sr. These elements have vacant *d* levels, which by taking electrons away from the sp^2, *p* bands, permit quite different electron distributions and orbital constructions. It is therefore correct to predict a distorted hexagonal close-packed lattice for Be, Mg, Zn, and Cd, as is observed. It is also correct to predict that Ca, Ba, and Sr will not have the same distorted *hcp* lattice. (Ca, Sr, and Ba have cubic lattices.)

DISCUSSION

When the antibonding population is subtracted from the bonding population a figure giving the net number of bonding electrons is obtained, Table II. As this number sums up only the electron populations of the several bands, and as the properties and electron dependencies of the bands differ, the number of net-bonding electrons by no means shows all the significances of the band systems. For example, if the property of plasticity were to be judged from changes in overlap accompanying nuclear displacements that do not alter internuclear distances, the *s* band would be plastic, the *d* bands hard. Moreover, as the character of the overlaps are different in the different *d* bands, the band populations do not always correctly evaluate the relative magnitude of even so specific

a property. As another example, the p band has consistently the lowest ionization potential and the lowest electron density (about 0.33 electrons per orbital) and may for these reasons be principally responsible for the properties of conductivity and paramagnetism in these metals. Nevertheless, other delocalized bands may on occasion also make important contributions to these two properties, as for example the d bands in the five-electron atoms.

In a more general way as well numbers for net-bonding electrons have less significance than the itemized list of their parts. This arises from the condition that in band systems electrons occupy successive levels and do not therefore all make the same contribution to the binding energy. This is possibly of most importance when the antibonding levels are just beginning to be occupied (the seven-, eight-, and nine-electron atoms). As the lowest levels of both bonding and antibonding bands are filled first, the net contribution to the binding energy of a bonding and antibonding band exactly cancel only when both bands are fully occupied. When the antibonding band is not completely full, it still cancels out a numerically equivalent population. To be correct from the binding energy point of view, however, the upper more weakly binding states in the bonding band are the ones to be selected. That is, the stablest states remain and give a binding energy contribution that is underemphasized in a number that by implication describes average electrons.

Whatever their deficiencies, it is nevertheless these numbers for net-bonding electrons that have the simplest correspondence with the concept of a numerical valence. They are therefore to be compared with the metallic valences proposed by Pauling (3) for the transition elements.

Valence electrons	1	2	3	4	5	6	7	8	9	10	11	12
Pauling's valence	1	2	3	4	5	6	6	6	6	6	5.5	4.5
Net-bonding electrons	1	2	3	3.9	5	6	7	7	4.6	3.8	3.0	2.0
Integral valence	1	2	3	4	5	6	7	6	5	4	3	2

It is evident that agreement is good until elements with an important antibonding population are encountered. In atoms with seven and eight valence electrons, the very weakly binding d_z band is being occupied. As it holds 0.6 and 1.0 binding electrons in the two elements respectively, the number 7 rather overestimates the effective situation. Also, in the atoms with 9 and 10 valence electrons, rather more than a justifiable weight is given to the antibonding population in $ccp\ d\epsilon'$, as has been mentioned. This cannot have a greater effect than to provide values for an 'average' valence of 5.0 and 4.0 for these elements respectively. In brief, that is, the concept of an integral valence can in fact be justified as a reasonable approximation to the net-bonding electron values, as shown above. Even with such adjustments to average values, a significant departure from the metallic valences proposed by Pauling for atoms with 9, 10, 11, and 12 valence electrons still remains. As additional support for the net-bonding electron values presented in this paper, their correspondence with conventional chemical valences for these elements may be pointed out. Moreover, the physical and chemical relationships that are evident in the series of elements, Be, Mg, Zn, and Cd strongly suggest divalent atoms throughout.

Lattice structures and band populations are the predictions made in this paper. Factual comparisons are possible for the lattices, but band populations have not yet been measured. Even in the comparison that is possible some ambiguity remains. For it is conceivable that a specific lattice and particularly a close-packed one can be set up from more than one set of orbital constructions, as was indicated in the case of the hexagonal

close-packed lattice. Agreement with respect to the lattice does not, therefore, necessarily prove the correctness of the orbital constructions. The corollary is also ambiguous. If a lattice is incorrectly predicted for one member of a family, it does not necessarily follow that the orbital constructions are wrong for the other members, though they must of course be wrong in the specific case.

Of the 30 transition elements, the lattices of Mn and Fe (and Hg) were incorrectly forecast. This deviation from expectations corresponds with the appearance of the property of ferromagnetism in the transition elements and may therefore have a somewhat special significance. The assumption, implied by the application of the population figures to all elements in a subgroup, that the relative levels of the ns, np, and $(n-1)d$ atomic orbitals are independent of n is certainly not altogether correct. A general expectation is that the separations become smaller as n becomes larger. Secondly, the overlaps in the n type and $(n-1)$ type bands are apt to have different magnitudes, even among near neighbors. This has a direct bearing on the binding energies and also on the density of states if the bands are delocalized. It is known that the ratio of the radii of the $(n-1)$ to the n shell has its smallest values in the first transitional period, and in that period the minimum occurs at Fe. Taken together, these two factors, the decreasing separation between the atomic orbital energy levels and the increasing relative radius of the $(n-1)d$-orbitals as n increases, imply that the $(n-1)d$ orbitals become consistently more important to the binding energy with larger values of the principal quantum number. This accounts for the singular observation that the melting and boiling points of transition metals (with 4 to 10 valence electrons) invariably increase, while the melting and boiling points of non-transitional metals invariably decrease, with increases in n (atoms with 3 and 11 valence electrons are intermediate in this respect: Zn, Cd, and Hg fall into the non-transitional group with Be and Mg).

As it happens, the impact of what might be called these n-type variations have their maximum effect precisely at the elements Mn, Fe, and Co. Moreover, as the antibonding d bands are here just beginning to be occupied, the disposition of bonding and antibonding electrons will, at the same time, be most responsive to these changes. That is, both the cause and the response to the cause are maximal at Mn, Fe, and Co, among the transition elements. The problem becomes therefore to relocate the orbitals in these elements as specific cases (Fe has four lattices; Mn, three; and Co, two) and discover thereby, in the particular instances of αFe and αCo, the location and properties of the ferromagnetic orbitals, presumably resident in the $(n-1)d$ band.

ACKNOWLEDGMENTS

The author would like to thank the Department of Mines and the University of Toronto for their accommodations during a Sabbatical Year. Special thanks are due Professor Maurice Lister, who was kind enough to read the manuscript in draft form.

REFERENCES

1. Bloch, P. Z. Physik. **52**, 555 (1928).
2. Brooks, H. Theory of alloy phases. Am. Soc. Metals, Cleveland. 1956. pp. 199–220.
3. Pauling, L. Theory of alloy phases. Am. Soc. Metals, Cleveland. 1956. pp. 220–242.
4. Griffith, J. S. and Orgel, L. E. Quart. Revs. **10**, 381 (1957).
5. Jaffe, H. H. J. Phys. Chem. **58**, 185 (1954).
6. Craig, D. P., Maccoll, A., Nyholm, R. S., Orgel, L. E., and Sutton, L. E. J. Chem. Soc. 332 (1954).
7. Craig, D. P., Maccoll, A., Nyholm, R. S., Orgel, L. E., and Sutton, L. E. J. Chem. Soc. 354 (1954).
8. Kimball, G. E. J. Chem. Phys. **8**, 188 (1940).
9. Pauling, L. Proc. Roy. Soc. A, **196**, 343 (1949).

THE KINETICS OF THE EVOLUTION AND DISSOLUTION OF HYDROGEN AT ELECTRODES[1]

J. O'M. Bockris and H. Mauser

INTRODUCTION

The kinetics of the electrolytic evolution of hydrogen at electrodes have been treated previously only in an approximate way (Frumkin (1) and Bockris and Potter (2)); or upon the assumption that only one step influences the reaction rate (Parsons (3)); or without regard to H coverage (Vetter (4)). In the work reported here, a rigorous treatment of the kinetics of two probable paths for cathodic and anodic reactions of hydrogen at electrodes is developed, with attention to the evaluation of quantities which are open to experimentation and have values specific to certain reaction mechanisms.

GENERAL

The concept of a rate-determining step for a given path in electrode kinetics is regarded as follows. General equations are deduced for the velocity of the given reaction by way of a chosen path, and the current density at the electrode for a given overpotential can thence be expressed as a function of a number of electrochemical rate constants characteristic of steps within the path. Relations among these rate constants are then found which lead to a current density which depends, at constant overpotential, only upon *one* rate constant, k_p. The relations among the rate constants which give rise to this special case are then regarded as the condition for the over-all reaction to have a rate-determining step, p.

The conditions to provide a given rate-determining step can be deduced in terms of chemical (potential-independent) rate constants, or two types of electrochemical (potential-dependent) rate constants.

Thus,

$$\bar{k}_p = k_p \, e^{\pm \beta \Delta\phi \, zF/RT} \qquad [1]$$

where $\bar{k}_p$ is the electrochemical rate constant for a reaction involving the transfer of a charge z at a current density (c.d.) of i, $0 < \beta < 1$, $\Delta\phi$ is the Galvani p.d. between metal and solution; and k_p is the corresponding chemical rate constant. The reversible electrochemical rate constant is then

$$\bar{k}_{p,R} = k_p \, e^{\pm \beta \Delta\phi_R \, zF/RT} \qquad [2]$$

i.e., it is the value of $\bar{k}_p$ at the reversible potential.

Then,

$$\bar{k}_p = \bar{k}_{p,R} \, e^{\pm \beta \eta \, zF/RT} \qquad [3]$$

where η is the overpotential associated with the c.d., i.

A. Reaction Paths Considered

Likely paths for the hydrogen evolution reaction have been discussed (Bockris (5) and Breiter (6)). Here, the kinetics of only the two most probable paths will be considered; they differ only by the reaction in which hydrogen is desorbed.

[1]*Manuscript received September 6, 1958.*
Contribution from the John Harrison Laboratory of Chemistry, University of Pennsylvania, Philadelphia, Pennsylvania, U.S.A. This paper was prepared for presentation at the Symposium on Charge Transfer Processes held at the University of Toronto, Toronto, Ontario, September 4 and 5, 1958 (see Can. J. Chem. **37**, *120 (1959)).*

(*i*) *The Electrochemical Desorption Path* (*Kobosew and Nekrassow, 1930*)

Protons are discharged onto free sites* on the metal surface. The resulting chemisorbed hydrogen is desorbed to form a hydrogen molecule upon discharge onto it of a further proton. Conversely, hydrogen molecules adsorb on the electrode surface to form one adsorbed hydrogen atom and a proton in solution, the latter also being formed by the dissolution of chemisorbed hydrogen atoms.

(*ii*) *The Hydrogen Atom Combination Desorption Path* (*Tafel, 1903*)

Protons are discharged onto free sites. The resulting chemisorbed hydrogen atoms combine to form molecules. In dissolution, hydrogen molecules adsorb dissociatively on free sites on the electrode surface, each molecule forming two chemisorbed atoms. These dissolve, forming protons in solution.

The common step in both paths of the evolution reaction is the discharge of protons (Smits (7), Bowden and Rideal (8), Baars (9), and Erdey-Grúz and Volmer (10)). Proton discharge may occur either from hydroxonium ions or from water, the latter source of protons being probable only in alkaline solutions (Parsons and Bockris (11) and Poltorak (12)).

Each of the above-mentioned steps may become the rate-controlling step in either hydrogen evolution or dissolution. Because of the dependence of electrochemical rate constants upon potential, the rate-determining step may change with current density for a given electrode–solution system.

The following assumptions are made. (i) The systems considered have reached a stationary state. (ii) The symmetry factors (cf. Bockris (13)) involved in various charge-transfer partial reactions have the same value. (iii) H is chemisorbed on the electrode surface (and does not dissolve into the metal at an appreciable rate). (iv) There is no lack of supply of ions in solution to the electrode.

B. The Electrochemical Desorption Path

(*i*) *General Equations*

The reactions are

$$[4] \qquad H^+ + e_0^- \underset{-1}{\overset{1}{\rightleftharpoons}} MH$$

$$[5] \qquad H^+ + MH + e_0^- \underset{-2}{\overset{2}{\rightleftharpoons}} H_2$$

where MH represents hydrogen atoms, chemisorbed on the metal surface.

Assuming a Langmuir isotherm,†

$$[6] \qquad v_1 = k_1(1-k'c_H)c_{H^+}\, e^{-\beta\Delta\phi\, F/RT}$$

$$[7] \qquad v_{-1} = k_{-1}c_H\, e^{(1-\beta)\Delta\phi\, F/RT}$$

$$[8] \qquad v_2 = k_2c_Hc_{H^+}\, e^{-\beta\Delta\phi\, F/RT}$$

$$[9] \qquad v_{-2} = k_{-2}p_{H_2}(1-k'c_H)\, e^{(1-\beta)\Delta\phi\, F/RT}$$

where k' is a constant, such that $k'c_H$ is the fraction of surface covered with chemisorbed

**Free sites means here those not already occupied by hydrogen atoms.*

†If a logarithmic, and not a Langmuir, isotherm were used, a different general expression for the over-all current density would be obtained. However, the results at limitingly low, and limitingly high, degrees of surface coverage would be almost the same as those obtained here; and it is these limiting conditions which are most commonly needed in the use of relations between current density and, e.g., potential, as criteria of mechanisms.

H at a given c.d., c_{H^+} is the hydroxonium ion concentration in the Helmholtz double layer; and other terms are as already defined.

In the steady state, the over-all velocity, v, is given by

$$v = v_1 - v_{-1} = v_2 - v_{-2}. \tag{10}$$

Eliminating c_H and remembering that the current density is related to v by

$$i = 2F\,v/\nu \tag{11}$$

where ν is the stoichiometric number,

$$i = \frac{2F}{\nu}\,\frac{\bar{k}_{1,R}\bar{k}_{2,R}c^2_{H^+}\,e^{-2\beta\eta\,F/RT} - \bar{k}_{-1,R}k_{-2,R}p_{H_2}\,e^{2(1-\beta)\eta\,F/RT}}{c_{H^+}(\bar{k}_{2,R}+\bar{k}_{1,R}k')\,e^{-\beta\eta\,F/RT} + (\bar{k}_{-1,R}+\bar{k}_{-2,R}k'p_{H_2})\,e^{(1-\beta)\eta\,F/RT}}. \tag{12}$$

Equation [12] shows that i is positive ("cathodic") if $\eta < 0$, negative ("anodic") if $\eta > 0$.

If $i = 0$, $\eta = 0$; then [11] yields

$$e^{\Delta\phi_R\,F/RT} = \sqrt{K_1K_2(c^2_{H^+}/p_{H_2})} \tag{13}$$

where $K_1 = k_1/k_{-1}$ and $K_2 = k_2/k_{-2}$. Equation [13] is a form of the Nernst equation, i.e., confirms [12].

(ii) Cathodic Tafel Region

By the "Tafel region" is meant that region of the current density – potential relation for which $i = Ae^{B\eta}$ where A and B are constants. From [12] and for a net cathodic current density, two limiting cases give Tafel relations, i.e., if

$$(\bar{k}_{2,R}+\bar{k}_{1,R}k')c_{H^+}\,e^{-\beta\eta\,F/RT} \gg (\bar{k}_{-1,R}+\bar{k}_{-2,R}k'p_{H_2})\,e^{(1-\beta)\eta\,F/RT} \tag{14}$$

then,

$$i = 2F\,\frac{\bar{k}_{1,R}\bar{k}_{2,R}c_{H^+}}{\bar{k}_{2,R}+\bar{k}_{1,R}k'}\,e^{-\beta\eta\,F/RT}. \tag{15}$$

But if

$$(\bar{k}_{-1,R}+\bar{k}_{-2,R}k'p_{H_2})\,e^{(1-\beta)\eta\,F/RT} \gg (\bar{k}_{2,R}+\bar{k}_{1,R}k')c_{H^+}\,e^{-\beta\eta\,F/RT} \tag{16}$$

then,

$$i = 2F\,\frac{\bar{k}_{1,R}\bar{k}_{2,R}c^2_{H^+}}{\bar{k}_{-1,R}+\bar{k}_{-2,R}k'p_{H_2}}\,e^{-(1+\beta)\eta\,F/RT}. \tag{17}$$

By virtue of its form, [16] cannot be applicable at large negative overpotentials, when it must go over into [14]. Remembering that the cathodic Tafel region occurs only for $\beta\eta\,F/RT > 1$, the necessary relation among the rate constants for the occurrence of [17] is

$$(\bar{k}_{-1,R}+\bar{k}_{-2,R}k'p_{H_2}) > (\bar{k}_{2,R}+\bar{k}_{1,R}k')c_{H^+}\,e^2. \tag{18}$$

(iii) Anodic Tafel Region

From [12], with condition [14]:

$$i = -2F\,\frac{\bar{k}_{-1,R}\bar{k}_{-2,R}p_{H_2}}{(\bar{k}_{2,R}+\bar{k}_{1,R}k')c_{H^+}}\,e^{(2-\beta)\eta\,F/RT} \tag{19}$$

Or, with condition [16], [12] becomes:

$$i = -2F\,\frac{\bar{k}_{-1,R}\bar{k}_{-2,R}p_{H_2}}{\bar{k}_{-1,R}+\bar{k}_{-2,R}k'p_{H_2}}\,e^{(1-\beta)\eta\,F/RT}. \tag{20}$$

Equation [19], as a consequence of the form of [14], can be applicable only at lower positive values of the overpotential. The condition for it to occur at any potential in an anodic Tafel region,

$$[21] \qquad (\bar{k}_{2,R}+\bar{k}_{1,R}k')c_{H^+} > (\bar{k}_{-1,R}+\bar{k}_{-2,R}k'p_{H_2})\, e^2.$$

(iv) "Reversible" Region

By the "reversible region" is meant the range of overpotentials for which the expansion of $e^{\pm\alpha\eta\, F/RT}$ can be written as $1\pm\alpha\eta\, F/RT$ to an accuracy not less than that corresponding to the experimental measurement of η.

Applying this condition to [12]:

$$[22] \qquad i = -4F\,\frac{\bar{k}_{1,R}\bar{k}_{2,R}c^2_{H^+}\,\eta F/RT}{(\bar{k}_{2,R}+\bar{k}_{1,R}k')c_{H^+}+(\bar{k}_{-1,R}+\bar{k}_{-2,R}k'p_{H_2})}$$

and

$$[23] \qquad \bar{k}_{1,R}\bar{k}_{2,R}c^2_{H^+} = \bar{k}_{-1,R}\bar{k}_{-2,R}p_{H_2}.$$

(v) Coverage of Electrode with Adsorbed Atomic Hydrogen

The explicit expression for c_H follows from [10], utilizing [6]–[9], as

$$[24] \qquad c_H = \frac{\bar{k}_{1,R}c_{H^+}\, e^{-\beta\eta\, F/RT}+\bar{k}_{-2,R}p_{H_2}\, e^{(1-\beta)\eta\, F/RT}}{(\bar{k}_{1,R}k'+\bar{k}_{2,R})c_{H^+}\, e^{-\beta\eta\, F/RT}+(\bar{k}_{-1,R}+\bar{k}_{-2,R}k'p_{H_2})\, e^{(1-\beta)\eta\, F/RT}}.$$

Defining the degree of surface coverage at an overpotential η, θ_η, as

$$[25] \qquad \theta_\eta = k'c_H,$$

two limiting values for the Tafel regions follow from [24] and [25] as:

$$[26] \qquad (\theta_\eta)_c = \bar{k}_{1,R}k'/(\bar{k}_{1,R}k'+\bar{k}_2),$$

$$[27] \qquad (\theta_\eta)_a = \bar{k}_{-2,R}k'p_{H_2}/(\bar{k}_{-1,R}+\bar{k}_{-2,R}p_{H_2}k').$$

(vi) Influence of Concentration of Hydrogen Ions in Solution and Hydrogen Pressure in the Tafel Regions

The pH effects are known (Frumkin (15), Parsons (3), Bockris and Potter (5), and Bockris and Watson (14)).

The effect of hydrogen pressure on overpotential may be calculated in terms of the coefficient $\left(\frac{\partial\eta}{\partial \ln p_{H_2}}\right)_i$.

In the cathodic region, they follow from [15], for the condition [14]. Thence,

$$[28] \qquad \left(\frac{\partial\eta}{\partial \ln p_{H_2}}\right)_i = \frac{RT}{2F}.$$

If [16] applies, [17] gives:

$$[29] \qquad \left(\frac{\partial\eta}{\partial \ln p_{H_2}}\right)_i = \frac{RT}{2F}-\frac{RT}{(1+\beta)F}\left(\frac{k_{-2}k'p_{H_2}}{k_{-1}+k_{-2}k'p_{H_2}}\right).$$

In the anodic region, condition [14], resulting in [19], gives

$$[30] \qquad \left(\frac{\partial\eta}{\partial \ln p_{H_2}}\right)_i = -\frac{RT}{2F}\,\frac{\beta}{2-\beta}$$

whereas [16] and [20] give:

$$[31] \qquad \left(\frac{\partial\eta}{\partial \ln p_{H_2}}\right)_i = -\frac{RT}{(1-\beta)F}\left(\frac{1+\beta}{2}-\frac{k_{-2}k'p_{H_2}}{k_{-1}+k_{-2}p_{H_2}}\right).$$

(vii) Limiting Cases for the Electrochemical Path

The general equations for the electrochemical desorption path (cf. page 476) give rise to two general divisions, depending upon whether [14] or [16] is applicable. In the following tables, limiting values are given for the Tafel equation, degree of coverage with atomic hydrogen, and pressure coefficient of overpotential at constant current density, on the further assumption that the heights of the energy barriers in the successive reactions differ by an amount greater than about 3 kcal mole^{-1}.

C. The Atomic Hydrogen Desorption Mechanism

1. General Equations

The reactions are:

[32] $$H^+ + e_0^- \underset{-1}{\overset{1}{\rightleftharpoons}} MH,$$

[33] $$MH + MH \underset{-2}{\overset{2}{\rightleftharpoons}} H_2 + 2M.$$

Hence,

[6] $$v_1 = k_1(1-k'c_H)c_{H^+}\, e^{-\beta\Delta\phi\ F/RT}$$

[7] $$v_{-1} = k_{-1}c_H\, e^{(1-\beta)\Delta\phi\ F/RT}$$

[34] $$v_2 = k_2 c_H^2$$

[35] $$v_{-2} = k_{-2}(1-k'c_H)^2 p_{H_2}.$$

In the steady state:

[36] $$2(v_1-v_{-1}) = v_2-v_{-2} = v.$$

From [6], [7], [34], [35], and [36]

$$\frac{1}{4}\left(\frac{k_2}{k'^2}-k_{-2}p_{H_2}\right)\left(\frac{i}{2F}\right)^2-\left(\bar{k}^2_{1,R}c^2_{H^+}\, e^{-2\beta\eta\ F/RT}+\frac{\bar{k}_{1,R}k_2}{k'^2}c_{H^+}\, e^{-\beta\eta\ F/RT}\right.$$

$$+2\frac{\bar{k}_{1,R}\bar{k}_{-1,R}}{k'}c_{H^+}\, e^{(1-2\beta)\eta\ F/RT}$$

[37] $$\left.+k_{-2}p_{H_2}\frac{\bar{k}_{-1,R}}{k'}\, e^{(1-\beta)\eta\ F/RT}+\frac{\bar{k}^2_{-1,R}}{k'^2}\, e^{2(1-\beta)\eta\ F/RT}\right)\frac{i}{2F}$$

$$+\bar{k}^2_{1,R}\frac{k_2}{k'^2}c_{H^+}\, e^{-2\beta\eta\ F/RT}-\frac{\bar{k}^2_{1,R}}{k'^2}k_{-2}p_{H_2}\, e^{2(1-\beta)\eta\ F/RT}=0.$$

From [37], with the condition $i = 0$ ($\eta = 0$), the first two terms vanish, whence, with [1] and [2],

[38] $$e^{\Delta\phi_R\ F/RT} = K_1K_2^{\frac{1}{2}}(c_{H^+}/\sqrt{p_{H_2}})$$

where $K_1 = k_1/k_{-1}$, $K_2 = k_2/k_{-2}$, the equilibrium constants of the partial reaction [32] and [33].

Also, from [37], with $\eta = 0$,

[39] $$\bar{k}^2_{1,R}k_2c^2_{H^+} = \bar{k}^2_{-1,R}k_{-2}p_{H_2}.$$

2. General Solution for Current Density (Cathodic and Anodic Currents)

From [37]:

$$\frac{i}{2F}=\frac{2}{(k_2/k'^2)-k_{-2}p_{H_2}}\left\{\left(\bar{k}^2_{1,R}c_{H^+}\,e^{-2\beta\eta\,F/RT}+\frac{\bar{k}_{1,R}k_2}{k'^2}c_{H^+}\,e^{-\beta\eta\,F/RT}\right.\right.$$
$$\left.+2\,\frac{\bar{k}_{-1,R}\bar{k}_{1,R}}{k'}c_{H^+}\,e^{(1-2\beta)\eta\,F/RT}+\frac{\bar{k}_{-1,R}k_2}{k'}p_{H_2}\,e^{(1-\beta)\eta\,F/RT}+\frac{\bar{k}^2_{-1,R}}{k'^2}\,e^{2(1-\beta)\eta\,F/RT}\right)(+)$$
$$\left(\bar{k}^4_{1,R}c^4_{H^+}\,e^{-4\beta\,F/RT}+2\,\frac{\bar{k}^3_{1,R}k_2}{k'^2}\,c^3_{H^+}\,e^{-3\beta\eta\,F/RT}+\frac{\bar{k}^2_{1,R}k_2k_{-2}}{k'^2}\,c^2_{H^+}p_{H_2}\,e^{-2\beta\eta\,F/RT}\right.$$
$$+4\frac{\bar{k}^3_{1,R}\bar{k}_{-1,R}}{k'}\,c_{H^+}\,e^{(1-4\beta)\eta\,F/RT}$$
$$[40]\quad+2\,\frac{\bar{k}^2_{1,R}\bar{k}_{-1,R}}{k'}\,c^2_{H^+}\left(k_{-2}p_{H_2}+2\,\frac{k_2}{k'^2}\right)e^{(1-3\beta)\eta\,F/RT}+2\,\frac{\bar{k}_{1,R}\bar{k}_{-1,R}k_2k_{-2}}{k'^3}\,c_{H^+}p_{H_2}\,e^{(1-2\beta)\eta\,F/RT}$$
$$+6\,\frac{\bar{k}^2_{1,R}\bar{k}_{-1,R}}{k'^2}\,c^2_{H^+}\,e^{(2-4\beta)\eta\,F/RT}$$
$$+2\,\frac{\bar{k}^2_{-1,R}\bar{k}_{1,R}}{k'^2}\,c_{H^+}(k_2+k_{-2}p_{H_2})\,e^{(2-3\beta)\eta\,F/RT}+4\,\frac{k_{1,R}\bar{k}^3_{-1,R}}{k'^2}\,c_{H^+}\,e^{(3-4\beta)\eta\,F/RT}$$
$$+\frac{\bar{k}_{-1,R}k_2k_{-2}p_{H_2}}{k'^4}\,e^{2(1-\beta)\eta\,F/RT}$$
$$\left.+2\,\frac{\bar{k}^3_{-1,R}}{k'^2}\,k_{-2}p_{H_2}\,e^{3(1-\beta)\eta\,F/RT}+\frac{\bar{k}^4_{-1,R}}{k'^4}\,e^{4(1-\beta)\eta\,F/RT}\right)^{\frac{1}{2}}\Bigg\}.$$

In [40], the minus sign before the last bracket is taken; for, then, with $-\eta$, i is positive; and, if η is positive, i is negative, i.e., the signs of the i values change with the sign of η, in accordance with physical sense. If the plus sign is taken, i has the same sign, independently of the signs of η, i.e., the solution is unreal.

To obtain Tafel equations from [39], we rearrange the expression in such a way that a simple assumption regarding the predominance of one term over all others can result in expressions with only one potential dependent term.

3. Special Case of Equation [40] for $\bar{k}^4_{1,R}c^4_{H^+}\,e^{-4\beta\eta\,F/RT}$ Predominating in the Square Root Term (Cathodic and Anodic Case)

With this condition,

$$\frac{i}{2F}=\frac{2}{(k_2/k'^2)-k_{-2}p_{H_2}}\left\{\left(\bar{k}^2_{1,R}c^2_{H^+}\,e^{-2\beta\eta\,F/RT}+\frac{\bar{k}_{1,R}k_2}{k'^2}\,c_{H^+}\,e^{-\beta\eta\,F/RT}\right.\right.$$
$$\left.+2\,\frac{k_{-1,R}k_{1,R}}{k'}\,c_{H^+}\,e^{(1-2\beta)\eta\,F/RT}+\frac{\bar{k}_{-1,R}k_{-2}}{k'}\,p_{H_2}\,e^{(1-\beta)\eta\,F/RT}+\frac{\bar{k}^2_{-1}}{k'^2}\,e^{2(1-\beta)\eta\,F/RT}\right)$$
$$-\bar{k}^2_{1,R}c^2_{H^+}\,e^{-2\beta\eta\,F/RT}\left(1+\frac{2k_2}{k'^2\bar{k}_{1,R}c_{H^+}}\,e^{\beta\eta\,F/RT}+\frac{k_2}{k'^2}\,\frac{k_{-2}p_{H_2}}{\bar{k}^2_{1,R}c^2_{H^+}}\,e^{2\beta\eta\,F/RT}+4\,\frac{\bar{k}_{-1,R}}{k'\bar{k}_{1,R}c_{H^+}}\,e^{\eta\,F/RT}\right.$$
$$+\frac{2\bar{k}_{-1,R}(k_{-2}p_{H_2}+k_2/k'^2)}{k'\bar{k}_{1,R}c_{H^+}}\,e^{(1-\beta)\eta\,F/RT}+\frac{2\bar{k}_{-1,R}k_2k_{-2}p_{H_2}}{k'^3}\,e^{(1+2\beta)\eta\,F/RT}$$
$$[41]\qquad+6\,\frac{\bar{k}^2_{-1,R}}{k'^2\bar{k}^2_{1,R}c^2_{H^+}}\,e^{2\eta\,F/RT}$$
$$+\frac{2\bar{k}^2_{-1,R}(k_2/k'^2+2k_{-2}p_{H_2})}{k'^2\bar{k}^3_{1,R}c^3_{H^+}}\,e^{(2+\beta)\eta\,F/RT}+4\,\frac{\bar{k}^3_{-1,R}}{k'^3\bar{k}^3_{1,R}c^3_{H^+}}\,e^{3\eta\,F/RT}$$
$$\left.+\frac{\bar{k}^2_{-1,R}}{k'^4}\,\frac{k_2k_{-2}p_{H_2}}{\bar{k}^4_{1,R}c^4_{H^+}}\,e^{2(1+\beta)\eta\,F/RT}\right.$$

$$+\frac{2\bar{k}^3_{-1,R}}{k'^3}\frac{k_{-2}p_{H_2}}{\bar{k}^4_{1,R}c^4_{H^+}}e^{(3+\beta)\eta F/RT}+\frac{\bar{k}^4_{-1,R}}{\bar{k}^4_{1,R}}\frac{1}{k'^4c^4_{H^+}}e^{4\eta F/RT}\Bigg)^{\frac{1}{4}}\Bigg\}.$$

If the square root term of equation [41] is expanded, it is necessary to continue the expansion to the fourth term, otherwise the terms from the root term cancel with the terms before the square root. Utilizing the fact that all the terms in the square root after the first are $\ll 1$, then one obtains:

[42] $$\frac{k_2}{k'^2\bar{k}_{1,R}c_{H^+}} \ll e^{-\beta\eta F/RT}$$

[43] $$\frac{k_{-2}p_{H_2}}{\bar{k}_{1,R}c_{H^+}} \ll e^{-\beta\eta F/RT}$$

[44] $$\frac{\bar{k}_{-1,R}}{k'\bar{k}_{1,R}c_{H^+}} \ll e^{-\eta F/RT},$$

or, utilizing [39], [44] becomes:

$$k_2/k'^2\, k_{-2}\, p_{H2} \ll e^{-2\eta F/RT}.$$

These conditions, in [41], yield:

[45] $$i = 2F(k_2/k'^2)(1- e^{2\eta F/RT}).$$

Equation [45] expresses the net current under cathodic or anodic overpotential when the condition [42], [43], and [44] applies. Limiting conditions of this equation will be considered below.

4. Special Case of [40] for which $\bar{k}^2_{1,R}c^2_{H^+}(k_2k_{-2}/k'^2)p_{H_2}\, e^{-2\beta\eta F/RT}$ Predominates in the Square Root Term

Applying this condition to [40] one obtains:

[46] $$k'^2\bar{k}_{1,R}\, c_{H^+}/k_2 \ll e^{\beta\eta F/RT},$$

[47] $$\bar{k}_{1,R}c_{H^+}/(k_{-2}\, p_{H_2}) \ll e^{\beta\eta F/RT}.$$

Then, in [41]:

[48] $$i = 4F\,\bar{k}_{1,R}c_{H^+}\frac{1-[k'^2(k_{-2}p_{H_2}/k_2)]^{\frac{1}{4}}}{1-k'^2(k_{-2}p_{H_2}/k_2)}\, e^{-\beta\eta F/RT}.$$

5. Special Case of [40] for which $(\bar{k}^2_{-1,R}/k'^4)/k_2k_{-2}p_{H_2}\, e^{2(1-\beta)\eta F/RT}$ Predominates in Square Root Term

Applying this condition to [40] one obtains:

[49] $$k'\bar{k}_{-1,R}/k_2 \ll e^{-(1-\beta)\eta F/RT}$$

[50] $$\bar{k}_{-1,R}/(k'k_{-2}p_{H_2}) \ll e^{-(1-\beta)\eta F/RT}.$$

Then, from [41]:

[51] $$i = 4F\frac{\bar{k}_{-1,R}}{k'}\frac{1-(k_2/k'^2k_{-2}p_{H_2})^{\frac{1}{4}}}{1-(k_2/k'^2k_{-2}p_{H_2})}\, e^{(1-\beta)\eta F/RT}.$$

6. Special Case for which $(\bar{k}_{-1,R}/k'^4)\, e^{4(1-\beta)\eta F/RT}$ Predominates in Square Root Term

Application of this condition to equation [40] necessitates expansion of the square root term to four terms. The resulting conditions are:

[52] $$k'k_{-2}p_{H_2}/\bar{k}_{-1,R} \ll e^{(1-\beta)\eta F/RT},$$

[53] $$k_2/k'\bar{k}_{-1,R} \ll e^{(1-\beta)\eta F/RT},$$

[54] $$k'\bar{k}_{1,R}c_{H^+}/\bar{k}_{-1,R} \ll e^{\eta F/RT}.$$

Or, utilizing [39], [54] becomes:

$$k'^2 k_{-2} p_{H_2}/k_2 \ll e^{-2\eta\, F/RT}. \tag{55}$$

With these conditions in [40], one obtains:

$$i = 2F\, k_{-2} p_{H_2}(e^{-2\eta\, F/RT} - 1). \tag{56}$$

7. Reversible Region

Near the reversible potential, i in [37] is limitingly small. This implies that the term in i^2 in [37] will be negligible compared with that in i. Correspondingly, η will be limitingly small. In this equation we expand the e function to the first term only in the i term (of [37]) and to the second term in the term independent of i (the first term vanishing). One obtains:

$$i = -(4\eta\, F^2/RT) \Big/ \left(\frac{1}{\bar{k}_{1,R} c_{H^+}} + \frac{k'^2}{k_2} + \frac{2\bar{k}_{-1,R} k'}{\bar{k}_{1,R} k_2 c_{H^+}} + \frac{k'}{\bar{k}_{-1,R}} + \frac{1}{k_{-2} p_{H_2}}\right). \tag{57}$$

Then, with [39],

$$i = -(4\eta\, F^2/RT) \Big/ \left[\frac{1}{\bar{k}_{1,R} c_{H^+}} + \left(\frac{k'}{\sqrt{k_2}} + \frac{1}{\sqrt{(k_{-2} p_{H_2})}}\right)^2 + \frac{k'}{\bar{k}_{-1,R}}\right]. \tag{58}$$

Several limiting conditions can be derived for equation [58] by regarding Figs. 1, 2, 3, and 6 (cf. Tables). Thus, from Fig. 1, $\bar{k}_{1,R}$ is the smallest rate constant so that:

$$i = -4\bar{k}_{1,R}\, c_{H^+}(F^2/RT)\eta. \tag{59}$$

From Fig. 2, $\bar{k}_{-1,R}$ is the smallest rate constant and thus gives

$$i = -4(\bar{k}_{-1,R}/k')(F^2/RT)\eta. \tag{60}$$

From Fig. 3, k_{-2} is the smallest rate constant and therefore

$$i = -4\, k_{-2}\, p_{H_2}\, (F^2/RT)\eta. \tag{61}$$

From Fig. 6, k_2 is the smallest rate constant and therefore

$$i = -4\,\frac{k_2}{k'^2}\,\frac{F}{RT}\,\eta. \tag{62}$$

The pH and p_{H_2} dependence of these current densities in the reversible region may be noted as an aid to diagnostic evaluation of mechanism.

8. Coverage at the Equilibrium Potential

From [34] and [35],

$$v_2 = v_{-2}. \tag{63}$$

Hence:

$$\theta = \sqrt{\left(\frac{k_{-2} p_{H_2} k'^2}{k_2}\right)} \Big/ 1 + \sqrt{\left(\frac{k_{-2} p_{H_2} k'^2}{k_2}\right)}. \tag{64}$$

9. Coverage in the Tafel Region

From [6] and [7] and

$$\tfrac{1}{2}v = v_1 - v_{-1} \tag{65}$$

$$c_H = \frac{1}{k'}\,\frac{\bar{k}_{1,R} c_{H^+}\, e^{-\beta\eta\, F/RT} - (v/2)}{\bar{k}_{1,R} c_{H^+}\, e^{-\beta\eta\, F/RT} + (\bar{k}_{-1,R}/k')\, e^{(1-\beta)\eta\, F/RT}}. \tag{66}$$

From [34] and [35], with: $v = v_2 - v_{-2}$

$$[67] \qquad c_H = \frac{1}{k'}\left[-\frac{k_{-2}p_{H_2}}{k_2/k'^2 - k_{-2}p_{H_2}} + \sqrt{\left(\frac{k_{-2}p_{H_2}k_2}{k'^2[(k_2/k') - k_{-2}p_{H_2}]^2} + \frac{v}{k_2/k'^2 - k_{-2}p_{H_2}}\right)}\right].$$

10. Limiting Cases for the Catalytic Desorption Mechanism

The equations derived in sections 5 and 6 are based upon certain mathematical restrictions, and, with these limitations, apply to both cathodic and anodic polarization. If further restrictions in regard to the relative values of the constants in equations [48] and [51] are taken into account, the simple limiting cases (equivalent to the existence of a predominant rate-determining step) shown in Tables V and VI arise.

DISCUSSION

The characteristic quantities given in Tables I, II, III, and IV allow a complete distinction to be made between (*a*) the electrochemical and catalytic desorption paths, and (*b*) the energy–distance profiles and thus the rate-determining step. The distinguishing criteria are summarized in Table V.

The use of these criteria is clearly restricted to the assumption that only either the electrochemical or catalytic desorption mechanisms occurs, and that the surface H atoms block part of the surface for the discharge of H^+ ions.

The Tafel equations deduced for various limiting conditions in Tables I–IV may be divided into two groups:

1. Those equations which have the form: current density = charge factors × equilibrium constant of reaction *before* the r.d.s. × rate constant of the r.d.s. × concentration factor × a potential factor.

In this type of equation there is agreement with the formulation of consecutive reactions proposed by Eyring (16) which implies that the free energy of activation of the over-all reaction is the difference in free energy between the initial state and the activated state of the rate-determining reaction.

2. Those equations which have the form: current density = charge factor × rate constant of r.d.s. and equilibrium constant of reaction *following* the r.d.s. × concentration factor* × potential factor.

In this latter type of relation, the only rate constant (apart from those which make up the equilibrium constants) is that for the step from the initial state of the over-all reaction to the state of highest energy in consecutive reactions, and, in this formal sense, the rate-determining step is consistent with the definition made by Eyring *et al.* (16) for the rate-determining step in consecutive reactions. However, consider, for example, (Table III) the expression

$$i = 4F\frac{\bar{k}_{1,R}}{k'}c_{H^+}\sqrt{\left(\frac{k_2}{k_{-2}p_{H_2}}\right)}e^{-\beta\eta F/RT}$$

with [39]:

$$i = 4F\frac{\bar{k}_{-1,R}}{k'}e^{-\beta\eta F/RT}.$$

Thus, in such expressions, the energy barrier which determines the over-all reaction rate is that between the energy of the surface-adsorbed H atom and the state of highest energy in the system. (In such cases, the surface of the electrode is highly covered.)

**Except in the case of equations containing k_{-1}, when no concentration factor occurs in the form of the relation given.*

TABLE I

The electrochemical desorption reaction under cathodic conditions

Relations among the constants	[14] or [16] applicable	Tafel eq.	Coverage	$\left(\frac{\partial\eta}{\partial \ln p_{H_2}}\right)_i$	Energy barrier
$\frac{k_{2,R}}{k'}c_{H^+} > \frac{k_{-1,R}}{k'} > k_{-2,R} > k_{1,R}c_{H^+}$ and $\frac{k_{2,R}}{k'}c_{H^+} > k_{-2,R}p_{H_2} > \frac{k_{-1,R}}{k'} > k_{1,R}c_{H^+}$	[14]	$i = 2Fk_1c_{H^+}e^{-\beta\eta F/RT}$	$(c_H)_0 \to 0$ $(c_H) \to 0$	$\frac{RT}{2F}$	$E(A)c$
$k_{-2,R}p_{H_2} > \frac{k_{2,R}c_{H^+}}{k'} > k_{1,R}c_{H^+} > \frac{k_{-1,R}}{k'}$ and $k_{-2,R}p_{H_2} > k_{1,R}c_{H^+} > \frac{k_{2,R}c_{H^+}}{k'} > \frac{k_{-1,R}}{k'}$	[16]	$i = 2Fk_{1,R}\frac{k_{2,R}}{k'k_{-2,R}}c^2_{H^+}e^{-(1+\beta)\eta F/RT}$	$(c_H)_0 \to \frac{1}{k'}$ $(c_H) \to \frac{1}{k'}$	$-\frac{RT}{2F}\frac{1-\beta}{1+\beta}$	$E(B)c$
$\frac{k_{-1,R}}{k'} > \frac{k_{2,R}c_{H^+}}{k'} > k_{1,R}c_{H^+} > k_{-2,R}p_{H_2}$ and $\frac{k_{-1,R}}{k'} > k_{1,R}c_{H^+} > \frac{k_{2,R}c_{H^+}}{k'} > k_{-2,R}p_{H_2}$	[16]	$i = 2F\frac{k_{1,R}}{k_{-1,R}}k_{2,R}c^2_{H^+}e^{-(1+\beta)\eta F/RT}$	$(c_H)_0 \to 0$ $(c_H) \to 0$	$\frac{RT}{2F}$	$E(C)c$
$k_{1,R}c_{H^+} > \frac{k_{-1,R}}{k'} > k_{-2,R}p_{H_2} > k_{2,R}c_{H^+}$ and $k_{1,R}c_{H^+} > k_{-2,R}p_{H_2} > \frac{k_{-1,R}}{k'} > \frac{k_{2,R}c_{H^+}}{k'}$	[14]	$i = 2F\frac{k_{2,R}}{k'}c_{H^+}e^{-\beta\eta F/RT}$	$(c_H)_0 \to \frac{1}{k'}$ $(c_H) \to \frac{1}{k'}$	$\frac{RT}{2F}$	$E(D)c$

TABLE II

The electrochemical desorption reaction under anodic conditions

Relations among the constants	[14] or [16] applicable	Tafel eq.	Coverage	$\left(\frac{\partial\eta}{\partial \ln p_{H_2}}\right)_i$	Energy barrier
$\frac{k_{2,R}}{k'}c_{H^+} > \frac{k_{-1,R}}{k'} > k_{-2,R}p_{H_2} > k_{1,R}c_{H^+}$ and $\frac{k_{2,R}}{k'}c_{H^+} > k_{-2,R}p_{H_2} > \frac{k_{-1,R}}{k'} > k_{1,R}c_{H^+}$	[14]	$i = -2Fk_{-1,R}\frac{k_{-2,R}p_{H_2}}{k_{2,R}c_{H^+}}e^{(2-\beta)\eta F/RT}$	$(c_H)_0 \to 0$ $(c_H) \to 0$	$-\frac{RT}{2F}\frac{\beta}{2-\beta}$	$E(A)a$
$k_{-2,R}p_{H_2} > \frac{k_{2,R}}{k'}c_{H^+} > k_{1,R}c_{H^+} > \frac{k_{-1,R}}{k'}$ and $k_{-2,R}p_{H_2} > k_{1,R}c_{H^+} > \frac{k_{2,R}}{k'}c_{H^+} > \frac{k_{-1,R}}{k'}$	[16]	$i = -2F\frac{k_{-1,R}}{k'}e^{(1-\beta)\eta F/RT}$	$(c_H)_0 \to \frac{1}{k'}$ $(c_H) \to \frac{1}{k'}$	$\frac{RT}{2F}$	$E(B)a$
$\frac{k_{-1,R}}{k'} > \frac{k_{2,R}}{k'}c_{H^+} > k_{1,R}c_{H^+} > k_{-2,R}p_{H_2}$ and $\frac{k_{-1,R}}{k'} > k_{1,R}c_{H^+} > \frac{k_{2,R}}{k'}c_{H^+} > k_{-2,R}p_{H_2}$	[16]	$i = -2Fk_{-2,R}p_{H_2}e^{(1-\beta)\eta F/RT}$	$(c_H)_0 \to 0$ $(c_H) \to 0$	$-\frac{RT}{2F}\frac{1+\beta}{1-\beta}$	$E(C)a$
$k_{1,R}c_{H^+} > \frac{k_{-1,R}}{k'} > k_{-2,R}p_{H_2} > \frac{k_{2,R}c_{H^+}}{k'}$ and $k_{1,R}c_{H^+} > k_{-2,R}p_{H_2} > \frac{k_{-1,R}}{k'} > \frac{k_{2,R}c_{H^+}}{k'}$	[14]	$i = -2Fk_{-2,R}\frac{k_{-1,R}p_{H_2}}{k_{1,R}k'c_{H^+}}e^{(2-\beta)\eta F/RT}$	$(c_H)_0 \to \frac{1}{k'}$ $(c_H) \to \frac{1}{k'}$	$-\frac{RT}{2F}\frac{\beta}{2-\beta}$	$E(D)a$

TABLE III

The catalytic desorption mechanism under cathodic conditions

Relations among the constants	From general equation	Tafel eq.	Coverage	$\left(\frac{\partial\eta}{\partial \ln p_{H_2}}\right)_i$	Energy diagram
$\frac{k_2}{k'^2 k_{1,R} c_{H^+}} \ll e^{-\beta\eta F/RT}$ $\frac{k_{-2} p_{H_2}}{k_{1,R} c_{H^+}} \ll e^{-\beta\eta F/RT}$ $\frac{k_{-1,R}}{k' k_{1,R} c_{H^+}} = \sqrt{\left(\frac{k_2}{k'^2 k_{-2} p_{H_2}}\right)} \ll e^{-\eta F/RT}$	[41]	$i = 2F\frac{k_2}{k'^2}$	$(c_H) \to \frac{1}{k'}$	—	—
$\frac{k_{1,R} c_{H^+} k'^2}{k_2} \ll e^{\beta\eta F/RT}$ $\frac{k_{1,R} c_{H^+}}{k_{-2} p_{H_2}} \ll e^{\beta\eta F/RT}$ $\frac{k_{-2} p_{H_2} k'^2}{k_2} \ll 1$	[48]	$i = 4F k_{1,R} c_{H^+} e^{-\beta\eta F/RT}$	$(c_H)_0 \to 0$ $(c_H) \to 0$	$\frac{RT}{2F}$	$T(A)c$
$\frac{k_{1,R} c_{H^+} k'^2}{k_2} \ll e^{\beta\eta F/RT}$ $\frac{k_{1,R} c_{H^+}}{k_{-2} p_{H_2}} \ll e^{\beta\eta F/RT}$ $\frac{k_2}{k_{-2} p_{H_2} k'^2} \ll 1$	[48]	$i = 4F\frac{k_{1,R} c_{H^+}}{k'}\sqrt{\left(\frac{k_2}{k_{-2} p_{H_2}}\right)} e^{-\beta\eta F/RT}$	$(c_H)_0 \to \frac{1}{k'}$ $(c_H) \to \frac{1}{k'}$	$-\frac{RT}{2F}\frac{1-\beta}{\beta}$	$T(B)c$
$\frac{k_{1,R} c_{H^+} k'}{k_{-1,R}} = \sqrt{\left(\frac{k_{-2} p_{H_2} k'^2}{k_2}\right)} \ll e^{\eta F/RT}$ $\frac{k_{-2} p_{H_2} k'}{k_{-1,R}} \ll e^{(1-\beta)\eta F/RT}$ $\frac{k_2}{k_{-1,R} k'} \ll e^{(1-\beta)\eta F/RT}$	[56]	$i = 2F\frac{k^2_{1,R} k_2 c^2_{H^+}}{k^2_{-1}} e^{-2\eta F/RT}$	$(c_H)_0 \to 0$ $(c_H) \to 0$	$\frac{RT}{2F}$	$T(C)c$

TABLE IV

The hydrogen desorption mechanism under anodic conditions

Relations among the constants	From general equation	Tafel eq.	Coverage	$\left(\frac{\partial\eta}{\partial \ln p_{H_2}}\right)_i$	Energy diagram
$\frac{k_{-2}p_{H_2}k'}{k_{-1,R}} \ll e^{(1-\beta)\eta F/RT}$ $\frac{k_2}{k_{-1,R}k'} \ll e^{(1-\beta)\eta F/RT}$ $\frac{k_{1,R}c_{H^+}k'}{k_{-1,R}} = \sqrt{\left(\frac{k_{-2}p_{H_2}k'^2}{k_2}\right)} \ll e^{\eta F/RT}$	[56]	$i = -2Fk_{-2}p_{H_2}$	—	—	—
$\frac{k_{-1,R}k'}{k_2} \ll e^{-(1-\beta)\eta F/RT}$ $\frac{k_{-1,R}}{k_{-2}p_{H_2}k'} \ll e^{-(1-\beta)\eta F/RT}$ $\frac{k_2}{k'^2k_{-2}p_{H_2}} \ll 1$	[48]	$i = -4F\frac{k_{-1,R}}{k'}e^{(1-\beta)\eta F/RT}$	$(c_H)_0 \rightarrow \frac{1}{k'}$ $(c_H) \rightarrow \frac{1}{k'}$	$\frac{RT}{2F}$	$T(B)a$
$\frac{k_{-1,R}k'}{k_2} \ll e^{-(1-\beta)\eta F/RT}$ $\frac{k_{-1,R}}{k_{-2}p_{H_2}k'} \ll e^{-(1-\beta)\eta F/RT}$ $\frac{k'^2k_{-2}p_{H_2}}{k_2} \ll 1$	[48]	$i = -4Fk_{-1,R}\sqrt{\left(\frac{k_{-2}p_{H_2}}{k_2}\right)}e^{(1-\beta)\eta F/RT}$	$(c_H)_0 \rightarrow 0$ $(c_H) \rightarrow 0$	$-\frac{RT}{2F}\frac{\beta}{1-\beta}$	$T(A)a$
$\frac{k_2}{k_{1,R}k'^2c_{H^+}} \ll e^{-\beta\eta F/RT}$ $\frac{k_{-2}p_{H_2}}{k_{1,R}c_{H^+}} \ll e^{-\beta\eta F/RT}$ $\frac{k_{-1,R}}{k'k_{-1,R}c_{H^+}} = \frac{1}{k'}\sqrt{\left(\frac{k_2}{k_{-2}p_{H_2}}\right)} \ll e^{-\eta F/RT}$	[41]	$i = -2Fk_{-2}p_{H_2}\frac{k^2_{-1,R}}{k_{1,R}c_{H^+}k'^2}e^{2\eta F/RT}$	$(c_H)_0 \rightarrow \frac{1}{k'}$ $(c_H) \rightarrow \frac{1}{k'}$	0	$T(D)a$

For the above general kinetics of the h.e.r., it is possible to calculate an expression for the stoichiometric number, ν (Horiuti and Ikusima (17)), namely:

[68] $$\nu = \frac{2\,i_0 F}{RT}\left(\frac{\partial \eta}{\partial i}\right)_{\eta \to 0}.$$

In the limiting cases where a r.d.s. appears (except those leading to a limiting current density), as assumed in Tables I–IV, simple values of ν, namely, those of 1 or 2, are obtained. These values are shown in Table VI.

TABLE V

Distinguishing criteria in catalytic and electrochemical desorption paths

Energy profile (cf., Tables I–IV)	Tafel slope		Coverage (high region)		Pressure effect	
	Cathodic	Anodic	Cathodic	Anodic	Cathodic	Anodic
Electrochemical A	β	$2-\beta$	0	0	$\frac{RT}{2F}$	$-\frac{RT}{2F}\frac{\beta}{2-\beta}$
Catalytic A	β	$1-\beta$	0	0	$\frac{RT}{2F}$	$-\frac{RT}{2F}\frac{\beta}{1-\beta}$
Electrochemical B	$1+\beta$	$1-\beta$	$\frac{1}{k'}$	$\frac{1}{k'}$	$-\frac{RT}{2F}\frac{1-\beta}{1+\beta}$	$\frac{RT}{2F}$
Catalytic B	β	$1-\beta$	$\frac{1}{k'}$	$\frac{1}{k'}$	$-\frac{RT}{2F}\frac{1-\beta}{\beta}$	$\frac{RT}{2F}$
Electrochemical C	$1+\beta$	$1-\beta$	0	0	$\frac{RT}{2F}$	$-\frac{RT}{2F}\frac{1+\beta}{1-\beta}$
Catalytic C	2	0	0	0	$\frac{RT}{2F}$	–
Electrochemical D	β	$2-\beta$	$\frac{1}{k'}$	$\frac{1}{k'}$	$\frac{RT}{2F}$	$-\frac{RT}{2F}\frac{\beta}{2-\beta}$
Catalytic D	0	2	$\frac{1}{k'}$	$\frac{1}{k'}$	–	0

A, B, C, D are the types of energy profiles drawn in Tables I, II, III, and IV.

TABLE VI

Values of the stoichiometric number

Electrochemical A	1
Catalytic A	2
Electrochemical B	1
Catalytic B	2
Electrochemical C	1
Catalytic C	1
Electrochemical D	1
Catalytic D	1

Thus, the values of ν enable a distinction to be made between the catalytic desorption mechanism A or B with rate-determining discharge step and the corresponding electrochemical desorption step. This distinction is of particular use because these steps have the same Tafel slopes.

It may be noted that the appropriate value of i_0 which should be substituted into [68] is that measured very near to the reversible potential. In practice it is usual to substitute the value of i_0 obtained from an extrapolation of the Tafel line. If use of this

i_0 value gives simple values of ν, the existence of the same mechanism in the region of the reversible potential, as that which occurs in the Tafel region, is confirmed (for experimental values, see Pentland, Bockris, and Sheldon (18)).

Vetter (4) stated that it was not possible to apply a determination of ν to distinguish between a rate-determining discharge mechanism (catalytic path) and a rate-determining electrochemical desorption (electrochemical path), without independent knowledge of other kinetic characteristics of the reaction occurring in a given case. He purported to show that indefinite values of ν could arise from such an attempt. However, values of ν differing from the integral values of Table VI arise only in the absence of the simple limiting conditions given in Tables I–IV, whereupon no single rate-determining step awaits identification and ν (which concerns a rate-determining step) has no simple meaning. If a simple integral value of ν is obtained from an application of [68], its use in the evaluation of a rate-determining step is possible (Table VI).

ACKNOWLEDGMENTS

The authors are indebted to the University of Pennsylvania for a Fellowship to H.M. and to the Yardney Electric Company for other financial assistance.

REFERENCES

1. Frumkin, A. N. Acta Physicochim. **7**, 474 (1937).
2. Bockris, J. O'M. and Potter, E. C. J. Electrochem. Soc. **99**, 169 (1952).
3. Parsons, R. Trans. Faraday Soc. **47**, 1332 (1951).
4. Vetter, K. J. Z. Elektrochem. **59**, 435 (1955).
5. Bockris, J. O'M. Modern aspects of electrochemistry. Butterworths Scientific Publications, London. 1954. p. 200.
6. Breiter, M. Habilitationsschrift. Munich. 1956.
7. Smits, A. The theory of allotropy. Longmans, Green and Co., Ltd., London. 1922. p. 115.
8. Bowden, P. and Rideal, E. Proc. Roy. Soc. (London), A, **120**, 59, 80 (1928).
9. Baars, M. Sitzber. Ges. Beförder. ges. Naturw. Marburg, **63**, 213 (1928).
10. Erdey-Grúz, T. and Volmer, M. Z. physik. Chem. **150**, 203 (1930).
11. Parsons, R. and Bockris, J. O'M. Trans. Faraday Soc. **47**, 914 (1951).
12. Poltorak, O. M. Zhur. Fiz. Khim. **28**, 1845 (1954).
13. Bockris, J. O'M. Modern aspects of electrochemistry. Butterworths Scientific Publications, London. 1954. p. 187.
14. Bockris, J. O'M. and Watson, R. G. H. J. chim. phys. **49**, 41 (1952).
15. Frumkin, A. N. Z. physik. Chem. **164**, 121 (1933).
16. Glasstone, S., Laidler, K. J., and Eyring, H. The theory of rate processes. McGraw-Hill Book Co., Inc., New York. 1941. p. 100. Bockris, J. O'M. Modern aspects of electrochemistry. Butterworths Scientific Publications, London. 1954. p. 181.
17. Horiuti, J. and Ikusima, M. Proc. Imp. Acad. (Tokyo), **15**, 39 (1939).
18. Pentland, N., Bockris, J. O'M., and Sheldon, E. J. Electrochem. Soc. **104**, 182 (1957).

INTERPRETATION OF LIGHT SCATTERING DATA OBTAINED FROM SOLUTIONS OF LARGE ROD-LIKE PARTICLES

M. E. REICHMANN

It has been shown that the number average molecular weight and particle size can be evaluated from the angular distribution of the intensity of scattered light in addition to the customary weight average molecular weight and z average particle size (1, 2, 3). An evaluation of two different averages is useful inasmuch as it provides an idea as to the width of the distribution function. It is the purpose of this note to show that although sound in theory, the evaluation of the number averages of rods is extremely inaccurate in practice.

Qualitative information concerning the width of the distribution can also be gained from an evaluation of both the z average and weight average particle size. It will be demonstrated that the latter can be determined in a more reliable way than the number average.

In all the derivations the assumption has been made of a one-to-one correspondence between polydispersity in molecular weight and length. As pointed out by Rice in the case of random coils, such a correspondence would not exist if the system was polydisperse in stiffness (4). An equivalent situation may arise in rigid rods if there was polydispersity in thickness. In this case it will be shown that the weight average length as determined from experimental data will be underestimated.

The correlation between the angular distribution of the intensity of scattered light and the molecular parameters is given by the following expression:

$$[1] \qquad Kc/R_\theta = (1/M_w P)+2Bc$$

(c = concentration in g/ml, R_θ = Rayleigh's ratio at angle θ, M_w = weight average molecular weight, B = second virial coefficient, and $K = 2\pi^2 n_0^2 (dn/dc)^2/N\lambda^4$, n_0 = refractive index of solvent, dn/dc = refractive index increment of solution, N = Avogadro's number, and λ = wave length in vacuum).

For rigid rods the function P is given by:

$$[2] \qquad P = \int_0^x \frac{\sin w}{w}\, dw - \left(\frac{\sin x}{x}\right)^2$$

$x = (2\pi/\lambda')\ L \sin \theta/2$ ($\lambda' = \lambda/n$, L = length of rod).

When x is small $1/P$ can be expressed by the first two terms of a power series (5):

$$[3] \qquad 1/P = 1+x_z^2/9$$

$$[4] \qquad (Kc/R_\theta)_{c=0} = \frac{1}{M_w}(1+x_z^2/9) \qquad (x_z = z \text{ average of } x).$$

Figure 1 demonstrates that this approximation represents the $1/P$ function in the range of $x^2 = 0$–3, and that the error in the evaluation of the limiting slope and intercept is not too large up to $x^2 = 15$. It requires therefore a distribution function with a negligible fraction of particles for which $x^2 > 15$.

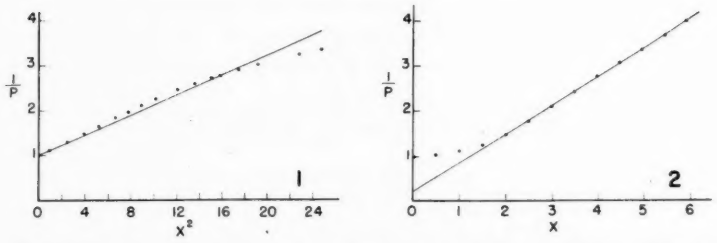

FIG. 1. Reciprocal of particle scattering function vs. x^2 (see text). Solid line was derived from approximation for small values of x.
FIG. 2. Reciprocal of particle scattering function vs. x (see text). Solid line was derived from approximation for large values of x.

When x is large P can be approximated by the following equation (1):

$$P = (\pi/2x_w)\ (1-1/\pi x_n) \qquad [5]$$

$$1/P = (2x_w/\pi)\ (1+1/\pi x_n+1/\pi^2 x_n^2+\ldots) \qquad [5a]$$

neglecting higher terms and introducing $x_w/x_n = M_w/M_n$

$$\frac{1}{P} = \frac{M_w}{M_n}\left(\frac{2}{\pi^2}+\frac{2x_n}{\pi}\right) \qquad [5b]$$

$$\frac{1}{PM_w} = \left(\frac{Kc}{R_\theta}\right)_{c=0} = \frac{1}{M_n}\left(\frac{2}{\pi^2}+\frac{2x_n}{\pi}\right). \qquad [5c]$$

In Fig. 2, $1/P$ for monodisperse rods ($M_w/M_n = 1$) is plotted as a function of x. The line is given by equation [5b]. As Fig. 2 indicates, equation [5b] is a good approximation provided $x > 2$.

Equation [5c] has been suggested as a basis for the evaluation of the number average molecular weight and length. Let us consider the expression in the brackets in [5c]. The value of the first term is 0.203. For $x > 2$ the second term will be larger than 1.30. Therefore the slope of $(Kc/R_\theta)_{c=0}$ versus $\sin\theta/2$ will be larger than an order of magnitude compared to the intercept. An average error of 3% in the slope will introduce an error of 30% or larger in the intercept, and since both M_n and L_n can only be evaluated with the aid of the intercept, this will also be the uncertainty in their determination.

Moreover, by neglecting the higher terms in [5a] the intercept is seriously affected. Remembering that it is the second term in the brackets that determines the intercept one can see that when $x = 2$ the third term will be 16% of the second, and with $x = 6$ the contribution of the third term will be 5% of the second term. Therefore, the intercept evaluated from experimental data will be too high, leading to too low values of the number average parameters.

Since the slope of $(Kc/R_\theta)_{c=0}$ vs. $\sin\theta/2$ can be evaluated with some precision, it would be useful to investigate whether independent information can be obtained from the slope alone. Introducing into [5c] $1/M_n = x_w/M_w x_n$ we obtain:

$$(Kc/R_\theta)_{c=0} = 2L_w/\pi^2 M_w L_n+(4L_w/M_w\lambda')\sin\theta/2. \qquad [6]$$

This is the equation derived by Casassa (6). M_w can be evaluated from the intercept of $(Kc/R_\theta)_{c=0}$ vs. $\sin^2\theta/2$ and thus the weight average length can be obtained from the slope of equation [6].

In the case of polydispersity in the thickness of the rod, the weight average molecular weight, as determined from the intercept of $(Kc/R_\theta)_{c=0}$ vs. $\sin^2 \theta/2$, will be given for a cylinder of radius r by:

$$M_w = \rho\pi N(r^2)_w L_w$$

whereas in the case of uniform thickness

$$M_w = \rho\pi N r^2 L_w' \qquad (\rho = \text{particle density}).$$

The slopes in equation [6] will be $4/\rho\pi N\lambda'(r^2)_w$ and $4/\rho\pi N\lambda' r^2$ respectively. Except in the case of a net side-to-side dissociation, $(r^2)_w > r^2$ resulting in the underestimation of the weight average length.

This can also be expressed in a different way. To preserve the one-to-one correspondence between molecular weight and length, we can formally replace the fluctuation in thickness by an equivalent fluctuation in length. A greater polydispersity in length than in the case of uniform thickness results. Rice has shown that any increase in polydispersity in length leads to a sharper downward curvature of $1/P$ vs. $\sin^2 \theta/2$ (4). The values of $1/P$ at high angles, and the particle length calculated from these values, would be consequently underestimated. Polydispersity in thickness can therefore be considered as the rod equivalent of polydispersity in stiffness in coils (4).

It is sometimes customary to examine polydispersity by comparing the particle length derived from the limiting slope of $1/P$ vs. $\sin^2 \theta/2$ (L_z), with the particle length derived from the best fit of the experimental data with a theoretical curve at high angles (7). It can be shown that the latter particle length will be very close to the weight average length, provided only that the distribution is not very wide. This follows from equation [5*a*]. Neglecting higher terms:

[7] $$1/P = 2x_w/\pi^2 x_n + 2x_w/\pi$$

and the explicit $1/P$ function reduces when x is large to:

[7*a*] $$1/P = 2/\pi^2 + 2x/\pi = 0.20 + 2x/\pi.$$

If x is large, $2x/\pi$ practically determines the value of $1/P$. The same applies to [7] provided x_w/x_n is not very large compared to one. Thus the x determined from the theoretical curve will be very close to x_w.

In a recent publication, light scattering data on tobacco mosaic virus have been reported (7). The particle size was determined from the limiting slope and from the best fit at high angles of the $1/P$ vs. $\sin^2 \theta/2$ curve. The small difference between these two values (10%), was taken as evidence in favor of a narrow distribution. What has been done in effect was a comparison between L_z and L_w. It is somewhat surprising that the length determined from high angle measurements (2900 Å) was lower than the length of the most frequent particle (3000 Å), as determined with the electron microscope. A similar discrepancy was obtained in our laboratory on potato X virus (see preceding article). These discrepancies resulted probably from polydispersity in thickness, as discussed above. The 10% difference would be a measure of the total polydispersity. In view of this it is not surprising that the distribution function of length in tobacco mosaic virus as obtained from electron microscope data was extremely sharp (8).

1. Holtzer, A. M. J. Polymer Sci. **17**, 432 (1955).
2. Benoit, H. J. Polymer Sci. **11**, 507 (1953).
3. Benoit, H., Holtzer, A. M., and Doty, P. J. Phys. Chem. **58**, 635 (1954).

4. RICE, S. A. J. Polymer Sci. **16**, 94 (1955).
5. ZIMM, B. J. Chem. Phys. **16**, 1099 (1948).
6. CASASSA, E. F. J. Chem. Phys. **23**, 596 (1955).
7. BOEDTKER, H. and SIMMONS, N. S. J. Am. Chem. Soc. **80**, 2550 (1958).
8. HALL, C. E. J. Am. Chem. Soc. **80**, 2556 (1958).

RECEIVED SEPTEMBER 22, 1958.
CONTRIBUTION NO. 7, CHEMISTRY DIVISION, SCIENCE SERVICE,
CANADA DEPARTMENT OF AGRICULTURE RESEARCH LABORATORY,
VANCOUVER, B.C.

THE DIELECTRIC CONSTANT AND DIPOLE MOMENT OF 1,3-DIOXANE[1]

R. WALKER[2] AND D. W. DAVIDSON

In contrast to 1,4-dioxane, which has been extensively investigated, neither the dielectric constant nor the dipole moment of 1,3-dioxane has been previously measured, although the dipole moment has been recently calculated (1). The present note reports the static dielectric constants of liquid and solid 1,3-dioxane and the dipole moment as measured in cyclohexane and benzene solutions.

EXPERIMENTAL METHODS

1,3-Dioxane was prepared from 1,3-propanediol and paraformaldehyde by essentially the method of Clarke (2), followed by distillation in a Todd still over calcium oxide and a second distillation over calcium hydride. Boiling point (757 mm) 104.9–105.1° (corr.), n_D^{25} 1.4171. The water content, estimated by the Fischer method, was 0.013% and the absence of significant quantities of hydroxyl- and carbonyl-containing impurities was shown by the infrared spectrum. Gas chromatographic analyses showed only a trace (less than 0.3%) of volatile impurities, except for one sample.

Solvents were dried by refluxing over calcium hydride, followed by distillation. Benzene, after 84 hours of refluxing, had a water content of less than 0.001%.

Dielectric measurements on the liquid and solid were made by a method previously described (3). Dipole moment determinations were made at 25.0° C with a cell of 37 $\mu\mu$f capacitance using a substitution method which involved a number of reiterations to increase the total capacitance measured. For the most dilute solutions 20 reiterations were made.

Refractive indices were measured at 25.0° C with an Abbé Refractometer.

RESULTS AND DISCUSSION

The dielectric constant is shown as a function of temperature in Fig. 1. The melting point is indicated by the break in the curve at −44° C. In the liquid there is no dependence of dielectric constant (ϵ') on frequency up to at least 500 kc/sec. In the solid there is some dispersion of ϵ' over a temperature range extending a few degrees below the melting point where the points in the figure refer to measurements made at 10 kc/sec. At higher frequencies the curve shows less curvature before the melting point is reached.

Between the melting point and 25° C the static dielectric constant values for the liquid may be represented by

$$\epsilon_0 = -5.29_5 + 5.62_3 \times 10^3/T$$

with an average deviation of ±0.2%.

[1]*Issued as N.R.C. No. 5019.*
[2]*Present address: Department of Chemistry, The University, Hull, England.*

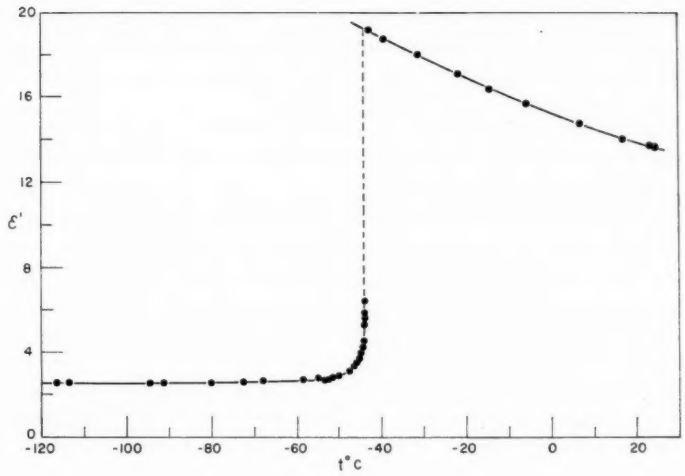

FIG. 1.

The dielectric results provide no evidence of the existence of more than one solid phase, although the possibility of a transition between two non-polar forms which do not differ greatly in density is not excluded. The value of ϵ_0 ($\sim$2.6) in the solid is about that to be expected for the square of the refractive index and shows the absence of any appreciable rotational polarization. 1,4-Dioxane exhibits a solid–solid transition some 11° below the melting point (4).

Figure 2 is a plot of Δ/w vs. w for the cyclohexane and benzene solutions. Here $\Delta = (\epsilon-\epsilon_1)-(n^2-n_1^2)$ and w is the weight fraction of dioxane. The dipole moment was calculated from

$$\mu^2 = \frac{27kT}{4\pi N_A}\frac{M}{(\epsilon_1+2)^2 d_1}\cdot\left(\frac{\Delta}{w}\right)_0$$

in which ϵ_1 and d_1 refer to the solvent and $(\Delta/w)_0$ to the value extrapolated to $w = 0$.

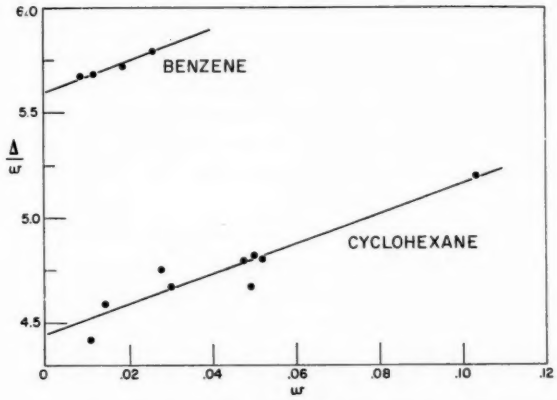

FIG. 2.

As pointed out by Guggenheim (5), a least squares treatment of a quantity like Δ/w as a function of concentration weighs too heavily the less accurate data at low concentrations. Consequently we have fitted the data by least squares to the equations

$$\epsilon - \epsilon_1 = \alpha w + \beta w^2$$
$$n^2 - n_1^2 = \gamma w + \delta w^2$$

and obtained $(\Delta/w)_0$ as $(\alpha - \gamma)$. The straight lines in Fig. 2 result from this treatment.

The dipole moments obtained are 2.14_5 D from the solutions in cyclohexane and 2.13_4 D for those in benzene, with an over-all accuracy estimated at ± 0.03 D.

By the use of the Onsager equation (6) an "effective" dipole moment for the undiluted dioxane may be calculated from the dielectric constant of the liquid. At 25° C, μ (Onsager) = 2.55 D, a value which is practically independent of temperature. The difference between the Onsager moment and the dilute solution moments implies a considerable correlation between the moments of neighboring molecules in the liquid.

The value of the dipole moment calculated by Le Fèvre, Le Fèvre, and Smith (1), for the purpose of establishing the configuration of dimethylene pentaerythritol, was 1.86_5 D. Our measured values are sufficiently close to this figure not to change these workers' conclusion that the two 1,3-dioxane rings having ring atom 5 in common are most likely both in the chair configuration.

The difference between the moment of 1,3-dioxane and that of 2-methyl-1,3-dioxane (1.89 D in benzene (7)) is probably primarily due to the effect of the methyl group in making the ring flatter and the OCO angle larger. The calculation of the moment of 1,3-dioxane referred to above (1) made use of an assumed moment for the C–O–C group of 1.25 D, which is one experimental value of the dipole moment of dimethyl ether. However, in general the C–O–C group appears to have a higher moment in cyclic ethers, the dipole moment of pentamethylene oxide, for example, being 1.87 D (8). In addition, the presence of two C–O–C groups in the ring will change the charge distribution in such a way as to reduce the effective dipole moment associated with each.

To the extent that the contribution of C–H bond moments is negligible, there is no difference between the dipole moments of the chair and boat forms of 1,3-dioxane. Some indirect evidence, however, for the predominance of the chair form is afforded by the magnitude of the difference between μ (Onsager) and μ (solution), which is unusually large for a liquid in which hydrogen bonding is absent (6). Figure 3 illustrates what are perhaps the most favorable relative positions for neighboring molecules, along with the directions of their dipole moments. In each configuration the dipole moment lies in the plane of symmetry of the molecule and each molecule is represented by its projection on this plane. It is evident that complexes of the type shown for the chair configuration, in which neighboring molecules have their moments parallel to one another, will lead to an effective dipole moment considerably higher than that of an isolated molecule. For

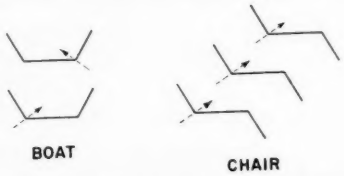

FIG. 3. "Favored" packing of molecules in 1,3-dioxane. Dipole moments are drawn through projections of O atoms on the planes of symmetry.

vertically stacked boat molecules, on the other hand, adjacent molecules have only a small (~1 D) vertical component of moment in common.

ACKNOWLEDGMENTS

We are indebted to R. Ironside and M. E. Bednas for Fischer, infrared, and gas chromatographic analyses, and to Mrs. G. Wheeler for technical assistance.

1. Le Fèvre, C. G., Le Fèvre, R. J. W., and Smith, M. R. J. Chem. Soc. 16 (1958).
2. Clarke, H. T. J. Chem. Soc. **103**, 1788 (1912).
3. Davidson, D. W. Can. J. Chem. **35**, 458 (1957).
4. Jacobs, C. J. and Parks, G. S. J. Am. Chem. Soc. **56**, 1513 (1934).
5. Guggenheim, E. A. Trans. Faraday Soc. **47**, 573 (1951).
6. Böttcher, C. J. F. Theory of electric polarization. Elsevier Pub. Co., Inc., Amsterdam. 1952. p. 323.
7. Otto, M. M. J. Am. Chem. Soc. **59**, 1590 (1937).
8. Allen, J. S. and Hibbert, H. J. Am. Chem. Soc. **56**, 1398 (1934).

Received October 19, 1958.
Division of Applied Chemistry,
National Research Council of Canada,
Ottawa, Canada.

ON THE CONSTITUTION OF 2-KETO-L-GULONIC ACID

N. J. Gaspar* and J. M. Los

In the course of a polarographic investigation of 2-keto-L-gulonic acid (1) the following constitutional features were observed.

In aqueous solution the compound exists in the free acid lactol form as proposed by Reichstein and Grüssner (2), in equilibrium with an extremely small concentration of the free keto acid. The solid state can be either a free keto acid or the corresponding lactone. The latter crystallizes from a solution either of high viscosity or of high ionic strength. Sometimes mixtures of the two solid forms were obtained. Each form was invariably found to contain one molecule of water of crystallization.

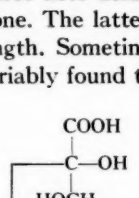

free acid lactol in solution

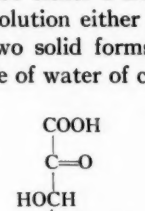

free keto acid in solid state

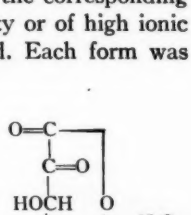

lactone

The lactone is, of course, the keto tautomer of L-ascorbic acid.

The solid 2-keto-L-gulonic acid was made by the method of Reichstein and Grüssner (2): 20 g of diacetone-2-keto-L-gulonic acid were dissolved in 200 ml of distilled water. The solution was heated to boiling and was allowed to stand over a boiling water bath for 45 minutes. The water was then evaporated *in vacuo* till a sirup remained. We found

Holder of a National Research Council of Canada Studentship.

that crystallization from a low-viscosity solution yielded a different substance from that crystallizing at high viscosity. At intermediate viscosity, mixtures of these two would form.

This conclusion was drawn primarily from the results of alkalimetric titration: the product from low-viscosity solution was found to be 99.9% pure if its molecular weight was assumed to be 212, i.e. that of the free acid plus one molecule of water of crystallization. The substance obtained from the high-viscosity solution showed the same degree of purity if its molecular weight was put at 194. This could mean either that the water of crystallization does not appear in the latter case, or that the lactone ring has closed during crystallization.

Heating of the higher molecular weight compound at 50° *in vacuo* for a few hours also produced the compound of molecular weight 194, the loss of weight corresponding to exactly one molecule of water.

The decision as to the nature of the lower molecular weight compound could be made on the basis of the infrared spectra of both solid compounds (Fig. 1). The spectra were taken from KBr pellets (about 1.5 mg of solid in 400 mg of KBr) with a Perkin–Elmer Model 21 spectrophotometer. The product of molecular weight 212 has a strong adsorption peak at 5.75 μ, characteristic of the carbonyl stretching band and much like the corresponding peak of pyruvic acid at 5.73 μ. The product of molecular weight 194, however, shows a peak at 5.67 μ, which is typical of a lactone. Therefore it is concluded that the water is lost in the closing of the lactone ring and not by giving up water of crystallization (the slight adsorption around 6.10 μ seems characteristic of free water).

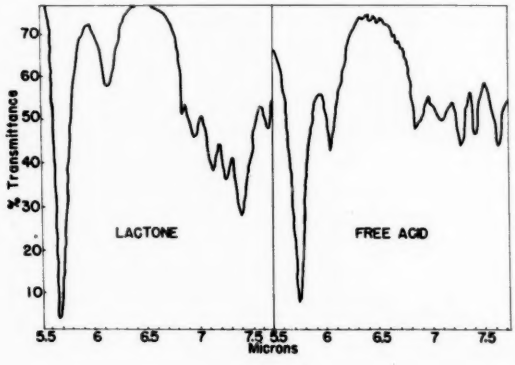

FIG. 1.

It is not likely that either of the two solid forms contains a lactol ring. Molecular models may show that the lactone cannot have a cyclohemiacetal ring as well. The most favorable case is a very strained double-ring structure obtained when the pyranose lactol has the boat conformation and the OH groups on C_2 and C_3 are *cis* to one another. Furthermore, it is not likely that a lactol ring exists in the solid free acid either: (*a*) the C=O adsorption peak at 5.75 μ is very large, (*b*) the above-mentioned transition of this free acid into the lactone form would probably require a total rearrangement within the crystal.

Both solid forms dissolve in water as the free acid, predominantly with a cyclohemiacetal ring. However, equilibrium with the free keto acid must exist, as borne out

by the completely rate-controlled current–voltage wave at the dropping mercury electrode (1). The ionization constant ($K = f\pm(c_{H^+}c_{A^-}/c_{HA})$) is 2.86×10^{-3} at 25° C and ionic strength 0.7 (1).

When KBr pellets were made not by mixing of the solid with KBr but by quickly freezing a solution of the free acid containing a high concentration of KBr, and then removing the water by freeze-drying, the lactone form was invariably produced.

In order to decide whether this is due to the high KBr concentration or to the lower temperature, the following experiment was carried out.

Two identical samples of the lactone (15 mg each) were dissolved in 10 ml of water. To one of these, 4 g of KBr was added. Each solution was then rapidly frozen in a dry ice – acetone mixture and the ice was sublimed *in vacuo*. The sample to which no KBr had been added was then mixed with 4 g of the latter. Identical pellets were made. The spectra showed clearly that the sample containing the KBr in solution had crystallized in the lactone form, the other as the free keto acid (in spite of the fact that it had its starting point in the solid lactone). We may therefore conclude that in the case of the first sample most of the water had been tied up as water of hydration of the K^+ and Br^- ions, lowering the activity of the water to such an extent that only the lactone could crystallize, just as if the crystallization had taken place from a very viscous solution.

Our thanks go to the National Research Council for financial assistance and to Merck and Company, Montreal, for providing the diacetone 2-keto-L-gulonic acid.

1. Los, J. M. and Gaspar, N. J. To be published.
2. Reichstein, T. and Grüssner, A. Helv. Chim. Acta, **17**, 311 (1934).

Received August 25, 1958.
Department of Chemistry,
University of New Brunswick,
Fredericton, New Brunswick.

ISOLATION OF OLIGOSACCHARIDES IN IMPROVED YIELD BY THE ENZYMATIC DEGRADATION OF POLYSACCHARIDES

T. J. Painter[1]

Theoretical considerations originating with Kuhn (1) predict that, for random degradation of a uniform linear macromolecule, the yield of the n-membered fragment is given by $n\alpha^2(1-\alpha)^{n-1}$, where α is the degree of scission. The maximum possible yield of the fragment is then $n[2/(n+1)]^2[(n-1)/(n+1)]^{n-1}$, and occurs when $\alpha = 2/(n+1)$. Further calculation shows that the maximum possible yield of dimer plus trimer occurs when $\alpha = 0.59$, and amounts to 46%.

In the hydrolysis or acetolysis of polysaccharides, lack of randomness in the degradation usually results in considerably lower yields, and study of the literature shows that the combined yield of di- and tri-saccharides has seldom exceeded 35% by weight of the total hydrolyzate. Apart from the wastage of material, examination of the oligosaccharides obtained in these cases would reveal only the dominant structural features of the parent polysaccharide. In addition, misleading artifacts may arise from the recombination (reversion) of simple sugars, although in the case of acetolysis this effect appears to be minimized (2).

[1]*Harold Hibbert Memorial Fellow, McGill University, Montreal, Quebec, 1957–58.*

As Kuhn pointed out, these yields can be considerably increased if the oligosaccharides, once formed, are protected in some way from further degradation. Cellobiose octaacetate, for example, is partly protected by crystallization during the acetolysis of cellulose, and yields of over 40% are not uncommon (3). When completely protected, the maximum yield of n-mer in a random degradation would be $2/(n+1)$, and the maximum yield of dimer plus trimer, if both were protected, would be 83.3%.

This note suggests a possible method of protection in which the lower oligosaccharides are continuously removed from the system by dialysis. To achieve this, it is clear that neither the catalyst, nor any saccharides higher than those desired, should be dialyzable and that the former should not attack the membrane. These conditions were met quite closely by using some fungal hemicellulases and pectinases* in conjunction with a cellophane membrane (4).

Aqueous solutions of a series of polysaccharides, together with the enzyme preparation, were enclosed in cellophane dialysis bags which were large enough to permit a 100% increase in volume of the solution, such as would arise through osmosis. The bags were placed in beakers containing relatively large volumes of water, maintained at 37° C. At intervals, the dialyzates were replaced with fresh water until no further carbohydrate material was removed from the reaction mixture. The combined dialyzates in each case were concentrated to yield syrupy mixtures of sugars, which were shown by paper chromatography to contain large amounts of di-, tri-, tetra-, and higher saccharides, in addition to monosaccharides.

Quantitative experiments were carried out with the four polysaccharides listed in Table I. Each was used in conjunction with a purified hemicellulase preparation, which effected rapid and nearly complete (80–95%) conversion into dialyzable material, while having little effect on the cellophane membrane. The sugars obtained in each case were weighed and then adsorbed on small charcoal columns. The monosaccharide components were selectively eluted and weighed, and the weights of the oligosaccharides were assumed to be represented by the difference.

TABLE I

Recovery of oligosaccharides from polysaccharides

Polysaccharide	Sample* (g)	Saccharides in dialyzate†			
		Total (g)	Mono- (g)	Oligo-‡ (g)	Oligo- (%)
Galactoglucomannan§	0.49	0.44	0.16	0.28	64
Galactoglucomannan‖	0.46	0.43	0.26	0.17	39
Arabogalactan‖	0.50	0.48	0.23	0.25	52
4-*O*-Methylglucuronoxylan¶	0.51	0.43	0.30	0.13	30

*Solution or suspension in water (40 ml), plus 1% w/v hemicellulase in water (10 ml).
†Dialyzates (1 l.) replaced by water every 8 hours for 24 hours, then combined.
‡From columns 3 and 4 by difference.
§From wood of loblolly pine (*Pinus taeda* Linn.) (5).
‖From inner bark of white spruce (*Picea glauca* (Moench) Voss) (6).
¶From wood of white birch (*Betula papyrifera* Marsh.) (7).

These figures provide merely an approximate indication of the possible general usefulness of the method. The yield of oligomers in a particular case will, of course, be greatly dependent upon the nature of the polymer and the enzyme preparation used, as well as conditions of temperature, pH, and concentration. It will also be dependent upon the

*Obtained from the Nutritional Biochemicals Corporation, Cleveland, Ohio.

dimensions of the dialysis vessel in which hydrolysis is carried out, and the rate at which the dialyzate is replaced by fresh water. A more detailed investigation of the optimum conditions for the partial hydrolysis of a number of polysaccharides is now in progress, and an apparatus has been constructed which provides for continuous replacement of the dialyzate, automatic collection of the oligosaccharides, and the use of suitable buffer solutions. It is also intended to construct a dialysis vessel such that the area of membrane for a given volume of reaction mixture is greatly increased, in order to facilitate rapid diffusion of the oligosaccharides.

The author wishes to thank Professor C. B. Purves for his kind interest in this work, and the National Research Council for financial assistance.

1. KUHN, W. Ber. B, **63**, 1503 (1930).
2. SMITH, F. and SRIVASTAVA, H. C. J. Am. Chem. Soc. **78**, 1404 (1956).
3. BRAUN, G. *In* Organic syntheses, Coll. Vol. **II**, 122 (1943).
4. JONES, J. K. N., MERLER, E., and WISE, L. E. Can. J. Chem. **35**, 634 (1957).
5. JONES, J. K. N. and PAINTER, T. J. J. Chem. Soc. 669 (1957).
6. PAINTER, T. J. Forthcoming publication.
7. GLAUDEMANS, C. P. J. and TIMELL, T. E. J. Am. Chem. Soc. **80**, 941, 1209 (1958).

RECEIVED OCTOBER 21, 1958.
MCGILL UNIVERSITY AND
PULP AND PAPER RESEARCH INSTITUTE OF CANADA,
MONTREAL, QUEBEC.

5-*O*-β-D-GALACTOFURANOSYL-D-GALACTOSE FROM GALACTOCARALOSE*

P. A. J. GORIN AND J. F. T. SPENCER

Galactocaralose, a polysaccharide formed by *Penicillium charlesii* G. Smith in Raulin-Thom medium has been shown to contain D-anhydrogalactofuranose units linked 1,5 linearly to a chain length of 9–10 units as indicated by the methylation (1, 2) technique. Its $[\alpha]_{5780}$ (−84°) suggested strongly that the galactose units have the β-configuration.

In the present work partial acid hydrolysis of galactocaralose, which contained smaller amounts of the more acid-stable mannocaralose, produced, as shown by paper chromatography, a homologous series of oligosaccharides. The mixture was fractionated on a cellulose column (3) and materials which appeared to be galactose (4.5%), galactobiose (1.8%), galactotriose (1.4%), galactotetraose (0.4%), and galactopentaose (0.8%) were obtained.

The galactobiose contained a furanose non-reducing end unit, since the sugar was rapidly hydrolyzed with 0.01 *N* sulphuric acid at 100° C (4). Only D-galactose was formed as shown by paper chromatographic examination and by preparation of the 1-methyl 1-phenylhydrazone derivative (5). Treatment of the disaccharide with excess lead tetraacetate in acetic acid resulted in nearly 2 moles of oxidant being consumed at a moderately rapid rate which ruled out 2-, 3-, and probably 4-substitution, and suggested that the glycosidic linkage was either 1,5 or 1,6 (6). A crystalline galactobiitol, obtained by sodium borohydride reduction (7) of the aldose, consumed in 2 minutes 4 molar equivalents of sodium periodate with concomitant release of 2 moles of formic acid; in a separate experiment 2 moles of formaldehyde were formed on sodium periodate oxidation. More prolonged treatment of the polyol resulted in overoxidation probably

**Issued as N.R.C. No. 5022.*

due to attack of the 2,3-*trans*-glycol of the anhydrogalactofuranose unit. Thus the only reasonable structure for the reducing disaccharide is the hitherto undescribed 5-*O*-D-galactofuranosyl-D-galactose, which complements the methylation data obtained from the original polysaccharide.

In agreement with the oxidation data, treatment of the galactobiitol with excess sodium periodate followed by sodium borohydride reduction gave a sirupy arabofuranosyl glycerol ($[\alpha]_D$ −129°). The latter, which gave an amorphous penta-*p*-nitrobenzoate, yielded arabinose and glycerol on acid hydrolysis and consumed 1 molar equivalent of sodium periodate which accords with the values expected from 2-*O*-L-arabofuranosyl glycerol. The configuration of the glycosidic linkage is deduced to be α by isorotational considerations mentioned later. It has been shown that in many glycopyranosyl-polyols the open-chain glycols are attacked preferentially by lead tetraacetate in acetic acid (8, 9). However, *trans* α-glycols in 5-membered ring systems may be oxidized relatively quickly with lead tetraacetate, and aqueous sodium periodate is a more specific oxidizing agent (10) for the required purpose. Based on Hudson's rules of isorotation (11), which have been used in the methyl glycopyranosyl and the glycopyranosyl glycerol series of sugars (8, 12), the specific rotation of 2-*O*-α-L-arabofuranosyl glycerol is calculated to be −108° using the following values: (*a*) 2-*O*-α-D-galactopyranosyl-glycerol, $[\alpha]_D$ +165° (13); (*b*) methyl-α-D-galactopyranoside·H_2O, $[\alpha]_D$ +179° (14); (*c*) methyl-α-D-arabofuranoside, $[\alpha]_D$ +123° (15).

EXPERIMENTAL

Optical rotations were measured at 27° C and evaporations done at 40° C. Solvents for paper chromatographic separations were ethyl acetate – acetic acid – water (9:2:2 v/v) for reducing oligosaccharides and butanol–ethanol–water (40:11:19 v/v) for other carbohydrates. *p*-Anisidine hydrochloride (16) was used as spray reagent for reducing and ammoniacal silver nitrate (17) for non-reducing sugars. R_{Gal} and R_{Rh} denote distances travelled by sugars on paper chromatograms compared to galactose and rhamnose, respectively.

Galactobiose from Galactocaralose

Trial hydrolyses of galactocaralose under a variety of pH's from 1 to 4 at 75° C for 18 hours (cf. the conditions of Andrews, Hough, and Powell (18) for partial hydrolysis of beet araban) showed that pH 2.2 gave the optimum yield of galactobiose (R_{Gal} 0.9), as judged from paper chromatograms. Therefore, galactocaralose (30.0 g), obtained by fermentation of Raulin-Thom medium by *Penicillium charlesii*, was dissolved in water (2 l.) and brought to pH 2.2 with sulphuric acid. After heating at 75° C for 18 hours the solution was neutralized ($BaCO_3$), filtered, and evaporated to a small volume which was added to excess methanol. The methanol-soluble material gave, on a paper chromatogram, a sugar corresponding to galactose and also four other slower moving yellow spots. The mixture of what appeared to be a homologous series of oligosaccharides was fractionated on a cellulose column. Ethyl acetate – acetic acid – water (9:2:2 v/v) eluted galactose (1.50 g); a 9:3:3 mixture gave galactobiose (0.55 g) then galactotriose (0.42 g) and a 9:4:4 mixture galactotetraose (0.12 g) and galactopentaose (0.24 g).

5-O-D-Galactofuranosyl-D-galactose

The sirupy material which appeared to be a galactobiose (19 mg), $[\alpha]_D$ −65° (*c*, 3.8 H_2O), was hydrolyzed as a 1% solution in 0.01 *N* sulphuric acid at 100° C. The specific rotation was −20° after 45 minutes, +5° (90 minutes), and +70° (16 hours; constant

value). The product was neutralized ($BaCO_3$), filtered, and evaporated to a sirup (17 mg) which corresponded to galactose on a paper chromatogram and was converted to its 1-methyl 1-phenylhydrazone (13 mg), m.p. and mixed m.p. 179° C, which had an X-ray diffraction pattern identical with known material.

The above galactobiose (18.8 mg) was oxidized with 4 moles per mole of lead tetraacetate in acetic acid (10 cc) containing water (0.5 cc). The oxidant uptake was 1.5, 1.6, 1.8, 1.9, and 2.2 moles after 2, 5, 15, 30, and 1260 minutes, respectively.

5-O-D-Galactofuranosyl-D-galactitol

The galactobiose (188 mg) was reduced by treatment with sodium borohydride (75 mg) in water (10 cc) for 3 hours. The solution was treated with excess acetic acid, followed by Amberlite IR120, and then evaporated to a crust which was repeatedly dissolved in methanol and evaporated. The product, which had R_{Gal} 0.6, crystallized and was recrystallized from methanol–ethanol. Yield 89 mg, m.p. 149–151° C, and $[\alpha]_D$ −65° (*c*, 0.9 H_2O). Calculated for $C_{12}H_{24}O_{11}$: C, 41.9%; H, 7.0%. Found: C, 41.8%; H, 7.2%. The polyol (15.0 mg in 10 cc water) was oxidized with 0.1 *M* sodium periodate (10 cc). After 2.5, 5, 7.5, and 10 minutes, 4.0, 4.3, 4.2, and 4.4 moles per mole of oxidant were consumed and 1.8 and 1.9 moles of formic acid produced after 2 and 7.5 minutes, respectively. About 0.5 moles of formic acid existed in each case as formate ester, as shown by titration with alkali. When a solution of the polyol (113γ) in 0.02 *M* sodium periodate (2.5 cc) was estimated for formaldehyde by the chromotropic acid method 2.1, 1.9, 2.0 moles per mole were produced after 2.5, 5, and 15 minutes, respectively.

2-O-L-Arabofuranosyl-glycerol

The galactobiitol (89 mg) was oxidized with aqueous sodium periodate (6 molar equivalents; 10 cc) for 1 minute and the solution then added to a suspension of Amberlite IR120 and Dowex-1 in water. The resin was filtered off and to the filtrate sodium borohydride (50 mg) was added. The solution was evaporated to a small volume and the mixture was worked up as in the previous sodium borohydride reduction. The sirupy derivative (41 mg) had R_{Rh} 0.95 and was purified on a cellulose column using *n*-butanol as solvent to give a material which had $[\alpha]_D$ −129° (*c*, 1.0 H_2O) and produced arabinose and glycerol on acid hydrolysis. The disaccharide consumed 0.96 moles per mole of sodium periodate after 1 hour, the specific rotation of the solution becoming constant after 30 minutes.

The purified glycerol derivative (19 mg) was heated for 30 minutes at 80° C in pyridine (2 cc) containing *p*-nitrobenzoyl chloride (0.20 g). The mixture was added to aqueous sodium bicarbonate and after this mixture was shaken for 30 minutes the precipitate was filtered off and reprecipitated twice from ethyl acetate with petroleum ether (b.p. 30–60° C). Yield, 62 mg. The powder had m.p. 88–92° and $[\alpha]_D$ 0° (*c*, 1.1 2,4-lutidine). Calculated for $C_{44}H_{31}O_{22}N_5$: C, 53.8%; H, 3.2%. Found: C, 53.2%; H, 3.5%.

The authors wish to thank Mr. J. A. Baignee and Mr. M. Mazurek for microanalytical determinations and Miss S. Lubin and Mr. N. Gardner for technical assistance.

1. Clutterbuck, P. W., Haworth, W. N., Raistrick, H., Smith, G., and Stacey, M. Biochem. J. **28**, 94 (1934).
2. Haworth, W. N., Raistrick, H., and Stacey, M. Biochem. J. **31**, 640 (1937).
3. Hough, L., Jones, J. K. N., and Wadman, W. H. J. Chem. Soc. 2511 (1949).
4. Haworth, W. N. Ber. A, **61**, 50 (1932).
5. Lobry de Bruyn, C. A. and van Ekenstein, W. A. Rec. trav. chim. **15**, 226 (1896).
6. Charlson, A. J. and Perlin, A. S. Can. J. Chem. **34**, 1200 (1956).

7. WOLFROM, M. L. and WOOD, H. B. J. Am. Chem. Soc. **73**, 2933 (1951).
8. CHARLSON, A. J., GORIN, P. A. J., and PERLIN, A. S. Can. J. Chem. **34**, 1811 (1956).
9. GORIN, P. A. J. and PERLIN, A. S. Can. J. Chem. **35**, 262 (1957).
10. MITRA, A. K. and PERLIN, A. S. Unpublished results.
11. HUDSON, C. S. J. Am. Chem. Soc. **38**, 1566 (1916).
12. CHARLSON, A. J., GORIN, P. A. J., and PERLIN, A. S. Can. J. Chem. **35**, 365 (1957).
13. PUTMAN, E. W. and HASSID, W. Z. J. Am. Chem. Soc. **76**, 2221 (1954).
14. DALE, J. K. and HUDSON, C. S. J. Am. Chem. Soc. **52**, 2536 (1930).
15. MONTGOMERY, E. and HUDSON, C. S. J. Am. Chem. Soc. **59**, 992 (1937).
16. HOUGH, L., JONES, J. K. N., and WADMAN, W. H. J. Chem. Soc. 1702 (1950).
17. PARTRIDGE, S. M. Nature, **158**, 270 (1946).
18. ANDREWS, P., HOUGH, L., and POWELL, D. B. Chem. & Ind. (London), 658 (1956).

RECEIVED SEPTEMBER 29, 1958.
NATIONAL RESEARCH COUNCIL OF CANADA,
PRAIRIE REGIONAL LABORATORY,
SASKATOON, SASKATCHEWAN.

THE CONDENSATION OF 1-PHENYL-2-PROPANONE WITH AROMATIC ALDEHYDES

R. A. ABRAMOVITCH AND A. OBACH

In connection with some other work it was necessary to determine whether, in the condensation of 1-phenyl-2-propanone (I) with aromatic aldehydes in the presence of piperidine, reaction took place at the methylene or at the ω-methyl group. If condensation took place at the methylene group the geometrical configuration would have to be determined, whereas the *trans*-isomer would be expected if reaction took place at the methyl group.

Previous work (1, 2, 3) had indicated that in the presence of aqueous alkali reaction took place at the methyl group

$$\underset{\text{(I)}}{C_6H_5{-}CH_2{-}CO{-}CH_3} + Ar{-}CHO \xrightarrow{OH^-} C_6H_5{-}CH_2{-}CO{-}CH{=}CHAr$$

whereas under acidic conditions reaction took place at the methylene group

$$C_6H_5{-}CH_2{-}CO{-}CH_3 + ArCHO \xrightarrow{H^+} \underset{\text{(II)}}{C_6H_5{-}\overset{\overset{Ar{-}C{-}H}{\|}}{C}{-}CO{-}CH_3}$$

Dickinson (4) reported that, with piperidine as a catalyst, salicylaldehyde reacted with 1-phenyl-2-propanone at the methyl group. In a reinvestigation of Dickinson's work Heilbron and Irving showed that condensation had actually taken place at the methylene group, but the geometry of the product was not established (5).

The condensation of 1-phenyl-2-propanone with benzaldehyde in the presence of piperidine and *n*-heptoic acid gave *cis*-1,2-diphenyl-1-butene-3-one (II; Ar=C_6H_5), whose structure and configuration were established by the fact that it reacted with sodium hypochlorite to give *cis*-α-phenylcinnamic acid (*cis*- with respect to the phenyl groups). The absence of a band for *trans*- CH=CH at 970 cm^{-1} in the infrared confirmed that condensation had not taken place at the terminal methyl group. The condensation with *m*-nitrobenzaldehyde similarly gave *cis*-1-*m*-nitrophenyl-2-phenyl-1-butene-3-one, which reacted with hypochlorite to give *cis*-1-*m*-nitrophenylcinnamic acid. The reaction of phenylpropanone with *o*-nitrobenzaldehyde, on the other hand, did not proceed as easily and only a 22% yield of *cis*-1-*o*-nitrophenyl-2-phenyl-1-butene-3-one was obtained

under the conditions used in the previous condensations. This ketone was obtained as an oil and was best analyzed as its 2,4-dinitrophenylhydrazone. Its structure and configuration were established by the reaction with sodium hypochlorite which gave *cis*-1-*o*-nitrophenylcinnamic acid. Although the ketone gave a positive iodoform reaction no cinnamic acid could be isolated by this method.

EXPERIMENTAL

1,2-Diphenyl-1-butene-3-one

1-Phenyl-2-propanone (12.09 g) and benzaldehyde (5.76 g) were dissolved in benzene (70 ml), and piperidine (6 drops) and *n*-heptoic acid (3 drops) were added. The mixture was boiled under reflux for 24 hours using a Dean–Stark water separator to remove the water azeotropically. Most of the benzene was then evaporated and the residue steam-distilled. The residual oil solidified in the refrigerator overnight; the solid was filtered off and recrystallized from aqueous ethanol giving 1,2-diphenyl-1-butene-3-one (52.7% yield), m.p. 54–55°. Goldschmiedt and Knöpfer (1) give m.p. 53–54° for this compound. Infrared spectrum (Nujol mull) (main peaks only): 1655 (s) (α,β-unsaturated C=O), 1618 (m) (C=C), 1598 (w) (phenyl), 793 (w), 752 (m), 722 (m), 696 (s), and 685 cm^{-1} (s).

The product (0.108 g) was treated with sodium hypochlorite (2 ml) (prepared by dissolving sodium hydroxide (4 g) in water (10 ml) and passing chlorine gas (2 g) through this solution at 0°), heated to 90°, and the flask stoppered and shaken vigorously. Heating at 90° and shaking was continued for ½ hour, water being added after 15 minutes to dissolve the solid which separated on cooling. The solution was filtered and the cold filtrate acidified with gaseous sulphur dioxide. The acid which precipitated was filtered and recrystallized from aqueous ethanol to give *cis*-α-phenylcinnamic acid (54% yield), m.p. 169.5–170.5°. Stoermer and Voht give m.p. 172° for this compound (6).

1-m-Nitrophenyl-2-phenyl-1-butene-3-one

This was prepared similarly from *m*-nitrobenzaldehyde (7.04 g) and 1-phenyl-2-propanone (12.034 g). It crystallized from aqueous ethanol as yellow prisms (57.2% yield), m.p. 79–80°. Calc. for $C_{16}H_{13}O_3N$: C, 71.90; H, 4.90. Found: C, 72.15; H, 4.83. Infrared spectrum (Nujol mull) (main peaks only): 1660 (s), 1625 (w), 1602 (w), 1532 (s) ($-NO_2$), 826 (m), 819 (m), 728 (m), 703 cm^{-1} (s).

Oxidation of the ketone with sodium hypochlorite gave *cis*-α-*m*-nitrophenylcinnamic acid, m.p. 178–180°. Bakunin (7) gives m.p. 181–182° for this acid.

1-o-Nitrophenyl-2-phenyl-1-butene-3-one

The residue, after steam distillation of the product of condensation of *o*-nitrobenzaldehyde (7.0 g) and 1-phenyl-2-propanone (12.06 g), was extracted repeatedly with ether, the dried ($MgSO_4$) extract was evaporated, and the residual oil distilled under vacuum, the fraction b.p. 142–180° at 0.5 mm being collected (21.8% yield). This was redistilled (b.p. 180–186° at 0.6 mm) giving the nitroketone as an orange-red oil (12.8% based on *o*-nitrobenzaldehyde). Infrared spectrum (liquid film) (main peaks only): 1685 (s), 1618 (m), 1585 (m), 1535 (s), 1505 (w), 865 (m), 790 (w), 755 (m), 720 (s), 700 (s), and 675 cm^{-1} (w). The 2,4-dinitrophenylhydrazone crystallized from an ethyl acetate – ethanol mixture in red prisms, m.p. 188–189°. Calc. for $C_{22}H_{17}O_6N_5$: C, 59.06; H, 3.80. Found: C, 59.32; H, 3.75.

With sodium hypochlorite the ketone gave *cis*-*o*-nitrophenylcinnamic acid, m.p. 193–194°. With sodium hypoiodite, iodoform, m.p. 115–118°, was obtained but the cinnamic acid could not be isolated. The melting point of the acid as reported in the literature (8) is 193–195°.

1. GOLDSCHMIEDT, G. and KNÖPFER, G. Monatsh. **18**, 437 (1897).
2. GOLDSCHMIEDT, G. and KRCZMAR, H. Monatsh. **22**, 659 (1901).
3. HARRIES, C. and MÜLLER, G. H. Ber. **35**, 966 (1902).
4. DICKINSON, R. J. Chem. Soc. 2234 (1926).
5. HEILBRON, I. M. and IRVING, F. J. Chem. Soc. 975 (1929).
6. STOERMER, R. and VOHT, G. Ann. **409**, 36 (1915).
7. BAKUNIN, M. Gazzetta chim. ital. **25**, 137 (1895).
8. PSCHORR, R. Ber. **29**, 496 (1896).

RECEIVED SEPTEMBER 17, 1958.
DEPARTMENT OF CHEMISTRY,
UNIVERSITY OF SASKATCHEWAN,
SASKATOON, SASKATCHEWAN.

CYCLIZATION OF 1,3-BIS-(β-CHLOROETHYL)-UREA*

M.-E. KRELING AND A. F. MCKAY

It was found that the double melting point property of 2-(β-chloroethylamino)-2-oxazoline hydrochloride (II*a*) is associated with its conversion in the molten state into 1,3-bis-(β-chloroethyl)-urea (I*a*). Although 2-(β-chloroethylamino)-2-oxazoline hydrobromide (II*b*) does not exhibit a double melting point, it also rearranges in the molten state to the corresponding urea (I*b*).

I*a*, X = Cl
b, X = Br

II*a*, X = Cl
b, X = Br

1-(β-Bromoethyl)-3-(β-chloroethyl)-urea and 1,3-bis-(β-chloroethyl)-urea on heating in water cyclized respectively to the hydrobromide and hydrochloride salts of 2-(β-chloroethylamino)-2-oxazoline. The conversion of 1-(β-bromoethyl)-3-(β-chloroethyl)-urea into the hydrobromide salt II*b* rather than the hydrochloride salt of 2-(β-bromoethylamino)-2-oxazoline can be attributed to the lower bond energy of the C–Br linkage in comparison with the C–Cl linkage.

EXPERIMENTAL†

1,3-Bis-(β-chloroethyl)-urea

1,3-Bis-(β-chloroethyl)-urea (m.p. 126.5–128° C) was prepared in 61.2% yield by the method of Bestian (1). A mixture melting point determination with a known (2) sample of 1,3-bis-(β-chloroethyl)-urea gave no depression.

2-(β-Chloroethylamino)-2-oxazoline Hydrochloride

1,3-Bis-(β-chloroethyl)-urea (20 g, 0.1 mole) in water (50 ml) was heated under reflux for 1 hour. After the clear solution was evaporated to dryness *in vacuo*, crystals were obtained, yield 20 g (100%). These crystals melted at 103–104° C, resolidified and remelted at 121–123° C. Three crystallizations from absolute ethanol–ether (1 : 1) solution raised the melting points to 107–109° C and 125–127° C. Anal. Calc. for $C_5H_{10}Cl_2N_2O$:

**Issued as Report No. 22 from the L. G. Ryan Research Laboratories, Monsanto Canada Limited, Ville LaSalle, Quebec.*

†All melting points are uncorrected. The microanalyses were determined by Micro-Tech Laboratories, Skokie, Ill., and Schwartzkopf Microanalytical Laboratory, Woodside, N. Y.

C, 32.45; H, 5.45; Cl, 38.32; N, 15.14%. Found: C, 32.77; H, 5.37; Cl, 37.86; N, 14.96%.

A picrate (m.p. 192–194° C) was formed in the usual manner from water. The product was identified by a mixture melting point determination with a known (2) sample of 2-(β-chloroethylamino)-2-oxazoline picrate (m.p. 193–194° C).

A sample of 2-(β-chloroethylamino)-2-oxazoline hydrochloride (m.p. 107–109° C and 125–127° C) was held in the molten state for 1 minute. The molten mass crystallized immediately on cooling and the crystals melted sharply at 125–127° C. These crystals no longer gave a picrate and they did not depress the melting point of a known sample of 1,3-bis-(β-chloroethyl)-urea.

2-(β-Chloroethylamino)-2-oxazoline hydrochloride (9.25 g, 0.05 mole) in absolute methanol (180 ml) was passed through a column of Amberlite IRA-400 resin (150 ml in the hydroxyl form). The column was washed with the same volume of methanol and the eluate and washings were evaporated to dryness *in vacuo* under nitrogen. The residual crystalline mass melted at 81–84° C, yield 7.43 g (100%). These crystals of 2-(β-chloroethylamino)-2-oxazoline were very soluble in water, alcohol, and acetone. Three crystallizations from acetone–hexane solution raised the melting point to 84–86° C. Anal. Calc. for $C_5H_9ClN_2O$: C, 40.40; H, 6.10; Cl, 23.85; N, 18.85%. Found: C, 39.78; H, 6.35; Cl, 23.50; N, 18.52%.

2-(β-Chloroethylamino)-2-oxazoline Hydrobromide

Gaseous hydrogen bromide was passed into a solution of 2-(β-chloroethylamino)-2-oxazoline (841 mg, 0.005 mole) in water (10 ml) until a pH of 3 was obtained. The solution was evaporated *in vacuo* at 45° C and the resulting oil crystallized on standing in a vacuum desiccator overnight, yield 1.3 g (100%). Crystallization from ethanol–ether solution gave a constant melting point of 118.5–119.5° C. Anal. Calc. for $C_5H_{10}BrClN_2O$: C, 26.17; H, 4.39; halogen, 50.27; N, 12.21%. Found: C, 26.41; H, 4.26; halogen, 49.88; N, 11.77%.

A sample of 2-(β-chloroethylamino)-2-oxazoline hydrobromide in water was converted into its picrate (m.p. 193–194° C) in 95% yield in the usual manner.

1-(β-Bromoethyl)-3-(β-chloroethyl)-urea

1-(β-Chloroethylamino)-2-oxazoline hydrobromide (76 mg, 0.00033 mole) was heated for 15 minutes in dry *o*-xylene (3 ml) to 130–140° C (temperature of the oil bath). The mixture upon cooling deposited crystals, which were collected by filtration; yield, 42 mg (55.3%). Crystallization from warm (50° C) ethanol–ether solution raised the melting point from 108.5–110° C to 109–111° C. Anal. Calc. for $C_5H_{10}BrClN_2O$: C, 26.17; H, 4.39; halogen, 50.27; N, 12.21%. Found: C, 26.02; H, 4.35; halogen, 50.30; N, 12.01%.

Cyclization of 1-(β-Bromoethyl)-3-(β-chloroethyl)-urea

1-(β-Bromoethyl)-3-(β-chloroethyl)-urea (80 mg) in water (2 ml) was heated for approximately 1 hour at 70–80° C until a clear solution was obtained. The clear solution on treatment with aqueous picric acid solution gave a 93.5% yield of 2-(β-chloroethylamino)-2-oxazoline picrate (193–194° C) which was identified by a mixed melting point determination.

1. Bestian, H. Ann. **566**, 210 (1950).
2. McKay, A. F., Weinberg, M. A., Picard, J. P., Hatton, W. G., Bedard, M., and Rooney, H. E. J. Am. Chem. Soc. **76**, 6371 (1954).

Received September 8, 1958.
L. G. Ryan Research Laboratories,
Monsanto Canada Limited,
Ville LaSalle, Quebec.

HELVETICA
CHIMICA
ACTA

SCHWEIZERISCHE
CHEMISCHE GESELLSCHAFT
Verlag Helvetica Chimica Acta
Basel 7 (Schweiz)

Seit 1918 **40** Jahre

Abonnemente: Jahrgang 1959, Vol. XLII $25.00 incl. Porto

Es sind noch lieferbar:

Neudruck ab Lager
Vol. I–XXIV (1918–1941)
Vol. XXV–XXVII (1942–1944) in Vorbereitung.

Originalausgaben, druckfrisch und antiquarisch.
Vol. XXVIII–XLI (1945–1958)

Diverse Einzelhefte ab Vol. XXII
Preise auf Anfrage. Nur solange Vorrat

Das wissenschaftliche Organ der SCHWEIZERISCHEN CHEMISCHEN GESELLSCHAFT

NOTES TO CONTRIBUTORS

Canadian Journal of Chemistry

MANUSCRIPTS

General.—Manuscripts, in English or French, should be typewritten, double spaced, on paper 8½×11 in. **The original and one copy are to be submitted.** Tables and captions for the figures should be placed at the end of the manuscript. Every sheet of the manuscript should be numbered. Style, arrangement, spelling, and abbreviations should conform to the usage of recent numbers of this journal. Greek letters or unusual signs should be written plainly or explained by marginal notes. Characters to be set in bold face type should be indicated by a wavy line below the characters. Superscripts and subscripts must be legible and carefully placed. Manuscripts and illustrations should be carefully checked before they are submitted. Authors will be charged for unnecessary deviations from the usual format and for changes made in the proof that are considered excessive or unnecessary.

Abstract.—An abstract of not more than about 200 words, indicating the scope of the work and the principal findings, is required, except in Notes.

References.—These should be designated in the text by a key number and listed at the end of the paper, with the number, in the order in which they are cited. The form of the citations should be that used in this journal; in references to papers in periodicals, titles should not be given and only initial page numbers are required. The names of periodicals should be abbreviated in the form given in the most recent *List of Periodicals Abstracted by Chemical Abstracts*. All citations should be checked with the original articles and each one referred to in the text by the key number.

Tables.—Tables should be numbered in roman numerals and each table referred to in the text. Titles should always be given but should be brief; column headings should be brief and descriptive matter in the tables confined to a minimum. Vertical rules should not be used. Numerous small tables should be avoided.

ILLUSTRATIONS

General.—All figures (including each figure of the plates) should be numbered consecutively from 1 up, in arabic figures, and each figure referred to in the text. The author's name, title of the paper, and figure number should be written in the lower left corner of the sheets on which the illustrations appear. Captions should not be written on the illustrations.

Line drawings.—Drawings should be carefully made with India ink on white drawing paper, blue tracing paper, or co-ordinate paper ruled in blue only; any co-ordinate lines that are to appear in the reproduction should be ruled in black ink. Paper ruled in green, yellow, or red should not be used. All lines must be of sufficient thickness to reproduce well. Decimal points, periods, and stippled dots must be solid black circles large enough to be reduced if necessary. Letters and numerals should be neatly made, preferably with a stencil (**do NOT use typewriting**), and be of such size that the smallest lettering will not be less than 1 mm high when the figure is reduced to a suitable size. Many drawings are made too large; originals should not be more than 2 or 3 times the size of the desired reproduction. Wherever possible two or more drawings should be grouped to reduce the number of cuts required. In such groups of drawings, or in large drawings, full use of the space available should be made; the ratio of height to width should conform to that of a journal page (5½×7½ in.) but allowance must be made for the captions. **The original drawings and one set of clear copies (e.g. small photographs) are to be submitted.**

Photographs.—Prints should be made on glossy paper, with strong contrasts. They should be trimmed so that essential features only are shown and mounted carefully, with rubber cement, on white cardboard, with no space between those arranged in groups. In mounting, full use of the space available should be made. **Photographs are to be submitted in duplicate;** if they are to be reproduced in groups one set should be mounted, the duplicate set unmounted.

REPRINTS

A total of 50 reprints of each paper, without covers, are supplied free. Additional reprints, with or without covers, may be purchased at the time of publication.

Charges for reprints are based on the number of printed pages, which may be calculated approximately by multiplying by 0.5 the number of manuscript pages (double-space typewritten sheets, 8½×11 in.) and including the space occupied by illustrations. Prices and instructions for ordering reprints are sent out with the galley proof.

Contents

Marshall Kulka—ω-Haloalkyl and ω-aminoalkyl sulphides. Cleavage of the alkyl–sulphur bond - 325

W. F. Forbes and A. R. Knight—The study of hydrogen bonding and related phenomena by ultraviolet light absorption. Part II. The effect of solvent–solute interactions on the intermolecular hydrogen bond in benzoic acids 334

E. A. Cherniak and W. M. Smith—The quenching of potassium resonance radiation by hydrocarbons - - - - - - - - - - - - - - - - - 341

Arthur A. Amos and P. Ziegler—Bromination of steroid 20-ketals - - - 345

James Trotter—Steric inhibition of resonance. I. 9-Nitroanthracene and 9,10-dinitroanthracene - - - - - - - - - - - - - - - - - - - 351

E. J. C. Curtis and J. K. N. Jones—The synthesis of 4-*O*-β-D-galactosyl-D-glucose (lactose) - 358

R. A. Abramovitch—The infrared spectra of some cyclic malonates - - - 361

Paul E. Gagnon and Brian T. Newbold—Peracetic acid oxidation of halogenated azobenzenes - 366

S. S. Berman and E. C. Goodhue—A new spectrophotometric procedure for platinum with tin (II) chloride - - - - - - - - - - - - - - - 370

Henry M. Papée—Microcalorimetry of adsorption of water vapor on lead diiodide - 375

M. E. Reichmann—Potato X virus. Part III. Light scattering studies - - 384

P. Kebarle and F. P. Lossing—Free radicals by mass spectrometry. XV. The mercury-photosensitized decomposition of formic acid, acetic acid, and methyl formate - 389

H. Favre, M. Lefebvre, and (in part) J-C. Richer—Dérivés du triméthyl-1,8,8 bicyclo[3,2,1]octane. III. Synthèse des triméthyl-1,8,8 bicyclo[3,2,1]octanols-2α et -2β et des triméthyl-5,8,8 bicyclo[3,2,1]octanols-2α et -2β - - 403

H. Favre and J-C. Richer—Dérivés du triméthyl-1,8,8 bicyclo[3,2,1]octane. IV. Détermination des configurations des deux diméthyl-5,5 cyclohexane-diols-1,3 - 411

H. Favre and J-C. Richer—Dérivés du triméthyl-1,8,8 bicyclo[3,2,1]octane. V. Réductions catalytique et chimique de la triméthyl-1,8,8 bicyclo[3,2,1]-octanedione-2,4 - 417

A. F. McKay and M.-E. Kreling—A new molecular rearrangement. IV. Further observations on the chemistry of 1-nitro-2,3,5,6-tetrahydro-1(H)-imidaz-(1,2-a)imidazole and 1-(β-chloroethyl)-2-imidazolidone - - - - - - 427

H. C. Clark and R. J. O'Brien—Co-ordination compounds of nickel(II). Part I. The spectra of salicylaldimine derivatives of nickel(II) in some organic solvents - 436

T. P. Yin and R. K. Brown—The reactivity of cellulose. III. The nitration of cotton linters alternately wetted with water at various temperatures and dried, and the probable distribution of the nitrate groups - - - - - 444

L. G. Stonhill—The determination of atomic ratios in the uranium–oxygen system by a thermogravimetric method - - - - - - - - - - 454

W. R. Trost—Orbital constructions and electron populations in the transition elements - 460

J. O'M. Bockris and H. Mauser—The kinetics of the evolution and dissolution of hydogen at electrodes - - - - - - - - - - - - - - - 475

Notes:

M. E. Reichmann—Interpretation of light scattering data obtained from solutions of large rod-like particles - - - - - - - - - - - 489

R. Walker and D. W. Davidson—The dielectric constant and dipole moment of 1,3-dioxane - 492

N. J. Gaspar and J. M. Los—On the constitution of 2-keto-L-gulonic acid - 495

T. J. Painter—Isolation of oligosaccharides in improved yield by the enzymatic degradation of polysaccharides - - - - - - - - - - - - - - - 497

P. A. J. Gorin and J. F. T. Spencer—5-*O*-β-D-Galactofuranosyl-D-galactose from galactocaralose - - - - - - - - - - - - - - - - - - 499

R. A. Abramovitch and A. Obach—The condensation of 1-phenyl-2-propanone with aromatic aldehydes - - - - - - - - - - - - - - - 502

M.-E. Kreling and A. F. McKay—Cyclization of 1,3-bis-(β-chloroethyl)-urea 504

Printed in Canada *by* University of Toronto Press